British and Fennoscandian Ice-Sheet interactions during the quaternary

Davies, Bethan Joan

BRITISH AND FENNOSCANDIAN ICE-SHEET INTERACTIONS DURING THE QUATERNARY

Bethan Joan Davies

A thesis presented for the degree of Doctor of Philosophy

Department of Geography
Durham University
February 2008

Declaration of Copyright

I confirm that no part of the material presented in this thesis has previously been submitted by me or any other person for a degree in this or any other university. In all cases, where it is relevant, material from the work of others has been acknowledged.

Bethan Davies

Department of Geography,
Durham University

09 April 2009

For Alan and Norma
My Parents

Abstract

Northeastern England and the North Sea Basin is a critical location to examine the influence of glaciation in the northern Hemisphere during the Quaternary. This region was a zone of confluence between the British and Fennoscandian Ice Sheets, and harboured several dynamic ice lobes sourced from northern Scotland, the Cheviots, the Lake District and the Southern Uplands. The region thus has some of the most complex exposures of Middle to Late Pleistocene sediments in Britain, with both interglacial and glacial sediments deposited in terrestrial and marine settings, and being sourced from both the British Isles and northern continental Europe.

The research undertaken involved a thorough reinvestigation of the Quaternary sediments of northeast England, making use of enhanced exposures in coastal sections following the cessation of colliery waste dumping, and in boreholes from the North Sea. It used detailed sedimentological, stratigraphical, chronostratigraphical, lithological, petrological, and geochemical techniques to investigate their depositional processes, age, provenance signatures, and regional correlatives to construct an independent model of the eastern margin of the British-Irish Ice Sheet (BIIS) throughout the Quaternary, and its interaction in the North Sea Basin with the Fennoscandian Ice Sheet (FIS). This region was a zone of confluence between ice lobes sourced from northern Scotland, the Cheviots, the Lake District and the Southern Uplands, and is ideally placed for investigating the geological record of the North Sea Lobe during the Late Devensian. In addition, County Durham has one of the most northerly exposures of Middle Pleistocene sediments in Britain, including a raised beach and a Scandinavian till.

This project focussed on a variety of localities in northeastern England and in the North Sea Basin, including Whitburn Bay, Shippersea Bay, Hawthorn Hive, and Warren House Gill. At Whitburn Bay, the Blackhall and Horden glacigenic members are exposed in superposition and are Late Devensian in age. The lower Blackhall Member here is interpreted as a subglacial traction till with a high percentage of locally derived erratics. A boulder pavement at the top of the till points to a switch in ice-bed conditions and the production of a melt-out lag prior to the deposition of the upper, Horden Member. This second traction till contains erratics and heavy minerals derived from crystalline bedrock sources in the Cheviot Hills and northeast Scotland, including tremolite, andalusite, kyanite and rutile. Within the Horden Member are numerous sand, clay and gravel-filled channels incised into the diamicton, which are attributed to a low energy, distributed, subglacial canal drainage system. Coupled with the hydrofractures and the boulder pavement, this suggests that a partly decoupled, fast flowing ice stream deposited the Horden Member. The eastward, on-shore direction of ice movement indicates that the ice stream was confined in the North Sea Basin, possibly by the presence of Scandinavian ice.

From Hawthorn Hive to Warren House Gill, the Blackhall and Horden members are separated by the Peterlee Sands and Gravels, ice-proximal outwash sediments. Beneath the glacial sequence, some 500 m to the south is the Easington Raised Beach. The partly calcreted interglacial beach lies directly on Magnesian Limestone bedrock at 33 m O.D., and consists of beds of unconsolidated, well-bedded, imbricated, well-rounded sands and gravels. It has been dated to MIS 7 by amino acid geochronology and OSL dating. The

beach contains exotic gravel, including flint, and previous workers have reported Norwegian erratics. The only currently extant source for these is the Scandinavian Drift at Warren House Gill.

Warren House Gill is a classic Middle Pleistocene site, and has a complex stratigraphy, consisting of a lower "Scandinavian Drift" with overlying estuarine sediments, and an upper "Main Cheviot Drift", which comprises two tills and glaciotectonised, interstratified sands and silts, traditionally interpreted as Devensian in age. The lowest grey Scandinavian Drift is a grey, laminated clay with dropstones. It contains marine bivalve fragments, foraminifera, and clasts of northeastern Scotland and Norwegian provenance, as well as Magnesian Limestone, chalk, flint, and Triassic red marl from the North Sea. Reworked palynomorphs include Eocene dinoflagellate cysts. This is interpreted as a Middle Pleistocene glaciomarine deposit, and is renamed the 'Ash Gill Member' of the Warren House Formation, with inputs from both Scottish and Scandinavian sources. It is dated to the Middle Pleistocene by AAR dates on the shell fauna, and by the relationship to the MIS 7 age raised beach. The overlying well sorted pink and red interbedded sands and silts contain carbonate nodules and rare clasts. These shallow subaqueous sediments were deposited through suspension settling and bottom current activity, and they may be reworked loess. They are named the 'Whitesides Member' and are the highest member in the Warren House Formation.

The overlying "Cheviot Drift" consists of two ice-marginal traction tills (the Blackhall and Horden members), separated by interbedded glaciofluvial red silts and sands. The till lithologies are indicative of a northern British provenance, and are rich in limestone, coal, sandstone, greywacke and dolerite. The Blackhall Member was deposited by ice during MIS 4, during a period of maximum extent of the British and Fennoscandian ice sheets and contact in the central North Sea. The Horden Member was deposited in an ice-marginal landsystem by the Late Devensian North Sea Lobe, and is correlative with the Skipsea Member in Yorkshire and the Bolders Bank Formation offshore.

The Swarte Bank, Coal Pit, Fisher and Bolders Bank formations from the North Sea Basin were also examined. These subglacial and glaciomarine sediments, ranging from MIS 12 to MIS 2 in age, were all found to show a similar provenance from the Grampians, Aberdeenshire and the Scottish Highlands, indicating repeat ice-flow pathways during the Quaternary.

This research has significant implications for British Quaternary stratigraphy, as it indicates that Fennoscandian ice was a significant influence on the BIIS throughout the Quaternary, and that on multiple occasions, Fennoscandian ice directly impacted the coast of eastern England. During MIS 12, a marine embayment opened in northeast England between the British and Fennoscandian ice sheets. Ice rafted material derived from both Scottish and Norwegian sources was deposited in this marine embayment. The Ash Gill Member of the Warren House Formation is an isolated remnant of this ancient glaciomarine environment, and it is separated from the overlying Devensian sediments by a substantial unconformity.

During the Early Devensian, ice sourced in Scotland flowed eastwards through the Tyne Gap, where it was joined by a minor component of Lake District ice. This was a stage of maximum configuration of the BIIS, with contact with the FIS offshore. During the Last Glacial Maximum, the North Sea Lobe was constrained by the FIS offshore, forcing the North Sea Lobe onshore. This project found no evidence of Lake District erratics in County Durham, but found detrital material in the subglacial tills from the coast of northeastern Scotland.

Acknowledgements

It has been my privilege to work with Dave Roberts, Dave Bridgland and Colm Ó Cofaigh during the last three years, who have continually provided guidance, inspiration, encouragement, teaching and support. Role models, teachers, researchers, thank you.

This PhD was funded by a bursary from the Geography Department and from Hatfield College. Hatfield also provided several generous grants to support the research and conference attendance. The Dudley Stamp Memorial Fund provided £500 towards thin-section analysis. The Research Development Fund of the Geography Department paid £1000 for the JCB excavations at Warren House Gill. INQUA gave £500 for travel to the INQUA conference in Cairns.

It was a pleasure to collaborate with Dr. Steve Pawley from RHUL, who came to Durham to sample for OSL and analysed the age of the Easington Raised Beach. This gave this work another dimension and greatly improved its international significance. This was under the auspices of the AHOB project, overseen by Professor Jim Rose. Dr. Ian Candy, also RHUL, analysed the cementation of the Easington Raised Beach, and dated the cement by U-series. Dr. Kirsty Penkman and Miss Beatrice Demarchi of York University did the AAR analysis on the shell fragments from Easington and Warren House Gill, again yielding interesting and scientifically important results. Bill Austin counted and identified the foraminifera from the Easington Raised Beach.

The laboratory staff at Durham University Geography Department (Frank Davies, Neil Tunstell, Eddie Million, Mervyn Brown, Amanda Hayton, and Martin West) made many resources available to me. Amanda and Martin did the ICP-MS and Atomic Absorption. Neil taught me many new techniques. David Sales of the Geology department made the thin sections. Dr. Nick Cox and Dr. Ian Evans kindly taught me relevant statistical techniques and helped me to operate STATA.

The British Geological Survey put their core store at my disposal and provided me with detailed logs of boreholes from the North Sea. They also gave permission to reproduce some of their maps. Dr. Jim Riding of the BGS kindly identified palynomorphs from the tills of County Durham and provided many useful comments. Dr. Emrys Phillips (also BGS) helped with interpretations of heavy-mineral data, clast-lithological data, and the soft-sediment deformation within the thin sections at Warren House Gill and Whitburn Bay, vastly adding to the quality of this research.

I owe many thanks to many other kind people at the British Geological Survey. Dr. Jonathon Lee, Dr. Brian Moorlock, Dr. Richard Hamblin, and Mrs Anna Harrison provided encouragement and employment after I finished my Undergraduate degree, aided me in my MSc Thesis, and continued to provide support and encouragement during my PhD research. Dr. Lee crosschecked my identifications of heavy minerals and erratics. I would like to thank Professor Jim Rose for his enthusiasm and support during my MSc degree, which continued unabated during my doctoral research.

I would like to thank the girls of S209 for their encouragement and the odd shoulder during the last two years, and everyone else on the SRIF top floor for support, laughter and cake. The protracted discussions in the coffee room and the field with Dr. Dave Evans, Dr. Aoibheann Kilfeather, Dr. Ian Evans, Tom White, and Dr. Wishart Mitchell were ever helpful and constructive. Thank you also to everyone who came out to help me in the field – Steve, Tom W, Stefan, Natasha, David, Merry, Tom S, and Tim.

I have been fortunate in having many great opportunities and exposures to glacial science. Dave, thank you for taking me to Greenland. Dr. Bob Dugdale, thank you for taking me to Iceland and encouraging me to pursue my academic interests. BSES gave me my first exposure to ice sheets in Iceland, and it was there that I became fascinated by them. In addition, thank you to my Geography teachers at school, Sarah Jacot and Clare Grindrod, who first inspired me.

My parents and sister Siân encouraged me, proofread, kept me going when I had had enough, and pretended to be interested in my lectures whenever I saw a moraine/drumlin/nappe fold on the way to France. Thank you also for the financial help! Stefan, finally, thank you, for your help, love and support throughout three degrees, and the days, weeks, months and years of fieldwork, lab work, and writing.

Table of Contents

Abstract ..... ***iii***
Acknowledgements ..... ***v***
Table of Contents ..... ***i***
List of Tables ..... ***iii***
List of Figures ..... ***v***

Introduction **1**
1.1 British and Fennoscandian Ice-sheet Interactions during the Quaternary 1
1.2 Quaternary Geology of Britain 9
1.3 Quaternary Geology of County Durham 23
1.4 Key Conceptual and Theoretical Frameworks addressed in this Thesis 33

Methodology and Techniques **34**
2.1 Introduction 34
2.2 A Scientific Methodology 35
2.3 Field Techniques 36
2.4 Thin-section analysis 44
2.5 The Interpretation of Glacigenic Sediments 52
2.6 Lithological and Geochemical Techniques 57
2.7 Erratic sources in Britain 76
2.8 Statistical Analysis of the Geochemical Data 92
2.9 Microfossil and Macrofauna Analysis 95
2.10 Dating Techniques 100

Whitburn Bay **105**
3.1 Introduction 105
3.2 Sedimentology, Stratigraphy, and Lithological and Geochemical Data 109
3.3 Lithological, Geochemical and Biological Analysis 124
3.4 Interpretation 130
3.5 Discussion 140
3.6 Conclusions 146

Hawthorn Hive to Blackhall Rocks **148**
4.1 Introduction 148
4.2 Research Aims and Objectives 150
4.3 Facies Architecture: Hawthorn Hive to Blackhall Rocks 153
4.4 Hawthorn Hive 161
4.5 Conclusions 172

The Easington Raised Beach **173**
5.1 Introduction 173
5.2 Sedimentology and Stratigraphy 176
5.3 Geochemical, Lithological, Biological and Chronostratigraphical Analysis 180
5.4 Discussion 195
5.5 Conclusions 200

Warren House Gill **201**
6.1 Introduction 201
6.2 Sedimentology and Stratigraphy 204
6.3 Geochemical, Lithological and Biological Analyses 284
6.4 Chronostratigraphy 306
6.5 Interpretation 310
6.6 Discussion 331

6.7 Conclusions 346

The North Sea Basin 348
7.1 Introduction 348
7.2 North Sea Stratigraphy 353
7.3 Sedimentology and Micromorphology 370
7.4 Lithological, Biological and Geochemical Analyses 393
7.5 Interpretation 414
7.6 Discussion and Conclusions 425
7.7 Conclusions 429

Discussion 430
8.1 Regional onshore / offshore correlations 430
8.2 Implications for British and Fennoscandian Ice Sheet Interactions during the Quaternary 451
8.3 Key findings of this research 465
8.4 Conclusions 469

References 472

Appendix I: Methodologies 494
Micromorphology 494
Lithological and Geochemical Analysis 496
Microfossil Techniques 499
Dating Techniques 500

Appendix II: Publications
On CD.
- Whitburn Bay manuscript (*Boreas*). In Press.
- Heavy Mineral Analysis: Methodologies. In: Bridgland, D.R., In Prep. *Clast Lithological Analysis: Technical Guide 4.* Quaternary Research Association, London. Submitted.
- Easington Raised Beach manuscript (*Proceedings of the Geologists' Association).* In press.

Appendix III: Photographs, Hawthorn Hive to Blackhall Rocks
On CD.

Appendix IV: Raw Data
On CD. All raw data from thesis, including:
- Heavy Mineral, Clast Lithological, Particle Size and Geochemical data
- Palynomorph reports from Jim Riding
- OSL Dating report from Steve Pawley
- Carbonates report from Ian Candy

List of Tables

Chapter 1: Introduction

Table 1.1: Thesis Outline. 7
Table 1.2: Revised stratigraphy of north Norfolk (Lee *et al.*, 2002; Hamblin *et al.*, 2005). 11
Table 1.3: Summary table of British ice streams during the LGM. Abbreviation refers to letters on Figure 1.3. 19
Table 1.4: Stratigraphy of eastern Yorkshire. Adapted from Lewis (1999). 22
Table 1.5: Quaternary stratigraphy in County Durham. From Thomas (1999). 28

Chapter 2: Methodologies

Table 2.1: Glossary of abbreviations used in section logs (Krüger & Kjaer, 1999; Evans & Benn, 2004)....38
Table 2.2: Descriptive clast-roundness categories. From Benn (2007). 40
Table 2.3: Approach for investigation of glacigenic sediments. Adapted from Carr, 2004. 46
Table 2.4: Glossary of common terms used in micromorphology (after van der Meer, 1993; Perkins, 1998; Carr, 2001; Carr, 2004a; Menzies *et al.*, 2006; Hiemstra, 2007). Refer also to Figure 2.3. 46
Table 2.5: Macroscopic and microscopic criteria for interpretation of some typical glacigenic sediments. Refer to Figure 2.4. 56
Table 2.6: The potential history of a heavy-mineral assemblage: an idealised sedimentary cycle (Bateman and Catt, 2007) 63
Table 2.7: Glossary of terms in Heavy-mineral analysis (Gribble and Hall, 1992; Mange and Maurer, 1992). 64
Table 2.8: Provenance zones of some common heavy minerals (Hubert, 1971; Gale & Hoare, 1991). 70
Table 2.9: Relative stability of detrital heavy minerals (Morton & Hallsworth, 2007) 71
Table 2.10: Indices of ultra-stable heavy minerals (Morton *et al.*, 2005). 72
Table 2.11: Divisions of the Carboniferous Period (Jones *et al.*, 1995) 85

Chapter 3: Whitburn Bay

Table 3.1: Summary diagram of Micromorphological analysis. 114
Table 3.2: Average particle size distribution. For detailed PSA, see Appendix IV. 124
Table 3.3: Average Clast lithology results from Whitburn Bay, 8-32 mm. Sandstones are distinguished on their quartz, feldspar and arenite content. For detailed raw counts, refer to Appendix IV 125
Table 3.4: Average Heavy Minerals (percent non-opaques) in glacial deposits at Whitburn Bay (excluding carbonates due to strong skew). Combined results of multiple samples. For raw mineral counts, refer to Appendix IV 126
Table 3.5: Average Heavy Metals results at Whitburn Bay 127
Table 3.6: Comparison of characteristics of Skipsea Member at Dimlington, and Horden Member at Whitburn Bay (Penny & Catt, 1967; Madgett & Catt, 1978; Evans *et al.*, 1995; Catt, 2007) 145

Chapter 4: Hawthorn Hive to Blackhall Rocks

Table 4.1: Particle size distribution, Hawthorn Hive. For detailed raw counts, refer to Appendix IV 164
Table 4.2: Average percentages of clast lithologies at Hawthorn Hive, 8-16, and 16-32 mm. For detailed raw counts, refer to Appendix IV 165
Table 4.3: Average percentages of heavy mineralogies (percentage non-opaques) at Hawthorn Hive, size fractions 63-125 and 125-250 μm. For detailed raw counts, refer to Appendix IV. 166
Table 4.4: Metals analysis of Hawthorn Hive. 167

Chapter 5: The Easington Raised Beach

Table 5.1: Sample locations, Easington Raised Beach 181
Table 5.2: Average particle size distribution of the beach sands and gravels and the diamicton above. 182
Table 5.3: Average percentages of clast lithologies at Shippersea Bay, 8-16, and 16-32 mm. For detailed raw counts, refer to Appendix IV 182
Table 5.4: Geochemical analysis of sediments in Shippersea Bay 183
Table 5.5: Average percentage heavy minerals in sediments in Shippersea Bay. For detailed raw counts, refer to Appendix IV 184
Table 5.6: Foraminifera of LFA 1, the Easington Raised Beach. Courtesy of Dr. William Austin. 185
Table 5.7: Results of OSL dates, Easington Raised Beach, courtesy of Dr. Pawley 188

Table 5.8: Amino acid data on Nucella shells from the Easington Raised Beach. Error terms represent 1 S.D. about the mean for the duplicate analyses for an individual sample. Each sample were bleached (b) with the free amino acid fraction signified by 'F' and the total hydrolysable fraction by 'H*'. Each sample thus has a unique identifier. Results courtesy of Beatrice Demarchi and Kirsty Penkman of the University of York. ..189
Table 5.9: Age of cementation from U-series dating. From Candy (2008); refer to Appendix IV. 194

Chapter 6: Warren House Gill

Table 6.1: Micromorphological summary of thin sections of LFA 1 at Warren House Gill. 216
Table 6.2: Summary of micromorphology of LFA 2, the Beige Silts. 235
Table 6.3: Micromorphological Summary of LFA 3. 246
Table 6.4: Micromorphological Summary of LF 4a. 274
Table 6.5: Average percentage particle size for the different lithofacies associations at Warren House Gill. LFA 4 is separated into the fine-grained sand (LF 4a) and coarse-grained gravel facies (LF 4b). 285
Table 6.6: Particle size distribution for LFA 1 samples. Samples from LF 3a are included for comparison. 285
Table 6.7: Particle size distribution for diamictons (E1 and E3) and sands (E2) at Exposure E, Warren House Gill. 287
Table 6.8: Average percentage clast lithologies at Warren House Gill, 8-16 and 16-32 mm. For detailed raw counts, refer to Appendix IV. 288
Table 6.9: Average percentage (non-opaques) heavy mineralogy at Warren House Gill, 63-125 and 125-250 μm fraction. For detailed raw counts, refer to Appendix IV. 295
Table 6.10: Geochemistry results, high abundance metals, for all samples at Warren House Gill. For detailed raw counts, refer to Appendix IV. 301
Table 6.11: Palynomorphs and dinoflagellate cysts at Warren House Gill (Riding, 2007). 305
Table 6.12: Comparison between the Briton's Lane Formation, the Bridlington Member and the Ash Gill Member. 333
Table 6.13: Comparison of tills at study site 343
Table 6.14: Revised Quaternary Formations of County Durham 345

Chapter 7: The North Sea Basin

Table 7.1: Pleistocene formations of the southern North Sea (Cameron et al., 1992; Gatliffe et al., 1994)...354
Table 7.2: Regional names and approximate correlatives of formations in the North Sea Basin (Andrews et al., 1990; Cameron et al., 1992; Gatliffe et al., 1994; Cameron & Holmes, 1999) 355
Table 7.3: Summary of thin sections from North Sea Boreholes 374
Table 7.4: Description of samples from Bolders Bank Formation 394
Table 7.5: Sub-2 mm particle-size analysis of North Sea Boreholes 395
Table 7.6: Average Percentage Non-Opaque Heavy minerals for formations of the North Sea Basin 397
Table 7.7: North Sea Boreholes matrix Geochemistry. High Abundance metals. 405
Table 7.8: Foraminifera of the North Sea Boreholes 409
Table 7.9: Age-Diagnostic Palynomorphs from the North Sea Basin (Riding, 2008). Non age-diagnostic palynomorphs are not shown 412
Table 7.10: Summary of stratigraphy and formations of the North Sea 427

Chapter 8: Discussion

Table 8.1: Summary of Quaternary Stratigraphy in Co. Durham 450

Appendix I: Methodologies

Table 1: Impregnation of unlithified sediments by David Sales (Murphy, 1986). 494
Table 2: Methodology for preparation of thin sections by David Sales. After Murphy, 1986. 494
Table 3: Methodology for Particle Size analysis. 496
Table 4: Methodology for separation of heavy minerals. 497
Table 5: Methodology by Atomic Absorption by Amanda Hayton. 497
Table 6: Methodology for ICP-MS Total Metals Extraction by Martin West 498
Table 7: Separation of Foraminifera. 499
Table 8: Principle steps in the palynological preparation procedure (Riding and Kyffin-Hughes, 2004) 499
Table 9: Methodology for preparation and analysis of intra-crystalline amino acids (Penkman *et al.*, 2008). Amino Acid Racemisation analysis was conducted by Beatrice Demarchi. 500
Table 10: Methodology for Optically Stimulated Luminescence Dating by Dr. Steve Pawley of RHUL. 501

List of Figures

Chapter 1: Introduction

Figure 1.1: Topographic map of northeastern England, showing location of key sites and places referred to in text....6
Figure 1.2: BRITICE overlain on topographical map of the UK. Adapted from Clark *et al.* (2004a)....16
Figure 1.3: Map of major British ice streams (red arrows) during the LGM....18
Figure 1.4: Buried valleys of County Durham. Modified from Smith and Francis (1967) and Smith (1994). 24
Figure 1.5: Map of striae orientations in northeastern England. Modified from Beaumont (1967)....30
Figure 1.6: Map to show distribution of the Horden Member, moraines, ice-contact slopes, and meltwater channels (after Smith & Francis, 1967)....32

Chapter 2: Methodologies

Figure 2.1: Schematic diagram illustrating (A) Jeffery Rotation and (B) March Rotation. In Jeffery Rotation clasts are continually rotated as a result of vertical velocity gradients, whereas in March Rotation (B), clasts passively trace the deformation of the surrounding medium (from Benn, 2007b)....42
Figure 2.2: Key to symbols used in presentation of thin sections in this thesis. Arrows on turbates do not indicate direction of rotation....46
Figure 2.3: Conceptual diagram illustrating the relationship between plasmic fabric and aligned grains in response to simple shear (A) and the relationship between unidirectional plasmic fabrics, turbates, and skelsepic plasmic fabrics (B). Adapted from Hiemstra and Rijsdijk (2003)....49
Figure 2.4: Microstructures and plasmic fabrics observed from glacigenic sediments in this study. After van der Meer (1993), Menzies (2000), Menzies *et al.* (2006), and Hiemstra and Rijsdijk (2003)....51
Figure 2.5: Flow-charts to aid identification of some common heavy minerals. Numerous sources (Gale & Hoare, 1991; Deer *et al.*, 1992; Mange & Maurer, 1992; MacKenzie & Adams, 2001; Walden, 2004)....69
Figure 2.6: Photographs of hand specimens of some Norwegian indicator erratics (courtesy of Dr. Jon Lee, BGS)....75
Figure 2.7: Simplified geology of northern Britain. Adapted from BGS Digimap database. © NERC....78
Figure 2.8: Geological map of the Lake District, from BGS Digimap database. © NERC. Granites: G_1: Eskdale Granite. G_2: Ennerdale Granophyre. G_3: Threkfeld Microgranite. G_4: Skiddaw Granite. G_5: Shap Granite (Firman, 1978). SLA is the Skiddaw Slate Series....82
Figure 2.9: Geology of northeast England. From BGS Digimap database. © NERC....84
Figure 2.10: The Zechstein and Bakevellia Seas in the Late Permian. Adapted from Smith (1995a)....87
Figure 2.11: Geology of the North Sea. Adapted from Gatliffe *et al.*, (1994) Cameron *et al.*, (1992) and Andrews *et al.* (1990)....90
Figure 2.12: Electron microphotographs of some common benthic calcareous foraminifera. Scale bar is 0.1mm unless otherwise stated (Korsun *et al.*, 2001)....96
Figure 2.13: Identification of critical parts of foraminifera (Bé & Tolderhund, 1971; Vincent & Berger, 1981; Korsun *et al.*, 2001)....97
Figure 2.14: Conceptual model for the effect of bleach on different amino acid fractions in a shell....102

Chapter 3: Whitburn Bay

Figure 3.1: Map to show location of sections investigated at Whitburn Bay....106
Figure 3.2: Facies architecture at Whitburn Bay....110
Figure 3.3 Photograph of Lithofacies Associations 1 and 2 and the boulder pavement in Section 1, Whitburn Bay. The trowel is 20 cm long....111
Figure 3.4: Photograph, photomicrographs, and sketch of thin section Sample 1a-3, taken from the boundary between LFAs 1 and 2 in Section 1....113
Figure 3.5: Photograph of pipe structures in Section 2a....116
Figure 3.6: Photograph of Section 10 with thin section and photomicrographs of Sample 10, taken from the basal diamicton of Section 10. The slide shows characteristic, strongly birefringent plasmic fabric, Type II Pebbles, lineations of clasts, rotational structures and grain stacking, indicative of ductile deformation in a high strain environment....118
Figure 3.7: Vertical profiles of Section 9....119
Figure 3.8: Photomicrograph of deformed bedding in thin section sample 9a-5, demonstrating strong masepic plasmic fabric development, which is highlighted on the sketch....120
Figure 3.9: Microfaults and water escape structures relating to overfolding in Section 2b....121
Figure 3.10: Photographs of Section 5....123

Figure 3.11: Principle Component Analysis and ternary diagram of heavy-mineral analysis, clast lithological analysis, and metals analysis. 129
Figure 3.12: Cartoon depicting formation of the boulder pavement and hydrofracture at Whitburn Bay. Ice overburden pressure is denoted by *P*. 132
Figure 3.13: Land-system development at Whitburn Bay. 141
Figure 3.14: Map showing inferred ice flow directions, overlain onto the BRITICE data set for the northeast region (Clark *et al.* 2004). Ice flow around the Tweed area from Raistrick (1931). 143

Chapter 4: Hawthorn Hive to Blackhall Rocks

Figure 4.1: Map of eastern County Durham, showing the location of Shippersea Bay. Sites investigated in greater detail in this thesis are highlighted (in bold). National Grid (NZ) lines are shown. 149
Figure 4.2: Facies Architecture: Hawthorn Hive to Blackhall Rocks 154
Figure 4.3: Facies Architecture: Hawthorn Hive to Foxholes Dene. Refer to Appendix III for larger photographs. 156
Figure 4.4: Facies Architecture: Foxholes Dene to Castle Eden Dene. Refer to Appendix III for larger photographs. 157
Figure 4.5: Castle Eden Dene to Blackhall Rocks. Refer to Appendix III for larger photographs. 158
Figure 4.6: Vertical profiles, Hawthorn Hive to Blackhall Rocks. 159
Figure 4.7: Section log, Hawthorn Hive. Lower clast fabric (LFA 1): $S_1 = 0.539$; $S_2 = 0.369$; $S_3 = 0.093$. Upper clast fabric (of LF 2a, gravels): $S_1 = 0.548$; $S_2 = 0.106$; $S_3 = 0.034$. 162
Figure 4.8: Photograph and detail of Hawthorn Hive. 163

Chapter 5: The Easington Raised Beach

Figure 5.1: Simplified stratigraphy of coastal glacigenic sediments in County Durham. Modified from Bridgland and Austin (1999). 174
Figure 5.2: Photograph of the Easington Raised Beach, Shippersea Bay, Grid Reference: NZ 44318; 45301. 176
Figure 5.3: Sedimentary logs of Sections A and B, showing LFAs 1 to 3, Shippersea Bay 178
Figure 5.4: Photographs of the Easington Raised Beach, Section B. 179
Figure 5.5: Pie charts of average clast-lithological analysis and bar charts of geochemical analysis, Shippersea Bay. 183
Figure 5.6: Location of samples EAS 04 and EAS 05. LF 2a, Section A, Easington Raised Beach. 187
Figure 5.7: Comparison of OSL ages with the marine isotope record derived from the ODP677 site (Shackleton et al., 1990). Image courtesy of Dr. Pawley. 188
Figure 5.8: D/L values of Asx, Ala, Vak and [Ser]/[Ala] for the free (FAA) and Total Hydrolysable Amino Acid (THAA) fractions of the bleached Nucella lapillus shells from the Easington Raised Beach, compared with shells from the Cromerian type site (West Runton), and Crag deposits of Early Pleistocene age (from Sidestrand and Bramerton). 190
Figure 5.9: Photomicrographs of the microstructure of the Easington beach cement. 192
Figure 5.10: Comparison of the stable oxygen and carbon isotopic composition of the Easington Raised Beach with groundwater and tufa sediments from British interglacials (MIS 7 and MIS 11). From Candy (2008). 193

Chapter 6: Warren House Gill

Figure 6.1: Map showing location of trial pits (letters A to I) and exposures (letters J and K) at Warren House Gill. 206
Figure 6.2: Simplified composite stratigraphy, Warren House Gill 207
Figure 6.3: Vertical profiles of exposures at Warren House Gill, showing lithostratigraphy and location of samples. Figure 6.1 shows the location of the exposures. 208
Figure 6.4: Vertical Profile of Exposure G, Warren House Gill, showing location of bulk (red writing) and thin section (blue writing) sampling points. Lower clast fabric (LF 1b; $S_1 = 0.517$; $S_2 = 0.337$; $S_3 = 0.147$). Upper clast fabric (LF 3a; $S_1 = 0.572$; $S_2 = 0.269$; $S_3 = 0.091$). 210
Figure 6.5: Sketch of LF 1a to LF 4a at Exposure G, Warren House Gill. 211
Figure 6.6: Photograph A. Exposure G, Warren House Gill. Photograph B: LF 1b, showing tectonised laminations. Pickaxe is 90 cm long. Photograph C: Detail of LF 1b. 212
Figure 6.7: Vertical Profile of Exposure F at Warren House Gill, showing location of bulk (red writing) and thin section (blue writing) sampling points. The clast fabric S vales are: $S_1 = 0.572$; $S_2 = 0.334$; $S_3 = 0.093$. 50 measurements were made. 213

Figure 6.8: Detailed sketch of Exposure E2, with photograph of LF 1c, the tectonised contact between LFAs 1 and 2. LFA 1 and LFA 2 are folded together. Clast fabric from LF 3a ($S_1 = 0.557$; $S_2 = 0.31$; $S_3 = 0.134$). 214
Figure 6.9: Photograph of thin section sample WHG TS F1. Box A (Figure 6.10) shows shears. Box B shows a crushed grain in detail. Grain lineations that are sub-resolution of the image and masepic plasmic fabric have been highlighted to show their orientation and position. 217
Figure 6.10: Photomicrographs, WHG TS F1, from LFA 1 Exposure F at Warren House Gill. 218
Figure 6.11: Scans of thin section sample WHG TS G 0 m, LF 1a. Boxes show location and context of photomicrographs in Figure 6.12. Location of sub-resolution features is annotated on the scan. 220
Figure 6.12: Photomicrographs, Thin section WHG TS G 0m. Locations are shown in Figure 6.11. 222
Figure 6.13: Warren House Gill thin section sample WHG TS G 1.9m. LF 1a, the Basal Shelly Diamicton. There is a large man-made vugh void in the centre of the slide (laboratory induced, due to poor impregnation). Location of masepic plasmic fabric and orientation and location of grain lineations are annotated onto the scan. 224
Figure 6.14: Photomicrographs of WHG S G 1.9 m, LFA 1, Warren House Gill. 225
Figure 6.15: Detailed Sketch of Exposure B, LF 2a and LF 3a. Clast fabric (LF 3a): $S_1 = 0.574$; $S_2 = 0.363$; $S_3 = 0.063$. 227
Figure 6.16: Photograph of LF 2a and LF 3a, Exposure B. LF 2a lies on bedrock, and is overlain by a diamict facies with some bedding, which pinches out on the northern side of the section (LF 3a). This is overlain by a clast-rich diamicton (LF 3a), which contains well-bedded sands which are recumbently folded (LF 3c). 228
Figure 6.17: Detailed photographs of LF 2a, Exposure B. Photograph A shows deformed sand laminae. Photograph B shows deformed black inclusions. Photograph C details the nature of the contact with the soft, dolomised bedrock. Knife is 19 cm long when extended, and the blade only is 8 cm long. 229
Figure 6.18: Detailed sketch of LF 2 at Exposure C, Warren House Gill, showing bulk (WHG C2; red cross) and OSL sampling locations (green cross). Numbers denote carbonate nodules in LF 2a. For vertical profile, refer to Figure 5.12. *Y*-axis shows height above bedrock (proved by coring but not observed in section to sketch). 230
Figure 6.19: Detailed Sketch of LF 2a and LF 2b (silts) and LF 3a (Diamicton) and LF 3c (sands and gravels) in Exposure D, Warren House Gill. Green crosses show OSL sampling locations. Lower clast macro-fabric (LF 3a): $S_1 = 0.531$; $S_2 = 0.356$; $S_3 = 0.112$. Upper clast macro-fabric (LF 3a): $S_1 = 0.577$; $S_2 = 0.32$; $S_3 = 0.103$ 232
Figure 6.20: Photographs and detail of LFA 2, Exposure D, Warren House Gill. 233
Figure 6.21: Location of thin section samples and OSL samples at Exposure D, Warren House Gill. Geological hammer is 32 cm long. Penknife is 19 cm long when extended. 234
Figure 6.22: Photograph of Thin Section sample WHG TS D*i*. The matrix material is deformed and intermixed, exhibiting ductile deformation. 236
Figure 6.23: Scan of WHG TS D*ii*, taken from LF 2a in Exposure D. LF 2a, height 1.65 m. Location of plasmic fabric development is noted. 238
Figure 6.24: Sketch and photographs of LF 3a, Exposure A, Warren House Gill. Clast Fabric: $S_1 = 0.478$; $S_2 = 0.402$; $S_3 = 0.120$ 240
Figure 6.25: Vertical profile of Exposure C, Warren House Gill, showing sample locations. 242
Figure 6.26: Vertical profile of Exposure E1. Clast macro-fabric values: Lower clast fabric (LF 3a); $S_1 = 0.600$, $S_2 = 0.312$, $S_3 = 0.154$. Upper clast macro-fabric (LF 3a): $S_1 = 0.558$; $S_2 = 0.327$; $S_3 = 0.114$ 243
Figure 6.27: Clast macro-fabric data from Warren House Gill 244
Figure 6.28: Thin section slide from WHG TS D*iv*, taken from LF 3a, Exposure D, 2.4 m. Locations of features which are sub-resolution of the scan are highlighted, such as grain stacks, strong plasmic fabric development and grain lineations. S - Sandstone. Q – Quartz grain. 247
Figure 6.29: Photomicrographs of WHG TS D*iv*, showing rotational structures and augen-shaped, rotated intraclasts. 248
Figure 6.30: Thin Section sample WHG TS C5, LF 3a, taken directly above laminations in Exposure C, Warren House Gill. Location of sub-resolution features is annotated on diagram. 249
Figure 6.31: Photomicrographs of WHG TS C5, showing edge-to-edge grain contacts, plasmic fabrics, and marine microfossils. 250
Figure 6.32: Thin section slide WHG TS E1, from LF 3a, Exposure E1, above sand fold. Location of sub-resolution features is annotated on slide. 252
Figure 6.33: Photomicrographs, WHG TS E1 253
Figure 6.34: Sketch of Exposure D2, LF 3b, Warren House Gill, showing contact between LFA 2 and LF 3b. 254
Figure 6.35: Photographs of Exposure D2, showing location of thin section sample WHG Ex D2 within the interbedded diamicton and red sands/silts (Photograph C). LF 3a shows pinching and swelling interbedded

sand, gravel and diamicton (Photograph B). LF 3b exhibits interbedded diamicton and sand, with stringer formation into LF 3a above. Geological hammer for scale is 32 cm long. 255
Figure 6.36: Thin section sampled from interfingering LFA 3 and 2 at Exposure D2, Warren House Gill. Location of strong plasmic fabric development is shown. S – Sandstone. Q – Quartz grain. 257
Figure 6.37: Photomicrographs of thin section WHG Ex D2, showing plasmic fabric, rotational structures, and bedding. 258
Figure 6.38: Photographs of tectonised sand lenses of LF 3c interbedded with LF 3a (the Middle Diamicton). LF 3c of Exposure B contains recumbently folded beds of coarse sand and well-sorted fine gravel. Exposure D contains poorly-sorted, coarse gravelly sand which pinches and swells. LF 3c of Exposure C contains a large recumbently folded bed of coarse, poorly-sorted sand and gravel. Spade is 1 m long. 259
Figure 6.39: Detailed sketch of sand fold in Exposure E1, Warren House Gill. Green crosses represent OSL samples. 261
Figure 6.40: Photographs of Exposure E1, Warren House Gill, showing location of thin section sample WHG TS E1. Detail of faulted beds in sand fold are shown (Penknife for scale is 19 cm long when extended). Contact between LFA 2 and 3 is shown. LF 2a can be seen as the pink-beige silts in the bottom-right picture. 262
Figure 6.41: Photographs and detail of LF 3f and LF 4a, Exposure C. Spade is 1 m long. Knife is 19 cm long when extended. 263
Figure 6.42: Photograph of thin section WHG TS C4, Warren House Gill. Taken from LF 3f, the Laminated Diamicton. Location of plasmic fabric development and other sub-resolution features is annotated on the scan. 265
Figure 6.43: Photomicrographs of WHG TS C4. Refer to Figure 6.36 for location of images. 267
Figure 6.44: Warren House Gill Exposure H. LFAs 1, 3, 4a and 5 are exposed in this vertical profile. 269
Figure 6.45: Photographs of Exposure H, LF 1a, LF 3a, LF 4a and LFA 5. Spade for scale is 1 m long. 270
Figure 6.46: Photo-mosaic of LF 4a: LF 4a, Exposure H. The clay is clearly visible at the base of the exposure, grading into well-sorted sands. 271
Figure 6.47: Detailed sketch of LF 4a; Exposure H, Warren House Gill. 272
Figure 6.48: Thin section sample WHG TS Ha. Locations of sub-resolution features are noted. 275
Figure 6.49: Photomicrographs of WHG TS Ha (LF 4a), showing detail of contacts, soft sediment deformation, and fluidised diamicton. 277
Figure 6.50: Thin Section sample WHG TS Hb (LF 4a). Locations of sub-resolution features are highlighted. 279
Figure 6.51: Photomicrographs of WHG T Hb, showing soft sediment deformation, water escape, and rotation and pelletisation of silt bed. 280
Figure 6.52: Detailed vertical profile of LF 4b, Exposure K, Warren House Gill, showing bulk samples (red) and OSL samples (green). 282
Figure 6.53: Particle-size distribution ternary diagram. 285
Figure 6.54: Differential Cumulative chart of particle-size analysis for LFA 1 286
Figure 6.55: Composition of gravel lithologies (percentage) in samples from Hawthorn Hive to Blackhall Rocks 289
Figure 6.56: Triplot showing variations in clast lithologies from Hawthorn Hive to Blackhall Rocks. LFA 1 at Hawthorn Hive (HAW 02) contains far higher percentages of limestone, while LFA 3 at Hawthorn Hive (HAW 03) contains less Permian material. 290
Figure 6.57: Near, Far, Durable and Non-Durable lithologies at Warren House Gill. 291
Figure 6.58: Cluster Dendrogram for Clast Lithological Analysis. Three principal groups are clearly distinguished; LFA 1, the Easington Raised Beach, and LFAs 3, 4 and 5. 292
Figure 6.59: Annotated PCA Correlation on Clast Lithological Data. Divisions are drawn on by eye to emphasise distinction. 293
Figure 6.60: Compound bar chart showing proportions of heavy mineral species. LFA 1 contains higher percentages of hypersthene and hornblende. LFA 3 (WHG E1 to WHG G4) contains more kyanite, micas, and less sphene. 296
Figure 6.61: Graphical representation of ratios of ultra-stable heavy minerals. Annotations are drawn on by hand to emphasise distinction. ATi: Apatite-Tourmaline index. MZi: Monazite-Zircon index. GZi: Garnet-Zircon index. RuZi: Rutile-Zircon Index. See Chapter 2, Section 2.5.4. 297
Figure 6.62: Ternary diagram and PCA plots of heavy mineral suites of lithofacies of Warren House Gill. 299
Figure 6.63: Dendrogram showing clustering of samples. 300
Figure 6.64: Cluster dendrogram, common metals analysis. 301
Figure 6.65: Annotated Principle Components Analysis (Covariance) of Common Metals 302
Figure 6.66: Percentages of foraminifera in LFA 1 and LFA 3 304

Figure 6.67: AAR from Hiatella shells from LFA 1, Warren House Gill, compared to Bithynia and Valvata. The Species Effect creates a different diagenesis of different acids in different shells, making the AAR ages inconclusive, but suggestive of the Middle Pleistocene. > Crom is before the Cromerian. 307
Figure 6.68: Cartoon displaying the four zones of glaciomarine sedimentation in tidewater glaciers. Modified from Hart and Roberts (1994). The principle foraminiferal assemblages are denoted by their likely dominant species. 313
Figure 6.69: Clast macro-fabric May (A) and Benn (B) Diagrams. 323
Figure 6.70: Uplift diagram for LFA 1 and the Easington Raised Beach. 335

Chapter 7: The North Sea Basin

Figure 7.1: Location of significant BGS Boreholes and thickness of Quaternary sediments (Cameron *et al.*, 1992; Gatliffe *et al.*, 1994). 349
Figure 7.2: Bathymetry of the North Sea (Cameron et al., 1992; Gatliffe et al., 1994). 350
Figure 7.3: Map of Pleistocene Sediments in the North Sea (Andrews et al., 1990; Cameron et al., 1992; Gatliffe et al., 1994). The Aberdeen Ground Fm does not crop-out at sea bed. Refer to the cross-section in Figure 7.4. 357
Figure 7.4: West-East cross-section to illustrate Quaternary formations in the northern North Sea. Figure 7.3 shows location of section AB. From Andrews et al., (1990) 358
Figure 7.5: Correlation of Boreholes 81/26, 81/29 and 81/34. 359
Figure 7.6: The Weichselian in the NSB (from Carr et al., 2006) 361
Figure 7.7: From Graham *et al.* (2007). Reconstruction of ice sheet limits for MIS 2 with location of fast flowing ice streams (solid arrows) for other independent evidence. The youngest Witch Ground Fm MSGLs are identified in the boxed area. One reconstruction for the Witch Ground Ice Stream as a divergent flow from the Norwegian Channel Ice Stream is shown. UK offshore moraines indicated by black lines. MF is Moray Firth ice stream (Merritt *et al.*, 2003). S is the Strathmore Ice Stream (Golledge & Stoker, 2006). Norwegian Channel Ice Stream from Ottesen *et al.* (2005). 364
Figure 7.8: From Bradwell *et al.* (2008), mapped from the Olex dataset. Solid lines are ridges (moraines). Dashed lines are negative linear features (channels and tunnel valleys). 365
Figure 7.9: Correlation of borehole logs. From Gatliffe et al. (1994). 369
Figure 7.10: BH 81/52a from BGS Log. Formations after Cameron et al., (1992) and Scourse et al., (1998). 371
Figure 7.11: BGS BH 81/45 and BH 81/46a, using additional information from Balson and Jeffery (1991). 372
Figure 7.12: Thin section of the Swarte Bank Fm. Locations and orientations of grain lineations are highlighted. 375
Figure 7.13: Thin Section BH 81/52a 40.5 m. Location of sub-resolution features is highlighted on the figure. 378
Figure 7.14: Thin Section of the Sand Hole Fm. Location of plasmic fabric development is highlighted. 379
Figure 7.15: Photomicrographs of thin section sample 81/52a 29.87 m. 380
Figure 7.16: BGS Borehole 81/29 from BGS logs. Interpretations after Sejrup and Knudsen (1993) 381
Figure 7.17: BH 81/34 from BGS core logs. Interpretations after Stoker et al. (1985) and Sejrup and Knudsen (1993). 382
Figure 7.18: Thin Section of the Fisher Fm (BH 81/34 18.4m). Location of sub-resolution features is noted. 384
Figure 7.19: BH 81/26 from BGS core logs (interpretations after Sejrup et al., 1987; Sejrup & Knudsen, 1993; Graham et al., 2007). 385
Figure 7.20: Thin Section slide BH 81/26 65.4 m. Location of sub-resolution features is highlighted. 387
Figure 7.21: The Bolders Bank Fm. From BGS core logs, Cameron and Holmes (1999), Cameron et al. (1992), and Gatliffe et al. (1994) 388
Figure 7.22: Thin Section of the Bolders Bank Fm (81/48 8.9 m). Locations of sub-resolution features are highlighted. 390
Figure 7.23: Photomicrographs of Thin Section BH 81/48 8.9 m 392
Figure 7.24: Particle-size distribution of North Sea Boreholes. 395
Figure 7.25: Results of heavy-mineral analysis for various North Sea Boreholes 398
Figure 7.26: Ternary plots of percentages of pyroxenes, phosphates and amphiboles, and for epidote group, amphiboles and pyroxenes, illustrating the tight clustering of the samples. 400
Figure 7.27: Indices of ultra-stable heavy minerals 401
Figure 7.28: Heavy-Mineral Principle Components Analysis and Cluster Analysis 403
Figure 7.29: Ternary plot of three abundant metals (potassium, aluminium and magnesium) in the North Sea samples. 406

Figure 7.30: Common metals Principle Components Analysis and Cluster Analysis....407
Figure 7.31: Foraminifera of the North Sea Boreholes....410

Chapter 8: Discussion

Figure 8.1: Dimlington Stadial ice limits proposed by BRITICE Map (From Clark et al., 2004a; Evans et al., 2005) and from the Olex dataset by Bradwell et al. (2008), over a topographical model. Red lines are ice margins. Blue areas are moraines; green areas are ice-dammed lakes, purple areas are erratic sources....435
Figure 8.2: Clast-Lithological Data from this study. The Horden Member consistently has less Limestone and more Igneous material than the Blackhall Member....437
Figure 8.3: Ternary charts of clast-lithological analysis....438
Figure 8.4: PCA Covariance on all clast lithological data....439
Figure 8.5: Cluster Dendrogram (Ward's Linkage) for all clast lithological data....440
Figure 8.6: Heavy-Mineral Indices. Circles are drawn on to highlight groups....441
Figure 8.7: Annotated ternary charts of heavy-mineral analysis....442
Figure 8.8: Annotated PCA Correlation on the heavy-mineral data. The first three components are shown.443
Figure 8.9: Cluster analysis (Ward's Linkage) for all heavy-mineral data....445
Figure 8.10: PCA Correlation, Common Metals Analysis....447
Figure 8.11: Cluster Dendrogram for abundant metals. Four groups are clearly distinguished, but they comprise a combination of lithofacies....448
Figure 8.12: Pleistocene ice limits in northwest Europe and tunnel valleys in the North Sea Basin. From Kristensen et al., (2007)....453
Figure 8.13: Saalian ice sheet limits in Europe. From Svendsen et al., (2004)....455
Figure 8.14: Extent of the European ice sheet at 20 cal. ka BP. From Svendsen et al., (2004)....459
Figure 8.15: Weichselian glaciations of the Britain and the North Sea. Flow lines adapted from Carr *et al.* (2006), Roberts *et al.* (2007), Graham *et al.* (2007), Golledge and Stoker (2006), and Livingstone *et al.* (in press); moraines and ice limits from Bradwell *et al.* (2008), Evans *et al.* (2005), Clark *et al.* (2004a). The Blackhall Member was deposited during the earlier MIS 4, and the Horden Member during the later readvance of the North Sea Lobe at the LGM (~22 ka BP). Original flowlines are highlighted in orange....462

Appendix I: Methodologies

Figure 1: Diagram illustrating set-up required for density separation of heavy minerals....497

CHAPTER 1

Introduction

1.1 British and Fennoscandian Ice-sheet Interactions during the Quaternary

1.1.1 Introduction and Rationale

A Climate Change Paradigm

Understanding dynamic cryosphere-ocean-atmosphere interactions throughout the Quaternary is essential to our ability to understand and interpret contemporary climatic variability and predict future climatic trends. The ability to constrain long-term ice sheet responses to cryosphere-ocean-atmosphere changes during the Quaternary is of critical importance in understanding contemporary and possible future climatic change (Elias, 2007). The British Isles are ideally located to identify these responses, as they are directly influenced by changes in the Polar Front and the Gulf Stream; oceanic current fluctuations have resulted in extreme climatic fluctuations here throughout the Quaternary. Placing Twentieth and Twenty-First Century climate change within the context of long-term climate fluctuations provides a context within which to identify unusual trends (Elias, 2007). In addition, constraining the western extent and dynamics of the Fennoscandian Ice Sheet throughout the Quaternary are important, as this was one of the largest ice sheets in the world. Constraining the size and volume of this ice sheet is important for constraining its contribution to sea level change during the Devensian. Accurate estimations of sea level rise and dynamic reactions to climatic change will enable a better understanding of cryosphere-ocean-atmosphere interactions, and allow better prediction of large ice-sheet responses to climatic change.

Reconstructions of past areal extents of ice sheets are important, because the volume of ice strongly influences global sea level and patterns of oceanic and atmospheric circulation. Reconstructing former ice sheets on the northwest European margin provides a means to understand this crucial region and past ice-ocean-atmosphere interactions. In addition, providing sound geological data and accurate reconstructions of the previous and

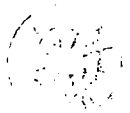

dynamic configurations of the last British-Irish Ice Sheet allows independent testing and training of ice sheet models.

The eastern section of the last British-Irish Ice Sheet during the Last Glacial Maximum was characterised by zones of rapid dynamic flow, with ice streams controlling local ice flow velocities and regional ice drawdown. Such ice flow pathways are important not only from a dynamic perspective, but also in overall influence on ice sheet behaviour and ice / ocean / climate interactions through time. However, to date, many ice-flow pathways have only been partly reconstructed, or remain hypothetical. Thus, the behaviour of the eastern margin of past British ice sheets and of the western margin of past Fennoscandian ice sheets throughout the Quaternary has remained poorly understood. This project will investigate the history of this interaction.

Understanding the role of Scandinavian ice in the North Sea during the Devensian, constraining a North Sea Lobe surging down the eastern coast of England, is therefore important for reconstructing the LGM ice sheet in Britain. The limits of the Devensian ice sheet in Britain are currently poorly constrained, and the role of a North Sea Lobe and of Scandinavian ice in the Quaternary glaciation of the North Sea is poorly understood. This lithostratigraphic investigation will lead to a better understanding of the complex dynamics of the eastern British-Irish Ice Sheet (BIIS) throughout the Quaternary.

In this thesis, the LGM is defined as the period of maximum ice sheet growth, with ice extending to the continental shelf. This occurred during MIS 29-22 cal. ka, peaking at 26 cal. ka BP. The Dimlington Stadial occurred around 22 cal. ka BP. All ages reported in this thesis are calibrated to calendar years BP using the CALIB Intcal 04 curve for terrestrial ages and the Marine 04 curve for marine shells (Stuiver & Reimer, 1993; Stuiver *et al.*, 2009).

Quaternary stratigraphical issues

Recent research in Norfolk has questioned the timing and frequency of Middle Pleistocene glaciations in Britain. In addition, the occurrence of Scandinavian ice at different times during the Middle Pleistocene has recently been questioned (Lee *et al.*, 2002; Lee *et al.*, 2004; Pawley *et al.*, 2004; Hamblin *et al.*, 2005; Gibbard *et al.*, 2008; Lee *et al.*, 2008; Pawley *et al.*, 2008). Under the recently proposed model, the FIS reached the British coastline only during MIS 6. This model details a multiple BIIS event stratigraphy stretching back to MIS 16, but is yet to be validated elsewhere in the UK. One of the major

obstacles to the validation of this model is the occurrence of the 'Scandinavian Drift' at Warren House Gill in County Durham (Trechmann, 1915, 1931b, 1952), as this is indirectly overlain by a raised beach dated to MIS 7 (Bowen *et al.*, 1991; Lunn, 1995). The Scandinavian Drift, or the 'Warren House Formation' (Thomas, 1999) survives in a buried valley of Warren House Gill (Francis, 1972), and is overlain by the 'Main Cheviot Drift' (Trechmann, 1952), with two tills attributed to the last glaciation. These tills were renamed the Blackhall and Horden tills by Francis (1972) and attributed to a two-stage LGM. They were renamed the Blackhall and Horden members by Thomas (1999). Until recently, these tills were inaccessible and covered by mining waste. However, recent work to clean the beaches (the 'Turning the Tides' programme) has led to erosion of mining waste and the re-exposure of the sediments (Bridgland, 1999).

During the Late Devensian, northeastern England was an area of competing ice lobes. Two ice-lobes sourced from northwest England and Scotland (depositing the Blackhall and Horden Members respectively) overran the area (Smith & Francis, 1967; Lunn, 1995). The recession of the first ice lobe prior to the advance of the second led to the development of large proglacial lakes (Smith, 1994). The second ice lobe, the North Sea Lobe, deposited the Horden Member during the Dimlington Stadial (Francis, 1972; Lunn, 1995). However, a Late Devensian North Sea Lobe surging down eastern England (Boulton *et al.*, 1977; Eyles *et al.*, 1994) is difficult to imagine without contact between the BIIS and the FIS in the North Sea. Recent research on the Devensian in the North Sea Basin has argued for a three-stage Devensian model, with no contact between the British and Fennoscandian ice sheets during the Dimlington Stadial (Sejrup *et al.*, 1994; Sejrup *et al.*, 2005; Carr *et al.*, 2006; Bradwell *et al.*, 2008). Without the FIS confining and redirecting the North Sea Lobe, the cause of the sharp southwards turn of the Tweed ice stream (Everest *et al.*, 2005) and the onshore flow direction of the North Sea Lobe remains unclear (Lunn, 1995; Catt, 2007). The dynamics of the last BIIS in eastern England are therefore poorly understood.

The North Sea Basin (NSB) is a deep sediment sink that contains vast thicknesses of Quaternary glacigenic sediments. However, the stratigraphy of these sediments remains uncertain (Carr *et al.*, 2000), and there have been few recent attempts to robustly interpret the age, genesis and provenance of these tills. Onshore-offshore correlations remain tentative (Catt, 1991a), and the offshore seismostratigraphic stratigraphy is hard to relate to the onshore lithostratigraphic stratigraphy (Gatliffe *et al.*, 1994).

Therefore, the flow phasing and dynamic interaction of the BIIS and FIS in eastern England during the Devensian has only been partly reconstructed. There has been little quantitative description of these tills, and no detailed analysis of their provenance, depositional processes, or type and style of deformation, leading to a limited understanding of Late Devensian ice-sheet dynamics and processes. Onshore-offshore correlations have not been quantitatively tested, and therefore wider regional ice-sheet dynamics are poorly understood. The northeastern coast of England, a focus of these ice lobes, is therefore critically located to examine Devensian interlobate ice-sheet history.

Correlation of the tills in County Durham to other glacigenic sediments in eastern England and the North Sea, in particular the Basement, Withernsea and Skipsea Members in northeast Yorkshire (Catt & Penny, 1966) and the Bolders Bank and Wee Bankie Formation offshore, is vital for understanding the behaviour and previous configurations of the last BIIS. The coastal sections in northeastern England potentially provide a wealth of information about Devensian and Quaternary ice-sheet dynamics, but they remain poorly studied. Little new data has been published since the work of researchers in the early Twentieth Century, and access has been difficult due to the dumping of colliery waste on beaches. This research therefore investigates a number of key sites along the eastern English coastline and in the North Sea. They include Whitburn Bay, Warren House Gill and Shippersea Bay. Warren House Gill has previously provided evidence of multiple glaciations and of Scandinavian ice impinging on eastern England, and is potentially the furthest north such exposure (Catt, 2007). In addition, it is ideally located to capture the signal of the Blackhall and Horden ice lobes. Whitburn Bay is situated in the region of coalescence of these competing ice lobes and at the head of Glacial Lake Wear, making it crucial for understanding ice-sheet flow dynamics and flow phasing at the Last Glacial Maximum (LGM). It is located immediately to the east of the Tyne Gap, and therefore should be the most northerly site to record evidence of this cross-Pennine ice lobe. Figure 1.1 shows the location of key sites referred to in this thesis.

1.1.2 Research Aims and Objectives

This thesis assesses the lithostratigraphy of Quaternary sediments exposed in coastal sections in County Durham and recovered from boreholes in the North Sea. The overall scientific aim of this thesis is to understand the dynamics, chronology, and interaction of different ice lobes and ice sheets within eastern England and the North Sea during the

Quaternary; essentially, the interaction between the BIIS and the FIS during the Quaternary. There are four main subsidiary objectives to this aim:

- To understand the depositional environments of glacigenic and interglacial sediments at Warren House Gill, Whitburn Bay, and in the North Sea;
- To develop a chronostratigraphical framework for the Quaternary sediments along the coast;
- To trace the provenance of these sediments in order to establish ice-flow pathways and flow phasing;
- To understand the interaction and dynamism of the BIIS and FIS during the Quaternary, including:
    - Understanding the spatially and temporally changing role of the North Sea Lobe flowing down the coast of eastern England;
    - Testing established regional correlations to the Basement, Skipsea and Withernsea Members.

This research will focus on the process history, provenance, age, and stratigraphic correlations of the glacial sediments, using lithostratigraphic, chronostratigraphic and biostratigraphic data into order to investigate the glacial sequence in northeast England and the North Sea. Ultimately, through the construction of a stratigraphic framework and provenance testing, this research will enable the development of a glacial/interglacial model of ice sheet development throughout the Middle and Late Pleistocene.

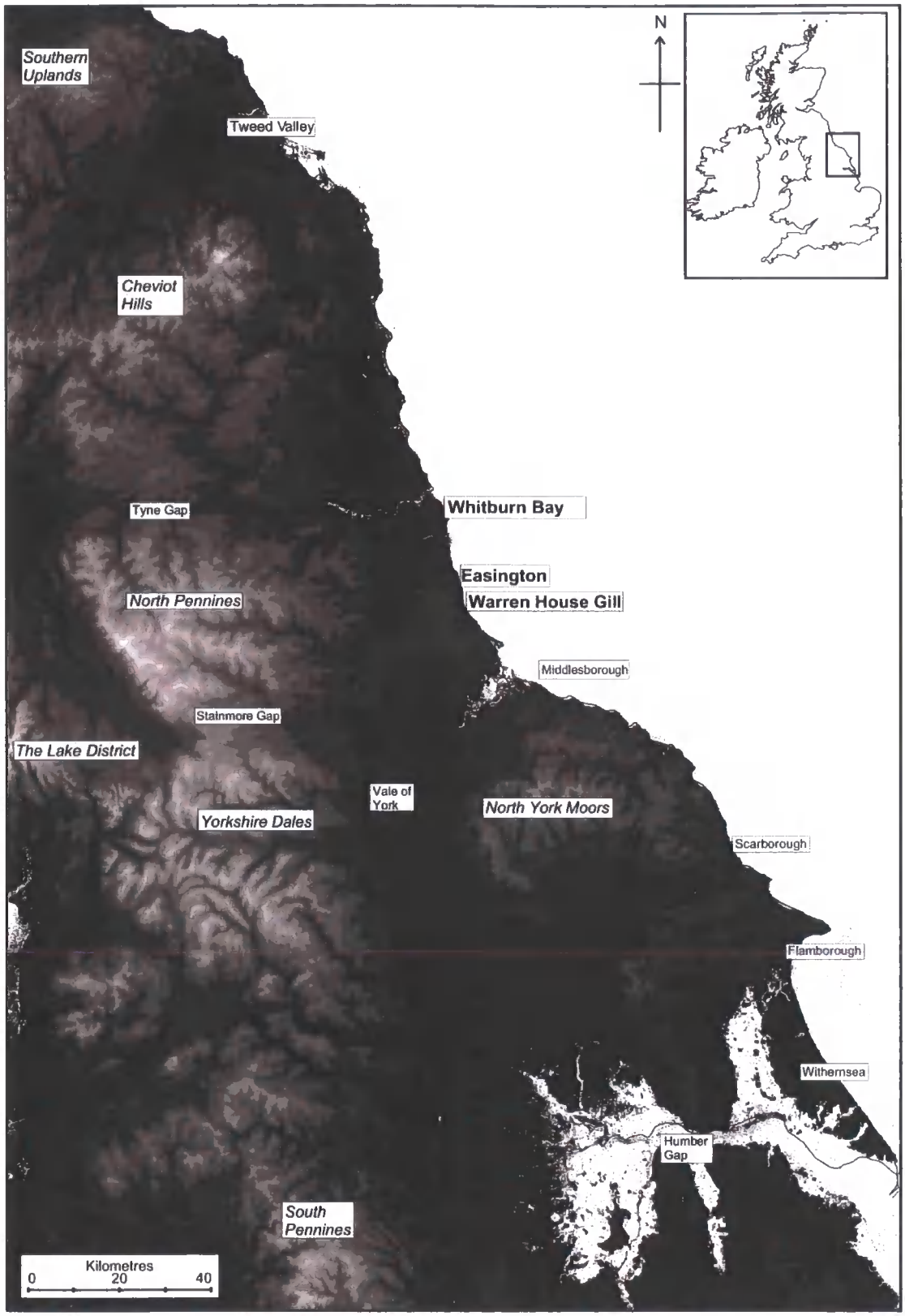

Figure 1.1: Topographic map of northeastern England, showing location of key sites and places referred to in text.

1.1.3 Scope of this thesis

This thesis therefore reports and interprets work from five localities: Whitburn Bay, Hawthorn Hive, Shippersea Bay, and Warren House Gill (and the sediments between), and from several boreholes from the North Sea Basin. Whitburn Bay contains excellent exposures of the Blackhall and Horden members, which are Devensian tills derived from the Lake District and the Southern Uplands respectively (Francis, 1972; Thomas, 1999). The 8 km from Hawthorn Hive to Blackhall Rocks show excellent exposures of these two tills. Here, the Peterlee Sands and Gravels separate them. In Shippersea Bay an interglacial beach, the Easington Raised Beach, is exposed. At Warren House Gill, the Scandinavian Warren House Formation is exposed (Thomas, 1999). The work in the North Sea focuses on the boreholes and formations nearest to northeastern England. This study therefore focused on the Bolders Bank Formation (Fm), the Coal Pit Fm, the Fisher Fm, the Swarte Bank Fm, and the interglacial Egmond Ground and Sand Hole formations.

Below is a summary of the eight chapters in the thesis (Table 1.1). This chapter outlines the key conceptual frameworks and the climatological paradigm in which this research is situated. It then contains a brief summary of the Quaternary in Britain and a more detailed analysis of Quaternary sediments in northern England. The Methodology chapter identifies and describes key field and laboratory techniques, and includes a discussion on erratic sources in the British Isles. Chapters 3 to 7 present results, data and interpretations from each of the key sites. The Discussion chapter attempts to draw all the evidence together, and to provide a synthesis and coherent theory for Quaternary stratigraphy in northern England.

Table 1.1: Thesis Outline.

Chapter 1	**Introduction** Introduces the key research themes. Research aims and objectives. Summary of Quaternary geology of Britain.
Chapter 2	**Methodology** Key field and laboratory methodological techniques, including examples, rationale for their use, and limitations. Interpreting glacigenic processes. Erratic sources in Britain.
Chapter 3	**Whitburn Bay** The first field locality, where complex Devensian glacial sediments are exposed.
Chapter 4	**Hawthorn Hive to Blackhall Rocks** Introduction to the area

	Facies architecture of the 8 km of Devensian and Quaternary sediments which are exposed. Detailed descriptions of Hawthorn Hive.
Chapter 5	**The Easington Raised Beach** Describes, interprets and dates the Easington Raised Beach.
Chapter 6	**Warren House Gill** Detailed lithostratigraphic and provenance analysis of glacigenic sediments at Warren House Gill. Site of the Warren House Formation (the Scandinavian till). Local correlations.
Chapter 7	**North Sea Basin** Analyses and interprets glacigenic and interglacial sediments in the North Sea. Determines processes of deposition and provenance of key formations.
Chapter 8	**Discussion** Explores possible correlations to sediments onshore and begins to reconstruct regional ice-sheet dynamics. Attempts to draw together all the strings, testing onshore-offshore correlations. Regional correlations. Creates of model of British and Fennoscandian ice-sheet interactions during the Quaternary. Conclusions: Summarises the findings of the thesis.
Appendix I	**Methodologies** Detailed methodological tables for laboratory techniques.
Appendix II (on CD)	**Publications** • Whitburn Bay *Boreas* manuscript (In Press). • Easington Raised Beach *Proceedings of the Geologists' Association* manuscript (Submitted). • Heavy-Mineral Analysis: Methodologies. In: Bridgland, D.R., *Clast Lithological Analysis. Technical Guide 4, Quaternary Research Association* (Submitted)
Appendix III (on CD)	**Photographs** Selected photographs of Hawthorn Hive to Blackhall Rocks.
Appendix IV (on CD)	**Raw Data** All raw data from this project. Palynomorph, U-series, and OSL reports.

1.2 Quaternary Geology of Britain

1.2.1 Middle Pleistocene glaciations

Introduction

There is substantial evidence for repeated glacials and interglacials during the Quaternary in Britain and in Fennoscandia; however, the number of Middle Pleistocene glaciations and the interactions between the Fennoscandian and British ice sheets remain unresolved. There is extensive evidence of large scale glaciation in Fennoscandia and in the North Sea during each of the main glacial stages (Ehlers *et al.*, 1984; Kleman & Stroeven, 1997; Sejrup *et al.*, 2004). Glaciations in Scandinavia are known from the Middle Miocene, based on small amounts of IRD in the Norwegian Sea from 12.6 Ma (Ebbing *et al.*, 2003). Ice-rafted debris (IRD) in the Norwegian Sea provides additional evidence of extensive glaciation extending to the shelf break on several occasions during the Middle Pleistocene (Hjelstuen *et al.*, 2004). A deep sea core off the Hebridean coast indicates that IRD was being delivered by British ice sheets from the Late Pliocene, at ~2.5 Ma (Sejrup *et al.*, 2005), although expansive glaciation of the continental shelf did not occur until the Middle Pleistocene. IRD in the Norwegian Sea provides additional evidence of extensive glaciation extending to the shelf break on several occasions during the Middle Pleistocene (Hjelstuen *et al.*, 2004).

Large-scale lowland glaciations in Britain are widely recognised in MIS 12, 6 and 2 (Clark *et al.*, 2004b). Coalescence of the Fennoscandian Ice Sheet (SIS) and the British-Irish Ice Sheet (BIIS) in the North Sea Basin (NSB) has been suggested during the Anglian (MIS 12), Wolstonian (MIS 6) and the Devensian (MIS 5d to 2) glaciations (Boswell, 1916; Perrin *et al.*, 1979; Catt & Digby, 1988; Bowen, 1999a; Catt, 2001a; Carr *et al.*, 2006), with Scandinavian ice reaching the British landmass during the Wolstonian and the Anglian (Perrin *et al.*, 1979). Evidence for this Scandinavian ice was principally found in Norfolk, but recent work by Lee *et al.* (2002) indicated that the Anglian North Sea Drift of East Anglia, which was thought to contain Scottish and Scandinavian tills, is purely of Scottish provenance. The North Sea Drift is now divided into the Happisburgh and Lowestoft Formations, which are dated by some authors to MIS 16 and MIS 12 respectively (Lee *et al.*, 2004). However, although this work has included robust and

detailed lithostratigraphical analysis, mapping and provenance analysis, the chronostratigraphy is poor and more accurate, direct dating on sediments is needed.

The acceptance of the Marine Isotope Stage record and of repeated major glaciations during the Quaternary (Emiliani, 1955; Shackleton, 1967; Shackleton & Opdyke, 1973), has led to many attempts to relate the Quaternary sedimentary deposits of the British Isles to the deep sea record (Bowen, 1999a). In the late 1980s, workers on the British Quaternary formally recognised six cold stages, and defined the transition from the Middle to Late Pleistocene at the start of MIS 5e, at 132 ka BP, which is still accepted today (Bowen *et al.*, 1987; Gibbard, 2003). Currently, the Anglian, Wolstonian and Devensian are the best known Middle Pleistocene glaciations (Bowen, 1999a). They are preceded by the Cromerian, which dates from MIS 21 to 13 inclusively, and are separated by the Hoxnian (MIS 11), unnamed interglacials equivalent to MIS 7 and 9 in the oceanic sequence, and the Ipswichian (MIS 5e) interglacial. However, evidence is accumulating to suggest that this is an oversimplification of the glacial sequence, and that up to five major lowland glaciations occurred in Britain in the Middle to Late Pleistocene (Clark *et al.*, 2004b; Lee *et al.*, 2004).

Glacial limits prior to the Devensian are poorly constrained in Britain, due to low preservation potential, on account of erosion during successive glaciations (Catt, 2007). Sejrup *et al.* (2005) argued that deep sea boreholes indicate that the British Ice Sheet has expanded during each of the main glacial stages (MIS 12, 10, 8, 6, 4 and 2). However, Bowen (1999b) proposed that only four major lowland glaciations occurred in the British Isles during the Bruhnes Chron, during MIS 16, 12, 6 and 2. Bowen (1999b) emphasised the danger of forcing an oversimplified continental stratigraphy into the marine isotope record. The terrestrial record is fragmentary and is poorly constrained by dating, and much more analysis and independent dating is therefore needed.

The Anglian (MIS 12)

North Norfolk contains vast thicknesses of Quaternary sediments, some of which have been attributed to the Anglian glaciation. In northeast Norfolk, three tills form the North Sea Drift Formation (Fm), which is overlain by the Lowestoft Till (Solomon, 1932; Banham, 1968; Eyles *et al.*, 1989). The Briton's Lane Formation, which contains Scandinavian and British lithologies, overlies the Lowestoft Fm. Both the North Sea Drift and Lowestoft formations are Anglian in age. The North Sea Drift is derived from the

Fennoscandian Ice Sheet (FIS), which entered the area from the north or north-north east, and the Lowestoft Fm from the 'British Eastern Ice Sheet' (Lunkka, 1994). These two ice-sheets were thought to coexist (Hart & Boulton, 1991).

Recent mapping and till petrography has produced some new theories regarding the age, provenance and stratigraphy of these Quaternary sediments (Hamblin *et al.*, 2005). These new theories are summarised below (Table 1.2). Lee *et al.* (2002) found no evidence for Scandinavian lithologies within the North Sea Drift Fm, although this has recently been challenged (Hoare & Connell, 2005). Mapping by the British Geological Survey found that the Walcott Till, formerly the North Sea Drift, was a facies of the Lowestoft Till (Hamblin *et al.*, 2005). Lee *et al.* (2004) argued that a terrace in the Bytham river contained till balls identical to newly-defined Happisburgh Fm. This terrace was tentatively dated to MIS 16 (Lee *et al.*, 2004).

Table 1.2: Revised stratigraphy of north Norfolk (Lee *et al.*, 2002; Hamblin *et al.*, 2005).

Lithostratigraphy	Sediment	Provenance and Processes	Chrono-stratigraphy
Briton's Lane Fm	Sands and Gravels	*North Sea, Scandinavian, North Britain* Glaciofluvial outwash	MIS 6
Sheringham Cliffs Fm		*North Sea, North Britain*	
Weybourne Till	Diamicton	Subglacial till	MIS 10
Bacton Green Till (North Sea Drift)	Diamicton	Subglacial till	MIS 10
Lowestoft Fm		*Scottish, NE Britain*	
Lowestoft Till	Chalky, clayey diamicton	Glaciation – subglacial till	MIS 12
Walcott Till (North Sea Drift)	Chalky, silty diamicton	Glaciation – subglacial till	MIS 12
Happisburgh Fm		*North Sea, northern Britain*	MIS 16
Corton Sands	Chalky, fine sand	Distal proglacial outwash	MIS 16
Leet Hill sands and gravels	Sands & gravels	Proximal proglacial outwash	MIS 16
Corton Till	Sandy, brown diamicton	Glaciation – subaqueous till	MIS 16
Happisburgh Till (North Sea Drift)	Sandy, grey diamicton	Glaciation – subglacial till	MIS 16
Bytham Sands and Gravels Fm	Coloured quartzose sand & gravel	Bytham river incision followed by deposition	Early Pleistocene
Wroxham Crag Fm	Quartzose sands & gravels	Coastal North Sea	Early Pleistocene
Norwich Crag Fm	Shelly sand & silt and clay	Coastal North Sea	Early Pleistocene

The new revised stratigraphy stretches from MIS 16 to MIS 2 and is composed of numerous complex formations (Hamblin *et al.*, 2005). Under this model, Scandinavian ice only reached the British coastline during MIS 6. However, the dating control for this model remains poor. The model is yet to be rigorously tested in other areas of Britain. Further work has questioned the validity of the model, as recent OSL dating has suggested that the Briton's Lane Fm is MIS 12 (Pawley *et al.*, 2008).

The Wolstonian (MIS 6)

The original 'Wolstonian' glaciation in Britain was based on the type site in the Midlands, which Keen *et al.* (1997) dated to MIS 12. The term 'MIS 6' is here preferentially used to describe the Wolstonian. It is generally accepted that Scandinavian ice impinged on the eastern coast of England at this time, in both Norfolk (Lee *et al.*, 2002) and northeastern England (Catt, 1991b; Bateman & Catt, 1996).

In the West Midlands, the Ridgacre Formation is regarded by Bowen (1999b) as providing evidence for an MIS 6 glaciation (Bowen, 1999b). The 'Older Drift' in North East Herefordshire is interpreted as evidence of a post-Hoxnian ice sheet that advanced across Herefordshire to the Malvern Hills (Richards, 1998). The Briton's Lane Fm provides indirect fluviatile evidence of an MIS 6 glaciation at Weybourne. These gravels contain Scandinavian lithologies, and based on this and their stratigraphical position, they are correlated to MIS 6 (Pawley *et al.*, 2004).

Other glacigenic deposits of inferred MIS 6 age include the Warren House Formation in Country Durham, the Basement Till (now the Bridlington Member; Lewis, 1999) in east Yorkshire and the Welton and Calcethorpe tills of Lincolnshire (Clark *et al.*, 2004b). These are all of Scottish, North Sea or Scandinavian provenance (Straw, 1983). The Bridlington Member is overlain by the Ipswichian Sewerby Raised Beach (Bateman & Catt, 1996), which is dated by its mammalian fauna (Catt & Penny, 1966; Boylan, 1967). Late Devensian amino acid ages have been obtained from the Bridlington Member (Eyles *et al.*, 1994). The technique used to obtain these ages has, however, been vastly improved, and these ages cannot now be held to be correct without further testing. The Bridlington Member is best exposed on the foreshore at low tide between Kilnsea and Holderness (Catt, 2007). Catt and Penny (1966) described it as a very dark grey diamicton with a wide range of arctic shells and erratics from northeast England (such as chalk, flint, Jurassic sandstones and shales, Magnesian Limestone, Carboniferous Limestone and shale, and

Whin Sill Dolerite), Scotland (granites, basalts and gneisses), and Scandinavia (larvikite and rhomb porphyries). At Dimlington and Bridlington, the Bridlington Member incorporates rafts of fossiliferous Pleistocene marine sediments, the Bridlington Crag (Catt & Penny, 1966), interpreted as an erratic mass picked up from the North Sea floor by the ice sheet that deposited the till. The absence of post-Anglian age indicators suggests that the Bridlington Crag is Anglian or older. Six species of ostracoda found in the Bridlington Member were also found in the Warren House Fm, and on this basis, the two deposits have been correlated (Catt & Penny, 1966; Catt, 2007).

The Welton Till overlies gravels containing an Acheulian hominid culture, dated to the Hoxnian. However, the discovery, from sites such as Boxgrove and Pakefield (Parfitt *et al.*, 2005), of human occupation of Britain during the Late Cromerian Complex, has undermined the value of using archaeological evidence to date these gravels. The mammalian fauna is stratigraphically undiagnostic, so the 'Wolstonian' age of the Welton Till is equivocal (Bridgland *et al.*, in prep). There are no clear grounds for assigning the Welton Till to a post-Anglian glaciation, and both the Welton Till and the overlying Calcethorpe Till could be Anglian age (Straw, 2005). The Welton site could indeed record evidence of three glaciations (Clark *et al.*, 2004b; Bridgland *et al.*, in prep). The Calcethorpe Till is overlain by the Marsh Till, correlative with the Skipsea Till of the Devensian Holderness Fm, which contains the Late Devensian Dimlington Silts (Lewis, 1999). A palaeosol developed on the Welton Till has been interpreted as representing an interglacial, possibly the Ipswichian (Straw, 1983). The Warren House Formation of Durham is correlated to the Bridlington Member due to its Scandinavian lithologies (Lunn, 1995). Other age suggestions for the Warren House Formation include Anglian and Devensian (Catt, 2007).

1.2.2 Devensian Glaciations

The Early Devensian

The British-Irish Ice Sheet (BIIS) was a mobile and sensitive ice sheet, with the Last Glacial Maximum (LGM) only one of many events (Clark & Meehan, 2001; Bowen *et al.*, 2002). There is possibly evidence of an MIS 4 glaciation in east Lincolnshire and east Yorkshire (Clark *et al.*, 2004b), with glacial deposits and glacial meltwater landforms associated with tills that are younger than the Ipswichian. They are associated with lacustrine and fluviatile sediments that have been dated to earlier than the Middle

Devensian. There is also evidence of an MIS 4 glaciation in Scotland, with the more extensive MIS 4 deposits separated from the less extensive MIS 2 deposits (Bowen, 1999). There is evidence of extensive glaciation of the North Sea Basin during MIS 4, the Ferder Episode of Carr *et al.* (2006). During the Middle Devensian, the British and Irish Ice Sheet (BIIS) reached its maximum size before 37 ka BP. The final retreat from the continental shelf around 25 ka led to first transgression of British and Irish seaways since that of the Ipswichian (Bowen *et al.*, 2002).

The Last Glacial Maximum

To avoid confusion, the term 'LGM' (Last Glacial Maximum) here refers to the period of global ice-sheet maxima, from 30-22 cal. ka BP, peaking at 26 cal. ka BP (Peltier & Fairbanks, 2006), when the last British-Irish Ice Sheet (BIIS) extended to shelf-wide glaciation (Bradwell *et al.*, 2008). The Dimlington Stadial (and Tampen Stadial) occurred around 22 cal. ka BP (Rose, 1985; Bateman *et al.*, 2008; Sejrup *et al.*, 2009).

Carr *et al.* (2006) and Sejrup *et al.* (2005) favoured a two-stage LGM model. In the earlier Cape Shore Episode (29-22 cal. ka BP), the FIS and the BIIS were confluent. The Dimlington Stadial (late LGM) in Britain, dated to ~21 cal. ka BP (Penny *et al.*, 1969; Rose, 1985), was more restricted than the LGM, and there is uncertainty about the eastern extent of the BIIS (Ballantyne *et al.*, 1998). This was addressed by Carr *et al.*, (2006), who argued that the eastern margin of the BIIS during the Dimlington Stadial corresponded to the edge of the Bolders Bank Fm. The Dimlington Stadial is also correlative with the Tampen Stadial in Norway and in the Norwegian Sea (Sejrup *et al.*, 2005; Sejrup *et al.*, 2009).

The last BIIS was a complex, dynamic system, with numerous waxing and waning ice streams, and different localised ice-accumulation areas competing for dominance (Bowen *et al.*, 2002). Ice-flow pathways changed through time, leading to complex, superimposed drumlin flowsets (e.g., Salt & Evans, 2004; Mitchell, 2007; Livingstone *et al.*, in press). Constraining these ice flow pathways was first attempted by Sutherland (1984), who supplied one of the first comprehensive reviews of the glaciation of Scotland, and identified key erratic sources and trains. Recently, the BRITICE database (Figure 1.2) has summarised erratics, drumlins, eskers, meltwater channels, ice-limits and more to provide a crucial tool in interpreting the LGM (Clark *et al.*, 2004a; Evans *et al.*, 2005).

The last Scottish Ice Sheet may have been thinner than in previous reconstructions (Boulton *et al.*, 1977). Earlier models assumed confluence with the FIS and extension to the shelf edge at the LGM, implying that even the highest Scottish mountains lay under the ice sheet. Revised models suggest a more restricted ice sheet with lower shear stresses, moving over a deformable bed. Over much of the Highlands, the ice surface altitude lay at 1000 m O.D., leaving many Scottish mountains as nunataks (Ballantyne *et al.*, 1998). The Grampian Highlands were another key ice-accumulation area, dispersing erratics (such as granites and the Dalradian quartz-mica-schist) southwards and eastwards through the Midland Valley of Scotland (Figure 1.2). The uplands of Dumfries and Galloway dispersed erratic trains northwards and southwards (Clark *et al.*, 2004a).

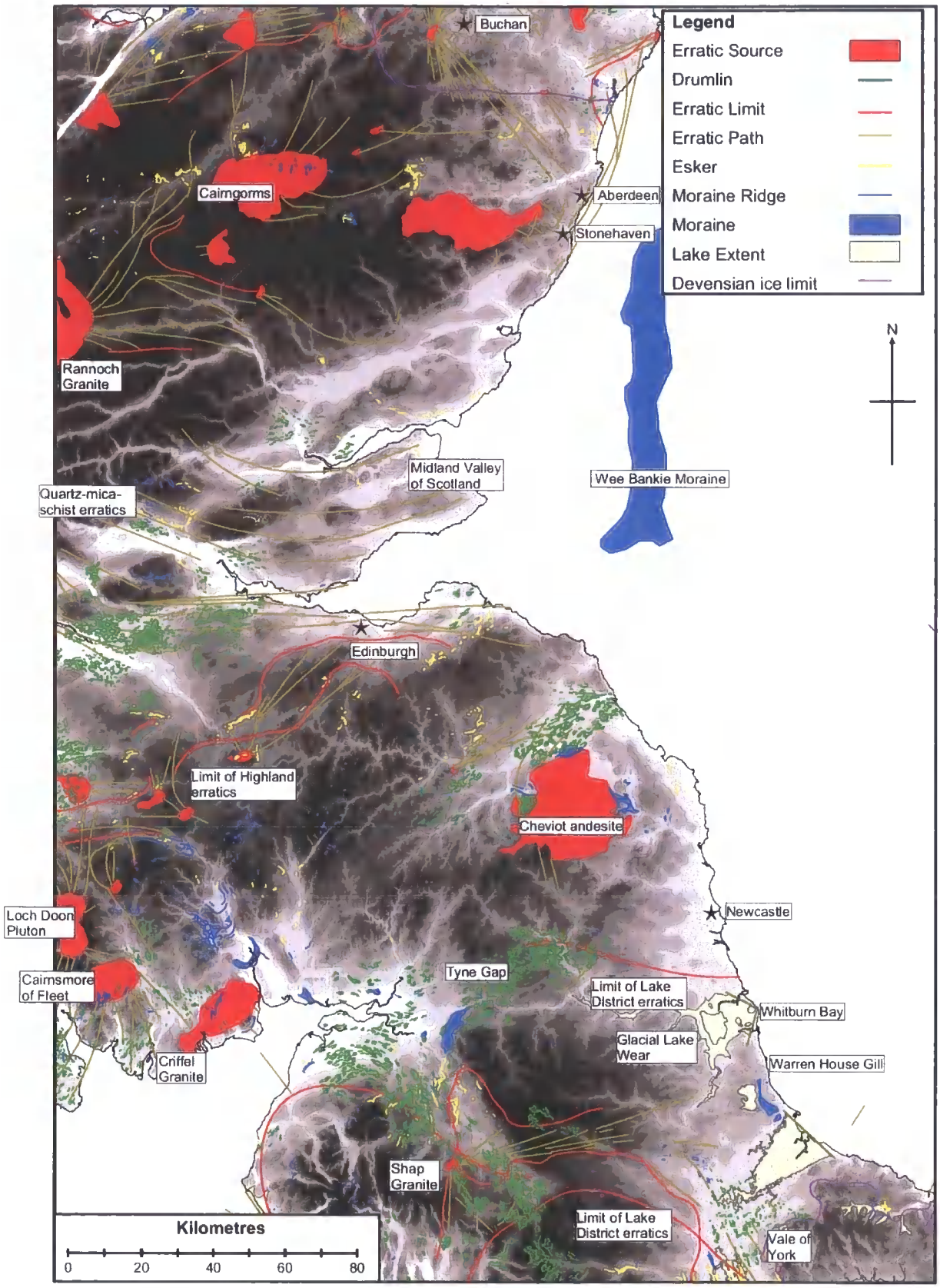

Figure 1.2: BRITICE overlain on topographical map of the UK. Adapted from Clark *et al.* (2004a).

In the North Minch Basin, the ice sheet extended no further west than the Greenstone Ridge, depositing a 60 km long submarine moraine. Stoker and Bradwell (2005) reported the presence of an ice-stream in the Minch during MIS 2 (Figure 1.3). The period of maximum ice extent is recorded in the Barra Fan (Knutz *et al.*, 2002), where the clastic input peaks at 27 to 26 cal. ka BP. They coincide with increased ice rafting from the northwestern sector of the BIIS, with IRD peaks associated with Heinrich Events 1 and 2.

The Dimlington Stadial

The Dimlington Stadial boundary in England lies between Dimlington and Norfolk (highlighted on Figure 1.3). In the Cheshire-Shropshire lowland, ice advanced to the Whitchurch Moraine, and was here coeval with Welsh ice from the west (Bowen *et al.*, 2002). During and after the LGM, ice from the Lake District and southern uplands extended into northeast England from the west, through breaches in the Pennine escarpment (Teasdale & Hughes, 1999). Erratic pathways defined flow pathways, and are shown on the BRITICE database (Figure 1.2). The ice flowed east or southeast, but as it thinned during deglaciation, the underlying topography exerted an increasing influence. Scottish ice coalesced with Lake District ice, which flowed radially out of the main mountain mass of the Lake District (Mitchell & Clark, 1994). The dominant Southern Uplands ice was deflected around the Lake District, a mountainous region that was able to develop an independent ice cap (Sutherland, 1991).

Recent workers have identified several ice-streams within the Devensian BIIS (e.g., Merritt *et al.*, 1995; Everest *et al.*, 2005; Stoker & Bradwell, 2005; Golledge & Stoker, 2006; Bradwell *et al.*, 2007; Roberts *et al.*, 2007; Bradwell *et al.*, 2008). Several of these may have operated repeatedly during several different glaciations. Figure 1.3 shows nine of the most important ice-streams during the Dimlington Stadial (various authors).

The competing ice lobes of the BIIS trapped vast quantities of meltwater in various proglacial lakes. The largest of these were Glacial Lake Humber (Bateman *et al.*, 2008), Glacial Lake Pickering, Glacial Lake Tees (Agar, 1954) and Glacial Lake Wear (as first described by Smith & Francis, 1967). These lakes were included in BRITICE (Clark *et al.*, 2004a) and are shown on Figure 1.2. In northeastern England, western ice may have retreated prior to the advance of the North Sea lobe, resulting in an ice free zone between glaciers in valleys and a lobe close to the coastline (Teasdale & Hughes, 1999). The term

'North Sea Lobe' refers to the southwards-flowing ice lobe in the eastern BIIS, as shown on Figure 1.3.

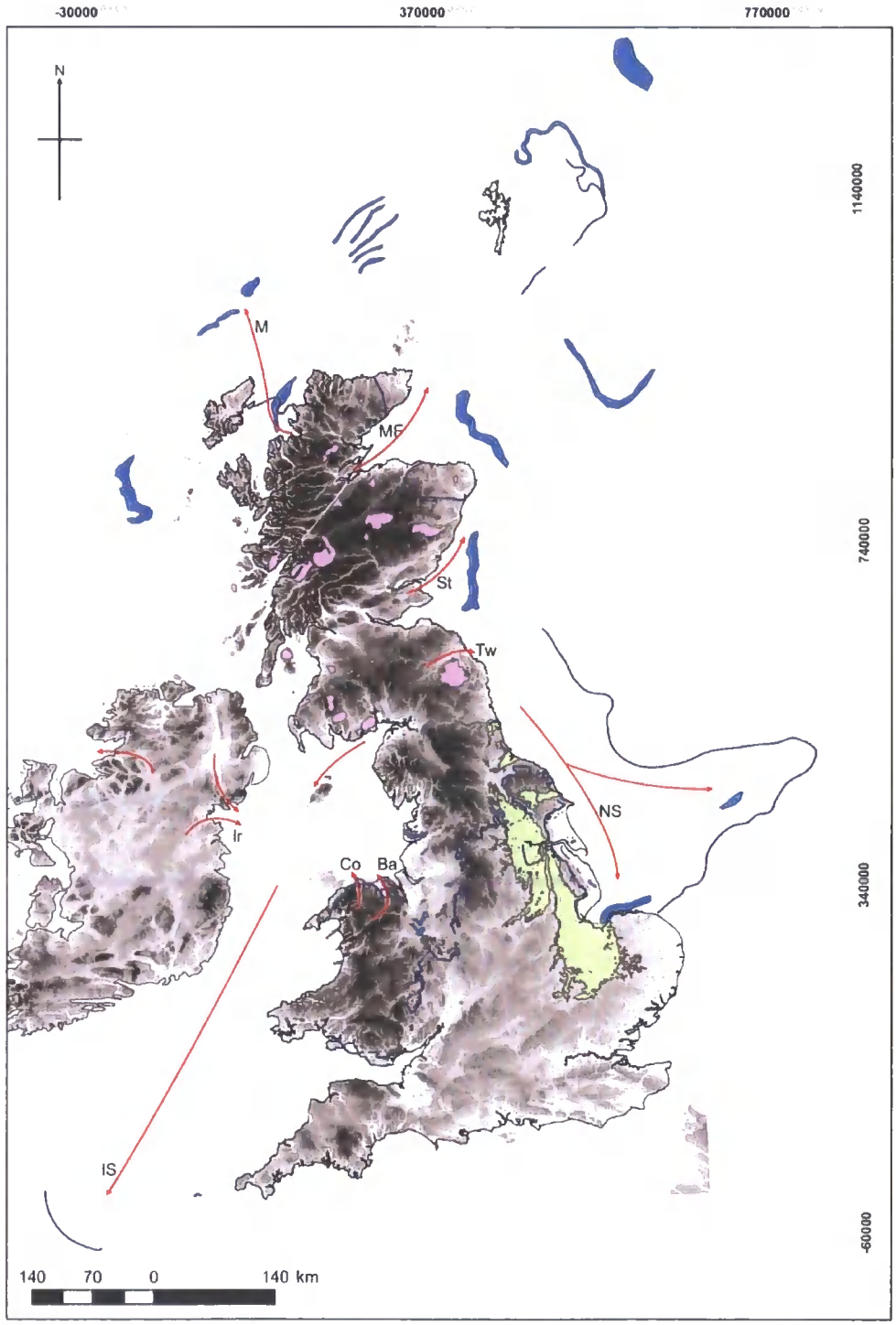

Figure 1.3: Map of major British ice streams (red arrows) during the LGM.
See Table 1.3 for description, location and references. Moraines, ice limits and ice-dammed lakes are taken from BRITICE database (Clark *et al.*, 2004a; Evans *et al.*, 2005).
IS: Irish Sea ice stream. IR: Irish ice streams. TW: Tweed ice stream. MF: Moray Firth ice stream. M: Minch ice stream. St: Strathmore ice stream. NS: North Sea ice stream.

Table 1.3: Summary table of British ice streams during the LGM. Abbreviation refers to letters on Figure 1.3.

	Name	Age	Characteristics and Evidence	Reference
IS	Irish Sea Ice Stream	14.9 – 14.8 cal. ka BP	Zone of flow convergence up-ice. Grounding line in the southern Celtic Sea. Deforming bed conditions.	Roberts *et al.* (2007) Ó Cofaigh and Evans (2001) Roberts *et al.* (2006)
IR	Irish ice streams	14.7 cal. ka BP	Differential modification of rogen moraine. Well-preserved outside ice-stream margins, and crosscut, streamlined and drumlinised within margins.	Knight and McCabe (1997) Knight *et al.* (1999) McCabe and Clark (1998)
MF	Moray Firth Ice Stream	ca. 13.0 cal. ka BP	Oscillating tidewater glacier in the Moray Firth.	Merrit *et al.* (1995)
St	Strathmore Ice Stream	MIS 2	Highly attenuated bedforms, abrupt lateral margins, glaciotectonics and deformed till. Trunk width of 45 km and length of >100 km. Wee Bankie is a lateral shear margin moraine.	Golledge and Stoker (2006)
M	Minch Ice Stream	MIS 2	Geophysical data from continental shelf. Bedrock megagrooves, elongate drumlinoid forms, mega-scale lineations.	Stoker and Bradwell (2005)
Co	Conway Ice Stream	Deglaciation	Drumlins in the Vale of Conway, meltwater channels. Uncoupling of Irish Sea Glacier and Welsh ice cap.	Jansson and Glasser (2005)
Ba	Bala Ice Stream	Deglaciation	Erratic trains and meltwater channels.	Jansson and Glasser (2005)
Tw	Tweed Ice Stream	Late MIS 2	Elongate bedforms, convergent ice-flow, abrupt lateral margins, pervasively deformed till.	Everest *et al.* (2005) Mitchell (2008)
NS	North Sea Ice Stream	Late MIS 2	Deformation tills from periodic surging over muddy marine sediments. Arcuate belts of hummocky moraine indicate stagnation. Ice sheet models cannot explain this lobe under steady-state models.	Eyles *et al.* (1994)

The North Sea Lobe created many ephemeral glacial lakes, such as Glacial Lake Wear, and led to the deposition of extensive lacustrine deposits in many valleys. Catastrophic drainage of these lakes may have led to the incision of the denes and gills of the Durham coast (Smith, 1994). Glacial Lake Wear (Raistrick, 1931) stood at different levels as outlets opened and closed during deglaciation. The lowlands around Sunderland and Newcastle were at one time almost entirely covered by this lake, in which the widespread 'Tyne-Wear Complex' deposits were laid down, consisting mostly of laminated clays (Catt, 1991a; Smith, 1994). These were later termed the 'Durham Member' by Thomas (1999). They range from interbedded laminated silty clays and clayey silts up to 55 m thick and extending up to 132 m Ordnance Datum (O.D.), to proximal proglacial gravels (Smith & Francis, 1967; Evans *et al.*, 2005). Finer fractions successively overlap the coarser fractions northwards, marking ice lobe recession. These glaciolacustrine sequences overlie the Blackhall Member (Evans *et al.* 2005). Towards the coast, the Horden Member overlies this earlier till (Catt, 2007).

Sediments along the northeast coast of England record one or more North Sea Lobes of the British ice sheet, which flowed southwards parallel to the coast (Eyles *et al.*, 1994). Eyles *et al.* (1994) interpreted it as an ice-stream sliding over slippy, deformable, marine sediments (Figure 1.3). The glaciofluvial landforms in Holderness are former ice contact, coalescent, subaqueous fans representing recessional positions of the North Sea Lobe (Evans *et al.*, 2005). Gaunt *et al.* (1992) argued that the westernmost penetration of a North Sea glacier up the Humber estuary is marked by the Horkstow Moraine, which corresponds with the westernmost limits of the Skipsea Member of the Holderness Fm (Table 1.4).

A Vale of York Lobe initially surged into Glacial Lake Humber to Wroot in Lincolnshire. This coalesced with glaciers in the dales south of Swaledale. There is evidence of palaeo-ice streams in the Vale of York, Vale of Eden, the Yorkshire Dales and the Tweed Valley (Evans *et al.*, 2005; Everest *et al.*, 2005; Mitchell, 2008; Bridgland *et al.*, in press). Eyles *et al.* (1994) used the limit of the Withernsea Member to support evidence of a surging ice sheet margin in east Yorkshire, and the edge of the overlying Skipsea Member (Lewis, 1999) provided the Dimlington ice limits in eastern England (Table 1.3 and Figure 1.2).

The till sheets in east Yorkshire off-lap eastwards, recording repeated surges of the North Sea ice lobe reaching less far inland during each surge (Teasdale & Hughes, 1999). Within Devensian tills along the east coast, the Skipsea Member has erratics indicating a

Southern Uplands and Cheviots source, and the Withernsea Member a Lake District and Pennines source. This indicates changing dominance of ice source areas during the last glaciation (Evans *et al.*, 2005).

During the Dimlington Stadial, the Irish Sea Basin was occupied by an ice stream flowing southwards (Roberts *et al.*, 2007). McCabe *et al.* (1998) argued that it was fed by centres of ice dispersion in the Lake District, Southern Uplands and Ireland. The Killard Point Stadial in Ireland records a readvance between 18.8 – 16.4 cal. kyr BP, during the North Atlantic Heinrich Event 1 (Thomas *et al.*, 2004; McCabe *et al.*, 2007). This ice stream may have impacted ice flowing eastwards across the Tyne Gap, as it would have created drawdown into the Irish Sea, resulting in stagnation and decline across the Pennines.

During Heinrich Event 1, the ice advanced to Dimlington Stadial limits once again. Between 10 and 45 cal. ka, IRD deposition increased every 2 to 3 ka, similar to the timing of Dansgaard-Oeschger Events (Bowen *et al.*, 2002).

Table 1.4: Stratigraphy of eastern Yorkshire. Adapted from Lewis (1999).

	Original Name	New Name	Stratotype	Sediments	Chronostratigraphy
Holderness Formation		**Flamborough member**	Flamborough Head	Laterally extensive flat-lying gravel that truncates the Skipsea Member.	
		Hornsea Member	East Holderness	Glacial deposits forming a belt of hummocky topography.	MIS 2
	Purple Till (Catt and Penny, 1966)	**Withernsea Member**	Dimlington Cliff	Massive, fine-grained diamict.	MIS 2
	Skipsea Till (Catt, 1991b). Drab Till (Catt and Penny, 1966)	**Skipsea Member** (Lewis, 1999)	Dimlington Cliff	Fine-grained diamicton characterised by banded structure, multiple stacked beds, chaotic clusters, stratified interbeds, deformed beds and pervasive shears and attenuation structures.	Overlies Dimlington Bed. MIS 2.
	Dimlington Silts	**Dimlington Bed**	Dimlington Cliff	Delicately laminated and rippled sand-silt containing detrital Arctic moss remains.	21.7 cal. yr BP (Penny *et al.*, 1969).
	Sewerby Raised Beach	**Sewerby Member** (Lewis, 1999)	Sewerby	Beach gravel with interglacial faunal assemblage (Ipswichian) overlain by blown sand, colluvium and coombe rock. Ipswichian Raised Beach.	MIS 5e (Bateman & Catt, 1996)
	Basement Till (Catt and Penny, 1966)	**Bridlington Member** (Lewis, 1999)	Dimlington Cliff	Muddy diamict with inclusions of fossiliferous marine muds. Scandinavian Till, Catt 1991.	Overlain by raised beach. MIS 6 (Catt, 1991b). AAR dates of MIS 2, (Lewis 1999).

1.3 Quaternary Geology of County Durham

1.3.1 Buried Valleys in County Durham

The Quaternary geology of the region in eastern County Durham is characterised by steep-sided denes, cutting through the Quaternary diamictons and locally into the Magnesian Limestone bedrock. These denes were probably rapidly cut through the soft Quaternary sediments post-glacially, in response to rapid isostatic uplift after deglaciation (Evans, 1999).

The soft Magnesian Limestone bedrock in these denes is also frequently eroded to well below sea level to form steep-sided palaeovalleys, which are infilled with Quaternary deposits. These buried palaeovalleys characterise the east coast, forming an anastomising network (Peel, 1956; Smith & Francis, 1967), and cut across the coastline at Hawthorn Hive, Warren House Gill, Limekiln Gill and Castle Eden Dene. Figure 1.4 shows the dendritic pattern of the buried valleys in County Durham. They could have been incised by ancient rivers, and possibly subsequently influenced by subglacial meltwater / proglacial meltwater during glacial periods.

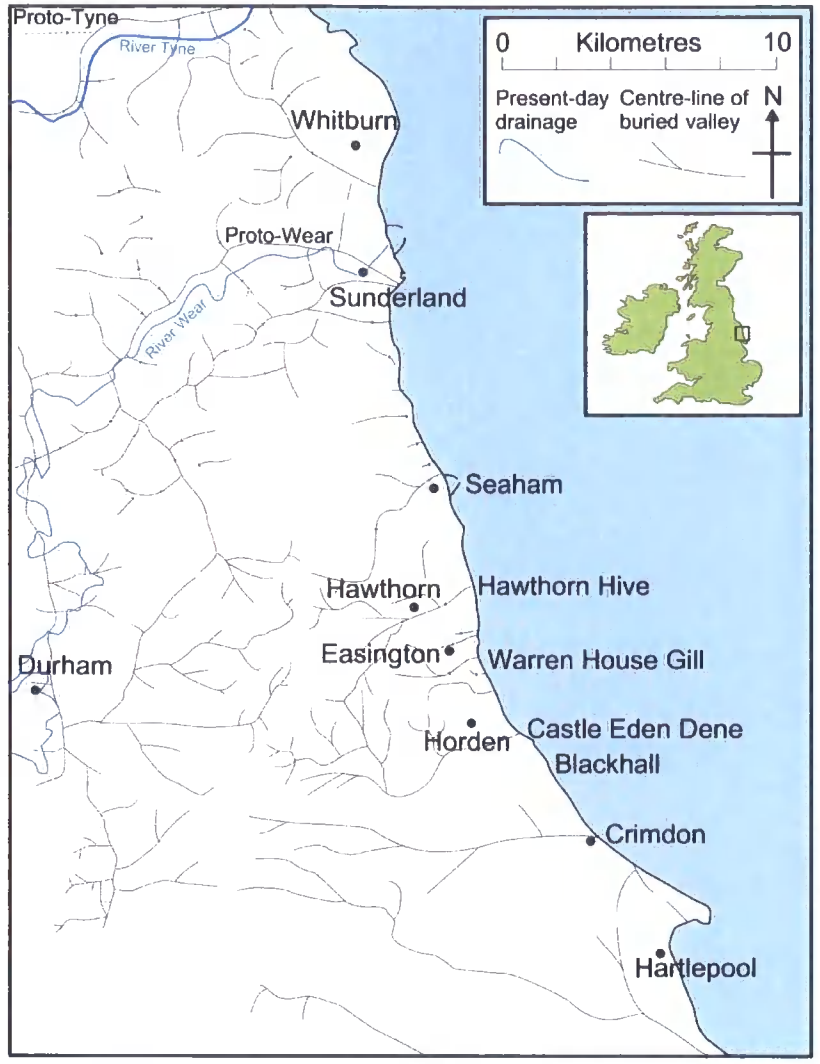

Figure 1.4: Buried valleys of County Durham. Modified from Smith and Francis (1967) and Smith (1994).

1.3.3 Middle Pleistocene Sediments in County Durham

Fissure Fills

Trechmann (1952) reported a series of fissure fills in the Permian Magnesian Limestone. These breccias and clays, now obscured, were said to contain seeds representing Tertiary woodland (Francis, 1972), with a later clay containing Middle Pleistocene flora and fauna (Reid, 1920). It contains freshwater shells, peat, tree trunks, insects, rodent teeth and elephant vertebra resembling *Archidiskodon meridionalis* (Lunn, 1995). This clay was named the Blackhall Colliery Formation (Table 1.5) by Thomas (1999).

Warren House Formation

Trechmann (1915) described a buried valley about 500 m wide in the Magnesian Limestone at the mouth of Warren House Gill, infilled at the base with "Scandinavian Drift", now the 'Warren House Till' (Francis, 1972) or 'Warren House Formation' (Table 1.5; Thomas, 1999). Trechman (1915) reported that this 'boulder clay' was overlain by loess, which in turn was overlain by Devensian 'boulder clay' and sands and gravels. The Warren House Formation reached a thickness of 2 or 3 m in the cliff section, but thinned out and disappeared as the bedrock rose at the side of the depression. The 'boulder clay' was locally coloured yellow by the presence of dolomitic Magnesian Limestone, and in places was slickensided and sandy (Trechmann, 1915). Beaumont (1967) described the Warren House Formation as a grey, sandy clay with rounded, Scandinavian, metamorphic crystalline erratics. Magnesian Limestone, the local parent rock, was present in low abundances (less than 6.5 %), and no Carboniferous Limestone was present. Boulders of larvikite, rhomb porphyries, and Norwegian rocks were also reported *in situ* and on the beach by Trechmann (1931b). Smith and Francis (1967) argued that the arctic shells, flint and chalk, red marl, belemnite fragments, and white limestone within the till were transported from the North Sea Basin. The clay and silt mineralogy of the Warren House Formation is substantially different to the other tills in the region. Beaumont (1967) proposed that the minerals were mainly derived from igneous rock material, and limestone material such as dolomite and calcite was added later. However, there has been no heavy-mineral or palynomorph analysis, which could provide valuable and detailed provenance information.

Smith and Francis (1967) suggested that the lack of exposures of the Warren House Formation implies that only pockets were preserved beneath younger drift in other buried valleys, and that the Scandinavian ice did not extend much further west than the present coastline. Subsequent glaciations removed the till, leaving only the small protected pocket in Warren House Gill (Beaumont 1967). Previous interpretations of the genesis of the Warren House Formation range from deposition as a subglacial till (Bridgland, 1999), to deposition from a grounded ice shelf, explaining the purity of the Scandinavian material (Beaumont 1967).

The age of the till is controversial. Trechmann (1931) stated that a substantial unconformity and interglacial separated the 'Scandinavian Drift' from the overlying last glacial tills. He argued that the evidence for this is present in the sequence at Warren House Gill in the form of a bed of loess, on which a palaeosol had developed (Trechmann,

1920, 1931b). Trechmann also argued that the apparently greater weathering of the 'Scandinavian Drift' than the 'Main Cheviot Drift' suggests that it pre-dated the last glaciation. This weathering must have occurred during an intervening warm period, such as the Ipswichian (Catt, 2007). However, the juxtaposition of abundant rotted and rounded clasts of granite and gneiss to a rich and apparently unweathered shell fauna in the till led Beaumont (1967) to question the interpretation of differential weathering. However, the calcareous groundwater would have preserved and protected the shell fauna.

Trechmann (1931a) stated that the Easington Raised Beach contained Scandinavian erratics derived from the underlying 'Scandinavian Drift'. Bowen *et al.* (1991) dated the beach to MIS 7, which Teasdale and Hughes (1999) have used to argue that the glaciation that deposited the Warren House Formation occurred in MIS 8 or earlier. However, the Warren House Formation was correlated with the Bridlington Member of Holderness due to the coincidence of lithology, fauna, stratigraphical position and biostratigraphical remains (Francis, 1972), and was therefore assigned an MIS 6 age by some workers (Catt & Penny, 1966; Catt, 1991b; Lunn, 1995; and Thomas, 1999). The age of the Warren House Formation, its precise genesis, and the provenance therefore remain unresolved. Additionally, dating the Warren House Formation by its relationship to the Easington Raised Beach is difficult. Their stratigraphical relationship is unclear, as they are not exposed in superposition. It is also illogical to assume that Scandinavian ice reached the British coastline only once, given the existence of at least 10 significant glaciations recognised from deep ocean cores (Shackleton & Opdyke, 1973). In addition, it is difficult to rationalise why the Fennoscandian ice sheet reached the British coastline at all before the British-Irish Ice Sheet, which had much shorter distances to travel. One possibility is that the BIIS disappeared completely in interglacials and so was initially slower to respond to abrupt climatic shifts, whilst ice remained in the highlands of Scandinavia even during interglacials, thus making the creation of a large ice sheet easier.

Interglacial Loess

Trechmann (1920) reported the pale brown or fawn-coloured upper beds as loess, with a thickness of approximately 0.3 m to 4 m. It is horizontally bedded, with seams of sand, fine gravel and occasional small boulders, and Trechmann interpreted it as having been resorted and redeposited by water after deposition. Towards the base of the section, Trechmann (1920) described undisturbed loess, which was uniform in colour and

appearance. It had no trace of shells or organic remains and was devoid of sand and stones. The loess in Warren House Gill was interpreted as interglacial by Trechmann (1920), but this is disputed by Francis (1972), as the loesses of Europe and North America were deposited in cold steppe environments. Francis (1972) suggested that the loess was deposited during the MIS 6 glaciation after the ice cap withdrew from the Durham locale.

The Easington Raised Beach

A raised beach at 33 m O.D. was first reported by Woolacott (1900) in Shippersea Bay, County Durham. Shippersea Bay is located near the small town of Easington, so Woolacott named the beach the 'Easington Raised Beach'. It is located some 800 m north of Warren House Gill. Later reinvestigations by Trechmann (1931a) suggested that the beach contained Scandinavian erratic material, which he argued must have been derived from the Warren House Fm. Trechmann proposed that the beach was from the last interglacial, and that the Warren House Fm (or 'Scandinavian Drift') was therefore from the previous glaciation. The beach was later dated by Amino Acid Racemisation by Bowen (1991), who stated that it was deposited during MIS 7 and that it contained a reworked fauna from MIS 9. This creates difficulty as the Warren House Fm was lithostratigraphically correlated to the MIS 6 age Basement Till (Bridlington Member; Lewis, 1999; Catt, 2001a).

Table 1.5: Quaternary stratigraphy in County Durham. From Thomas (1999).

	Original Names	New Name	Stratotype	Sediments	Chronostratigraphy
Wear Fm		**Framwellgate & Butterby members**		Overlies Durham Member in Wear Valley. Thin, patchy and discontinuous tills, represent ice-marginal flow tills.	Correlated with the 'Middle Sands and Gravels' (Francis 1972)
	Tyne-Wear Complex (Smith, 1994)	**Durham Member**	Central and SW Durham	Thick and extensive sequence of glaciofluvial sands and gravels and glaciolacustrine silts and laminated clays, fining southwards, Smith and Francis (1967)	
		Winch Gill Member	Central and SW Durham	Stiff grey basal till, resting on bedrock, contains tuffs, lavas and granite from the Lake District, granite from Scotland and red Triassic and Devonian sandstone.	
East Durham Fm	Main Cheviot Drift (Trechmann, 1952). Upper Boulder Clay (Smith and Francis 1967). Horden Till (Francis, 1972).	**Horden Member**	Horden	Overlies and interdigitates with Peterlee Member. brown sandy till passing downwards into red silty sand at base and westwards into the laminated clays of the Durham Member	MIS 2
	Peterlee Sands and Gravels (Francis, 1972)	**Peterlee Member**	Durham coast	Extensive fine sand, silts and clays passing up into gravels. Ice marginal and glaciolacustrine (Francis 1972)	MIS 2
	Lower Boulder Clay. Blackhall Till (Francis, 1972)	**Blackhall Member**	Blackhall Rocks	Extensive outcrops. Thick, grey-brown stony basal till on bedrock. Permian and Carboniferous erratics. Correlated with the Drab Till (Francis, 1972)	MIS 2
Easington Fm	Easington Raised Beach (Trechmann, 1952)	**Easington Formation**	Shippersea Bay	Cemented fine gravel and sand with a temperate molluscan fauna overlying a rock platform at 32 m OD	MIS 7 from AAR on shells (Bowen *et al.*, 1991)
Warren House Fm	Scandinavian Drift (Trechmann, 1952). Warren House Till (Francis, 1972).	**Warren House Formation**	Warren House Gill	Grey sandy till along coast of Northumberland and Durham bearing Scandinavian erratics, shells, and North Sea Tertiary erratics. Overlain locally by loess.	As old as MIS 6 (Francis, 1972; Thomas 1999). MIS 8 (Lunn, 1995)
Blackhall Colliery Fm	Fissure fills	**Blackhall Colliery Formation**	Blackhall Colliery	Fissure fillings in Triassic rocks containing clay with pyritised plant fragments and seeds. Lower Pleistocene flora (Reid, 1920). Overlain by clay containing molluscs, insects, peat, rodent teeth, and vertebra of *Elephus.*	Early Pleistocene

1.3.4 Devensian Tills in County Durham

The 'Main Cheviot Drift' of the Durham coast, as first described by Trechmann (1915), overlies the earlier Pleistocene sediments and widely caps the Magnesian Limestone cliffs (Bridgland, 1999). It comprises two tills separated by sand and gravel (Figure 4.2). In some places, sand and gravel also cap the sequence (Teasdale & Hughes, 1999).

The Blackhall Member (Lower Till)

Francis (1972) named the lower till the 'Blackhall Till', with a stratotype at Blackhall Rocks, where it is overlain by the Peterlee Sands and Gravels (or Peterlee Member; Thomas, 1999). The Blackhall Till was renamed the 'Blackhall Member' of the 'East Durham Formation' by Thomas (1999; Table 4.1). Francis (1972) described the Blackhall Member as a deeply weathered, thin, sandy, subglacial till resting directly on the Magnesian Limestone, and containing a high percentage of Magnesian Limestone clasts. Carboniferous Limestone and sandstones are present in small quantities. The sandstone abundance varies inversely with that of the Magnesian Limestone (Beaumont, 1967, 1971). Both red sandstones and greywackes are present. There are very small percentages of coal, ironstone, quartzose and igneous clasts. The Peterlee Member consists of a lower, red, fine-grained sand with beds of silt and clay, sporadic beds of coarser sand, and an upper gravel. These sands were interpreted as glaciofluvial outwash by Francis (1972).

The Tyne Gap was a major artery of the BIIS, directing ice from Scotland, the Pennines and the Lake District towards eastern England (Yorke *et al.*, 2007; Livingstone *et al.*, in prep). Beaumont (1967) argued that striae on both stones and bedrock and clast macro-fabrics in County Durham indicate a strong west-to-east movement (Figure 1.5), suggesting that an ice sheet came through the Tyne Valley, overrode Gateshead Fell and continued eastwards into the North Sea. The till therefore represents the maximum glaciation of the Durham area, and was deposited by an ice sheet which moved south-eastwards across eastern Durham from sources in the Pennines, the Lake District and the Southern Uplands (Beaumont, 1967). Beaumont proposed that this eastward flow reflected the build up of ice in the Irish Sea basin, which caused an overflow eastwards across the Pennines, entering the Durham area via the Tyne Gap (Beaumont, 1971). In the early stages, it coalesced with a Weardale Glacier to form a piedmont-lobe glacier in northern Durham. At maximum glaciation, it was probably coalescent with Scandinavian ice

offshore, and with Tees ice moving over the Stainmore depression in the south (Beaumont, 1967).

Francis (1972) correlated the Blackhall Till with the Drab Till of Holderness (as described by Catt & Penny, 1966). The Drab Till directly overlies Dimlington Silts of the LGM, and therefore dates from 21-22 cal. ka BP (Penny *et al.*, 1969). The Drab Till was renamed the Skipsea Till by Madgett and Catt (1978), and the Skipsea Member by Lewis (1999). At the type site in Holderness, the Skipsea Member is overlain by the Withernsea Member (Lewis, 1999), formerly the Purple Till (Catt & Penny, 1966) or Withernsea Till (Madgett & Catt, 1978). They form the 'Holderness Formation', as defined by Lewis (1999; refer to Table 1.4).

Figure 1.5: Map of striae orientations in northeastern England. Modified from Beaumont (1967).

The Horden Member (Upper Till)

The Horden Member (Table 1.5) is the youngest glacial deposit exposed along the Durham coast, and is the uppermost member of the East Durham Formation (Thomas,

1999). It overlies the Peterlee Member and its type section is located on the southern side of Warren House Gill, where Francis (1972) observed 9 m of brown stony clay with lenses of red silty sand near the base.

Beaumont (1967) described the clay mineralogy of the Blackhall and Horden members as very similar, being largely derived from the Coal Measures. Beaumont's (1967) clast lithological data from the Horden Member revealed that the Magnesian Limestone content of the till was less than 40 %, and he suggested that the Horden Member was partly derived from the underlying Blackhall Member. Variations in the Carboniferous Limestone content within the Horden Member were larger than in the Blackhall Member. Sandstone was higher in the Horden Member, and red sandstones, greywacke, coal and siltstone were present in small quantities (Beaumont, 1967).

Various processes have been proposed to explain the formation for the Blackhall and Horden Members, such as a tiered, stacked ice sheet with the Horden and Blackhall Members representing the dirty base of the two ice sheets (Catt & Penny, 1966). Beaumont (1967) argued that this explanation was unlikely and that there are no present day examples of this phenomenon; it is glaciologically implausible. The Horden Member is more likely to be a basal till from an ice sheet that overrode the Blackhall Member after the recession of Lake District ice (Beaumont, 1967).

The Horden Member has a much-localised distribution, and extends 10 km west of the Durham coastline (Figure 1.6). Clast macro-fabric data and bedrock striae indicate that the ice sheet flowed from the northeast to southwest. Teasdale and Hughes (1999) suggested that the till was possibly deposited by the Late Devensian North Sea Lobe, sourced from the Cheviots and the Firth of Forth. It passed the coast of northeast England and advanced south along the Yorkshire coast, before terminating to the northeast of Norfolk. The North Sea Lobe was perhaps held in this position by Scandinavian ice in the North Sea Basin (Teasdale & Hughes, 1999; Svendsen *et al.*, 2004).

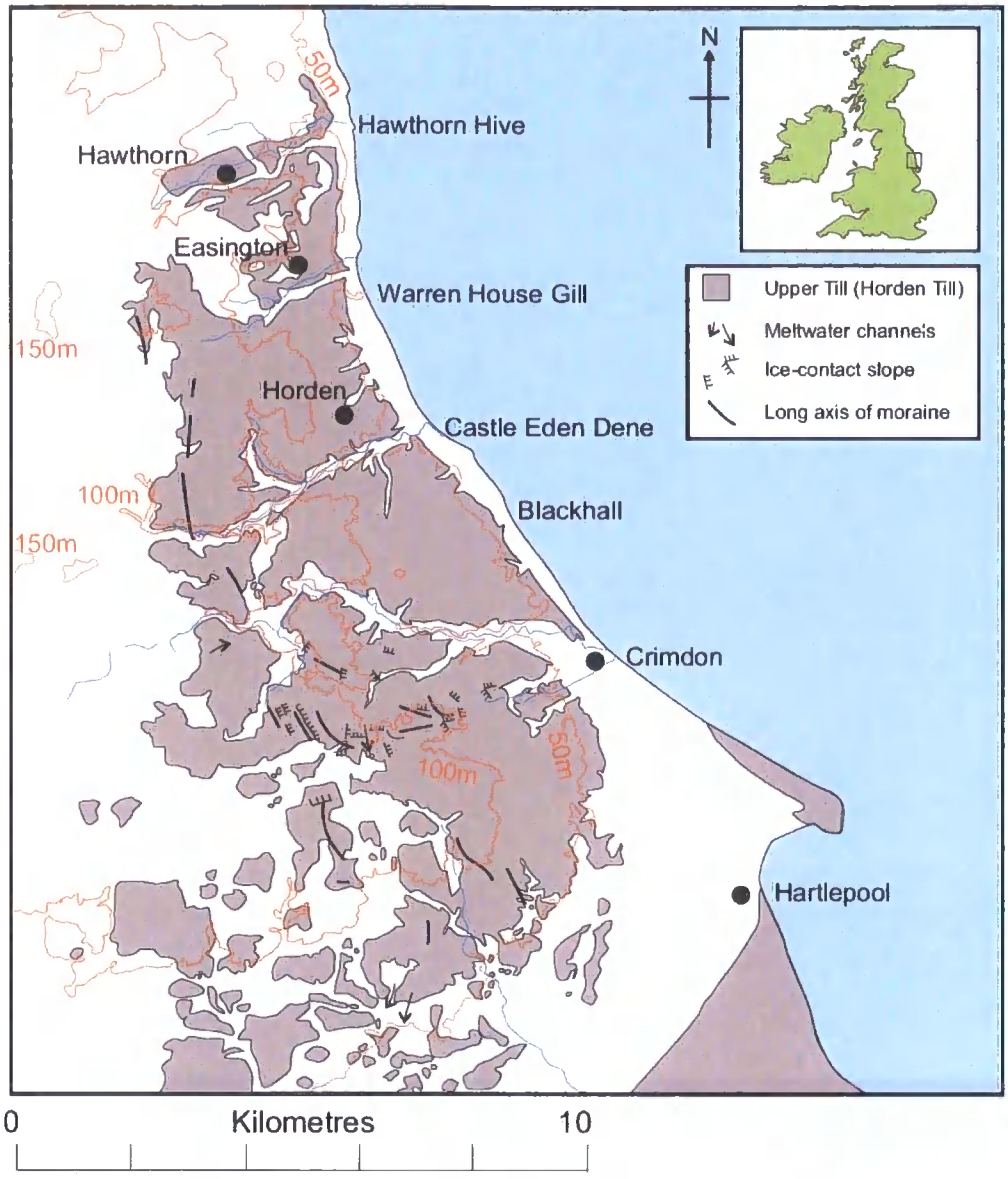

Figure 1.6: Map to show distribution of the Horden Member, moraines, ice-contact slopes, and meltwater channels (after Smith & Francis, 1967).

1.4 Key Conceptual and Theoretical Frameworks addressed in this Thesis

British Quaternary stratigraphy therefore has several key knowledge gaps that this thesis will address. This thesis attempts to address key issues regarding, firstly, the depositional processes, interlobate dynamics and ice flow pathways of Devensian glacigenic sediments in County Durham. The key issues include whether these ice lobes were contemporary or whether there was a period of subaerial exposure, the evidence for a North Sea Lobe, and the reasons for the its existence. Critical to this discussion is the influence of changing ice divides, and the influence this has on the glaciation of County Durham.

Secondly, this thesis looks at the long-term Quaternary history of County Durham, and examines the evidence for onshore Fennoscandian ice in eastern England. The goal of this research is to investigate the glaciological conditions that will allow the Fennoscandian ice sheet to reach eastern England before the British ice sheet. Additionally, the site at Warren House Gill is ideally located to test new stratigraphic models proposed in Norfolk (see Chapter 1.2.1).

Thirdly, this thesis examines an interglacial raised beach with the aim of establishing its age and stratigraphical relationship to the Warren House Fm. Constraining the age of the raised beach has implications regarding long-term tectonic uplift of the United Kingdom, which again is important to accurately identify to predict future sea level changes and crustal responses to isostatic loading. Finally, this thesis attempts to constrain onshore-offshore correlations, and to investigate the provenance of some key formations in the North Sea Basin, on order to identify any evidence for Fennoscandian ice in the western North Sea.

CHAPTER 2

Methodology and Techniques

2.1 Introduction

The procedures outlined in this section have four goals: correlation of lithofacies between sites, provenance of sediments, processes of deposition, and chronology of the sediments (cf. Walden, 2004). The geochemical and lithological properties of a sediment can be used to identify a likely source. Chemical, lithological or mineralogical 'fingerprinting' of a sediment, as illustrated in this chapter, is the only definitive method for defining ice sources and ice flow pathways. Therefore, in order to reconstruct the ice sheet history of the UK, this project uses a quantified, multi-proxy approach to create a coherent description and characterisation of the sediments present. This approach enhances each individual technique and the combined, integrated results of multiple data sources results in robust and detailed interpretations. The use of multivariate statistical analysis on the fully quantified data identifies trends and correlations that are otherwise difficult to discern objectively.

This chapter outlines the methods used and explains their applications and relevance. Field techniques include section logging, clast macro-fabrics, striae measurements, clast shape, used in conjunction with thin-section analysis. Quantitative lithological and geochemical techniques include sedimentary descriptions, particle-size analysis, heavy-mineral analysis, clast-lithological analysis, and ICP-Mass Spectrometry, combined with statistical analysis of the data (Principle Components Analysis and Cluster Analysis), and biostratigraphical data (foraminifera, palynomorphs, and macrofauna). This chapter also summarises the relevant dating techniques used (U-series, Optically Stimulated Luminescence (OSL) and Amino Acid Racemisation (AAR)), as conducted by workers at Royal Holloway, University of London, and the University of York.

2.2 A Scientific Methodology

This section outlines the scientific methodologies used during this project and identifies the rationale behind them. One of the key principles of the modern philosophy of science is the deductive creation of hypotheses to critically test in the course of scientific research. The initial structuring of the model depends in part on the operational constraints, such as what experiments will be required, what instruments and techniques are available, and what field and laboratory techniques exist (Goudie *et al.*, 1994). However, Quaternary geology often necessitates an inductive approach due to the incomplete stratigraphical record.

Case studies are common in geological and geomorphological research. However, they can be limited and unrepresentative, becoming trivia and embroiled in minutiae. It is therefore important to establish representation, by using multiple case studies and previous work. By using secondary data, the case study is situated within the wider area of research, which establishes its representativeness (Richards, 1996). The research presented in this thesis uses detailed case studies, but the wider data regarding ice sheet dynamics is fully considered in this thesis.

This research therefore is situated within the paradigm of reconstructing climate change, with a wider justification of understanding the long term trends and fluctuations of ice sheet behaviour and driving mechanisms, so that it can be used as a predictive tool for future climate change (Boulton *et al.*, 1991; Bowen *et al.*, 2002; Boulton & Hagdorn, 2006). This research uses five intensive case studies (Whitburn Bay, Hawthorn Hive, Shippersea Bay, Warren House Gill and boreholes from the North Sea Basin) to critically test well-defined hypotheses. Each of the sites is an intense observational study. These case studies are situated within a wider area of research into the BIIS during the Quaternary.

2.3 Field Techniques

2.3.1 Lithostratigraphy

Lithostratigraphy

Lithostratigraphy is the 'classification of bodies of rock based on the observable lithological properties of the strata and their relative stratigraphic positions' (Weerts & Westerhoff, 2007). Stratigraphy includes information about processes, geographical distributions, and the palaeo-environment of past glaciers and glaciation. It involves an attempt to determine the chronological sequence of geological events over a wide area. Lithofacies associations, landform-sediment assemblages, depositional processes, syn-depositional tectonics, landsystems, and geochronology are combined in a hierarchical structure to form a 'stratigraphy', through which the history and patterns of past glaciations and their associated environments can be reconstructed and interpreted (Rose & Menzies, 1996; Weerts & Westerhoff, 2007).

Sedimentological approaches should be based upon the 'lithostratigraphic unit', which has distinctive lithological properties, should be capable of being mapped and is typically tabular (Salvador, 1994; McMillan, 2005). The lithostratigraphic unit has a hierarchical system with the Group, Formation, Member and Bed sub-categories (Rawson *et al.*, 2002), and each new mappable lithostratigraphic unit must be formally proposed with a stratotype, and described emphasising lithological properties (Salvador, 1994; Weerts & Westerhoff, 2007). A lithostratigraphic scheme therefore:

1. has a hierarchical structure with the formation as the central (top) unit;
2. has a clear nomenclature;
3. describes each facies properly;
4. Contains mappable units only.

Therefore, in this research, the overall facies architecture and different lithofacies associations are mapped, logged and described in detail. The lithofacies associations are ultimately interpreted within a sediment-landform association, primarily in order to assess the processes by which glacigenic sediments were deposited and deformed. Through detailed lithological and petrological analysis, correlations between lithofacies associations and to regional stratotypes, based on processes of deposition, lithological and petrological

similarity, and chronostratigraphy, are possible. Ultimately, it is possible to make statements about provenance, age, and regional glacial lithostratigraphy.

Vertical Profiles

Lithostratigraphy must take a hierarchical approach. The first stage is individual sediment logging. Vertical profiles are a method of recording detailed sedimentological information from a section, and they can be used for the comparison and correlation of different localities. They highlight gradual, particularly vertical, trends, and provide a representative summary of exposures (Jones *et al.*, 1999). Detailed sketches of macro-scale features such as deformation structures can provide information regarding the genesis and depositional history of glacigenic sediments. The colour of a sediment is the most immediately visible property, and can indicate more fundamental differences in composition, such as mineralogy (Gale & Hoare, 1991). Identifying the colour of a sediment is essential if the lithology is to be fully characterised. Facies characteristics are noted using standard facies codes (Table 2.1).

Therefore, in each on-shore field location, a GPS, photography and sketches were utilised to accurately map the overall facies architecture and to record spatial relationships between lithofacies. Specific exposures were sketched and logged according to standard procedures (Evans & Benn, 2004), noting the sedimentary structures, contacts, deformation structures, Munsell colour, texture, particle size, clast lithology and shape, grading, and sorting of each facies. All sections were levelled to metres O.D. using standard levelling techniques.

Table 2.1: Glossary of abbreviations used in section logs (Krüger & Kjaer, 1999; Evans & Benn, 2004).

Diamicton	
Dm	Diamicton, matrix-supported
Dmm	Diamicton, massive, matrix-supported
Dms	Stratified matrix-supported diamicton
Dcm	Clast-supported diamicton
Dmg	Matrix-supported, graded
Dml	Matrix supported, laminated
--- (p)	Includes clast pavement
--- (g)	Graded diamicton
--- (b/s)	Banded / sheared
Silts and Clays (<0.063 mm)	
Fm	Fines, massive
Fl	Fines, laminated.
Flv	Fine lamination with rhythmites or varves.
Frg	Graded or climbing-ripple cross-lamination
Fcpl	Cycopels
Fp	Intraclast or lens
---(d)	with dropstones
--- (w)	with dewatering
Sands (0.063 to 2 mm)	
Sm	Massive sand
St (A)	Ripple cross laminated (Type A)
St (B)	Ripple cross laminated (Type B)
St (S)	Ripple cross laminated (Type S)
Scr	Climbing ripples
Ssr	Starved ripples
Sr	Sand, ripple-cross laminated
Sh	Very fine to very coarse and horizontally / planar bedded or low angle cross lamination
Sd	Deformed bedding
St	Medium to very coarse trough cross-bedded
Sp	Medium to very coarse planar cross-bedded
Sl	horizontal or draped lamination
Sh	Sheared sand
Sfo	Deltaic foresets
Sfl	Flasar bedded
Se	Erosional scours with intraclasts and crudely cross-bedded
Su	Fine to coarse with broad shallow scours and cross-stratification
Sc	Steeply dipping planar cross bedding
Suc	Upward coarsening
Suf	Upward fining
Srg	Graded cross-lamination
SB	Bouma sequence
Scps	Cycoplasms
--- (d)	with dropstones
--- (w)	with dewatering
Fine Gravel (2-8 mm)	
GRcl	Massive with clay laminae
GRch	Massive and infilling channels
GRh	Horizontally bedded
GRm	Massive and homogenous
GRmb	Massive and pseudo-bedded
GRmc	Massive with isolated outsize clasts
GRmi	Massive with isolated, imbricated clasts
GRmp	Massive with clast stringers
GRo	Openwork structure
GRruc	Repeated upward-coarsening cycles
GRruf	repeated upward-fining cycles
GRt	Trough cross-bedded gravel
GRcu	Upward coarsening (inverse grading)
GRfu	Upward fining (normal)
GRp	Cross-bedded
GRfo	Deltaic foresets
Coarse Gravel (8-256 mm)	
Gms	Matrix supported, massive gravel
Gm	Clast supported, massive
Gsi	Matrix supported, imbricated
Gmi	Clast supported, massive, imbricated
Gfo	Deltaic foresets
Gh	Horizontally-stratified gravel
Gt	Trough cross-bedded gravel
Gp	Gravel, planar-cross bedded
Gfu	Upward fining (normal grading)
Gcu	Upward coarsening (inverse grading)
Go	Open framework gravels
Gd	Deformed bedding
Glg	Palimpsest (marine) or bedload lag
Boulders (>256 mm)	
B	Boulders
Bh	Horizontally-bedded boulders
Bms	Matrix supported, massive
Bcg	Clast supported, graded
BL	Boulder lag or pavement
Bfo	Deltaic foresets
Bmg	Matrix supported, graded
Structure	
Bo	Boudinage
Be	Bedding
Ba	Banding

Lithofacies Associations

Each facies is characterised by its individual properties in the vertical profile. On the basis of physical similarities, these sedimentary facies are correlated to form 'lithofacies' (Evans & Benn, 2004). Lithofacies are sediments with a distinctive combination of properties, classified on the basis of their colour, texture, the lithology of clastic particles, thickness and geometry, presence / absence of fossils, and other sedimentary structures (Eyles & Lazorek, 2007). Their spatial organisation is logged using an overall facies architecture sketch. It is important to separate detailed field description and labelling from genetic perspectives and terminology. Inadequate field descriptions thwart later sophisticated environmental re-interpretation (Eyles & Eyles, 1983), as the interpretation of a genetic facies is subject to revision as ideas and knowledge change and the science develops. Lithofacies therefore are identified only on their physical, biological and chemical characteristics, with no inferred genesis (Evans & Benn, 2004). This separation of description and interpretation ensures a more objective approach, less prone to bias, error and subjectivity. In this thesis, each chapter is analysed separately and the sediments are assigned to lithofacies associations particular to that specific site. Regional correlations are drawn together in Chapter 8.

A hierarchical approach to sedimentology is a powerful tool for describing how sediments, landforms and landscapes fit together, and in determining how the landscape reflects depositional processes and external controls on the environment (Benn & Evans, 2004). However, sediments are laid down in associations; these assemblages reflect a range of processes active in any one given environment (Benn & Evans, 2004), which can be deposited at a range of scales. 'Lithofacies Associations' (LFAs) are distinct vertical successions of genetically related lithofacies (Eyles & Lazorek, 2007). Through recognising these packages, ancient glacial settings can be recognised and reconstructed.

Landsystems

Lithofacies associations can be analysed in conjunction with landforms to create sediment-landform associations (Evans & Benn, 2007). Sediment-landform suites are indicative and characteristic of specific styles of glaciation ('glacial landsystems'), such as surging glaciers, ice streams, plateau ice fields, sub-aquatic landsystems, and active-temperate terrestrial ice margins (Evans, 2003b). Glacial landsystems are composed of 'land units' (geomorphological features such as drumlin fields, moraine belts, etc.) and 'land elements' (a tunnel valley, a moraine, an esker, and the associated sediments), which

together form a landsystem, a 'recurrent pattern of genetically linked land units' (Evans, 2007b). Recent analyses of glacial landsystems stress their complexity and the fact that sediment-landform associations are dictated by the location and style of deposition (e.g., Alexanderson *et al.*, 2002; Evans & Twigg, 2002; Jennings, 2006; Lukas, 2006; Ottesen *et al.*, 2008)

2.3.2 Clast Shape, Till Fabrics and Striae Orientation

Clast Angularity-Roundness

Clasts inherit their shapes from the surrounding environment; erosion, transportation and weathering give clasts distinctive geomorphological signatures (Benn, 2007a). Angularity-roundness is simple to measure in the field when undertaking till-fabric analysis. Descriptive criteria are used to assign clasts to a roundness category (Table 2.2). A semi-quantitative approach is used, considering the whole shape of the clast. The sharpest edge may not be representative of the whole roundness. Clasts are therefore assigned to categories based on descriptive criteria (Benn, 1994). First order clast morphology was not conducted due to time constraints.

Table 2.2: Descriptive clast-roundness categories. From Benn (2007).

Very Angular (VA)	Edges and faces unworn, sharp, delicate protuberances.
Angular (A)	Faces and edges unworn.
Subangular (SA)	Faces unworn, edges worn.
Subrounded (SR)	Faces and edges worn but clearly distinguishable
Rounded (R)	Edges and faces worn and barely distinguishable
Well Rounded (WR)	No edges or faces distinguishable

Clast Macro-Fabric Analysis

The measurement of the arrangement of clasts within a diamicton can be a powerful tool in the analysis of Quaternary sediments (Benn, 2004), and it is traditionally used, in conjunction with striae data, as a standard quantitative tool in the analysis of past ice flow directions. More recently, till fabric data has been used to infer process (Carr & Rose, 2003). In this thesis, till fabric data is used together with striae data to reconstruct ice flow direction, and where possible it has been used to help interpret depositional processes. The resulting data are three mutually orthogonal eigenvectors (V_1, V_2 and V_3), with the principal eigenvector, V_1, being parallel to the axis of maximum clustering in the data. V_3 is normal to the preferred plane of the fabric. The degree of clustering about the

eigenvectors is given by the eigenvalues S_1, S_2, and S_3, with their relative magnitudes reflecting the fabric shape (Hubbard & Glasser, 2005). A-axis fabric data has a long history of research (Lawson, 1979; Hicock *et al.*, 1996; Benn, 2004). Coulomb plastic behaviour involves slippage between clasts and the surrounding, faster-flowing matrix. Therefore, more elongate clasts assume a minimum cross-sectional area, orientating the a-axis parallel to main stress direction. This makes strong, consistent till macro-fabrics in tills useful in interpreting palaeo ice-flow directions (Jónsdóttir *et al.*, 1999).

Jæren, south-west Norway, forms the onshore border of the Norwegian Channel ice stream. The Jæren escarpment, separating Low Jæren from High Jæren, was formed by erosion by the ice stream, which occupied the Norwegian Channel on multiple occasions during Pleistocene glaciations (Jónsdóttir *et al.*, 1999). Early analysis of the till macro-fabrics indicated a strong westerly to south-westerly flow direction, but in Stavnheim, further south in Jæren, till fabrics measured a northwest to west component (Andersen *et al.*, 1987). Andersen *et al.* (1987) argued that the glacier in Low Jæren moved north-westwards in an earlier phase, and then later moved in a westerly direction. Jónsdóttir *et al.* (1999) analysed till macro-fabrics and striations, aiming to delineate the pattern of regional glacial movements using macro-fabrics and clast lithology. They interpreted the glacigenic sediments as lodgement tills. The upper till had a strong, unimodal clustering of clast axes around the mean axis, resulting in a high significance value. The clast fabric from the lower till had a weak, equatorial, near random orientation of clast axes (Jónsdóttir *et al.*, 1999). The direction of maximum clustering (V_1 157° to 161°) coincided with the direction of the Jæren escarpment axis. Jónsdóttir *et al.* (1999) interpreted the upper fabric as representing palaeo ice flow direction as towards the northwest. The lower fabric was, however, probably influenced by cobbles and boulders, leading to a local fabric probably unrelated to glacier flow.

Recently, eigenvalues (S values) and vectors (V values) have been used to infer the genesis of glacial materials, indicating factors such as the rheology of the sediment. For example, debris-rich basal ice subjected to high cumulative strains tends to have strongly clustered clast macro-fabrics, whereas tills formed under low strain can have either strongly clustered or highly variable clast macro-fabrics (Benn, 2004). Other researchers have found strong fabrics at low strains (Iverson *et al.*, 1995; Hooyer & Iverson, 2000). Hicock *et al.* (1996) advise caution in using till fabrics to infer genesis of sediments, and suggest that they only be used as a starting point. Eigenvalues cannot be used alone, given the complexity of the subglacial environment (Hicock *et al.*, 1996).

Some researchers have argued that Jeffery-type rotation (Figure 2.1) is incompatible with the deforming bed hypothesis (Piotrowski *et al.*, 2001). March-type rotation (Figure 2.1) through plastic deformation has been identified as the dominant mode of clast orientation in deforming tills (Benn & Evans, 1996). Weak clast macro-fabrics have often been reported as typical of deforming bed tills (Hart, 1997), suggesting that particles are here free to rotate in a viscous medium (Evans *et al.*, 2006). Inhomogeneous deformation may produce a range of clast macro-fabric strengths, and localised fabric patterns reflect the deformation history and local strain conditions of the sediment (Evans *et al.*, 2006).

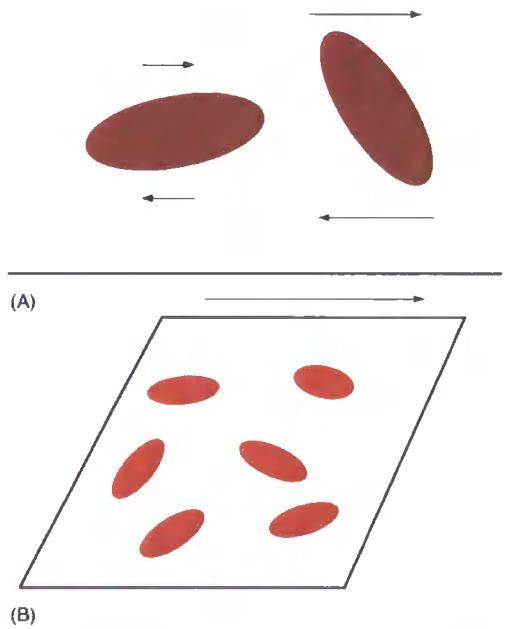

Figure 2.1: Schematic diagram illustrating (A) Jeffery Rotation and (B) March Rotation. In Jeffery Rotation clasts are continually rotated as a result of vertical velocity gradients, whereas in March Rotation (B), clasts passively trace the deformation of the surrounding medium (from Benn, 2007b)

Carr and Rose (2003) concluded that "particle orientations in subglacial diamictons reflect the strain response of the sediment to the applied total stress during subglacial deformation", and that particles of different size are rarely consistently orientated in relation to ice flow direction. Therefore it is important to limit the size range in the sample (Carr & Rose, 2003).

To obtain the clast measurements, clasts in the approximate size range 8-32 mm were excavated and the long axis (a-axis) and dip angle of 50 clasts per exposure was recorded, using a compass-clinometer (Benn, 2007b). The data are presented in equal-area stereonets and rose diagrams, according to procedures in Evans and Benn (2004) and Benn (2007b).

Clasts were sampled from a 2 m^2 area. Only clasts with elongate a-axes were measured, with ratios of >1.5:1 (Benn, 2004). All three eigenvalues are given.

Striae Orientation

Striae are used in conjunction with till-fabric analysis to reconstruct past ice-flow directions. Striae on individual *in situ* clasts and boulders were measured using a compass-clinometer. Up to 50 striae sets were collected per exposure, and at least 10 per clast. If a clast showed several sets of striae, then these were also noted. The data were collated and presented in rose diagrams.

Striae orientation has been often been used successfully in conjunction with clast macro-fabric analysis to determine palaeo ice flow directions (Hicock & Fuller, 1995). In addition, striae on bedrock forms can be used to infer palaeo ice flow directions (Haavisto-Hyvärinen, 1997; Ballantyne, 1999; Roberts *et al.*, 2007). Striations are important as they provide an independent evidence for ice flow (Benn, 2004).

2.4 Thin-section analysis

2.4.1 Introduction

Micromorphology is the microscopic examination of the composition and structure of sediments. It was originally developed in soil science, with concepts of plasmic fabric and morphological features and structures dating from the early 1960s (Bullock *et al.*, 1985). The undisturbed sediments are examined for a range of recognised microstructures, such as those first described by van der Meer (1993) and Menzies and Maltman (1992). They introduced key terms and concepts still used today, such as 'plasmic fabrics', and identified key structures indicative of subglacial deformation, such as rotational structures, necking structures, and crushed grains (van der Meer, 1997; Menzies, 2000; Menzies *et al.*, 2006). These structures can be used to account for the origins of a sediment, its transport pathways, and the processes of deposition and deformation (Ó Cofaigh & Dowdeswell, 2001; McCarroll & Rijsdijk, 2003). Micromorphology now provides detailed information to aid the interpretation of sediments that are often massive at macroscale, and can give valuable information regarding genesis, deformation history and strain rates (Carr, 2004a).

Later developments attempted to quantify micromorphology and introduce guidelines into its application to glacial sediments (Carr, 2001; Carr, 2004a). Structural geology recently influenced the development of micromorphology, and analysis of structural features in subglacially and proglacially deformed materials can additionally identify different types of characteristic subglacial deformation (Phillips *et al.*, 2007). Systematic structural analysis gives a deeper understanding of tectonostratigraphic sequences in soft sediments, and the glacier-induced stresses responsible for their development (Phillips *et al.*, 2002).

Now, the combined use of sedimentology and micromorphology is important in determining the processes of deposition, post-depositional deformation, and porewater fluctuations in glacigenic sediments. It can be used carefully to discriminate between macroscopically similar diamictons, such as debris flows, traction tills, and glaciomarine and glaciolacustrine sediments (Licht *et al.*, 1999; Carr, 2001). Furthermore, thin-section microfabrics give valuable information regarding genesis and strain directions in the absence of other directional features, such as clast macro-fabrics (Carr, 2001). Micromorphology can be used to account for the origins of a sediment, its transport

pathways, and the processes of deposition and deformation. These can be combined to create an understanding of sediment-landform associations and landsystems.

2.4.2 Sample Collection and Preparation

Thin sections were sampled using Kubiena tins. Representative (and replicate samples where pragmatically possible) samples were collected from each lithofacies. These undisturbed samples were then prepared according to standard techniques (Murphy, 1986; van der Meer, 1993; Lee & Kemp, 1994) by Mr David Sales (Department of Earth Sciences, Durham University. See Appendix I).

2.4.3 Sample analysis

The unlithified, undisturbed samples were analysed at multiple magnifications under petrological microscopes (*Leica DM EP* and *Meiji Techno EM2-13TR* models). The optical properties and relative orientations of the particles can determine the genetic stress history of the sediments. Using both plane- and cross-polarised light highlights the textural and structural characteristics of the sample. Thin sections were investigated at low magnifications between x10 and x100, as higher magnifications observe individual grains, which may not be helpful for structural interpretation.

The analysis of thin sections must employ a systematic, standardised description to be used meaningfully (Carr, 2001), such as that outlined in Table 2.3. Presentation of all data in a single table allows easy comparison between samples. A table of symbols used in the presentation of data is given in Figure 2.2. A glossary of terms used in analysis of thin sections is given in Table 2.4. Where possible, photomicrographs and scans show distinct features. Where this is not possible due to the magnification of the image, features that cannot be seen have been marked on to show their position and orientation. Arrows on rotational structures have no inferred direction.

Table 2.3: Approach for investigation of glacigenic sediments. Adapted from Carr, 2004.

1. Characterisation of Thin Section Sample identification Sample location Macroscopic description of sample.	
2. Textural Analysis *A. Skeleton* Size ranges Particle shape and form Distribution Composition *B. Plasma / Matrix* Texture Density Distribution	**3. Structural Analysis** *A. Voids* Void ration, type, distribution *B. Macrofabric* Horizontal / vertical *C. Structures* Sedimentary structures Deformation structures Diagnostic features for specific environments Diagenesis and post depositional alteration
4. Plasma Fabric Plasma fabric types, distribution, strength	
5. Interpretation	

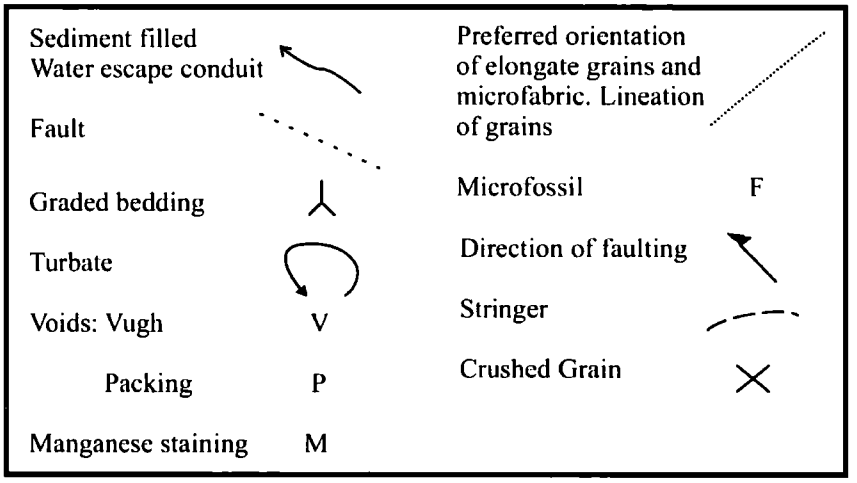

Figure 2.2: Key to symbols used in presentation of thin sections in this thesis. Arrows on turbates do not indicate direction of rotation.

Table 2.4: Glossary of common terms used in micromorphology (after van der Meer, 1993; Perkins, 1998; Carr, 2001; Carr, 2004a; Menzies *et al.*, 2006; Hiemstra, 2007). Refer also to Figure 2.3.

Anisotropic	The anisotropic skeleton grains and plasmic matrix of the slide transmit plane polarised light, but under cross-polarised light they extinguish (i.e. transmit no light) four times per complete rotation, every 90°. The refractive index therefore varies with direction.
Birefringence	Optical property in which interference colours become visible by turning the stage of the microscope; cause by double refraction of light under crossed polarisers and consequent polarising of bundles of light.

Cross polarised light (XPL)	When passing plane polarised light through a second filter at 90° to the first (the upper polariser), we see the light through crossed polars. Cross-polarised light is used to determine properties such as dispersion, birefringence, and extinction.
Domain	Small zones in which clay particles are orientated parallel to each other, causing them to behave (optically) as a single crystal. Subglacial tills may exhibit multiple domains with banding and stratification.
Edge-to-edge crushing	Clast fragments touching at the edges with visible breakage contacts. Breaking and grinding may have occurred in response to high stress levels resulting in significant grain-to-grain contacts along grain edge asperities. More common in areas with low pore water content.
Galaxy / turbate / Rotational structure	Circular alignments of grains around cores of consolidated sediment or larger grains; indicative of rotation. Closely associated with planar features. For example, van der Meer (1993) and Hart (2007).
Grain stacks	Edge-to-edge grains forming to support developing stresses. Develop perpendicular to the stress field. For example, Menzies (2000) and Menzies *et al.* (2006).
Grain alignments	Preferred long axis of skeleton grains. Numerous grains in a row with aligned long axes. E.g., Hiemstra & Rijsdijk (2003).
Interference colours	The colour of anisotropic minerals under crossed polars varies, and the same mineral shows different colours depending on crystallographic orientation. These colours are on Newton's Scale, divided into several orders: • 1st Order: grey, white, yellow, red • 2nd Order: violet, blue, green, yellow, orange, red • 3rd Order: indigo, green, blue, yellow, red, violet • 4th Order and above: pale pinks and greens.
Isotropic	Isotropic minerals remain black in all positions when viewed under cross-polarised light. They have random atomic structures, so that structure and refractive index are the same in all directions.
Lineations	Lines of skeleton grains with aligned long axes. May indicate shear zone. For example, Hart (2007).
Microfabric	Skeleton grains commonly show preferred long axis. The vertical arrangement of skeleton grains. For example, Carr (2001).
Necking structure	Squeezing of plasma between skeleton grains. Indicative of matrix flowage.
Plane polarised light (PPL)	In normal, unpolarised light, waves vibrate in all directions. Filtering the light beam in the microscope with the lower polariser makes all the light waves vibrate in one direction, parallel to a particular plane.
Plasma (matrix)	Grains of colloidal size (< 2 μm); may consist of clay minerals, oxides and hydroxides of Fe, Al and Mn, soluble salts, etc. Often used to refer to matrix – all material smaller than the thickness of the thin section. Individual particles cannot be seen.
Plasmic fabric:	Birefringence models of the plasma. Based on optical properties of the particles as well as the optical properties caused by the orientation of particles relative to each other. For example, see Khatawa & Tulaczyk (2001) and Carr (2001).

- ***Skelsepic***	Plasma particles orientated around a skeleton grain. May form in several ways, such as grain rotation under shear stress, or following massive deformation resulting in homogenisation of the bulk sediment.
- ***Masepic***	Plasma particles orientated in bands
- ***Omnisepic***	Plasma particles orientated randomly, revealing many different orientation directions.
- ***Unistrial***	Anisotropic clay with clear birefringence bands in one direction. Indicates a very strong preferred but horizontally localised orientation of thin lines of clay-sized particles within the till facies, indicative of the prolonged application of high stress.
- ***Lattisepic***	Plasma separations occur in two very short, discontinuous sets, orientated at right angles to each other.
Polyphase microstructures	Fluctuating porewater pressure and content resulting in overprinting of ductile and brittle features.
Pressure shadows	Symmetric or asymmetric tails of material on the stoss and lee of large grains. Indicative of planar shearing (symmetric) or rotation (asymmetric). For example, Phillips (2006)
Short distance lineations	Lineations no longer than 15mm in length and never touching adjacent larger clasts (for example, Menzies *et al.*, (2006)).
Skeleton grains	Single sand or coarse silt grains which are larger than the thickness of a thin section (20 to 30 μm).
Till Pebbles:	Soft sediment intraclasts; torn up and reworked fragments of unconsolidated sediment.
- ***Pebble Type I***	Arrangement of brecciated sediment such that it appears to form a series of rounded intraclasts delineated by packing voids.
- ***Pebble Type II***	Soft sediment intraclasts of material similar in nature to the surrounding sample, but with a clearly defined discrete internal plasmic fabric.
- ***Pebble Type III***	Soft sediment intraclasts of material different in nature to the surrounding sample: evidence of reworking of pre-existing sediments.
Vugh void	Irregularly shaped area with diffuse boundaries filled with resin. Caused by poor impregnation of thin section. Packing voids are caused during field sampling.

Recent research has expanded greatly on van der Meer's (1993) classic interpretations, and the development of criteria to identify different depositional environments. Hiemstra and Rijsdijk (2003) used artificially induced strain in potter's clay to investigate typical features found in subglacial diamictons. They found a close relationship between unistrial plasmic fabrics and rotational structures (Figure 2.3), and both increased in number with increasing strain. Grain lineations commonly occur in association with rotational structures such as turbates (Hiemstra & Rijsdijk, 2003).

Detailed micromorphological study has highlighted the importance of grain size variation in the production of rotational structures (Hart *et al.*, 2004). Individual larger

clasts may generate perturbations, allowing characteristic rotational structures to develop. Increases in grain size allow for more perturbations. As a result, a poorly sorted, coarse-grained till will be more micromorphologically inhomogeneous than a finer-grained till. Stringer initiation and deformable clasts with tails also indicate syntectonic rotation in a ductile, shearing medium (Roberts & Hart, 2005). The combination of lateral shear (Hart, 2007) and rotational movement results in a variable response to the applied stress field according to grain size.

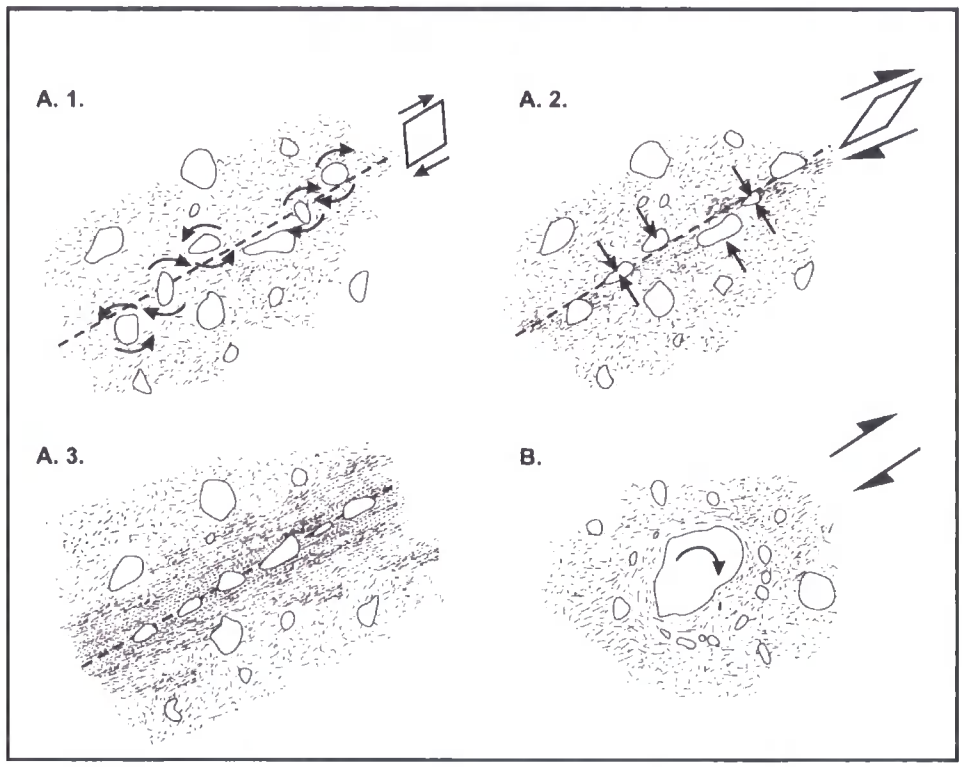

Figure 2.3: Conceptual diagram illustrating the relationship between plasmic fabric and aligned grains in response to simple shear (A) and the relationship between unidirectional plasmic fabrics, turbates, and skelsepic plasmic fabrics (B). Adapted from Hiemstra and Rijsdijk (2003).

Hart *et al.* (2004) argued that the rotational process mobilises particles by incorporating grains from the subjacent undeformed bed, as evidenced by van der Meer's 'Till Pebbles' (van der Meer, 1993). Hart *et al.* (2004) therefore proposed that subglacial deformation tills contain associations of rotational features, such as skelsepic plasmic fabrics, orientations of smaller skeleton grains around larger ones, and rotated, augen-like features with tails, with intermediate and linear features. Linear features include inclined clasts, lines of grains (lineations) and fragmentation of clasts. Intermediate features include mini-shear zones with internal rotation, and clay intraclasts with internal plasmic fabric

(Hart *et al.*, 2004). They argued that deformation tills contain a juxtaposition of rotational and linear features. This is a result of dynamism within the subglacial deforming till layer at the microscale, and is related to temporal and spatial variations in porewater content and pressure. The overprinting of ductile and brittle deformation within the same area of till is evidence of sudden phase changes related to fluctuating porewater pressure (Menzies *et al.*, 2006).

These structures are illustrated in the conceptual diagrams (Figure 2.3 and Figure 2.4). Figure 2.4 was developed from work by Van der Meer (1993), Menzies (2000), Hiemstra and Rijsdijk (2003), and Menzies *et al.* (2006). The structures are categorised by their genesis. These images only reflect structures observed in glacigenic sediments at Whitburn Bay, Warren House Gill, and in various boreholes in the North Sea.

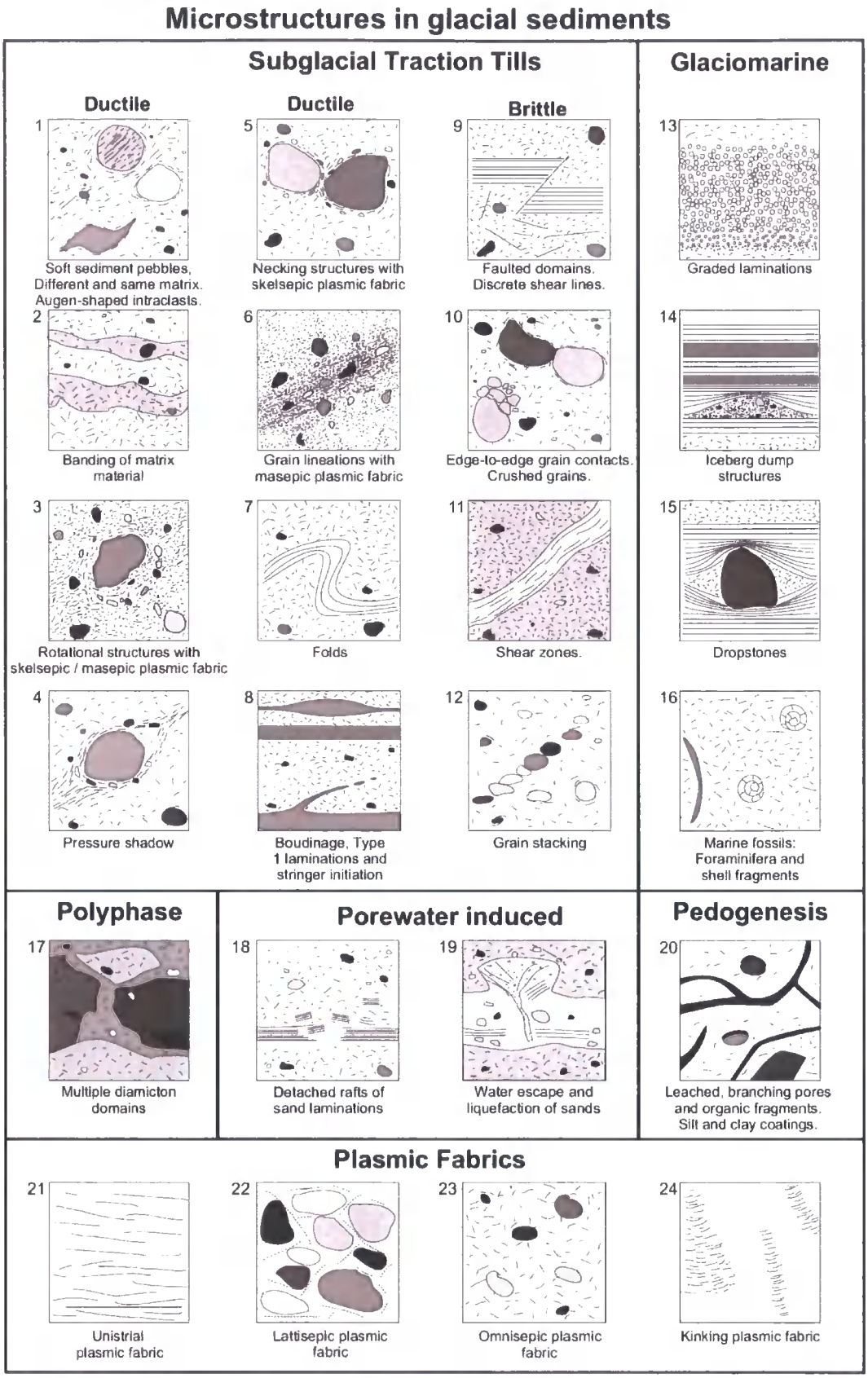

Figure 2.4: Microstructures and plasmic fabrics observed from glacigenic sediments in this study. After van der Meer (1993), Menzies (2000), Menzies *et al.* (2006), and Hiemstra and Rijsdijk (2003).

2.5 The Interpretation of Glacigenic Sediments

Thin-section analysis can therefore be used in conjunction with macroscale sedimentological analysis to identify subglacial processes. Traditionally, tills have been subdivided based on the typical processes assumed to have been dominant in their formation. These were thought principally to be sliding (Brown *et al.*, 1987), lodgement (Dreimanis, 1989) and deformation (Alley *et al.*, 1986). Lodgement till has a long history of research, being originally defined by Chamberlin (1895) as,

> *Sediment deposited by plastering of glacial debris from a sliding glacier sole due to the combined effects of pressure melting and frictional drag.*

This process resulted in massive or fissile tills, with slickensides resulting from shearing (Boulton, 1970). Clasts are lodged into the substrate and have typical bullet-shaped ends and clear stoss-and-lee ends. Alternatively, deformation till (Elson, 1961; Benn & Evans, 1998) refers to a,

> *Rock or sediment that has largely been homogenised by shearing in the subglacial layer.*

Subglacial deformation of soft sediments is considered to account for much of the forward motion by glaciers (Alley *et al.*, 1986; Humphrey *et al.*, 1993). Massive tills are thought to record evidence of high cumulative strains (Hart *et al.*, 1990). Others have argued that massive tills are simply the product of melt-out (Clayton *et al.*, 1989). Larsen *et al.* (2004) argued that a melt-out / deformation continuum was responsible for thick sequences of massive tills, with vertical accretion of subglacial sediments being melted out at the ice-bed interface, and then deformed. However, if deformation of soft beds is widespread, then deformation tills should be more prevalent (cf. Piotrowski *et al.*, 2001), and macroscopically massive 'deformation' tills often overly undeformed sediments (Boulton & Hindmarsh, 1987).

Glacier motion by sliding and lodgement over soft beds (cf. Clark & Hansel, 1989) was thought to occur by the decoupling of the glacier from its bed due to increased basal water pressures, which would prevent the transmission of stress to the substrate (Brown *et*

al., 1987). This theory evolved into an proposal of 'slip-stick' sliding at the ice-bed interface, with areas of high water pressure inducing decoupling (Fischer & Clarke, 1997). Clay-rich tills are less permeable (cf. sandy tills), encouraging the development of high water pressures; stick-slip behaviour and decoupling may therefore be at least partially lithologically controlled (Boulton, 1996; Evans *et al.*, 2006). Piotrowski and Kraus (1997) were among the first to propose a mosaic of sliding bed conditions and deforming conditions, where the ice is coupled to the bed. This explains the heterogeneity in tills in Germany.

A continuum with lodgement and deformation end-members will lead to progressive changes in bed properties at a particular location (Lian & Hicock, 2000; Boulton *et al.*, 2001; Nelson *et al.*, 2005). This viewpoint highlights the spatial and temporal variability of glacier beds, with ice-bed coupling variability brought about by changes in pore-water pressure. Piotrowski *et al.* (2004) argued that the spatial variability in sliding intensity resulted in a mosaic with sliding conditions and deforming spots. During sliding, ploughing of clasts may take place. 'Glaciotectonite' (as originally defined by Banham, 1977; and Pedersen, 1988) refers to sheared rocks and sediments, which still retains some of structural characteristics of its parent material (Benn & Evans, 1998). They can display both brittle and ductile deformation, or a combination of the two processes.

Mass flow diamictons (or flow tills) originate from water and sediment released by ablation from debris-rich basal ice. These deposits are typically macroscopically massive. They may have microscopic near-horizontal laminations. Rotational structures, kinking plasmic fabrics, and tile structures form as primary depositional features on a micromorphological scale (Lachniet *et al.*, 2001). Debris flows share many characteristics in common with subglacial sediments, such as pressure shadows, folds, laminations, shears, faults, water-escape structures, and rotational structures (Phillips, 2006). Mass flow diamictons, however, can be distinguished by the presence of 'tile structures' in close association with rotational structures (Menzies & Zaniewski, 2003). This long and extensive history of thin-section analysis of glacigenic sediments has given rise to a set of well-defined criteria, summarised in Table 2.5.

Recently, several researchers have argued that processes at the ice-bed interface are a result of a continuum of processes, including melt-out, lodgement, deformation, and sliding (van der Meer *et al.*, 2003; Nelson *et al.*, 2005; Evans *et al.*, 2006; Menzies *et al.*, 2006). It is therefore difficult to pin an exact genetic name onto a specific outcrop of diamicton. Evans *et al.* (2006) argued that the subglacial processes of deformation, flow,

sliding, lodgement and ploughing all exist contemporaneously at the base of temperate ice. These processes result in the mobilisation, transportation and deposition of sediment. This results in stratified or folded to texturally homogenous diamictons. Evans *et al.* (2006) argued that, while specific processes can and should be recognised in the sedimentary record, genetic 'finger-printing' of subglacial tills should be less process-specific. Subglacial tills are polygenetic, and till classification must recognise the range of processes involved by the subglacial till 'production continuum' (Evans *et al.*, 2006). Evans *et al.* (2006) proposed the use of the terms, 'glaciotectonite', as defined above, and 'traction till', which includes sediments deposited by sliding or deforming at the glacier bed, sediment released by pressure melting, and sediment homogenised by shearing. While 'traction till' is a generic term for all these processes, they can still be individually recognised in the geological record. Evans *et al.* (2006) also formally recognise 'melt-out till', as a sediment released by melting or sublimation at stagnant or slowly-moving, debris-rich ice, without subsequent transport or deformation.

Glaciotectonic deformation of subglacial sediments can result in tectonic laminations, which are distinct from glaciomarine or subaqueous laminations. Roberts and Hart (2005) identified two types of lamination. Type 1 laminations / stringers typically emanate from soft sediment clasts (e.g. chalk), are discontinuous, subhorizontal, and ungraded. In thin section, Type 1 laminations have sharp, undulatory contacts with silty or sandy stringers. Isoclinal folds are common. Type 2 laminations are laterally continuous, subhorizontal, and poorly sorted with dropstone-like structures and often exhibit reworked soft sediment clasts. Contact boundaries are sharp and unconformable, and dropstone structures are evident. Microfabric birefringence is low, but there are some areas of high birefringence sub-parallel to silty lamination contacts (Roberts & Hart, 2005). Type 1 laminations are the result of subglacial deformation by ductile, inter-granular, pervasive shear. Hart and Roberts (1994) argued that this type of lamination occurs as a result of high extensional shear, leading to boudinage. Smaller, less competent perturbations, such as chalk clasts, can become stretched out into a lamination under this high shear strain. The laminations can deform and rotate within the deforming layer, producing tails to appear as sedimentary augens (Hart & Roberts, 1994).

Type 2 laminations have a subaqueous signal, despite often containing a number of syntectonic ductile deformation structures (Roberts & Hart, 2005). At West Runton, Norfolk, the subhorizontal lateral continuity and dropstone structures with down-warped lower contacts and draped upper contacts are indicative of primary subaqueous origin

followed by secondary subglacial deformation. The planar, bedded nature of the strata, with sharp contact boundaries, are characteristic of sediments deposited by underflows, overflows, suspension fallout, ice-rafted debris processes and subaqueous debris flows, with each lamination representing a clear separate depositional event (Roberts & Hart, 2005). The clear characteristics of these laminations enable easy discrimination of glaciomarine and glaciolacustrine diamictons.

Several additional criteria can distinguish massive and laminated glaciomarine diamictons from subglacial diamictons (Table 2.5). Glaciomarine diamictons usually have a coarse, winnowed structure with dropstones; common, *in situ* marine microfossils; a lack of deformation structures; laminations, banding, or graded bedding structures; and a lack of plasmic fabric development (Carr, 2001; Hiemstra, 2001; Roberts & Hart, 2005). Distal glaciomarine sediments are characterised by their bedding and lamination; a medium to fine matrix; uniform grain shapes; few deformation structures; dropstone features and no plasmic fabric development; and the presence of bioturbation (Carr, 2001). Glaciolacustrine sediments share many characteristics of glaciomarine diamictons; however, they lack *in situ* marine microfossils and are mostly geographically more limited in extent (Ó Cofaigh & Dowdeswell, 2001). Menzies *et al.* (2006) argued that plasmic fabrics indicate the presence of orientated clay particles by strong birefringence. The type of plasmic fabric is indicative of a suite of orientations induced by ductile deformation. Lodgement tills, formed in a high-strain environment with considerable shear and deformation, undergo complete homogenisation and demonstrate unistrial plasmic fabrics (Khatawa & Tulaczyk, 2001).

Subglacial traction tills can therefore have ductile, brittle, polyphase or intermediate structures (Figure 2.4). Ductile deformation structures include soft sediment pebbles (Type II and III), banding and flow of matrix material, rotational structures with associated skelsepic / masepic plasmic fabrics, and strain caps and pressure shadows. Planar features such as grain lineations are commonly associated with rotational structures, and occur in plastically deforming sediments (Hiemstra & Rijsdijk, 2003). Brittle deformation structures include edge-to-edge grain contacts and grain crushing, grain stacking, and brittle faulting and discrete shear zones. Grain stacks form to support stresses developing in a sediment, and form perpendicular to the stress field (Hiemstra & Rijsdijk, 2003). Glaciomarine deposits are characterised by graded laminations, iceberg-dump and dropstone structures, and *in situ* marine microfossils. Porewater-induced soft-sediment

deformation structures include liquefaction and homogenisation of sands, rafting, and water-escape structures (Figure 2.4).

Table 2.5: Macroscopic and microscopic criteria for interpretation of some typical glacigenic sediments. Refer to Figure 2.4.

<table>
<tr><th>Glacially overridden soft sediments</th><th>Mass flow diamictons</th><th>Debris Flow</th></tr>
<tr><td>• Water saturated
• High porewater pressure and content
• Associations of:
- Clay-lined normal faults,
- Sand -filled hydrofractures,
- Soft-sediment deformation,
- Liquefaction of sands, and
- Brecciation associated with hydrofractures

(Phillips et al., 2002; Menzies & Zaniewski, 2003; Hiemstra et al., 2006; Phillips et al., 2007)</td><td>• Kinking plasmic fabric.
• Possibly laminations.
• Turbates.
• Tile structures.

(Menzies & Zaniewski, 2003)</td><td>• Laminations.
• Poorly developed plasmic fabric.
• Grain clusters.
• Turbates.
• Pressure shadows.
• Folds and Faults.
• Water-escape.

(Lachniet et al., 2001; Phillips, 2006)</td></tr>
<tr><th>Tectonic Laminations (Type 1)</th><th>Lodgement</th><th>Glaciolacustrine</th></tr>
<tr><td>• Non-graded laminations, not onlapping.
• Point source for laminations.
• Sinking clasts with laminations 'flowing' around them.
• Pressure shadows, boudins and preserved folds, tectonic folds.
• Discontinuous beds
• Décollement surface at base.

(Hart & Roberts, 1994; Roberts & Hart, 2005)</td><td>• Homogenised due to high strain.
• Unistrial plasmic fabrics.
• Planar features.
• Strong clast macro-fabrics

(Menzies et al., 2006)</td><td>• Laminated
• Normally graded.
• Conformable contacts.
• Rhythmites / varved.
• Weak plasmic fabrics.

(Ó Cofaigh & Dowdeswell, 2001)</td></tr>
<tr><th>Traction Till</th><th colspan="2">Glaciomarine Diamictons</th></tr>
<tr><td>• Variable clast macro-fabrics.
• Associations of planar and rotational movement.
• Strong masepic / skelsepic plasmic fabrics.
• High birefringence.
• Brittle deformation and ductile deformation together.
• May have Type 1 (tectonic) Laminations
• Associations of:
- Grain lineations,
- Grain stacking,
- Edge-to-edge clasts,
- Multiple direction lineations,
- Matrix flowage (necking)
- Rotations / turbates.
- Rounded soft sediment pebbles.
- Pressure shadows.
- Multiple diamicton domains.

(Carr, 2001; Hiemstra & Rijsdijk, 2003; Hart et al., 2004; Ó Cofaigh et al., 2005; Roberts & Hart, 2005; Evans et al., 2006; Menzies et al., 2006; Hiemstra, 2007).</td><td colspan="2">• Coarse, winnowed texture.
• Horizontal microfabric
• Laminations / graded bedding / stratification.
• Type 2 (sedimentary) laminations.
• Conformable contacts.
• Onlapping beds.
• Laterally continuous.
• Dropstones, IRD, iceberg dump structures.
• Weak plasmic fabrics.
• In situ Tephra layers.
• In situ Arctic / sub- Arctic / turbid water foraminifera.
• Sedimentary base to structure.
• Gravitational flow folds.
• Post depositional minor micro-faulting.

(Hart & Roberts, 1994; Licht et al., 1999; Carr, 2001; Hiemstra, 2001; Ó Cofaigh & Dowdeswell, 2001; Roberts & Hart, 2005).</td></tr>
</table>

2.6 Lithological and Geochemical Techniques

2.6.1 Introduction

Quantified lithological and petrological analysis of glacigenic sediments provides a robust tool in the interpretation and delineation of ice-flow pathways. However, no one technique on its own can provide sufficiently detailed and robust provenance data. In addition, large bulk samples are required for clast-lithological analysis, which are not always possible to obtain; for example, only very small samples are available from offshore boreholes. Therefore, it is important to apply a number of quantified lithological techniques in order to accurately constrain ice accumulation areas, identify ice flow pathways, and provide robust lithological correlations (Passchier, 2007). This thesis uses a variety of techniques to achieve these broad goals. Firstly, qualitative sedimentary description provides an initial assessment of the lithological properties of a sediment. Particle-size analysis is the first necessary quantitative step, as the grain size and degree of sorting is the most fundamental property of any sediment (Bridgland, 1986; Gale & Hoare, 1991; Hoey, 2004). In order to constrain lithological correlations, three principal techniques are used: whole-sample geochemistry, heavy-mineral analysis, and clast-lithological analysis. The results are subjected to vigorous multivariate statistical analysis, which has previously been shown to work well (e.g., Ryan *et al.*, 2007).

The use of several independent techniques adds robustness to lithological cross-correlations (Passchier, 2007). Each technique is subject to its own, different, limitations, as outlined below. Heavy-mineral analysis and clast-lithological analysis are the most useful tools in provenance interpretation, as erratics may be traced back directly to outcrop. Although erratic train identification has been used before (e.g., Harmer, 1928; Sutherland, 1991), this is the first study to quantitatively apply all these techniques to north-eastern England. When used in conjunction with palynomorph analysis (see below, Chapter 2.9.2), robust provenance interpretations can be made.

2.6.2 Sampling Procedure

Where possible, samples were collected from open field sections, allowing the full variability of the stratigraphy to be sampled. The sampling strategy aimed to collect several bulk samples from each facies at each site. Where possible, samples were collected from a

vertical profile, demonstrating vertical lithological variations. Surface exposures were carefully cleaned and logged prior to sampling. Material was collected well away from the land surface and anywhere exhibiting signs of pedogenesis. Careful notes were taken of the lithofacies sampled, and sample location including depth / height. Where pragmatically possible, a series of vertically spaced samples was collected, to ensure each facies is sampled in a representative fashion (Walden, 2004). Due to the spatial variability of glacigenic diamictons, multiple samples were taken from several vertical profiles to ensure that inter-facies variation is accounted for and that representative samples are taken. Multiple sample collection is important to show replicability and robustness of data, and to determine errors (Hoey, 2004). In addition, multiple samples from each lithofacies are needed for statistical analysis.

Multiple and replicate bulk samples for detailed sedimentary description, heavy-mineral analysis, particle-size analysis, geochemistry and microfossil analysis were therefore collected from each lithofacies at each location. For well-sorted sands and clays, 500 g samples were collected. For diamictons, bulk samples of at least 10 kg were needed. These are stored in tightly sealed strong, air-tight polythene bags until laboratory analysis. Samples were clearly labelled to ensure easy identification. Samples with biogenic matter or high water content were kept in cold storage to minimise biological activity.

For diamictons, in the laboratory, most of the sample was set aside for particle-size analysis. 1 kg was retained and the air-dried sample was then gently manually disaggregated, then sieved through a 2 mm sieve. Sub-sampling for various lithological analyses of the sub-2 mm fraction was achieved through the use of a riffle box.

2.6.3 Sediment Description

Various laboratory methods can aid the description and characterisation of sediments in conjunction with field descriptions. Visually identifying and recording the fundamental properties of a sediment is highly important to give context to other analyses. The first stage in the laboratory analysis is the description of the sediments. Before drying, the sediments are laid out on a tray, and are inspected for reaction to 10 % Hydrochloric acid (HCl); colour according to a Munsell colour chart; fossils (shells, wood fragments); texture; sorting; and clast shape, number, and lithology (Gale & Hoare, 1991). The sediments are then thoroughly air-dried.

2.6.4 Particle-Size Analysis (PSA)

The particle size distribution is amongst the most fundamental physical properties of any geological materials (Bridgland, 1986; Drewey, 1986), and is essential in characterising the lithology of unconsolidated rocks (Gale & Hoare, 1991). PSA is a sensitive indicator of the physical and environmental conditions, under which the sediment was deposited (Benn & Gemmell, 2002). The size and sorting of sedimentary particles (and statistical distribution, for example, skew) is therefore indicative of the processes of erosion, transportation and deposition of sediments (Hoey, 2004). Glacial tills often have very similar particle size distributions over very wide geographical areas (Gale & Hoare, 1991), which can be used to indicate correlations or differences between different stratigraphical units. This thesis uses PSA primarily as a descriptive tool, and to aid the correlation and differentiation of lithofacies. The method used for determining particle size is given in Appendix I.

The principal limitation of PSA is that, for diamictons with occasional large clasts, extremely large samples are required to obtain an accurate approximation of the particle size distribution. Ideally, the largest grain (up to 32 mm diameter) should represent no more than 0.1% of the entire sample weight (Gale & Hoare, 1992). For larger grains (up to 128 mm diameter), 1% of sample weight is allowed (Church *et al.*, 1987). Required sample size increases dramatically in very poorly-sorted sediments (Hoey, 2004). This is unrealistic to achieve due to the enormous effort needed to sample and sieve tonnes of material. Pragmatically, samples of 10 to 20 kg provide a suitable trade-off between statistical reliability and efficiency. In addition, because deposits with large particles are usually heterogeneous, multiple repeat samples are needed (Hoey, 2004).

The particle-size distribution of tills can allow interpretations of processes acting at a multitude of scales (Benn & Gemmell, 2002). For example, Sharp *et al.* (1994) used particle-size analysis and Gaussian component analysis to resolve the PSA into a series of Gaussian curves, representing debris entrainment, communition and depositional processes (Sharp *et al.*, 1994). Haldorsen (1981) used different particle size modes in subglacial tills in Norway to differentiate between a residual-clast mode, particles produced by crushing, and a mode consisting of fine abrasion products (Haldorsen, 1981). Hooke and Iverson (1995) analysed the distribution as a whole, aiming to identify key processes acting at all scales within the sediment (Hooke & Iverson, 1995).

2.6.5 ICP-Mass Spectrometry

ICP-Mass Spectrometry (Total Metals Extraction) identifies the geochemistry of a sediment. It can provide a provenance signature and can be used to correlate between and within lithofacies. In this study, the multivariate statistical analysis of the whole-rock geochemistry provides an additional tool in the cross-correlation of sediments (cf. Walden, 2004), and it is supported by heavy-mineral analysis.

The sample must first undergo Atomic Absorption before it can be analysed by the ICP-MS machine (see Appendix I). Amanda Hayton and Martin West (Durham University Geography Department) carried out this work. In this project, only the abundant metals were analysed. The rare elements occur in such low percentages that the data can be unreliable, and small fluctuations are artificially exaggerated in statistical analysis.

Whilst till geochemistry has been little used in the UK, in America and Canada geochemical anomalies are successfully and widely used in conjunction with heavy-mineral analysis to define ice flow pathways. In particular, geochemical analysis is used in prospecting gold and diamonds; geochemical analysis helps to pinpoint areas immediately down-flow of diamondiferous dykes (McClenaghan, 1992; Klassen, 1999; Thomas & Gleeson, 2000). Identifying clastic dispersal trains, including palimpsest trains, can clearly identify and locate bedrock sources (Parent *et al.*, 1996). Parent *et al.* (1996) note that clastic dispersal trains are large and are therefore more easily located than small mineralised outcrops. The Canadian Geological Survey have therefore compiled large maps detailing clastic erratic trains, resulting in a detailed understanding of the last ice sheet. In Britain, this approach is not possible due to the lack of till geochemical data, making it difficult to identify anomalies. In this study, therefore, matrix geochemistry is used as a correlative tool alone.

2.6.6 Heavy-Mineral Analysis

> *Each heavy mineral is a unique messenger of coded data, carrying the details of its ancestry and the vicissitudes of its sedimentary history.*
>
> Mange and Wright, 2007
> *Heavy Minerals in Use*

Introduction

A version of this chapter is submitted to the *QRA Technical Guide: Clast Lithological Analysis*. Heavy-mineral analysis (HMA) is the microscopic identification of mineral grains with densities greater than 2.85 g cm^3, typically 1-2 % of sand samples. Applications for the technique in Quaternary Science include sediment description, provenance testing (for example, Mange & Otvos, 2005), reconstructing sediment transport paths, the correlation of lithostratigraphic units, mapping sediment dispersal patterns and delineating sediment-dispersal provenances (Lee, 2003). Many of the 50 translucent heavy minerals described by Mange and Maurer (1992) have restricted paragenesis, providing crucial and important information which cannot be gained by other means (Morton & Hallsworth, 2007). HMA is very useful when sediments are clast poor, such as in matrix-supported diamictons and well-sorted sands (Gale & Hoare, 1991). HMA should be used as part of a multi-proxy study, utilising other techniques such as clast-lithological analysis, X-ray diffraction of clay minerals, calcium carbonate determination, matrix geochemistry, and biostratigraphical techniques.

HMA has a long history of use as a correlative tool in eastern England. It was used by Boswell (1916) and Solomon (1932) to qualitatively correlate the glacial deposits in north Norfolk with those in Yorkshire, Lincolnshire and Cambridgeshire (Boswell, 1916). HMA also demonstrated that the Hunstanton Till of northwest Norfolk was the lateral equivalent of the Devensian Skipsea Member of east Yorkshire (Catt & Penny, 1966; Madgett & Catt, 1978; Lee, 2003). The stratigraphical correlation of the chalky tills of East Anglia was proved through HMA by Perrin *et al.* (1979). More recently, heavy-mineral analysis correlated and differentiated the fluvial and glacial sediments in the Norfolk-Suffolk borders (Lewis, 1999).

Factors controlling Heavy-Mineral Assemblages

Heavy minerals form a small but varied part of the sand fraction, and may be more resistant to weathering than lighter minerals. There are rarely more than 20 heavy mineral species identified in any one sample. There are four principal factors controlling heavy-mineral assemblages in glacial sediments: composition of the source rock, mechanical resistance of the minerals, dissolution caused by diagenesis and chemical weathering during glacial-interglacial sedimentation, and the density and morphology of mineral grains, which affects the deposition of minerals in water-saturated or water-lain sediments (Passchier, 2007). During glacial transport, rock fragments and minerals from the ice/bed interface are comminuted to their terminal grades. The effect of crushing and abrasion decreases with particle size (Passchier, 2007). The terminal grade represents a particle-size range for each mineral in the till matrix, depending on the mineral size in the source rock and mechanical stability. Garnets, a resistant mineral, reach their terminal size after 80-180 km of glacial transport, whereas mechanically unstable minerals such as dolomite are crushed to their terminal size after 0-3 km (Passchier, 2007).

Detrital heavy minerals are additionally subjected to a wide range of processes during erosion, transportation, deposition and diagenesis. These processes have the potential to modify an assemblage radically, leading to the obscuration of provenance signatures. Examples include hydraulogical sorting, mechanical weathering, pedochemical weathering, geochemical weathering, authigenesis and anthropogenic addition (Bateman & Catt, 2007). Resistant minerals such as tourmaline may be reworked from sedimentary rocks. An awareness of these processes and attention to their consequences can substantially improve the interpretations from the dataset. The complex history of a heavy-mineral assemblage can be summarised as below (Table 2.6).

Table 2.6: The potential history of a heavy-mineral assemblage: an idealised sedimentary cycle (Bateman and Catt, 2007).

A.	**Pre-erosional phase** *Pedochemical weathering, at source*
B.	**In transit phase** *Hydraulic sorting* *Mechanical weathering*
C.	**Post-depositional, pre-burial phase** *Pedochemical weathering, at sink* *Authigenic growth*
D.	**Post-burial phase** *Geochemical weathering* *Authigenic growth*
E.	**Exhumation phase** *Pedochemical weathering, at (re)exposure* *Authigenic growth* *Anthropogenic addition*

Separation of Heavy Minerals

HMA is particularly useful when undertaken on a narrow size selection, and so was undertaken on the 63-125 μm and 125-250 μm size fractions. Heavy minerals are most easily obtained by density separation using the full-freezing technique (see Appendix I), which is developed from earlier work by Carver (1971) and Gale and Hoare (1991). The recommended heavy liquid is sodium polytungstate ($3Na_2WO_4.9WO_3.H_2O$), which is non-toxic and, although expensive, is recyclable.

Identification of heavy minerals

Line counting should be employed, where the microscope slide is moved by means of the mechanical stage along linear traverses. All non-opaque grains intersected by the crosshairs are identified and counted, and all opaque grains intersected are counted. The results are number frequencies. This method is grain-size sensitive, which emphasises the importance of counting within a narrow size band (Mange & Maurer, 1992). Under the petrological microscope, various optical properties of the heavy minerals can aid identification. Opaque minerals are defined here following the pedological approach (rather than mineralogical) in that they are black in plane polarised light (PPL) and black or very dark brown in crossed polarised light (XPL). This was in order to enable comparison with other regional data sets, such as Madgett and Catt (1978). Non-opaque minerals transmit plane polarised light. 200 to 300 non-opaques were counted under the microscope for each sample as this is a statistically significant number and gives a

representative sample (Hubert, 1971; Bridgland, 1986; Walden, 2004). The proportions of opaque to non-opaque minerals should be calculated, and the mineral data is presented as percentage non-opaque.

Under PPL, the shape, pleochrosim, cleavage, colour, and relief of the mineral are the most obvious properties (Table 2.7 and Table 2.4). The mineral is then observed under XPL. The extinction of the mineral upon rotation of the stage, the birefringence, and the interference colours of the mineral (Table 2.7) provide further clues as to its identification (Mange & Maurer, 1992; Walden, 2004). The flow charts below (Figure 2.5) can aid the identification of heavy minerals, but they must be used in conjunction with colour photographs and detailed descriptions of mineral species, such as in Mange and Maurer (1992), or with a reference collection. Reference to a Michel Levy chart aids identification of interference colours (Gribble & Hall, 1992; MacKenzie & Adams, 2001).

Table 2.7: Glossary of terms in Heavy-mineral analysis (Gribble and Hall, 1992; Mange and Maurer, 1992).

Angle of extinction	Anisotropic minerals go into extinction four times during a complete rotation of the stage. All uniaxial minerals possess straight or parallel extinction. A prism face or edge, or a prismatic cleavage, is parallel to one of the cross-wires when the mineral is in extinction. Biaxial minerals possess straight or oblique extinction. Orthorhombic minerals show straight extinction against a prismatic cleavage or a prism face edge. All other biaxial minerals possess oblique extinction. The angle through which a mineral has to be rotated to bring the cleavages parallel to the crosswire is the extinction angle.
Anisotropic	The anisotropic skeleton grains slide transmit plane polarised light, but under cross-polarised light they extinguish (i.e. transmit no light) four times per complete rotation.
Birefringence and Interference Colours	The colour of anisotropic minerals under crossed polars varies, and the same mineral shows different colours depending on crystallographic orientation. These colours are on Newton's Scale, divided into several orders: • 1st Order: grey, white, yellow, red • 2nd Order: violet, blue, green, yellow, orange, red • 3rd Order: indigo, green, blue, yellow, red, violet • 4th Order and above: pale pinks and greens.
Cleavage	Most minerals cleave along specific crystallographic directions, related to planes of weakness in the mineral's atomic structure. These planes are straight, parallel, and evenly spaced, which indicate crystallographic orientation. When a cleavage is poorly developed, it is a parting.

Cross polarised light (XPL)	When passing plane polarised light through a second filter at 90° to the first (the upper polariser), we see it through crossed polars. Cross-polarised light is used to determine properties such as dispersion, birefringence, and extinction.
Habit / Form	The shape that a mineral exhibits in different rock types. E.g., euhedral, with well-defined crystal faces; anhedral, with no crystal faces apparent; prismatic, when the crystal is elongate in one direction; acicular, when the crystal is needle-like; fibrous, when the crystals resemble fibres. Flat, thin crystals are tabular or platy.
Interference Colours	Newton's Scale represents interference colours. They depend on the thickness of the mineral and the birefringence, and can be compared to a Michel Levy chart. Interference colours depend on the retardation of different wavelengths, which depends on atomic structure, orientation, birefringence, and thickness of a crystal. Some minerals have anomalous interference colours, which are not represented on the Michel Levy chart. They may result if minerals have abnormally high dispersion, or are deeply coloured. Examples include chlorite, epidote, zoisite, tourmaline and sodic amphiboles.
Interference Figure	All non-opaque minerals show interference Figures, excepting cubic minerals. There are two types, uniaxial and biaxial.
Isotropic	Isotropic minerals remain black in all positions when viewed under cross-polarised light. Minerals belonging to the cubic system are isotropic; they have the same properties in all directions.
Plane polarised light (PPL)	In normal, unpolarised light, waves vibrate in all directions. Filtering the light beam in the microscope with the lower polariser makes all the light waves vibrate in one direction, parallel to a particular plane.
Pleochroism	Some coloured minerals display characteristic colour changes on rotation of the stage under PPL. The two extremes of colour occur twice during 360° rotation. Ferromagnesian minerals such as amphiboles, biotite, and staurolite possess this property. Pleochroism is due to the unequal absorption of light by the mineral in different orientations.
Relief and Refractive Index	The refractive index of resin is 1.54 and of clove oil is 1.535. The surface relief of a mineral is essentially constant and depends on the difference between the RI of the mineral and the RI of the clove oil. The greater the difference between the RI of the mineral and the oil, the rougher the appearance of the surface of the mineral. If the RIs are similar, the surface appears smooth.

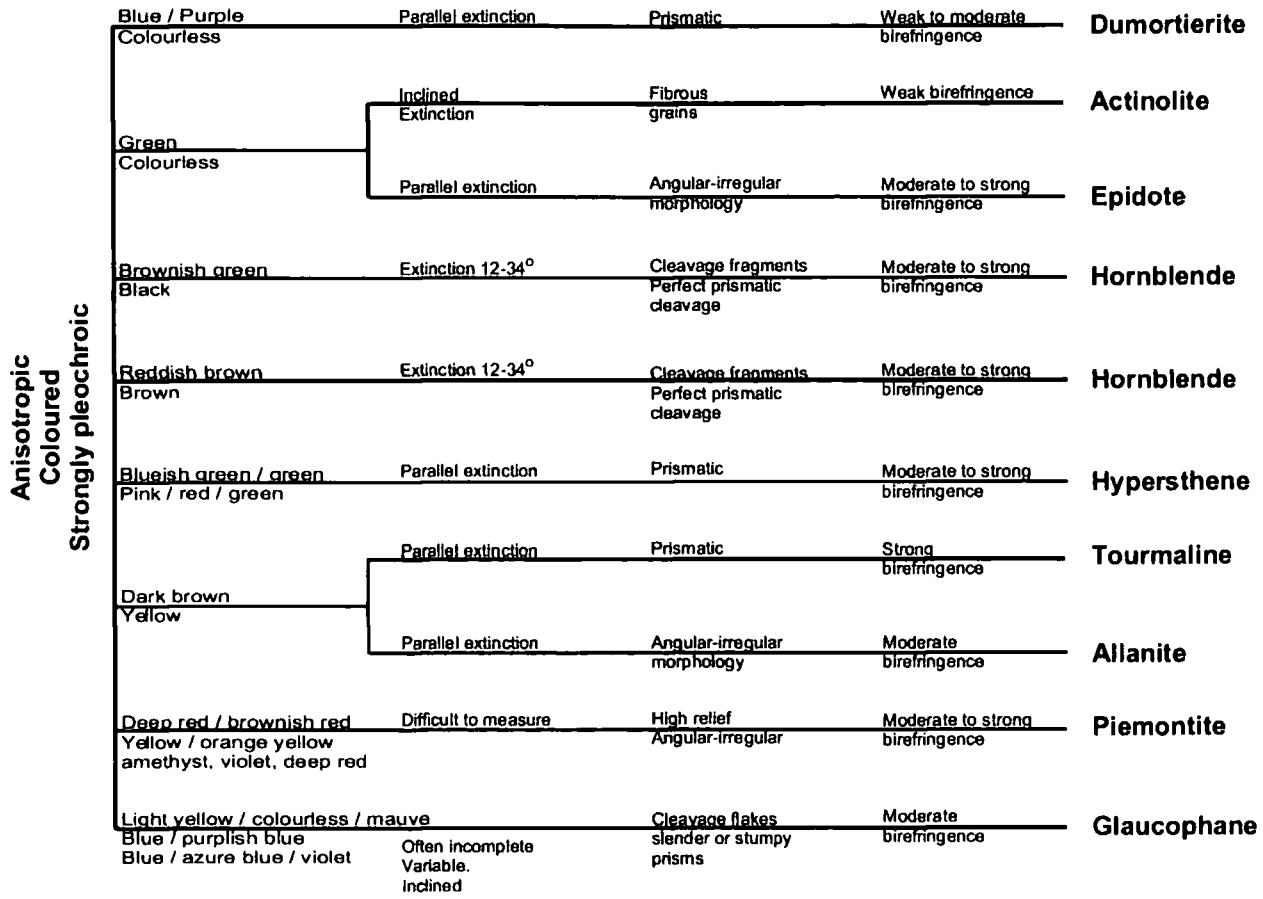
Anisotropic
Coloured
Strongly pleochroic
Blue / Purple
Colourless
Parallel extinction
Prismatic
Weak to moderate birefringence
Dumortierite
Green
Colourless
Inclined Extinction
Fibrous grains
Weak birefringence
Actinolite
Parallel extinction
Angular-irregular morphology
Moderate to strong birefringence
Epidote
Brownish green
Black
Extinction 12-34°
Cleavage fragments Perfect prismatic cleavage
Moderate to strong birefringence
Hornblende
Reddish brown
Brown
Extinction 12-34°
Cleavage fragments Perfect prismatic cleavage
Moderate to strong birefringence
Hornblende
Blueish green / green
Pink / red / green
Parallel extinction
Prismatic
Moderate to strong birefringence
Hypersthene
Dark brown
Yellow
Parallel extinction
Prismatic
Strong birefringence
Tourmaline
Parallel extinction
Angular-irregular morphology
Moderate birefringence
Allanite
Deep red / brownish red
Yellow / orange yellow
amethyst, violet, deep red
Difficult to measure
High relief
Angular-irregular
Moderate to strong birefringence
Piemontite
Light yellow / colourless / mauve
Blue / purplish blue
Blue / azure blue / violet
Often incomplete
Variable.
Inclined
Cleavage flakes slender or stumpy prisms
Moderate birefringence
Glaucophane

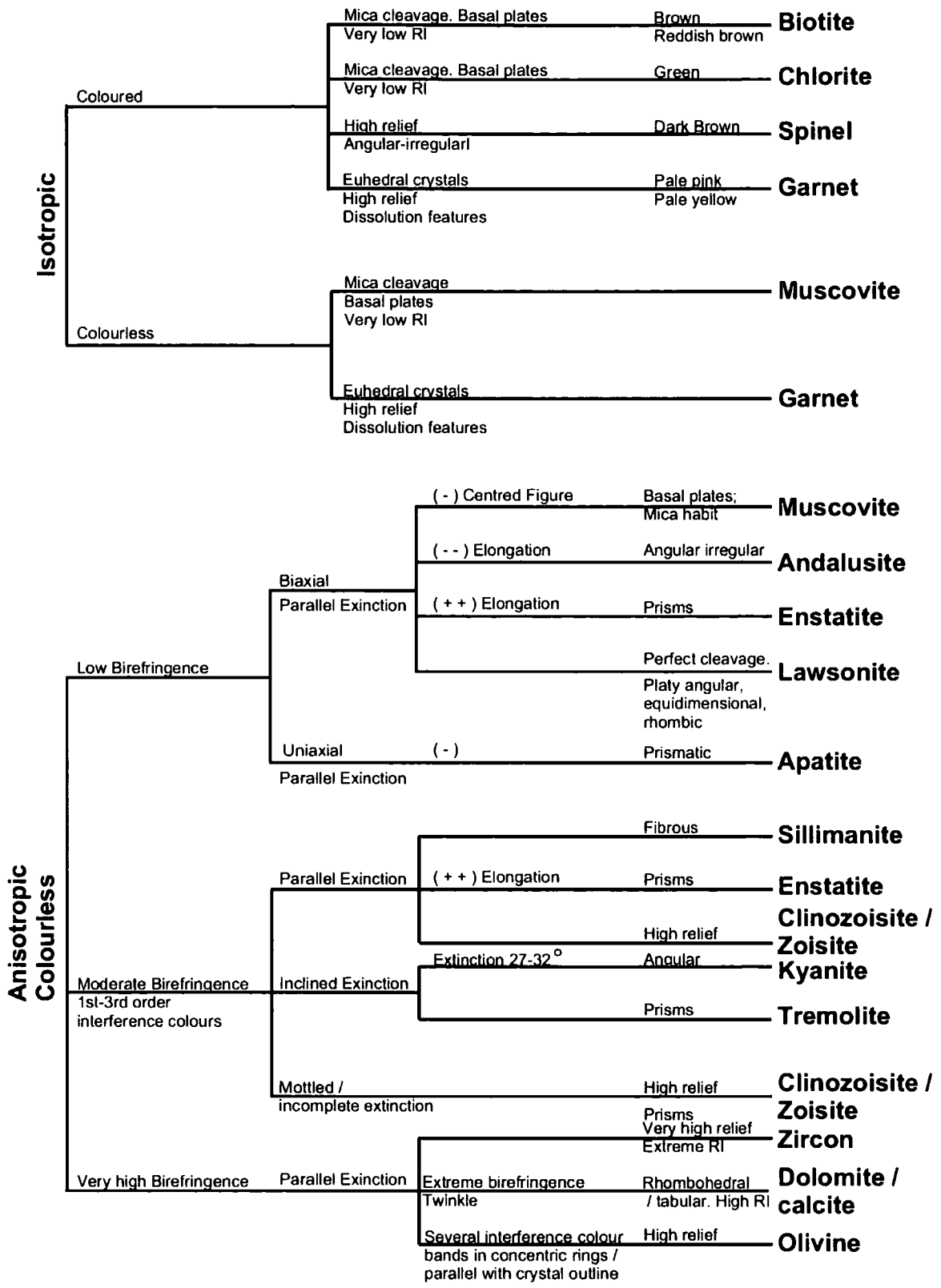
Isotropic
Coloured
Mica cleavage. Basal plates
Very low RI
Brown
Reddish brown
Biotite
Mica cleavage. Basal plates
Very low RI
Green
Chlorite
High relief
Angular-irregularl
Dark Brown
Spinel
Euhedral crystals
High relief
Dissolution features
Pale pink
Pale yellow
Garnet
Colourless
Mica cleavage
Basal plates
Very low RI
Muscovite
Euhedral crystals
High relief
Dissolution features
Garnet
Anisotropic
Colourless
Low Birefringence
Biaxial
Parallel Exinction
(-) Centred Figure
Basal plates;
Mica habit
Muscovite
(- -) Elongation
Angular irregular
Andalusite
(+ +) Elongation
Prisms
Enstatite
Perfect cleavage.
Platy angular,
equidimensional,
rhombic
Lawsonite
Uniaxial
Parallel Exinction
(-)
Prismatic
Apatite
Moderate Birefringence
1st-3rd order
interference colours
Parallel Exinction
Fibrous
Sillimanite
(+ +) Elongation
Prisms
Enstatite
High relief
Clinozoisite /
Zoisite
Inclined Exinction
Extinction 27-32°
Angular
Kyanite
Prisms
Tremolite
Mottled /
incomplete extinction
High relief
Clinozoisite /
Zoisite
Very high Birefringence
Parallel Exinction
Prisms
Very high relief
Extreme RI
Zircon
Extreme birefringence
Twinkle
Rhombohedral
/ tabular. High RI
Dolomite /
calcite
Several interference colour
bands in concentric rings /
parallel with crystal outline
High relief
Olivine

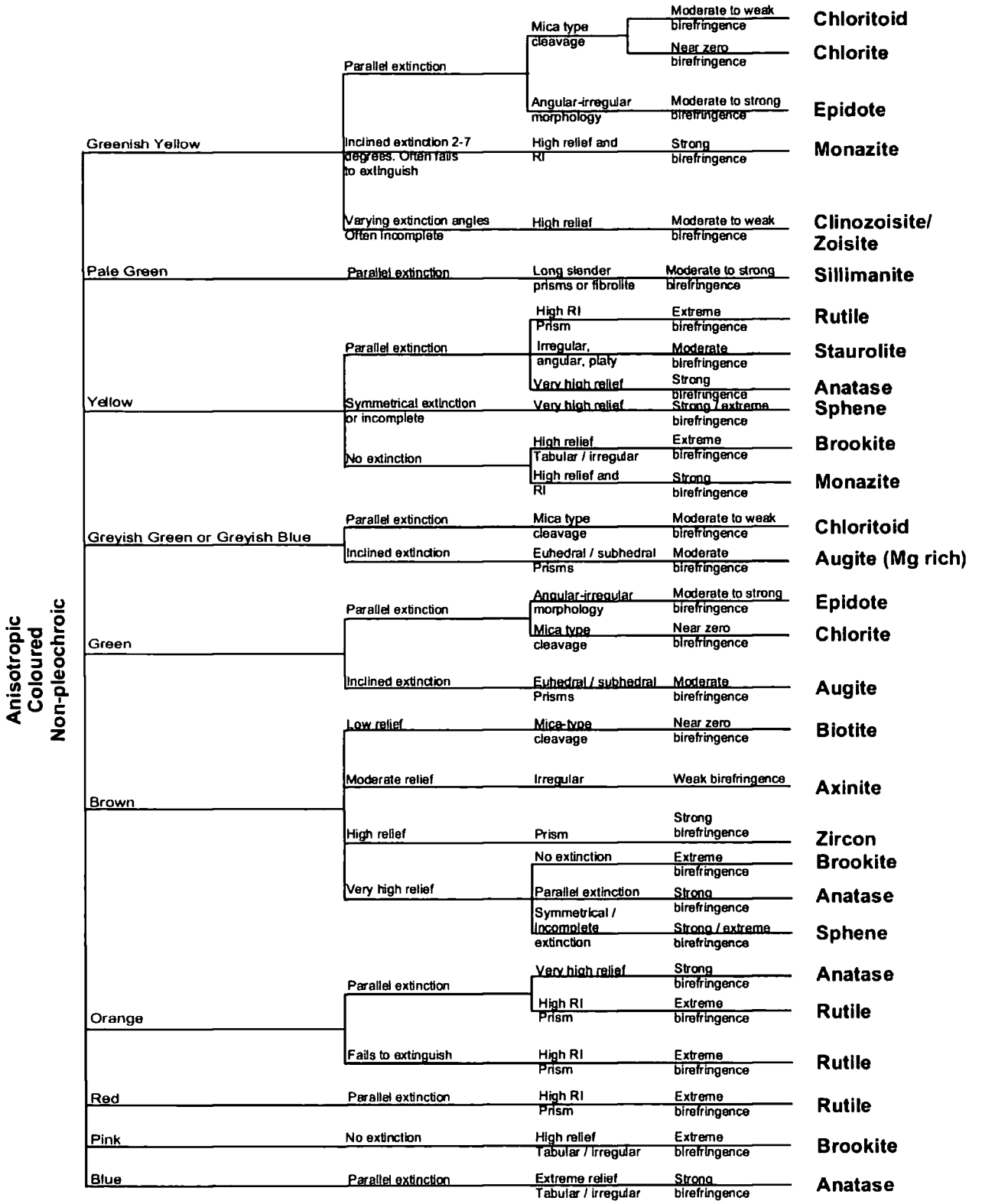
Anisotropic
Coloured
Non-pleochroic
Greenish Yellow
Pale Green
Yellow
Greyish Green or Greyish Blue
Green
Brown
Orange
Red
Pink
Blue
Parallel extinction
Inclined extinction 2-7 degrees. Often fails to extinguish
Varying extinction angles Often incomplete
Parallel extinction
Symmetrical extinction or incomplete
No extinction
Parallel extinction
Inclined extinction
Parallel extinction
Inclined extinction
Low relief
Moderate relief
High relief
Very high relief
Parallel extinction
Fails to extinguish
Parallel extinction
No extinction
Parallel extinction
Mica type cleavage
Angular-irregular morphology
High relief and RI
High relief
Long slender prisms or fibrolite
High RI Prism
Irregular, angular, platy
Very high relief
Very high relief
High relief Tabular / irregular
High relief and RI
Mica type cleavage
Euhedral / subhedral Prisms
Angular-irregular morphology
Mica type cleavage
Euhedral / subhedral Prisms
Mica-type cleavage
Irregular
Prism
No extinction
Parallel extinction
Symmetrical / incomplete extinction
Very high relief
High RI Prism
High RI Prism
High relief Tabular / irregular
Extreme relief Tabular / irregular
Moderate to weak birefringence
Near zero birefringence
Moderate to strong birefringence
Strong birefringence
Moderate to strong birefringence
Extreme birefringence
Moderate birefringence
Strong birefringence
Strong / extreme birefringence
Extreme birefringence
Strong birefringence
Moderate to weak birefringence
Moderate birefringence
Moderate to strong birefringence
Near zero birefringence
Moderate birefringence
Near zero birefringence
Weak birefringence
Strong birefringence
Extreme birefringence
Strong birefringence
Strong / extreme birefringence
Strong birefringence
Extreme birefringence
Extreme birefringence
Extreme birefringence
Strong birefringence
Chloritoid
Chlorite
Epidote
Monazite
Clinozoisite/ Zoisite
Sillimanite
Rutile
Staurolite
Anatase
Sphene
Brookite
Monazite
Chloritoid
Augite (Mg rich)
Epidote
Chlorite
Augite
Biotite
Axinite
Zircon
Brookite
Anatase
Sphene
Anatase
Rutile
Rutile
Rutile
Brookite
Anatase

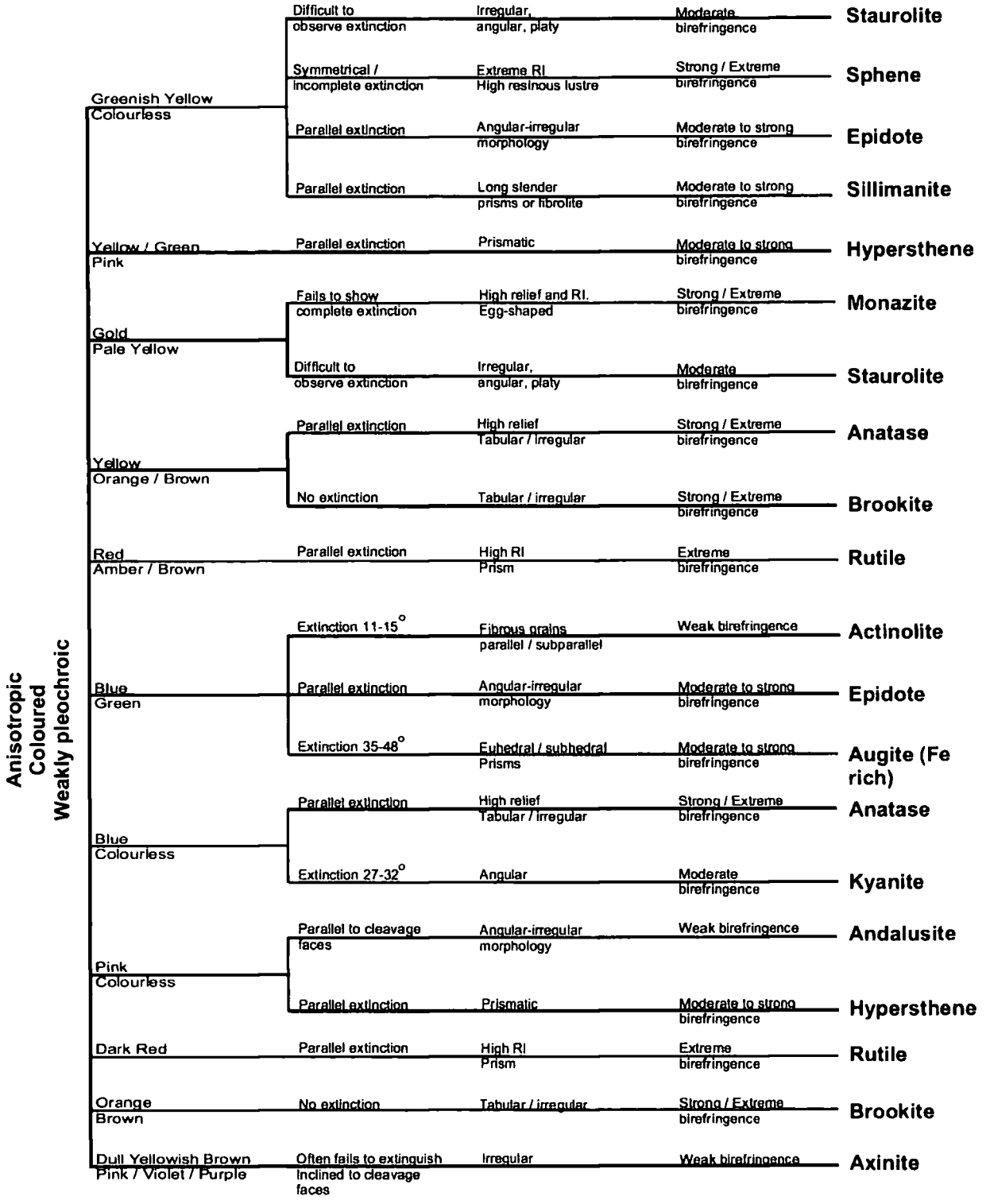

Figure 2.5: Flow-charts to aid identification of some common heavy minerals. Numerous sources (Gale & Hoare, 1991; Deer *et al.*, 1992; Mange & Maurer, 1992; MacKenzie & Adams, 2001; Walden, 2004).

Provenance studies using heavy-mineral analysis

Characteristic suites of heavy minerals can be used to identify key provenance zones, especially when used in conjunction with clast-lithological data. Multivariate statistical

analysis can be used to identify groups of minerals (Davis, 1986; Kovach, 1995). Principle components analysis on fully quantified heavy-mineral data can be used to tease out subtle relationships and related groups of minerals, as well as identifying trends in the data which may otherwise be obscured (Bateman & Catt, 2007; Ryan *et al.*, 2007). Cluster analysis (dendrograms) can also identify correlative samples. Mineral groups comprising less than 2 % of the dataset (such as sulphides and sulphates) were excluded due to low numbers, which would have a disproportional effect on the statistical analysis. Raw counts were square-rooted to reduce strong skew. To aid provenance interpretation, heavy minerals can also be grouped into genetic suites (Hubert, 1971), such as reworked sedimentary, low- and high-rank metamorphic, igneous, pegmatitic, and authigenic suites (Table 2.8).

Table 2.8: Provenance zones of some common heavy minerals (Hubert, 1971; Gale & Hoare, 1991).

Reworked sediments	Well-rounded grains of rutile, tourmaline, and zircon.
Low-rank metamorphic	Biotite, chlorite, spessartite garnet, tourmaline, (especially small, euhedral, brown crystals with graphite inclusions).
High-rank metamorphic	Actinolite, andalusite, apatite, almandine garnet, biotite diopside, epidote, clinozoisite, glaucophane, hornblende, ilmenite, kyanite, sillimanite, sphene, staurolite, tourmaline, tremolite, zircon, zoisite.
Sialic / Acidic Igneous	Apatite, biotite, hornblende, ilmenite, monazite, muscovite, rutile, sphene, tourmaline, zircon.
Mafic / Basic Igneous	Anatase, brookite, augite, diopside, epidote, hornblende, hypersthene, ilmenite, olivine, pyrope garnet, topaz, serpentine.
Pegmatites	Apatite, diopside, cassiterite, garnet, monazite, muscovite, rutile, tourmaline.
Ash Falls	Euhedral crystals of apatite, augite, biotite, hornblende, zircon.
Authigenic	Tourmaline, zircon, euhedral crystals of anatase, brookite, pyrite, rutile, sphene.

Some heavy minerals have specific paragenesis and occur in only limited regions. For example, olivine and clinopyroxenes occur in the Carboniferous volcanic rocks (olivine and clinopyroxene phyric basalts) and high-level intrusions of northern Britain, the Midland Valley of Scotland, and locally within the Southern Uplands. The Highlands and Islands of Scotland are the sole source for chloritoid (Mange *et al.*, 2005); assemblages of garnet-staurolite-chloritoid are characteristic of Stonehavian-type metamorphism, developed in a small area to the east of Stonehaven close to the Highland Boundary Fault (Stephenson & Gould, 1995; Trewin, 2002). A garnet-andalusite-kyanite assemblage (possibly with sillimanite) is a higher grade assemblage developed in the Buchan-type

metamorphism, developed along the Scottish coast north of Aberdeen (Stephenson & Gould, 1995).

The relative stability of heavy minerals varies (Table 2.9). The effects of diagenesis can cause the loss of valuable provenance information. Parameters used for the interpretation of provenance must therefore reflect source characteristics, rather than subsequent diagenetic processes. Two complementary approaches should be used, one using multivariate statistics to evaluate the whole assemblage, and one concentrating on the ratios of specific ultra-stable heavy minerals (Morton & Hallsworth, 1994; Morton *et al.*, 2005; Morton & Hallsworth, 2007).

Table 2.9: Relative stability of detrital heavy minerals (Morton & Hallsworth, 2007).

Least Stable
Olivine
Orthopyroxene, Clinopyroxene
Calcic amphibole, Andalusite, Sillimanite
Epidote
Titanite
Kyanite
Sodic amphibole
Garnet, Chloritoid
Tourmaline, Monazite, Spinel
Rutile, Anatase, Brookite, Zircon, Apatite
Most Stable

Ratios of specific stable heavy minerals with similar hydrodynamic behaviour reflect source area characteristics. Determining the relative proportions of minerals that behave in a similar way during the processes of transport, deposition and diagenesis, which have similar chemical and mechanical stability and hydraulic behaviour can give a more reliable indication of sediment provenance (Morton & Hallsworth, 1994). For example, changes in the percentages of staurolite, kyanite, epidote, amphibole and pyroxene could be attributed to their instability. Several pairs of common ultra-stable minerals fulfil the criteria for similar hydraulic behaviour. These are apatite-tourmaline, rutile-zircon, monazite-zircon, garnet-zircon and chrome spinel-zircon (Morton *et al.*, 2005). These are expressed as index values, given below in Table 2.10.

Table 2.10: Indices of ultra-stable heavy minerals (Morton *et al.*, 2005).

ATi	Apatite-Tourmaline index	$\frac{10 \times \text{apatite count}}{\text{Total apatite + tourmaline}}$
GZi	Garnet-Zircon index	$\frac{100 \times \text{garnet count}}{\text{Total garnet + zircon}}$
RuZi	Rutile-Zircon index	$\frac{100 \times \text{rutile count}}{\text{Total rutile + zircon}}$
MZi	Monazite-Zircon index	$\frac{100 \times \text{monazite count}}{\text{Monazite + zircon}}$
CZi	Chrome spinel-Zircon index	$\frac{100 \times \text{chrome spinel count}}{\text{Total chrome spinel + zircon}}$

Sources of Error in Heavy-Mineral Analysis

Common sources of error in HMA predominantly involve operator error. This begins with contamination of the sample, errors in splitting the bulk sample, errors in sieving to the correct size fractions, errors in the density separation technique (such as mineral inclusions making light minerals denser), and errors in the identification and counting of heavy minerals (Hubert, 1971). Tracing heavy-mineral associations to source regions demands an exacting knowledge of regional geology, and is susceptible to error. Finally, diagenesis, hydraulogical sorting, and other depositional and post-depositional processes can severely affect the heavy-mineral suite. However, careful acknowledgement of this means that heavy mineral associations can impart valuable and useful provenance information for glacigenic diamictons, and it remains an important correlative tool.

Summary

HMA has a long and involved history of use in Quaternary Science. Although it became unfashionable in the late twentieth century, it is now regaining recognition as a useful and important tool. When used within a framework of understanding the limitations and controls on heavy mineral deposition, HMA can provide important information regarding provenance, stratigraphic correlation and even depositional processes. HMA works well as a complementary technique to the study of glacial tills, and is an invaluable tool in the examination of clast-poor diamictons and well-sorted sands.

2.6.7 Clast-Lithological Analysis

Methodology

Clast identification is used in the description and characterisation of a sediment, and in the correlation or differentiation of stratigraphical units. It is a powerful provenance tool, and it can also be used in reconstructing variations in the mode of deposition (Bridgland, 1986). The analysis of erratics within tills is a powerful tool in the reconstruction of ice-sheet dynamics and flow patterns (Evans, 2007a). For example, clast-lithological analysis has recently been used extensively in Norfolk to test the case for a Scandinavian ice sheet during the Middle Pleistocene (Lee *et al.*, 2002). Black flint and Cretaceous chalk were traced to the bedrock of north Norfolk and the North Sea Basin. Carboniferous lithologies are distinctive of the Westphalian of northern England. Although the provenance of some crystalline erratics was ambiguous, the lack of distinctive Norwegian indicator erratics compared to evidence of northern British erratics precluded a Scandinavian origin.

Over 300 clasts greater than 4 mm and less than 32 mm diameter were sampled from a 2 m^2 area per site to give a statistically significant, representative sample (Bridgland, 1986). Pebbles should be carefully washed in water and separated into *phi* size fractions (4-8 mm, 8-16 mm, 16-32 mm, and over 32 mm) by sieving. Whilst the under 8 mm size stones are too small to accurately identify, they should be retained, and can be used if the sediment in question lacks any stones greater in size. It is normally difficult to obtain stones in the greater than 32 mm size fraction in numbers sufficient for quantitative analysis, but nonetheless they should be included in stone counts as in some cases, especially for durable erratics, examples may only occur in the large size fractions. These fractions should be identified and counted and noted during analysis.

Clasts in the 8-16 cm, 16-32 cm and >32 cm fractions were identified using a low powered binocular microscope (model '*Motic SMZ-168*'), a reference collection collected at outcrop, and standard rock identification criteria (Gale & Hoare, 1991; Walden, 2004). A geological hammer was used to break open the clasts to open a fresh surface for identification (Bridgland, 1986). A steel probe was used to test for hardness, and 10 % 1M HCl was used for the identification of carbonates (cf. Bridgland, 1986). Statistical analysis is then performed on the data (see Chapter 2.7). Strongly skewed data were square-rooted. The classes were divided into lithological categories to reduce the number of variables and simplify the dataset.

Provenance studies using Clast Lithology

Investigations of provenance using clast lithology use a geological map and a reference collection to identify overall source regions. Suites of lithologies can be used to

identify likely sources. Statistical groupings of suites of lithologies clearly helps define lithological correlations.

'Indicator erratics' are distinctive clasts which can be traced back to outcrop. They are usually granites or distinctive lavas, and these have been used to trace ice-flow pathways in the British Isles (Harmer, 1928; Sissons, 1967; Sutherland, 1984; Evans *et al.*, 2005). A classic indicator erratic from the Lake District is the 'Shap Granite' from Shap, near Penrith. Distinctive Scottish erratics include Grampian granites such as the Rannoch Granodiorite, and the Essexite erratic train from Lennox-town. These were all visited and sampled at outcrop; comparison to reference samples enabled identification of key lithologies.

Distinctive Scandinavian lithologies (Figure 2.6) have been used to infer the presence of Scandinavian ice (e.g., Trechmann, 1931b; Pawley *et al.*, 2004). However, these are durable lithologies that may be reworked, and their presence must be interpreted with care (Catt, 1991a). The concentration of indicator erratics decreases with distance from the outcrop. Concentrations down-ice of the outcrop increase rapidly as new material is added, but concentrations decrease rapidly at the outcrop margin (Evans, 2007a).

Drammensgranit

Oslo Basalt

Rhomb Porphyry

Larvikite

Nepheline Syenite

Rhomb prophyry conglomerate

Figure 2.6: Photographs of hand specimens of some Norwegian indicator erratics (courtesy of Dr. Jon Lee, BGS).

2.7 Erratic sources in Britain

2.7.1 Introduction

This section examines the pre-Quaternary geology of Britain, with particular reference to areas reported to be principle erratic sources and ice-accumulation areas, such as the Southern Uplands, Grampian Highlands, and the Lake District (Harmer, 1928; Sissons, 1967; Sutherland, 1984; Sutherland, 1991; Bowen *et al.*, 2002). The chapter also examines the geology of critical regions, such as the Midland Valley of Scotland. The reviews by Sutherland (1984; 1991) highlighted several key erratic sources, and used much of the work of the Yorkshire Boulder Committee (Howarth, 1908; Woolacott, 1910; Harmer, 1928). These regions were again emphasised in the recent review by Evans *et al.* (2005). They include distinctive and easily recognisable granites, such as the Lake District Shap Granite, the Criffel and Loch Doon granites from the Dumfries and Galloway region, and the Cheviot andesite. Glaciological models by Bowen *et al.* (2002) and Boulton and Hagdorn (2006) identified the Lake District, the Southern Uplands, and the Grampian Highlands as key ice-accumulation areas.

In order to reconstruct and interpret the Quaternary geology of an area, it is important to have a thorough understanding of the regional geology. Changing bedrock lithologies between sites can explain clast-lithological variations, which can occur over a very short distance. Ice-flow pathways can therefore only be reconstructed through a robust and thorough examination of the lithological and petrological properties of a till.

2.7.2 The Grampian Highlands

The Grampians and the Northern Highlands of Scotland are large region of structurally complex, high-grade metamorphic rocks (Figure 2.7) within the Caledonian orogenic belt of Scotland (Strachan *et al.*, 2002). The Grampian Terrane is part of the Dalradian Supergroup, and is bounded to the south by the Highland Boundary Fault (Strachan *et al.*, 2002). Igneous granites (including the Rannoch Muir, Cairngorm, Mount Battock, Glen Fyne, Etive, and Glencoe granites) were emplaced during the deposition of the Dalradian Supergoup, and were linked to crustal stretching associated with the opening of the Iapetus Ocean (Stephenson & Gould, 1995).

The Dalradian sediments of the Grampians were deposited as marine sands, silts, muds and limestones in the Iapetus Ocean during the Neoproterozoic until the Early Ordovician. These were subsequently deformed and metamorphosed during the Mid-Ordovician Grampian orogeny (Strachan *et al.*, 2002), forming complex quartz-mica-schist facies which are a prominent erratic, dispersed south-eastwards through the Midland Valley (Harmer, 1928; Sutherland, 1984).

Stephenson and Gould (1995) described a suite of basic and ultramafic rocks that were intruded into the Dalradian during a late phase of the Grampian orogeny (Strachan *et al.*, 2002). The bodies occur along the Portsoy-Duchray Hill Lineament, and are associated with areas of high-temperature, low pressure 'Buchan' metamorphism (Stephenson & Gould, 1995). Buchan metamorphism is associated with the mineral sequence garnet-andalusite-kyanite, with accessory minerals biotite, sillimanite and cordierite (Strachan *et al.*, 2002). To the southwest, 'Stonehavian metamorphism' records decreasing pressure. It is typified by the mineral assemblage garnet-chloritoid-staurolite, with accessory biotite minerals.

2.7.3 The Midland Valley of Scotland

Lower Palaeozoic

The Midland Valley is bounded by the Southern Uplands Fault to the south and the Highland Boundary Fault to the north (Bluck, 2002). It spans the gap between the deeper parts of the Caledonian orogen to the north, where the Dalradian block underwent Cambro-Ordovician burial, metamorphism and cooling (Bluck, 2002), and the more superficial, subduction-related region to the south. Lower Old Red Sandstone rocks and a series of Carboniferous basins dominate the present Midland Valley (Figure 2.7).

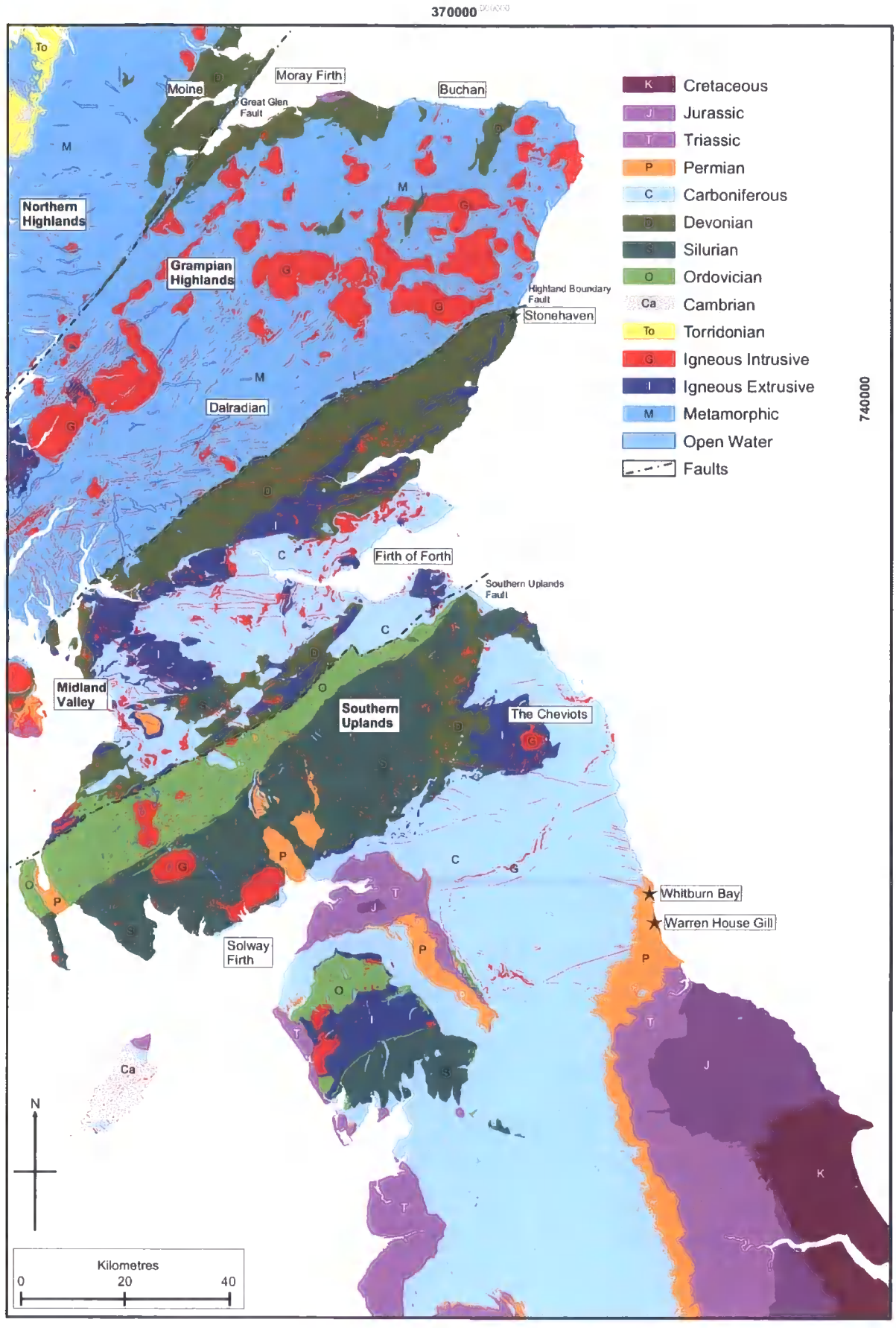

Figure 2.7: Simplified geology of northern Britain. Adapted from BGS Digimap database. © NERC

The Devonian

The effects of the final closure of the Iapetus Ocean continued into the Devonian, with the formation of many granites in Scotland and northern England resulting from the Caledonian Orogeny (Toghill, 2000), such as the Cheviot, Southern Uplands, Shap, Skiddaw and Weardale granites and the granophyre-gabbro complex of Carrock Fell in the Lake District (Robson & Johnson, 1995). The Old Red Sandstone deposits are about 418 to 362 Ma, and the basal parts of the Old Red Sandstone occur in the Silurian.

The Old Red Sandstone Continent landmass was high, arid, and had low humidity. Coarse sediments were laid down in lakes and rivers in the inter-montaine basins of the mountainous areas (the Caledonides), and on coastal plains to the south. Shallow-shelf seas in the Rheic Ocean provided environments for the deposition of Devonian limestones and sandstones (Toghill, 2000).

The Old Red Sandstone sediments consist of fine- to medium-grained red or buff-coloured sandstones (Cameron & Stephenson, 1985), with darker red siltstones or mudstones. Quartz grains are predominant. Old Red Sandstone deposits outcrop in five principle areas in the UK, which broadly reflect the original sedimentary basins in which they were deposited (Barclay *et al.*, 2005). These are:

- The Orkney and Shetland islands and north east Scotland,
- The Midland Valley of Scotland, in an amalgamation of several basins of which the largest was the Strathmore Basin (Figure 2.7),
- The Scottish Borders and Northumberland, in the Scottish Border Basin (Figure 2.7),
- South Wales,
- The Welsh Borderland and Bristol, in the Anglo-Welsh Basin.
- Rare conglomerates in the northern Lake District, the Mell Fell Conglomerate, and in the inliers around the Northern Pennine Faults may belong to the Old Red Sandstone.

Carboniferous Volcanism

Igneous activity was widespread in the Midland Valley during the early to middle Viséan. Cameron and Stephenson (1985) described thick plateaux of alkali olivine-basalt and related lavas. Smaller, localised pyroclastic activity continued until the Lower Permian. The later volcanic episodes were accompanied by the intrusion of thick sills of

alkali dolerites, mainly during the Namurian and early Westphalian (Cameron & Stephenson, 1985). Cameron and Stephenson (1985) portrayed the basaltic lavas as porphyritic, and classified them on the size and occurrence of plagioclase, clinopyroxenes and olivine phenocrysts.

2.7.4 The Southern Uplands

A large part of Scotland is underlain by Caledonian and older rocks. The Caledonian Orogeny was an important feature of Scottish geological history, because the Iapetus Ocean sutured along the Scottish border. The Southern Uplands terrane is a Lower Palaeozoic accretionary thrust belt to the northwest of the Iapetus Suture (Oliver *et al.*, 2002), and southeast of the Southern Uplands Fault. Oliver *et al.* (2002) noted that the Southern Uplands terrane comprised Ordovician and Silurian greywackes and siltstones. Caradoc and Ashgill greywackes are dominant in the northwest, Llandovery in the centre, and Wenlock greywackes in the southeast.

Harris (1991) argued that in the northern belt, the wedges of dipping greywackes contain pillow lavas, cherts and black shales. Intruded into these are granitic plutons, the 'Newer Granites', emplaced at 400 Ma (Harris, 1991). The largest and most important early Devonian igneous complexes are the Loch Doon, Cairnsmore of Fleet, and Criffel granitic masses (Floyd, 1999), and these were all identified by Sutherland (1984) as key erratic sources. They are all calc-alkali granites of Ordovician to Silurian age (Greig, 1971), intruded as part of the Caledonian orogeny (Floyd, 1999). The Loch Doon is a white biotite-granite with quartz, biotite, orthoclase, muscovite and hornblende. The Cairnsmore of Fleet muscovite-biotite-granite mass lies between the Loch Doon and Criffel granites (Greig, 1971; Pankhurst & Sutherland, 1982). The Criffel igneous complex is principally a biotite-hornblende-granodiorite and the inner Dalbeattie Granite is porphyritic with microperthite megacrysts (Pankhurst & Sutherland, 1982).

2.7.5 The Lake District

The oldest rocks in the Lake District are the Ordovician Skiddaw Slate Series ('SLA' on Figure 2.8) and the Borrowdale Volcanics ('A' on Figure 2.8). The Skiddaw Slates formed about 500 Mya in a shallow sea. There are at least 4000 m of mudstones, now slates, and siltstones and sandstones (Toghill, 2000). The thick, andesitic Borrowdale

Volcanics were erupted from ancient island volcanic island arcs and marginal volcanic basins, and are interbedded with marine sediments that are often full of fossils (Eastwood, 1946). They succeed the Skiddaw Group in the Central Lake District (Millward *et al.*, 1978). There are up to 6000 m of Llandeilo- to mid-Caradoc-age volcanics, which are mainly andesitic lavas, ash fall tuffs and ignimbrites, formed at different volcanic centres (Toghill, 2000).

A major unconformity separates Borrowdale Volcanic Group from the overlying Coniston Limestone Group, which encompasses up to 200 m of sandstones, shales and limestones with a rhyolite lava to the east. These Ashgill Epoch rocks are overlain conformably by dark shallow-water Silurian shales with graptolites (Toghill, 2000).

The Shap, Eskdale and Skiddaw Granites (Figure 2.8) are the exposed parts of a large, composite, acid batholith that underlies the central and northern Lake District (Firman, 1978). They have been loosely dated to the Devonian, but their ages range considerably. Firman (1978) argued that the oldest, possibly Ordovician intrusions, are part of the Carrock Fell Complex (the gabbros are indicated on Figure 2.8). Gabbro, granophyre and diabase were intruded along the junction between the Skiddaw Slates and the Eycott Volcanics, and were later metamorphosed by the Lower Devonian Skiddaw Granite. The Ennerdale Granophyre was intruded at a higher structural level than the Eskdale Granite, but it only penetrates the lowest andesites of the Borrowdale Volcanic Group (Firman, 1978). Firman (1978) described it as a fine-grained, pink, quartz-alkali feldspar rock, with rare porphyries. The younger Eskdale Granite is a perthite-muscovite granite, which penetrates the Ordovician Borrowdale Volcanic group. The Skiddaw Granite is a biotite-granite with oligoclase and quartz.

The distinctive Shap Granite (Figure 2.8), identified as a key erratic by the Yorkshire Boulder Committee (Howarth, 1908; Harmer, 1928), is a small outcrop of only 8 km^2. It reached a higher stratigraphic level than the other Lake District intrusions. Firman (1978) argued that it was contemporaneous with the Skiddaw Granite. The Yorkshire Boulder Committee (Kendall & Howarth, 1902), Howarth (1908) and Harmer (1928) carefully mapped its distribution in the drifts of eastern England. The Shap Granite contains characteristic, idiosyncratic, large pink orthoclase perthite phenocrysts up to 50 mm long in a coarsely crystalline matrix of quartz, orthoclase and oligoclase, with some biotite (Firman, 1978).

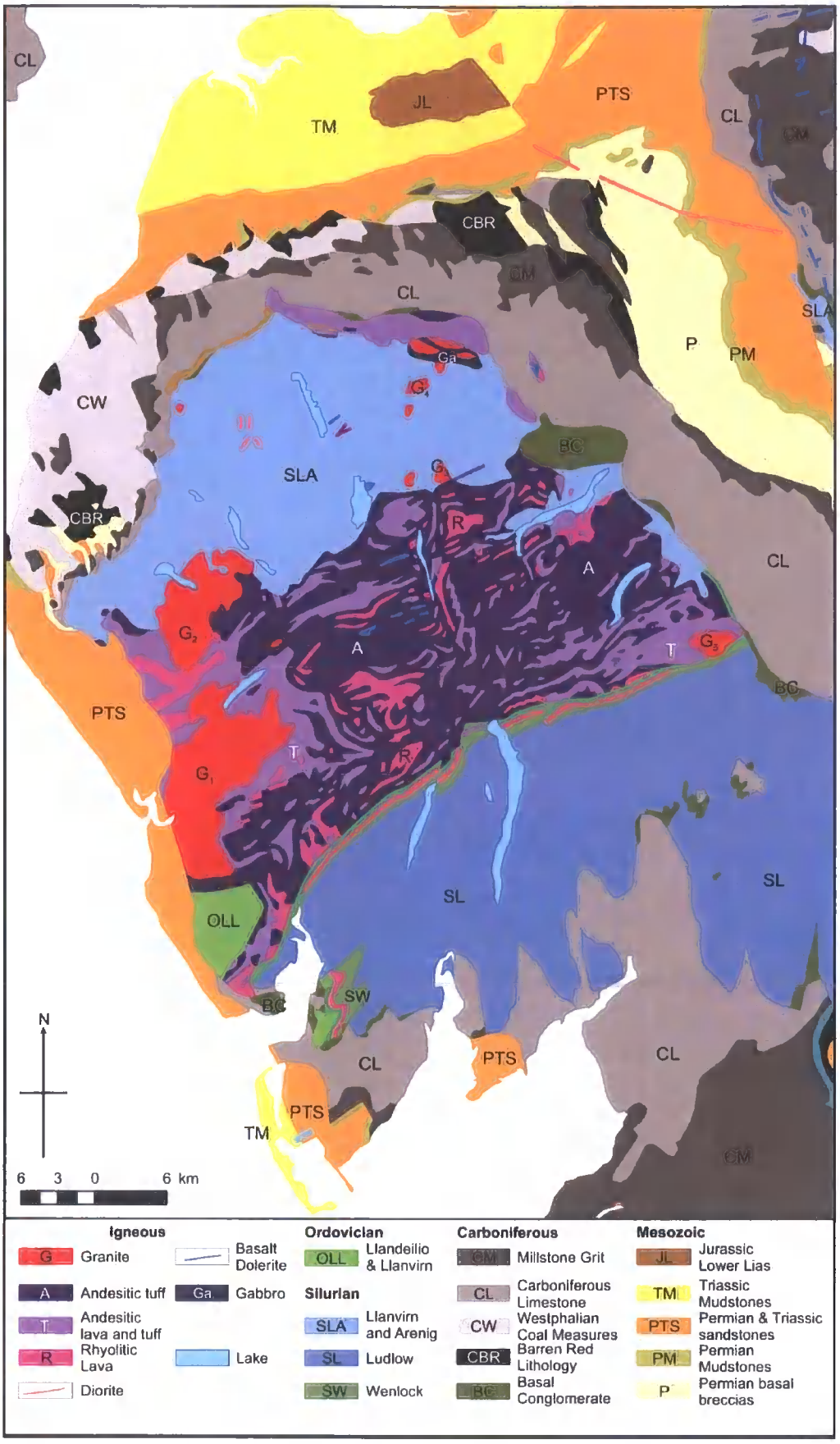

Figure 2.8: Geological map of the Lake District, from BGS Digimap database. © NERC. Granites: G_1: Eskdale Granite. G_2: Ennerdale Granophyre. G_3: Threkfeld Microgranite. G_4: Skiddaw Granite. G_5: Shap Granite (Firman, 1978). SLA is the Skiddaw Slate Series.

2.7.6 The Cheviots

Old Red Sandstone sediments occur in the Cheviot Hills (Figure 2.9) where the Lower Old Red Sandstone includes red siltstones with palaeosols, sandstones and conglomerates. These are overlain by the Cheviot Volcanic Group (Toghill, 2000).

A number of igneous episodes took place during the Devonian (Robson, 1976). The Scandian Orogen, from about 435 to 425 Ma, was of Himalayan proportions, and resulted from the compression of the Laurentian crust, of which the Scottish Highlands were part (Barclay *et al.*, 2005). This caused volcanism and thrusting along major northeast-trending faults, with low-grade metamorphism in northern Britain. The volcanic rocks were originally extensive, and their eroded remnants are located at Ben Nevis, Glen Coe, Lorn and north of the Highland Boundary Fault. Volcanic rocks also occur extensively in the Southern Uplands, and granitic intrusions such as the Cheviot Granite were emplaced (Barclay *et al.*, 2005).

Robson (1976) argued that igneous activity in the Cheviots began with numerous volcanic centres issuing pyroclastic material. Some beds are fine-grained tuffs or ashes, whilst others are coarse agglomerates. The ash cones have mostly eroded away, but the pyroclastic material was preserved under lava flows. Fifteen metres of rhyolite overlies the western pyroclastic flows. They contain phenocrysts of biotite mica, distinguishing them from the overlying andesites (Robson, 1976). The Cheviot andesite, a pitchstone-pyrite, is grey to black, with fresh plagioclase laths (labradorite), thin red veins, and phenocrysts of rhombic pyroxene and augite (Robson, 1995), set in a matrix of feldspar and glass. It is a key indicator erratic, long recognised in the Quaternary deposits of eastern England (Howarth, 1908; Trechmann, 1952; Catt & Penny, 1966; Eyles *et al.*, 1982; Sutherland, 1984; Teasdale & Hughes, 1999).

Some millions of years later, after the end of volcanic action, a major granitic intrusion was injected into the mass of lavas (Robson, 1976). The Cheviot Granite has a surface area of approximately 70 km^2. The junction between the granite and the lava is seldom straight, and ramifying veins of fine-grained granite run into the andesites. Dykes associated with the major granitic intrusion (Robson, 1976) are concentrated in the south eastern, the southern and the south western perimeter of the granite. They are aligned along two trends, the north-north-east and north-north-west. Four varieties are recognised, in order of decreasing abundance: mica-porphyrites, quartz-porphyries, felsites and pyroxene-

porphyrites. They have a strong red or pink colour against the prevailing purple or grey extrusive rocks (Robson, 1976).

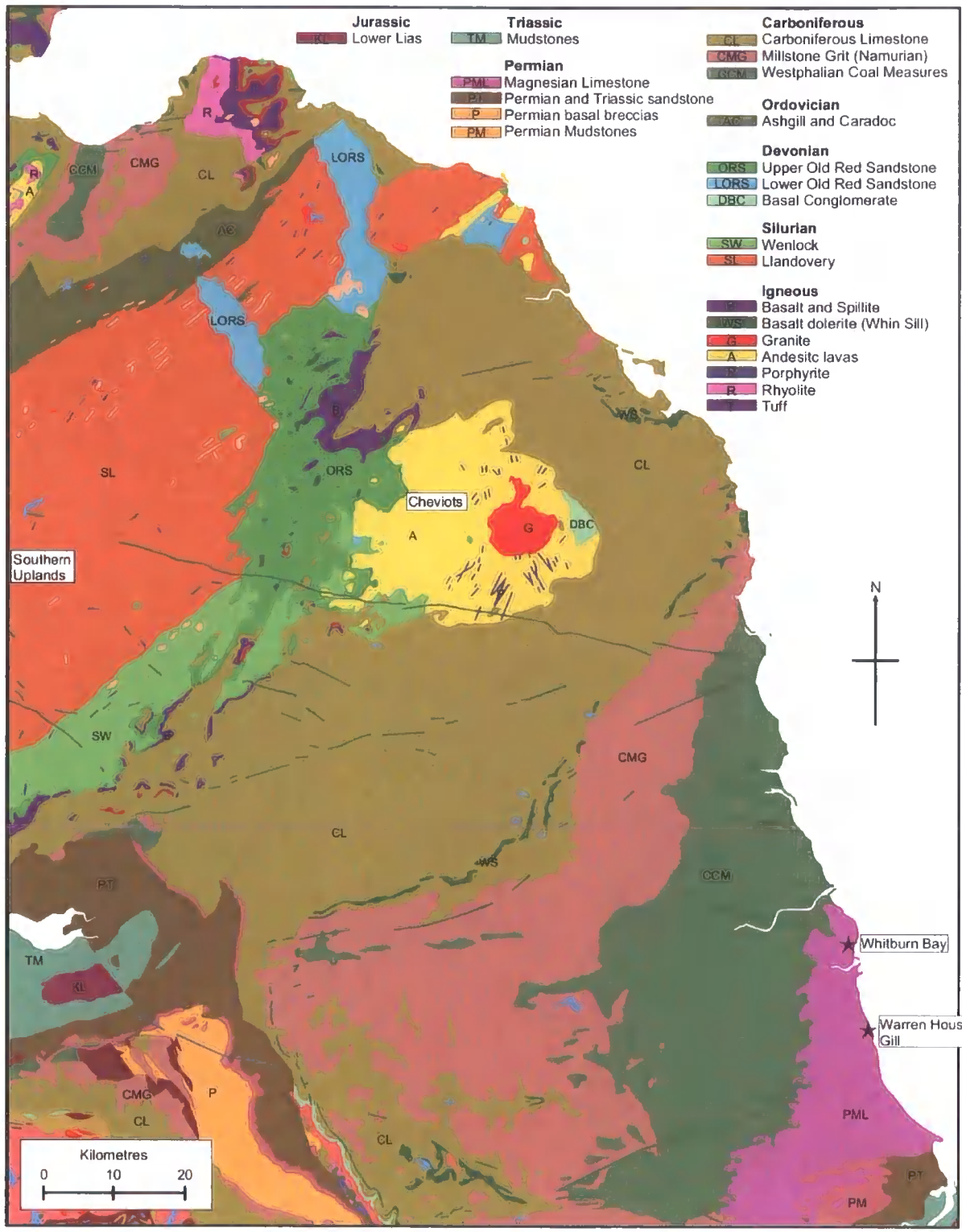

Figure 2.9: Geology of northeast England. From BGS Digimap database. © NERC

2.7.7 Northeast England

The Carboniferous

The eroded Old Red Sandstone Continent was invaded by the shallow shelf seas of the Rheic Ocean, caused by a eustatic sea level rise. The British area was close to the equator with warm, shallow tropical seas, into which the Carboniferous Limestone (Figure 2.9) was deposited. Rivers deposited deltaic sediments, the Millstone Grits (Table 2.11), into these shallow seas (Toghill, 2000). The climate then became humid and these deltas supported swamps and tropical rain forests. Changes in sea level resulted in numerous marine transgressions during the Westphalian, and the burial and decay of vegetation led to the formation of coal seams, the Coal Measures (Toghill, 2000).

Table 2.11: Divisions of the Carboniferous Period (Jones *et al.*, 1995)

Period	Age (Ma)	Epoch	Stages	Formation	Sediments
Carboniferous	290	Stephanian		*Whin Sill*	Quartz Dolerite
	300	Westphalian	D		
			C	*Upper Coal Measures*	Mudstone, siltstone, sandstone, coals
			B	*Middle Coal Measures*	
			A	*Lower Coal Measures*	
	315	Namurian	Yeadonian	*Millstone Grit*	Cyclic succession of sandstone, siltstone, mudstone, limestone and coal
			Marsdenian Kinderscoutian Sabdenian Arnsbergian Pendelian		
	325				
		Dinantian	Viséan	*Carboniferous Limestone*	Sandstone, limestone, mudstone
			Tournaisian		Interbedded shales, dolomitic limestones, sandstones
	363				

The Dinantian Carboniferous Limestone group (Table 2.11) comprises sandstone, mudstone, limestone and coal. The sandstones are fine to medium-grained and are yellow in colour. The argillaceous limestones are hard, grey to dark grey, with conspicuous crinoids, brachiopods and corals (Cameron & Stephenson, 1985). The Westphalian Coal Measures of Northumberland and Durham (Figure 2.9) incorporate a series of deltaic sediments 900 m thick (Jones *et al.*, 1995). Sandstones, siltstones and shales predominate with many seams of coal and underlying seatearths.

The Great Whin Sill

The Whin Sill Complex (Figure 2.9) was intruded into Carboniferous rocks from the Late Carboniferous to earliest Permian (Randall, 1995). It was formed by a series of basaltic dykes linked at depth. The Whin Dykes associated with the Whin Sill have a general east-north-east trend. The Whin Sill Complex intersects the Coal Measures of the Westphalian, but not the Permian rocks and was thus emplaced during the time represented by the unconformity of the Upper Carboniferous and the Permian of the north of England (Randall, 1995).

The Whin Sill dolerite is highly variable and complex. Petrologically, the 'normal' rocks were described by Randall (1995) as a dark, blue-grey quartz-dolerite with a grain size average of 0.5 to 1.0 mm. This varies according to speed of cooling, so higher-level sills and dykes have a smaller grain size. It bears plagioclase laths forming an interlacing network, showing a sub-ophitic texture with granular aggregates of augite. Other types include fine-grained rocks of basaltic composition with small phenocrysts of plagioclase and pyroxene, and coarse-grained rocks will all the mineral constituents visible to the naked eye (Randall, 1995).

The Permian

The Permian forms the bedrock for County Durham and is the local bedrock for the onshore field sites. Smith (1995b) argued that during the Early Permian, northern Europe was similar to the Sahara today. Widespread barren uplands were gradually eroded, to form an extensive peneplain of vast areas of Carboniferous rocks. Post-orogenic subsidence resulted in the formation of extensive sub-sea-level basins in the areas now occupied by the North and Irish Seas (Smith, 1995a).

The Early Permian Basal Breccias (Figure 2.9) are yellow, 0.6-1.8 m thick, and consist of angular to subangular rock fragments in a tough grey matrix of calcite in dolomite-cemented fine-grained sandstone. The component clasts are Carboniferous Limestone. Patination and scattered dreikanter suggest that the breccias may have formed part of a stony desert pavement (Smith & Francis, 1967). The younger Yellow Sands are a distinctive unfossiliferous formation of weakly cemented aeolian desert sand in eleven parallel ridges, characterised by large scale trough cross lamination (Smith & Francis, 1967).

During the Late Permian, a marine transgression from the north established a shallow saline sea, the Zechstein Sea, over northern Europe, the North Sea and northeast England (Figure 2.10). They infilled the deep basins formed by subsidence in the North Sea region, separated by a persistent Pennine Ridge (Smith and Francis, 1967). Thicknesses of dolomitic limestones and evaporites were deposited as it dried up (Toghill, 2000). Woodcock and Strachen (2000) stated that the preservation of the dune topography when sands were still friable indicates rapid transgression by quiet marine waters. Smith (1995a) argued that after the transgression, most of east Durham lay in the marginal shelf zone of the Zechstein Sea. The Permian Rocks of northern England (Figure 2.9) are therefore a thick cyclic succession of marine limestones and dolomites, which outcrop in the eastern and southern parts of Tyne and Wear and County Durham (Smith, 1995b).

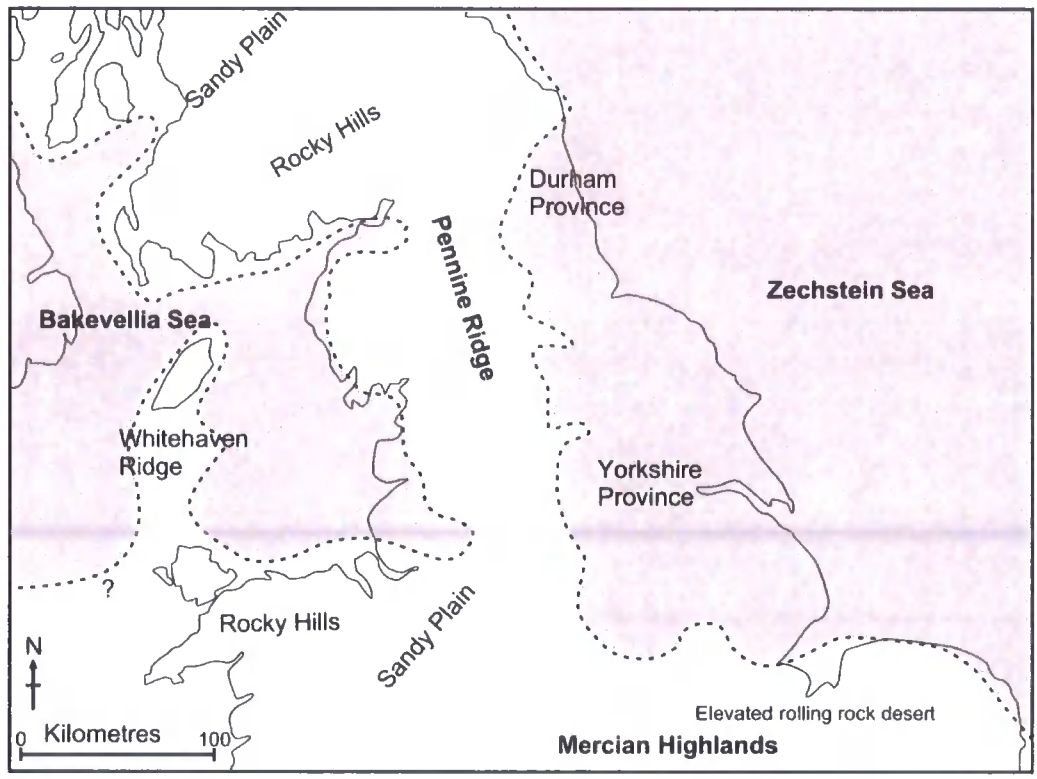

Figure 2.10: The Zechstein and Bakevellia Seas in the Late Permian. Adapted from Smith (1995a).

Smith (1979; 1994) argued that the Zechstein Sea modified the immediate climate, increasing rainfall and enabling plants to become re-established in former desert areas. Large-scale cyclicity was caused by glacio-eustatic sea-level oscillations. The sediments are subdivided into four evaporite cycles (Smith, 1995b). Each cycle consists of varying proportions of mudstone, limestone, dolomitic limestone and evaporite, deposited in a

number of discrete phases. The concentration of salts in each cycle results from the desiccation of the surrounding playas and Salinas with continued evaporation in the basin (Woodcock & Strachan, 2000). The upward concentration of salts and the increasing aridity of the environment through each cycle is mirrored in the complete Zechstein succession.

North of the West Hartlepool Fault, no strata higher than the Magnesian Limestone occur. Their former presence is indicated by fragments of red and green mudstones of Upper Permian Marl lithology and in collapse breccias in the Middle and Upper Magnesian Limestone (Smith & Francis, 1967). Abundant plant debris in the lower parts of the carbonates suggests that after each transgression, climatic amelioration occurred around the margins of the sea (Smith, 1995b).

The local bedrock in the study area is the Late Permian Roker Dolomite and Concretionary Limestone formations (Smith, 1995b), part of Cycle 2 of the Zechstein evaporites. They span a continuum of depositional environments, ranging from shelf-crest oolite banks (Roker Dolomite facies) to unstable slope deposits (Concretionary Limestone facies). The Concretionary Limestone is a grey to brown laminated dolomitic limestone or dolomite with abundant turbiditic and slumped beds of cream-coloured dolomite and oolite (Smith, 1995b). The Roker Dolomite Formation comprises well-bedded cream to buff-coloured granular dolomite, often oolitic, with some lamination.

2.7.8 The North Sea

Pre-Permian and Permian Geology

Pre-Permian rocks in the North Sea Basin are exposed along the British coastline, but are covered eastwards by younger lithologies (Gatliffe *et al.*, 1994). The Devonian Old Red Sandstone was deposited in the Orcadian Basin around the Moray Firth (Figure 2.11). Most of the Central North Sea was a region of continental deposition during the Upper Devonian (Gatliffe *et al.*, 1994), and the Upper Old Red Sandstone has been found in many wells.

There were two major depocentres (the Southern and Northern Permian Basins) in the North Sea during the Permian (Gatliffe *et al.*, 1994). Gatliffe *et al.* (1994) stated that the Lower Permian in the Northern Basin comprised red, clastic sediments deposited in continental desert, fluvial and sabkha environments. The overlying Upper Permian (Zechstein) sediments were deposited after a transgression (Figure 2.10) and consist of

evaporites and carbonates (Smith, 1995b). These sediments continue onshore to eastern England. They include red Upper Permian Marls, which have been eroded from the English coastline.

The Jurassic and Triassic

The North Sea was a major Mesozoic basin, with over 3000 m of deposits occurring in the most rapidly subsiding part east of Scotland (Figure 2.11). Lias does occur in quantity in the Viking Graben area east of the Shetlands (Hudson & Trewin, 2002). The North Sea contains some of the principle oil reservoirs, located in Middle Jurassic sequences. Massive, coarse- to fine-grained sandstones are overlain by mixed shales, sandstones and thin coals, with an upper facies of bioturbated marine sands (Hudson & Trewin, 2002). Kimmeridgian bituminous shales from the Upper Jurassic are widely distributed in the North Sea (Figure 2.11).

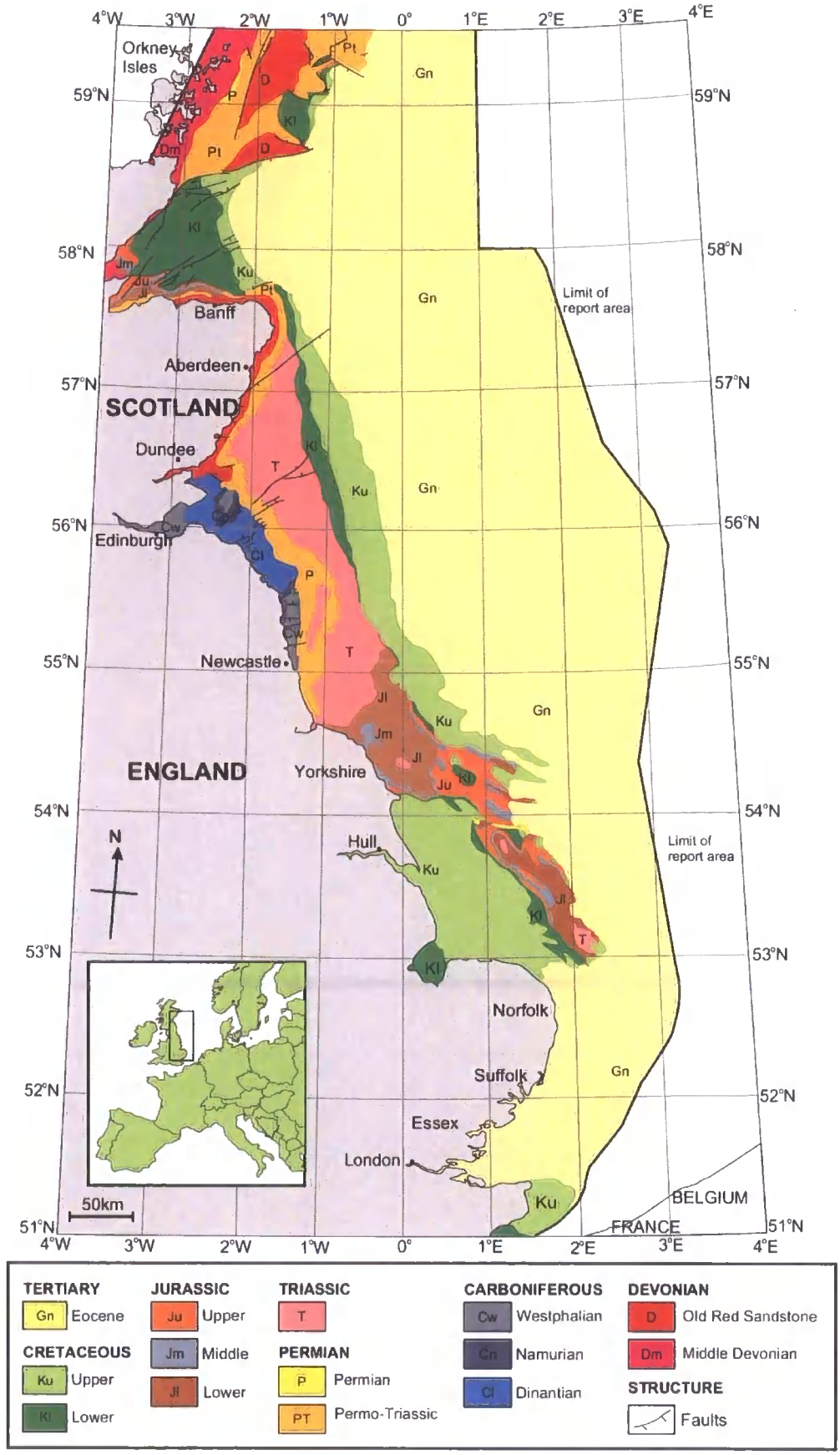

Figure 2.11: Geology of the North Sea. Adapted from Gatliffe *et al.*, (1994) Cameron *et al.*, (1992) and Andrews *et al.* (1990).

The Cretaceous and Palaeogene

The Jurassic-Cretaceous boundary occurs within the Kimmeridge Clay Fm (Gatliffe *et al.*, 1994). Sudden eustatic sea-level fall caused the cessation of Kimmeridge Clay deposition. Across a large area in the Mid North Sea High towards the Aberdeen Platform, uniform, argillaceous, calcareous sediments were deposited during the Early Cretaceous. During the Late Cretaceous and earliest Palaeocene, warm, oxygenated waters transgressed the North Sea and Britain. Thick chalk and chalk-marl sequences were deposited in the central North Sea (Figure 2.11). Lithospheric cooling led to downwarping in the central North Sea, and accumulation of sediments along the central axis (Gatliffe *et al.*, 1994).

Gatliffe *et al.* (1994) mapped Palaeogene sedimentary rocks over large areas of the central North Sea (Figure 2.11). There is an erosional limit 100 km east of the UK coast. The Palaeogene represents the end of quiescence, uplift of the Hebrides-Shetland axis, and extensive volcanicity in the northeast Atlantic Ocean. This was associated with sea-floor spreading and the opening of the Atlantic Ocean (Gatliffe *et al.*, 1994). According to Gatliffe *et al.* (1994), the Palaeogene and Eocene rocks of the North Sea comprise deltaic, shelf and basin systems, mostly hemipelagic mudstones and sandstones, deposited in shallow seas.

2.8 Statistical Analysis of the Geochemical Data

2.8.1 Principle Components Analysis

Multivariate statistical analysis of the heavy mineral, metals and stone lithology counts allowed simplification of variables in the dataset. Ordination techniques attempt to represent the relationships of the objects of study in a continuum of one or more dimensions. Numerous variables, such as numbers of different heavy mineral species, give a multidimensional dataset. The main objective of ordination techniques therefore is to reduce the number of dimensions necessary for depicting the major trends in a data set (Kovach, 1995).

Eigenanalysis is an ordination technique that performs linear transformations on multidimensional data to extract axes that summarise as much of the data as possible. Principle Component Analysis (PCA) is an eigenanalysis of a covariance or a correlation matrix, calculated from the original measurement data (Kovach, 1995). It is a method of displaying several correlated variables so that the maximum variation is displayed (Ryan *et al.*, 2007). The PCA method uses all the data and requires no factor weighting. Data are plotted in hyperspace.

The elements of the eigenvectors used to compute scores of observations are "Principle Component Loadings". These are coefficients of the linear equation that the eigenvector defines. The PCA axes represent the variation of the data (Davis, 1986). The longest axis, which describes the greatest variance, is the first PCA axis; the second longest axis, perpendicular to then first, represents the next set of variance, etc. (Kovach 1995). In two dimensions, a graph can be plotted with new axes, the first of which is a best-fit line through the data, and the second of which is the axis with least variation (Ryan *et al.*, 2007). A PCA based on a covariance matrix relates to the squared standard deviation within the variables. A PCA based on a correlation matrix relates to the skew of the variables. An eigenanalysis is then performed on the matrix (Kovach, 1995).

For example, Bateman and Catt (2007) used PCA to summarise the numerous variables (mineral categories) into a single diagram. In a periglacial landscape in northwest England following the Younger Dryas, multidirectional winds deposited the Shirdley Hill Sand coversands. Their depositional environments and provenance remain controversial (Bateman & Catt, 2007). Likely provenance sources for these reworked sands include

Quaternary deposits, the Carboniferous Lower Coal Measures, and the Triassic Bunter Sandstones. PCA revealed three main groups. The SHS formed three main groups; the uppermost was highest in the succession and was weathered. The other groups indicated an origin by aeolian reworking of earlier glaciofluvial sands, i.e., outwash from the Late Devensian ice sheet (Bateman & Catt, 2007).

Principal components analyses (covariance and correlation) and cluster analyses on the heavy-mineral assemblages involved first simplifying the mineral phases or lithological types into their wider family groups to reduce the number of variables (i.e., silicates, epidote group, pyroxenes, amphiboles, micas, oxides and phosphates). In heavy-mineral analysis, sulphides and sulphates were excluded from the analysis due to very low numbers (less than 2 % of total), and carbonates were excluded due to strong skew. Statistical analyses on the stone lithological counts involved simplifying the dataset into groups of igneous, Permian, quartzose, Cretaceous, Jurassic, Carboniferous, Southern Uplands, sandstone, and Triassic lithologies. Statistical analyses were only conducted on the abundant metals in the matrix geochemistry, due to the strong variations and skew in the rare metal abundances.

2.8.2 Cluster analysis

Cluster analysis is a set of numerical techniques used to divide the observations into discrete groups. The clusters are based on the characteristics of the objects (samples), the most similar being clustered most closely together (Kovach, 1995). 'Non-hierarchical' techniques divide samples into groups without showing the relationships between the groups. 'Hierarchical methods' arrange the clusters into a hierarchy, making the relationships between different groups apparent (Kovach, 1995). This produces a tree-like diagram termed a 'dendrogram'. Agglomerative hierarchical cluster analysis starts with all the samples separately, and combines successively the most similar samples until all are in a single, hierarchical group. This technique is useful in geochemical analysis of tills, for example, as a clear dichotomy between lithofacies, with a high degree of dissimilarity and a low degree of clustering, can indicate separate depositional events. Agglomerative hierarchical cluster analysis operates by first calculating a similarity matrix for all samples. The most similar samples cluster as a pair and are then considered a single object. The similarity matrix is recalculated and compared with this new group (Kovach, 1995).

'Ward's Linkage' cluster analysis focuses on determining how much variation there is within a cluster. The clusters joined in the next round of clustering are chosen by determining which two would give the least increase in within-cluster variation (Kovach, 1995). The clusters are as distinct as possible, as the criterion for clustering is to have the least amount of variation.

Bell *et al.* (1989) used cluster analysis of erratics within the drifts of northern Labrador to distinguish regional and local ice events, and to define ice-flow patterns and ice limits in the study area. Gneissic clasts indicated deposition by an easterly flow of the Laurentide ice sheet, and the absence of such clasts indicates deposition by a local ice source (Bell *et al.*, 1989, 1990).

Richards (1998) used quantified clast-lithological analysis and matrix geochemistry to distinguish different lithostratigraphical units within between the Risbury Fm of Herefordshire. PCA and cluster analysis allowed differentiation of individual groupings. Multivariate analysis of the clast lithological and fine-fraction geochemical data defined consistent populations within diamicton facies from the Risbury Fm of northeast Herefordshire. The first population is a subglacial till. Melt-out or secondary processes in a proglacial, ice-marginal environment deposited the second population. The matrix composition was therefore dependent on the mode of deposition by the ice sheet (Richards, 1998).

Thamó-Bozsó and Kovács (2007) used numerical analysis of heavy-mineral data to reconstruct the evolving Quaternary fluvial network of the Hungarian Plain. Heavy-mineral composition the borehole data and modern river sediments, evaluated by cluster analysis, showed two, three or four major clusters. This cluster analysis allowed full differentiation of the sediments of various palaeo-rivers.

Parallel with cluster analysis, Thamó-Bozsó and Kovács (2007) performed PCA on all samples. Results identified garnet, chlorite, amphibole and pyroxene as the most important heavy minerals in the differentiation between the assemblages of the modern and ancient Danube and the tributaries of the Tisza River. Comparison of the heavy mineral compositions of the modern river samples and the boreholes samples by PCA showed the modern river samples to cluster to the right, being devoid of chlorite, with the Quaternary sediments clustering to the left, influenced by high percentages of chlorite. This allowed inferences regarding transport directions.

2.9 Microfossil and Macrofauna Analysis

2.9.1 Foraminifera

Foraminifera live in very specific marine environments, either as plankton or as benthos. They are amoebas with granular reticulopods, two-way cytoplasm streaming, and which either secrete calcareous shells, or agglutinate sediment particles into a shell (a test). The test is composed of a series of chambers; different species display diversity in architecture and arrangements (Loubere & Austin, 2007). There are about 10,000 species of benthic foraminifera, which are taxonomically organised based on their test structure. Tests are usually from 50 μm to 2000 μm in size. The identification of different species by their tests and their abundances in an assemblage can give clues as to the environmental conditions at the time of deposition. This thesis uses qualitative foraminifera analysis to infer between glaciomarine conditions, open-water conditions, and subglacial conditions.

The separation of foraminifera (forams) follows the methodology outlined in Appendix I (cf. Knudsen & Austin, 1996). In each sample, 200-300 specimens are picked out from a black tray and placed onto a counting tray for identification and counting. Identification of foraminifera and their palaeo-ecology is determined with reference to described samples in the literature (Hansen & Lykke-Andersen, 1976; Murray, 1979; Hald & Korsun, 1997; Jennings *et al.*, 2004). Some examples are shown in Figure 2.12. The specimens are identified by their visual characteristics, including whether they are triserial, biserial, planispiral, trochospiral, evolute, involute, how many chambers there are, and the presence of septal bridges (Figure 2.13, Loubere & Austin, 2007).

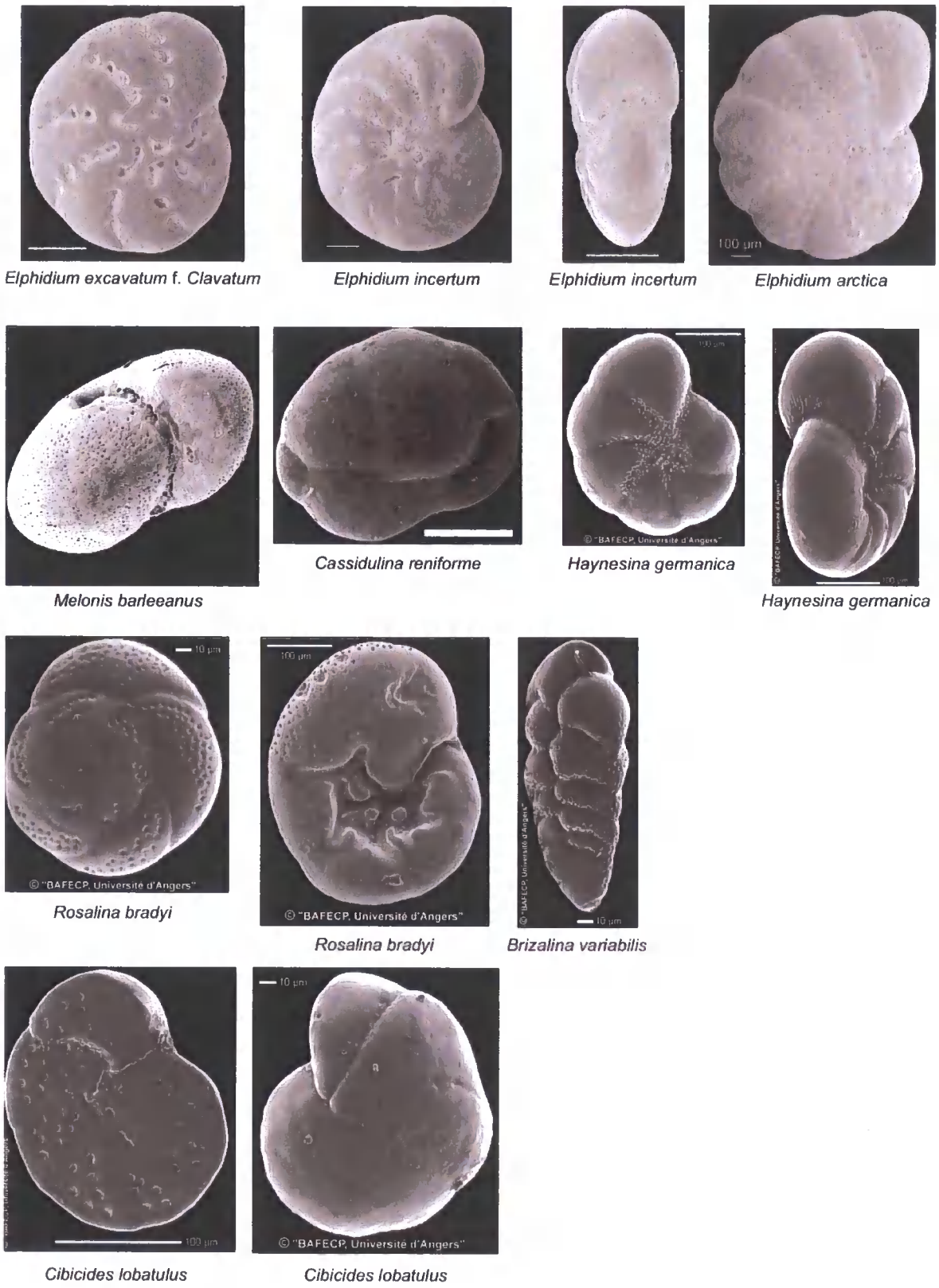

Figure 2.12: Electron microphotographs of some common benthic calcareous foraminifera. Scale bar is 0.1mm unless otherwise stated (Korsun *et al.*, 2001)

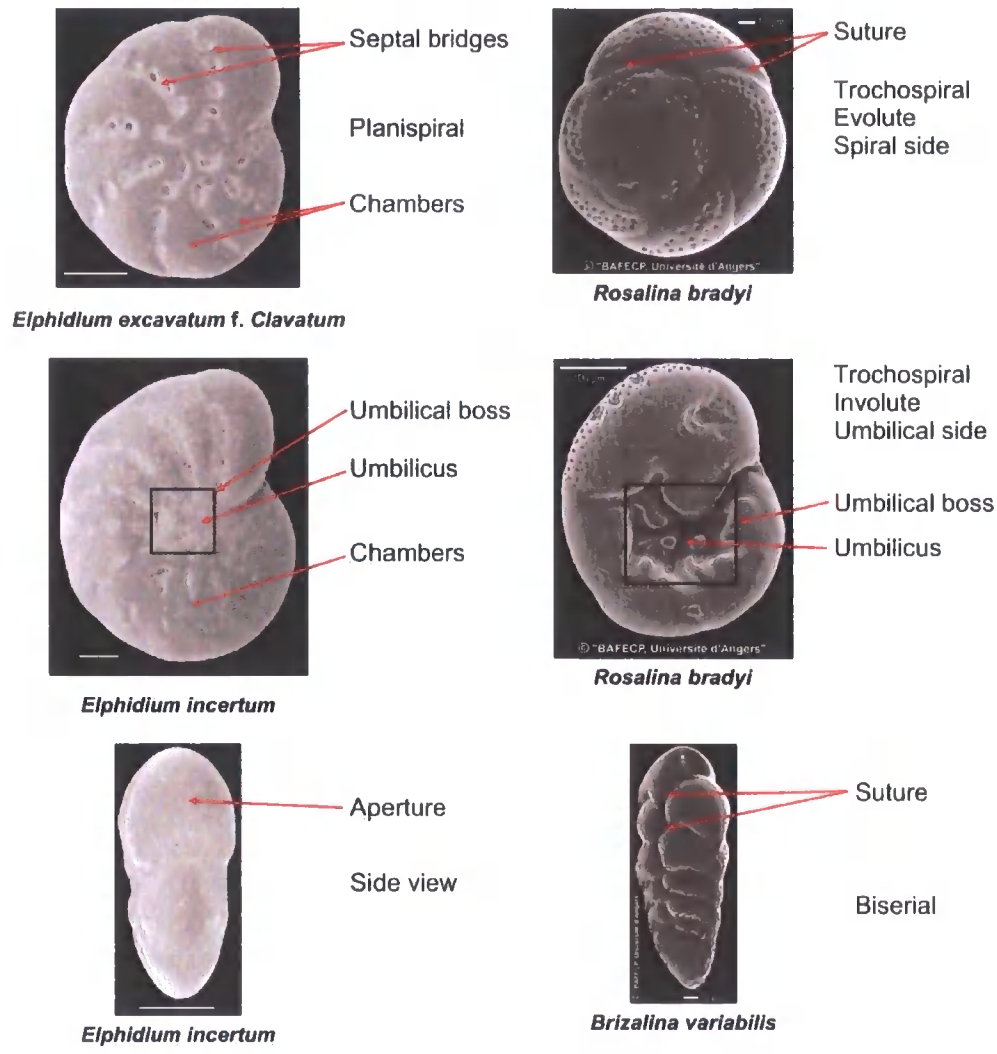

Figure 2.13: Identification of critical parts of foraminifera (Bé & Tolderhund, 1971; Vincent & Berger, 1981; Korsun *et al.*, 2001).

A number of typical faunal assemblages have been identified in modern glaciomarine environments, such as Svalbard, and can be used as analogues to interpret assemblages in ancient glacigenic sediments. For example, the *Cassidulina reniforme* assemblage is negatively related to salinity and temperature. It typically occupies the inner parts of glacially-influenced fjords in Svalbard (Hald & Korsun, 1997). Subsidiary species include *Cibicides lobatulus, Elphidium excavatum* f. *clavata,* and *Buccella frigida.* These assemblages are common in modern glaciomarine environments.

An *Elphidium excavatum* f. *clavata* assemblage is a typical proximal glaciomarine fauna (Jennings *et al.*, 2004). These environments are characterised by seasonal sea-ice cover, turbid water and high sedimentation rates. It usually occurs with the *C. reniforme* assemblage, with *E. excavatum* increasing in dominance close to the glacier snout. The *C.*

reniforme assemblage also extends beyond the areal distribution of the *E. excavatum* assemblage (Hald & Korsun, 1997). A *Cibicides lobatulus* assemblage with accessory species *I. norcrossi* and *A. gallowayi* is typical of high energy/low sedimentation rate environments. The species has a cosmopolitan distribution (Hald & Korsun, 1997), is common in the outer parts of glacier fjords, and is indicative of a high energy bottom-water environment.

2.9.2 Palynomorphs

Allochthonous palynomorph analysis was also used to establish provenance and help in the ice-flow pathway reconstruction (Lee *et al.*, 2002; Riding *et al.*, 2003), based on known and established geological and geographical distributions. Palynomorph analysis was carried out by Dr. Jim Riding of the British Geological Survey, Keyworth, using the separation method outlined in Appendix I (see Riding & Kyffin-Hughes, 2004; Riding & Kyffin-Hughes, 2006). 'Palynomorphs' are organic-walled microfossils with a plant or animal affinity (Riding & Kyffin-Hughes, 2004), and can be derived from either terrestrial or marine terrains. They are abundant in sedimentary deposits, and their small size, ubiquity, and high preservability means they can provide detailed biostratigraphical and palaeo-ecological information (Riding & Kyffin-Hughes, 2004). Palynomorphs include acritachs, dinoflagellate cysts, chitinozoa, fungal spores, green/blue algae, plant spores, pollen grains, and scolecodonts (Jansonius & McGregor, 1996). They do not include wood fragments, plant cuticles or other amorphous organic material.

Dinoflagellates are unicellular organisms occupying most aquatic environments. Most species are planktonic and use two flagella to swim in a spiral-like motion (de Vernal *et al.*, 2007). Their cysts (dinocysts) yield microfossils, and these are good biostratigraphical markers and indicators of changes in sea-surface water masses (de Vernal *et al.*, 2007). Dinocysts are the most common organic-walled microfossils or palynomorphs in marine sediments. Their presence in Quaternary glacigenic sediments and tills is useful as they can be used to determine the source regions for ice sheets; for example, Eocene dinoflagellate cysts can only be derived from the Late Cretaceous chalk of the northeastern North Sea, whereas Carboniferous palynomorphs typically indicate a provenance in northern England (Riding *et al.*, 2003). Palynomorph analysis has been used extensively to test for a Scottish or Scandinavian ice source in tills in Norfolk (Lee *et al.*, 2002; Riding *et al.*, 2003).

2.9.3 Macrofauna

Marine macrofauna can impart valuable information regarding depositional environments and palaeo-environmental conditions (e.g., freshwater / brackish / marine / littoral / shelf / temperate / arctic conditions). Additionally, shell fragments can be used for amino acid racemisation dating. The shells of different species racemise at different rates (Lajoie *et al.*, 1980; Penkman *et al.*, 2007), so that only racemisation data from the same taxon can be meaningfully compared, making species identification particularly important. Shells such as marine bivalves and littoral gastropods were identified with reference to a specimen guide book (Campbell & Nicholls, 1986) were observed through a low-powered binocular microscope (*Motic SMZ-168*).

2.10 Dating Techniques

The cliffs along the Durham coastline contain directly dateable sediments. Techniques utilised for this part of the research include amino acid racemisation (AAR) on marine gastropods within the Warren House Formation and the Easington Raised Beach, Optically Stimulated Luminescence (OSL) dating on beach, fluvial and marine sediments, and U-series on the cement of the Easington Raised Beach.

2.10.1 Amino Acid Racemisation (AAR)

Amino acids are organic molecules linked by peptide bonds (Miller & Clarke, 2007), and make up all proteins. All protein amino acids have one asymmetric carbon atom or centre of symmetry; these are 'chiral' molecules. The mirror images of chiral molecules are not superimposable; they exhibit 'handedness' (Miller & Clarke, 2007). They can exist in two different configurations or 'enantiomers'. Chiral forms of the same amino acid were originally identified by the way they rotated plane-polarised light passed through a solution containing the pure enantiomer. Enantiomers rotating light to the left are L-amino acids (levorotatory); those rotating light to the right are D-amino acids (dextrorotatory). Living organisms utilise exclusively L-amino acids to build protein (Miller & Clarke, 2007). Upon the death of an organism, diagenetic reactions degrade proteinaceous residues into their constituent amino acids, which spontaneously interconvert to their D-configurations in a regular and predictable manner into an equilibrium mixture (Penkman *et al.*, 2007). This is 'racemisation'. The initial status of 100 % L-configuration means that amino acid racemisation can be used as a dating technique.

Amino acid racemisation was carried out on shell fragments of known species using a pioneering technique developed by Dr. Kirsty Penkman and Miss Beatrice Demarchi (University of York). Improvements in the methodology developed by Dr. Penkman mean that multiple amino acids are analysed from the intra-crystalline fraction (Penkman *et al.*, 2007; Penkman *et al.*, 2008). Refer to Appendix I for detailed methodology.

Organic matter within fossil biominerals is subject to contamination. The degradation products of the organic matter also need to be retained within the biomineral as diagenetic reactions are used to assess the original properties and burial history of the sample. Investigation of fossil organic material therefore requires a "closed system" (Penkman *et*

al., 2008). A closed system is essential for the application of amino acid geochronology, because the majority of organic matter within fossil biominerals is subject to contamination and / or leaching. In closed systems, diagenetic reactions of indigenous biomolecules should be predictable, and the original molecules and their degradation products can be used to interpret the burial history of the sample (Penkman *et al.*, 2008). As diagenetic reactions are used to assess the original properties and burial history of the sample, the degradation products of the organic matter must be retained within the biomineral: this is the case in closed systems (Penkman *et al.*, 2008). The method is based on the extent of protein decomposition, which increases with time, although there is an increased rate of breakdown during warm stages and a decrease in cold stages. Amino acids can exist in two forms, L and D, and only L-amino acids are formed in shells; modern shells have a DL ratio of close to zero. However, when an organism dies a spontaneous reaction occurs called racemisation, until there is an equal number of D- and L- amino acids, i.e., a D/L value of 1.

A substantial proportion of molluscan shell protein is subject to diagenesis and dissolution after burial. However, a residual fraction of shell protein is retained by amino acids, and can be isolated by extensive bleach treatment of shell powders. This intra-crystalline fraction traps organic material within crystals, and is superior for AAR dating. Exposure of the powdered mollusc shells to concentrated NaOCl (bleach) for 48 hours reduces the amino acid content to residual levels; this procedure effectively removes the readily accessed organic matrix that resides between mineral crystals while isolating the intra-crystalline fraction (Figure 2.14). The intra-crystalline fraction of mollusc shells is a closed system for the retention of amino acids.

Rates of racemisation vary between species (the "species effect"), as does diagenesis (Lajoie *et al.*, 1980); therefore for an age to be determined from the ratios of amino acids, a thorough database of species that have been independently dated is needed.

In this research project, shell fragments were separated from bulk sample by gentle wet sieving, and appropriate species were analysed by AAR. The goal was to constrain the age of the shell to provide a minimum age estimate for the sediment.

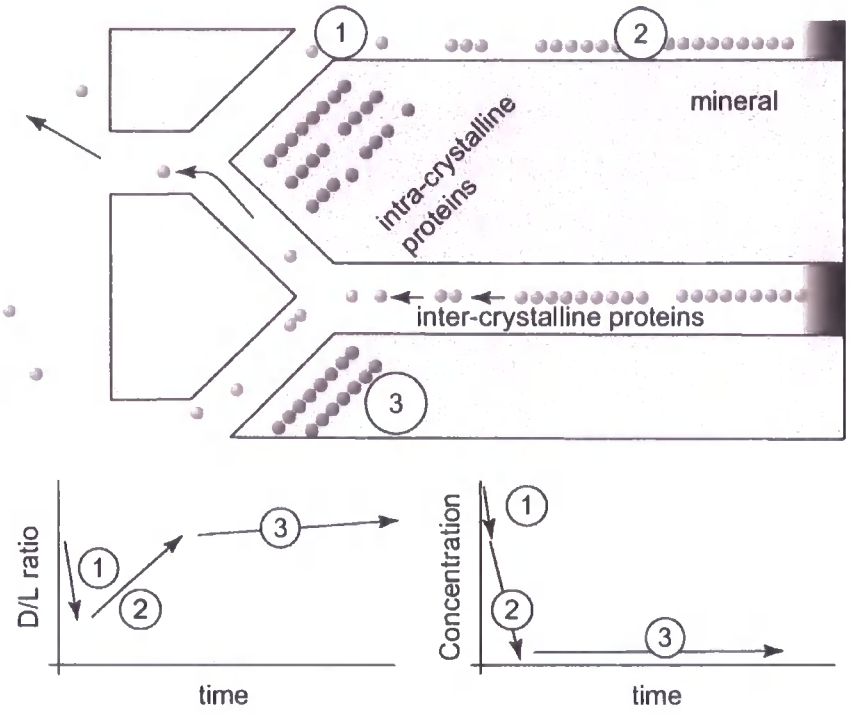

Figure 2.14: Conceptual model for the effect of bleach on different amino acid fractions in a shell.

The highly racemised FAA in the matrix (1) are removed first, leading to a small drop in the concentration but a decrease in the D/L value.

A rise in D/L coincides with a rapid drop in concentration as the intact proteins of the matrix (2) are removed. Prolonged bleaching may selectively remove amino acids in the intra-crystalline fraction or begins to etch the carbonate, exposing intra-crystalline acids (3). From Penkman *et al.*, (2008).

2.10.2 Optically stimulated luminescence (OSL)

Optically Stimulated Luminescence (OSL) dating is a direct method of dating glacigenic sediments. It can only be used on sediments that have been exposed to light at the time of deposition, such as glaciofluvial, glaciolacustrine and loessic sediments. The context and depositional environment of the sample sites must be well understood if the dates are to be correctly interpreted. OSL is only applicable on sediments with a significant amount of quartz and feldspar grains, so is particularly suited to quartz-rich sand deposits typical of glaciofluvial sandurs. Luminescence dating works with sediments from a few years to several hundred thousand years old (Lian & Roberts, 2006), making it a considerably more viable radiometric technique than others due to its longevity and the fact that organic remains are not required. OSL dating at Warren House Gill was carried out and interpreted by Dr. Stephen Pawley (Department of Geography, Royal Holloway University of London), using the methodology outlined in Appendix I.

Recent examples of direct OSL dating on glaciolacustrine sediments include the ice-dammed Glacial Lake Humber (Bateman *et al.*, 2008). The dates of 16.6 ± 6 kyr constrain the advance of the Last British-Irish Devensian ice sheet in the area, as it could only exist when ice advanced through the Humber Gap. Glaciofluvial sediments from a sandur and other glaciofluvial sediments in west Norfolk were dated by OSL to MIS 12 (Pawley *et al.*, 2008), contesting recent models proposed for north Norfolk that suggest that these sediments are as old as MIS 16. This new research suggests that the Cromer Ridge was formed in MIS 12 instead of MIS 6 (Pawley *et al.*, 2008). Refer to Chapter 1.2.1.

Natural minerals absorb and store ionising energy; when exposed to sunlight, this energy is lost (Lian, 2007). In the environment, this energy comes from naturally occurring radiation emitted from radioisotopes within the mineral grain, from its immediate surroundings, and from cosmic rays. The dose rate is therefore proportional to the concentration of radioisotopes, and to the intensity of cosmic rays. The amount of uranium (U), potassium (K) and thorium (Th) in a sample significantly affect the upper and lower limits of the technique. The optical age of the sample is determined by the laboratory dose of radiation that produces the same OSL as did the environmental dose; this is the equivalent dose. The age of the sediment is the equivalent dose divided by the dose rate (Lian, 2007). Optical dating therefore gives the time since the last exposure to sunlight or heat (Murray & Roberts, 1997).

The physical models used to explain OSL are complex and remain poorly understood. There are numerous reviews about the mechanisms involved (e.g., Murray & Wintle, 2000; Lian & Roberts, 2006; Lian, 2007). The crystal lattice is imperfect and contains impurities and structural defects (Lian, 2007), some of which are attractive to electrons which have been freed from their normal sites in the valance bands of atoms. These are 'electron traps'. Free electrons occur when atoms absorb naturally occurring ionising radiation. Free electrons are then held in electron traps; the duration depends on the strength / thermal lifetime of that particular trap. Some of these traps will be emptied on exposure to light (Lian, 2007). The sediment must have been deposited sub-aerially or in only shallow subaqueous conditions, to ensure that the electron traps are fully emptied prior to burial.

2.10.3 Uranium-Series Dating and Stable Isotope Analysis

Stable isotope analysis can impart valuable information regarding the climatic conditions (i.e., interglacial / glacial / wet / dry), as isotopes of oxygen and carbon vary

according to the prevailing climatic conditions (Candy *et al.*, 2006; Preece *et al.*, 2007). This was conducted by Ian Candy according to standard procedures (Candy *et al.*, 2006).

Uranium-series (U-series) has been used extensively to date carbonates (e.g., Candy, 2002; Candy & Schreve, 2007; Preece *et al.*, 2007). U-series utilises the natural decay of uranium into its daughter isotopes. There are three U-series decay chains that start with the naturally occurring radioactive isotopes ^{238}U, ^{235}U (Uranium), and ^{232}Th (Thorium), and end with the stable isotopes of lead: ^{206}Pb, ^{207}Pb, and ^{208}Pb respectively (Thompson, 2007). The solubility of uranium is relatively high. Therefore, carbonates precipitated from natural waters frequently contain significant uranium and negligible thorium and protactinium (Pa) concentrations, allowing the radioactive decay of uranium to be charted. These are ideal conditions for U-series, which requires an initial state of disequilibrium due to its very long half life (Thompson, 2007).

The isochron method is most appropriate for surficial carbonates, including calcretes, as it corrects for detrital contamination (Candy *et al.*, 2005). U-series sample preparation, separation geochemistry and mass spectrometry followed the procedures of Seth *et al.* (2003), Luo *et al.* (1997) and Pin and Joannon (2001). U-series dating was conducted by Dr. Candy, of Royal Holloway, University of London (see Candy, 2008 in Appendix IV).

CHAPTER 3

Whitburn Bay

3.1 Introduction

A version of this chapter is in press in *Boreas* (see Appendix II). The behaviour of the British-Irish Ice Sheet (BIIS) along the eastern coast of Britain during the Last Glacial Maximum (LGM) is poorly understood (Carr *et al.*, 2006). Competing ice lobes from both northwest Britain and Scotland overran the area, but the flow phasing of these lobes, and their dynamic interaction have only been partly reconstructed. Whitburn Bay in County Durham, northeast England (Figure 3.1), is located in an area of coalescence of several competing ice lobes, making it crucial for understanding ice-sheet flow dynamics and flow phasing during the LGM. This region captures the signal of ice flowing eastwards from the Tyne Gap and ice flowing southwards down the coast. It is ideally located to determine the palaeo ice-flow direction here, to establish whether there is an onshore signal for the North Sea Lobe. Sites located further south are within city limits; further north and the Tyne Gap signal is not present. In addition, the Glacial Lake Tees is located immediately inland of Whitburn Bay, so this is a key site to determine the mechanism and cause of this proglacial lake. Furthermore, there is little chronostratigraphic control on the glacial sediments associated with both the advance and retreat phases of the BIIS in this area.

It has been suggested that ice from northwest Britain crossed the coast first, before ice sourced from the Cheviot/Tweed area flowed north to south down the coast (Teasdale & Hughes, 1999). The sediments and landforms related to the latter phase of ice flow suggest a surge lobe may have operated along this coast (Eyles *et al.*, 1982; Catt, 1991a; Eyles *et al.*, 1994; Evans *et al.*, 1995; Teasdale & Hughes, 1999; Boulton & Hagdorn, 2006). This late-phase readvance of ice has been linked to Heinrich Event 1 forcing (McCabe *et al.*, 2005). The coast-parallel flow direction of the ice has also been linked to deflection of the BIIS by Fennoscandian ice in the central North Sea (Boulton *et al.*, 1991), but this remains contentious (Carr *et al.*, 2006). Whitburn Bay (Figure 3.1) is therefore an important site as

it exposes both of the Blackhall and Horden members, and was a focal point for ice emanating from the Lake District, the Southern Uplands and the Cheviots.

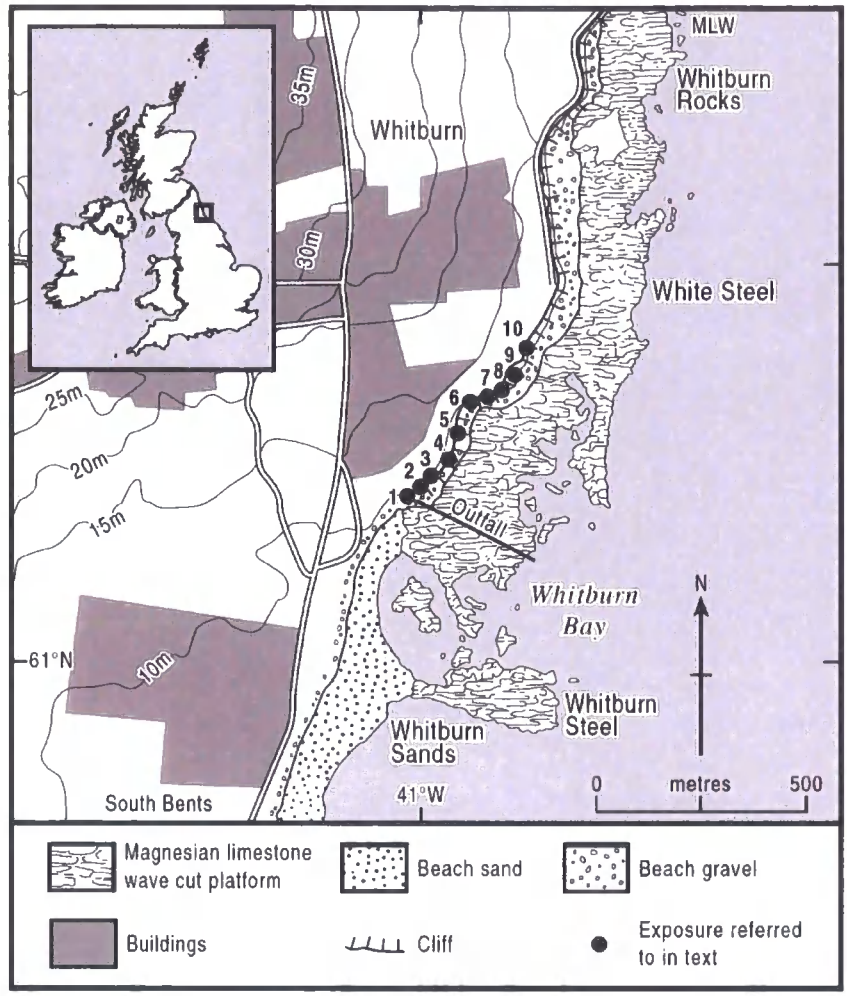

Figure 3.1: Map to show location of sections investigated at Whitburn Bay.

Trechmann (1915) was the first to propose the existence of two tills in County Durham (now called the Blackhall and Horden members; Thomas, 1999), where they cap the local Magnesian Limestone bedrock (Smith & Francis, 1967; Francis, 1972; Bridgland, 1999; Bridgland & Austin, 1999). However, there has been little quantitative description of these tills and no detailed analysis of their provenance, depositional processes, and type and style of deformation, leading to a severely limited understanding of ice-sheet dynamics and processes. In the lowlands of Sunderland and County Durham, large proglacial lakes were formed, trapped between east coast ice and the higher ground to the west. Extensive lacustrine clays, the 'Durham Member', were deposited in this lake (Smith, 1994). These

lakes may have had impacts on ice lobe response to climatic forcing and the stability of the ice lobes.

Francis (1972) correlated the lower Blackhall Member with the Skipsea Member in the Holderness cliffs on the basis of stratigraphic position and lithology (Madgett & Catt, 1978), the type locality of the LGM in Britain (Rose, 1985), where it overlies the Dimlington Silts, dated to 21350 - 22080 cal. yr. BP (Penny *et al.*, 1969; Sejrup *et al.*, 2009). These correlations are not quantitative and are based on little empirical evidence beyond matrix colour, stratigraphic position and erratic content. The glaciofluvial Peterlee Sands (tabular sands and gravels) overlie the Blackhall Member and are in turn overlain by the Horden Member (Francis, 1972; Thomas, 1999). Catt and Penny (1966) proposed that the Horden and Blackhall members were deposited from the dirty basal parts of a contemporaneous, two-tiered (stacked) ice sheet, producing two separate tills. However, the Horden Member is more likely to be a basal till from an ice sheet that overrode the Blackhall Member after the recession of Lake District ice (Beaumont, 1967).

Detailed process-based research on Devensian glacigenic sediments further north in Northumberland (Eyles *et al.*, 1982) identified till sequences interpreted as lodgement till complexes with 'shoestring channels' cut subglacially into the till bed, often containing irregular debris masses. These were inferred to have originated from the glacier sole, dropping from the roof of the channel. Eyles *et al.* (1982) argued that variable palaeo-discharges were the result of ponding episodes, possibly resulting from the closure of the channel downstream by ice or deformation of the till bed. The tills and glaciofluvial sediments were all deposited during a single, complex episode of wet-based subglacial sedimentation (Eyles *et al.*, 1982).

Hence, there is substantial scope for new research to contribute to the understanding of ice sheet dynamics in the region during the Late Devensian. This work provides new empirical, quantitative data and detailed sedimentological analysis to critically test the proposed genesis of the tills, provenance models, regional stratigraphic correlations, and the interaction between the British and Fennoscandian ice sheets during the Late Devensian. This research aims to reconstruct the glacial processes operating during the Late Devensian at the northeast margin of the BIIS, as typified in glacigenic sediments exposed at Whitburn Bay. Firstly, it uses macroscale and microscale lithofacies analysis to reconstruct the subglacial and ice-marginal processes, as well as patterns and phasing of flow occurring during ice sheet advance and recession. Secondly, the paper seeks to

determine the ice-flow pathways in the region, using lithological, palynological, heavy-mineral and heavy-metal provenancing techniques. Thirdly, the paper considers the glacial land-system operating along the east coast during the LGM and evaluates the evidence for a surging ice lobe in the North Sea. Finally, the implications of this research for regional Quaternary stratigraphic correlations are considered. Two key testable hypotheses are tested. The first is that Whitburn Bay contains two separate tills, with the first recording ice advance through the Tyne Gap, with an ice accumulation area in the Lake District. The second hypothesis is that the second till was deposited by the North Sea Lobe, sourced in the Cheviots and flowing southwards along the eastern British coastline, and constrained to the east by Fennoscandian ice.

3.2 Sedimentology, Stratigraphy, and Lithological and Geochemical Data

3.2.1 Site location and general description

At Whitburn Bay (Figure 3.1), glacigenic sediments are well exposed above the Roker Formation Magnesian Limestone bedrock (Figure 3.2). Two lithofacies associations (LFAs) are identified as superimposed lower (LFA 1) and upper (LFA 2) diamictons, separated by a boulder pavement. Incised into LFA 2 is a laminated sand and clay facies (LF 2b), rippled sand, and bedded coarse sand and gravel (LF 2c). The presence of two distinct tills supports interpretations by Francis (1972), but the stratigraphy crucially differs in relation to the Peterlee Sands, as in the glaciofluvial sediments are considerably more variable and complex than previously presented. Instead of the planar outwash described by Francis (1972), sands and gravels exist as discrete channels within LFA 2.

3.2.2 Lithofacies Association 1: massive, matrix-supported diamicton

Macroscale Sedimentology

LFA 1, the lower diamicton, is inconsistently exposed at Whitburn Bay (Figure 3.2 and Figure 3.3). It is a yellowish brown (10YR 4/4), matrix-supported, over-consolidated, diamicton with abundant fine to coarse gravel and cobbles. The upper contact is sharp and unconformable. The diamicton incorporates faceted and striated clasts of both local and far-travelled provenance, such as limestones, sandstones, granites, andesites, rhyolites and quartz. In places, the diamicton is fissile and faintly stratified. Clast macro-fabrics show a moderately strong, clustering around the S_1 axis of 0.6 from north-west to southeast, with a low dip angle to the southeast. A boulder pavement is occurs at the top of LFA 1.

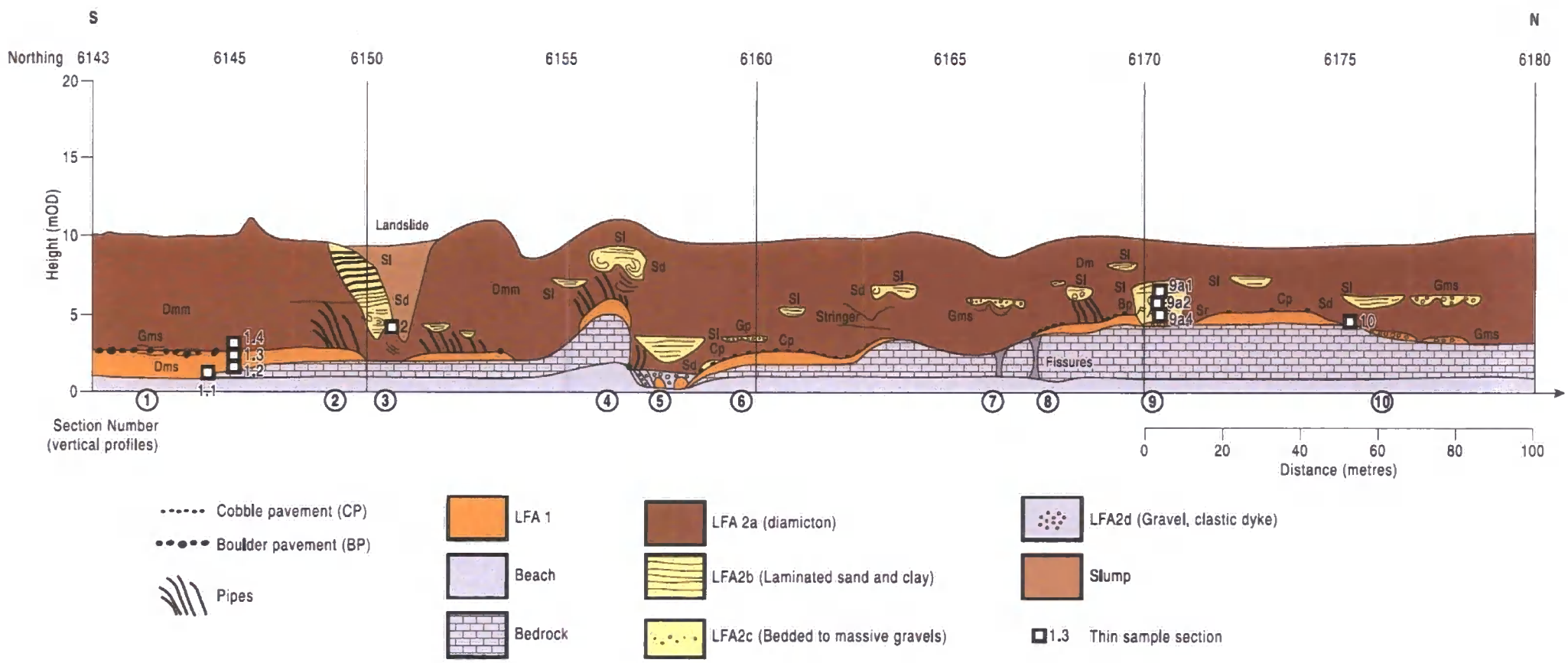

Figure 3.2: Facies architecture at Whitburn Bay.

The Boulder Pavement

The boulder pavement occurs consistently at the top of LFA 1 and is laterally extensive across Whitburn Bay. It consists of well faceted, striated boulders up to 50 cm diameter (Figure 3.3), predominantly of Carboniferous Limestone, Magnesian Limestone and sandstone. The spacing between the boulders here ranges from a few centimetres up to 60 cm. In between and above the boulders there are channelised, massive, poorly sorted gravels with a sharp, undulating lower contact. The mean dip direction of the boulders is 141° and the mean dip is 08.5°. Multiple measurements on many of the boulders indicate a consistent and strong striae orientation from north-north-east to south-south-west. These overprint fainter and less numerous striae orientated from north-west to southeast. Boulders lodged below the pavement into LFA 1 have numerous and well-clustered striae orientated from north-west to southeast (Figure 3.3).

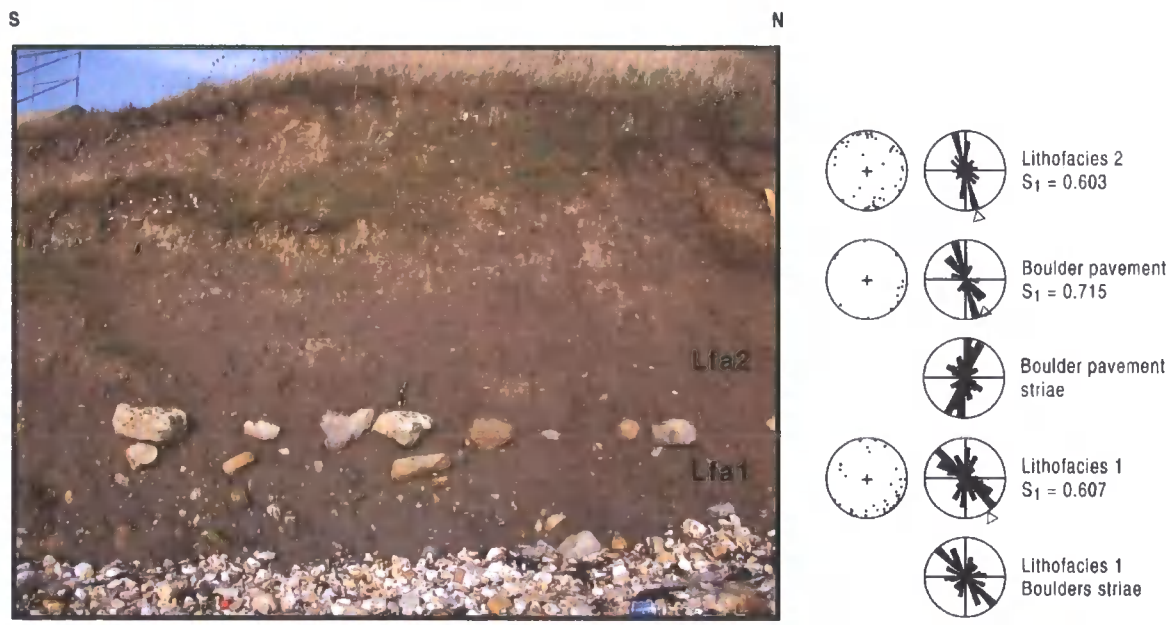

Figure 3.3 Photograph of Lithofacies Associations 1 and 2 and the boulder pavement in Section 1, Whitburn Bay. The trowel is 20 cm long.
LFA 1 is a matrix-supported diamicton, with a boulder pavement at the top. The boulders are striated. The diamicton is clast-rich and is 60 cm thick. It is a dark yellowish brown (10YR 4/4), it is fissile and it is faintly stratified. It has an unconformable upper contact. Clast fabric: $S_1 = 0.607$; $S_3 = 0.072$; $V_1 = 149°$.
LF 2a is a clast-poor diamicton with coal, Carboniferous Limestone and sandstone gravel. It has a sandy texture and is a dark greyish brown (10YR 4/3). LF 2a clast fabric: $S_1 = 0.603$; $S_3 = 0.098$; $V_1 = 164°$.

Micromorphology

In thin section, LFA 1 is a light brown, matrix-supported, massive diamicton of even density (Table 3.1). Rotational structures and Type II Pebbles are common, and there is a

strong skelsepic plasmic fabric. The skeleton grains are poorly sorted. Larger skeleton grains exhibit edge rounding, while smaller grains are generally angular. Elongated grains are commonly lineated and aligned. The plasmic fabric is very localised and patchy, with a strong skelsepic plasmic fabric around skeleton grains (Table 3.1).

Sample 1-3, which crosses the contact between LFA 1 and LFA 2 in Section 1 (Figure 3.4), is a brown, silty, matrix-supported diamicton, divided by a deformed, folded bed of clast-supported skeleton grains, with sharp contacts dissected by micro-scale water-escape structures. There are rare microfossils, possibly originating from the limestone clasts present. The sample exhibits well-developed rotational structures with associated pressure shadows, lineations of aligned elongate skeleton grains, and rounded Type II and III Pebbles (van der Meer, 1993). These intraclasts are coherent, well rounded, and display no intergranular disintegration or stringers. Small numbers of crushed grains and necking structures between grains are also apparent (cf. Menzies, 2000; Table 3.1). Microfabric analysis indicates a strong degree of alignment of skeleton grains. There is a strongly developed bimasepic and skelsepic plasmic fabric where clay-sized matrix material is abundant.

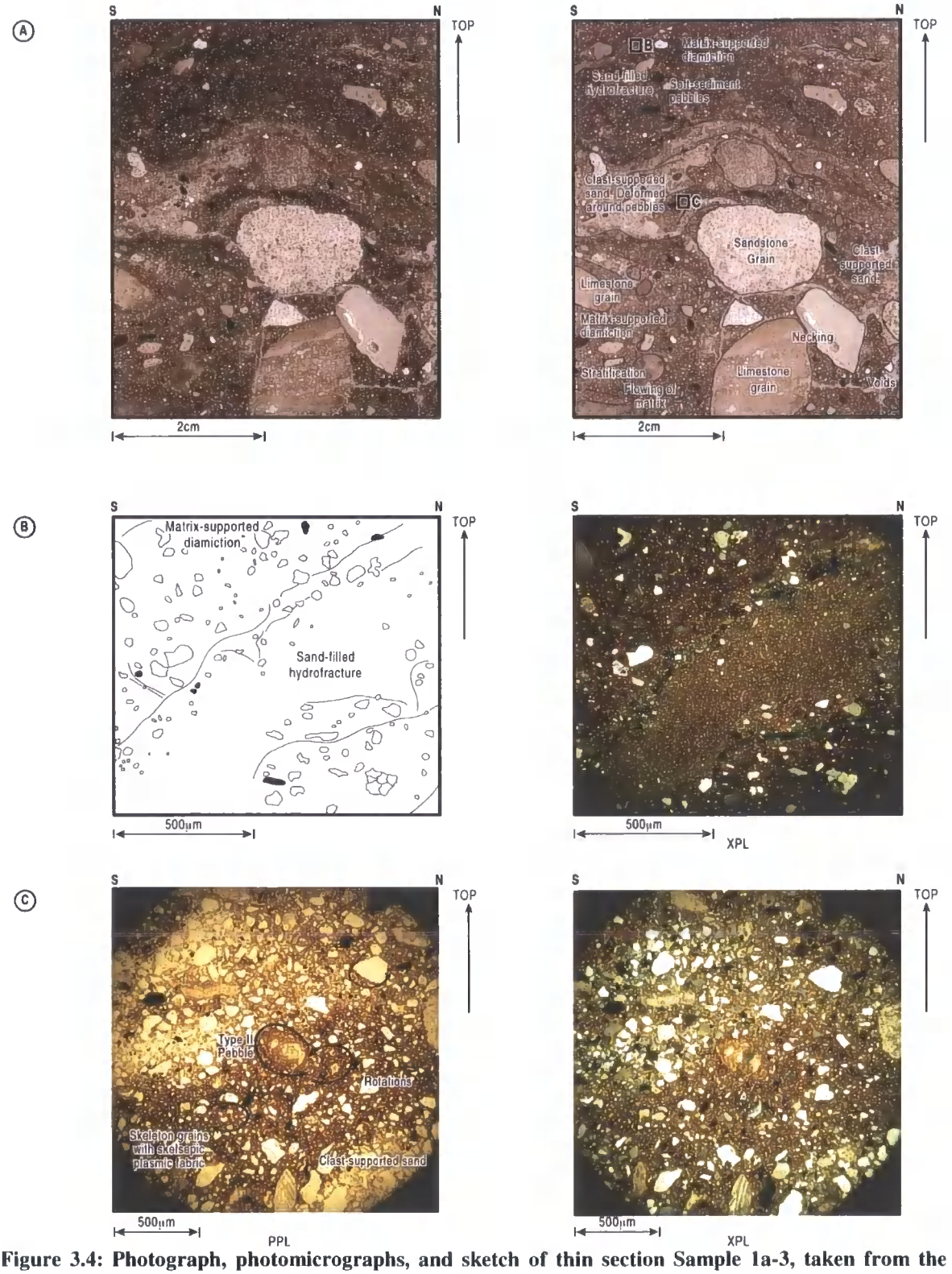

Figure 3.4: Photograph, photomicrographs, and sketch of thin section Sample 1a-3, taken from the boundary between LFAs 1 and 2 in Section 1.

Photograph A: LFA 1 and LFA 2 in thin section are separated by a bed of clast-supported sand. Extensive deformation and mixing can be seen between the two diamictons. On a microscopic scale, folded and strongly deformed sand laminations show stringer initiation into the diamicton. Boudinage structures are associated with this.

Photograph B: Sand-filled hydrofracture with sharp, erosive contacts cuts across a matrix-supported diamicton.

Photograph C: Graded sand lamination with rotations and reworked silt pebbles.

Table 3.1: Summary diagram of Micromorphological analysis.

Sample		Skeleton grains		Texture	Voids		Deformation structures										Fluvial / marine features			Plasmic Fabric				
		Shape <500 um	Shape >500 um	Texture	Voids	Void Type	Section Elements	Rotation	Pressure shadow	Crushed grains	Pebble I	Pebble II	Pebble III	Water escape	Lineations	Folds	Dropstones	Microfossils	Laminae	Lattisepic	Skelsepic	Omnisepic	Masepic	Kinking
LFA 1	1_1	SR	SA	F	•	L		•••		••		•••									•••			
	1_2	SR	SA	F	•	L		•••	•	•		••			••						•••		••	
Pipes	2_1	SR	SR	F/M/C	••	L	S; Be							••	•••	•••			•••		•••			•
LF 2a	10	SR / SA	SR / SA					•••			•	••		•							•••		•••	
	1_3	SR	SA	F/C	•	L/P	Ba	•••		••		•••			••			•			•••		•••	
	1_4	SR	SA	F	•	P		••		•		••			••						•••		••	
LF 2b	2_2	SR / SA	A	F	•	L/P	F	•••							•••					••	•		•••	
	9a_1		SA / A	M			Be	•													•			
	9a_2		SA / A	M			Be								••						•			
	9a_3	SR / SA	SR / SA	M/C	•	L	Be; Bo	•							•	••	••		•••		•		•	

One dot indicates that a feature is present. Two or three dots indicate that it is more common.
Voids: L – Laboratory induced; P – Packing induced.
Shape: SR – sub-rounded; SA – sub-angular; R – rounded; A – angular.
Texture: C – coarse; M – Medium; F – Fine.
Section elements: Be – bedding; Ba – banding, S – shear; Bo – boudinage.

3.2.3 Lithofacies Association 2: Massive, matrix-supported diamicton, with coarse sands and gravels, and laminated sand and clay.

LFA 2 is an association of several different lithofacies, including a dark brown, matrix-supported diamicton with abundant fine gravel but rare coarse gravel (LF 2a; Figure 3.3; Table 3.2), pipe-injection structures (Figure 3.5), several different facies of laminated sand and clay bodies nested within the diamicton (LF 2b), and coarse sand and gravel facies (LF 2c and LF 2d).

LF 2a: Diamicton facies

The general characteristics of the diamicton are the rare coarse gravel clasts, ranging from subangular to angular, and which are faceted and striated, and clast macro-fabrics indicating a moderate to strong clustering of a-axes from north-north-east to south-south-west and north-east to south-west. LF 2a is a dark brown colour (10YR 3/3), and contains far-travelled erratics (Table 3.3). In some places, the two diamictons (LFA 1 and LF 2a) are exposed in superposition (Figure 3.2), but in others, LF 2a overlies either bedrock or sands and gravels. In Section 2a, pipe structures are exposed (Figure 3.5). The injection structures are similar in colour to LFA 1; they occur repeatedly along Whitburn Bay and appear to be associated in particular with the laminated sands (Figure 3.2).

In Section 10 three facies are exposed (Figure 3.2). Firstly, a coarse, poorly sorted sand and gravel rests directly on soft, dolomitised bedrock (LF 2c; Figure 3.6A). This is unconformably overlain by a clast-rich, massive, dark yellowish brown (10YR 3/3) diamicton (LF 2a). The diamicton is truncated by a coarse, poorly sorted sand and gravel, with a convex, undulating base (LF 2c; Figure 3.6A). Above this facies, coal grains pick out planar laminated fine sands and sand-silt couplets (LF 2b). Beds 5 and 6, Section 10, are laminated sands and silts deformed by dewatering, loading-style soft-sediment deformation such as flame and ball and pillow structures. Bed 7 above incorporates extended climbing Type A Ripples (Allen, 1963, 1982; Evans & Benn, 2004). Within these sands is a small, lenticular, detached diamicton block, surrounded by flame, ball and pillow and other dewatering structures. This is overlain by planar laminated sand and clay (LF 2b; Figure 3.6A), truncated by the overlying, dark brown diamicton (LF 2a). This diamicton is clast-poor, dark brown, and massive.

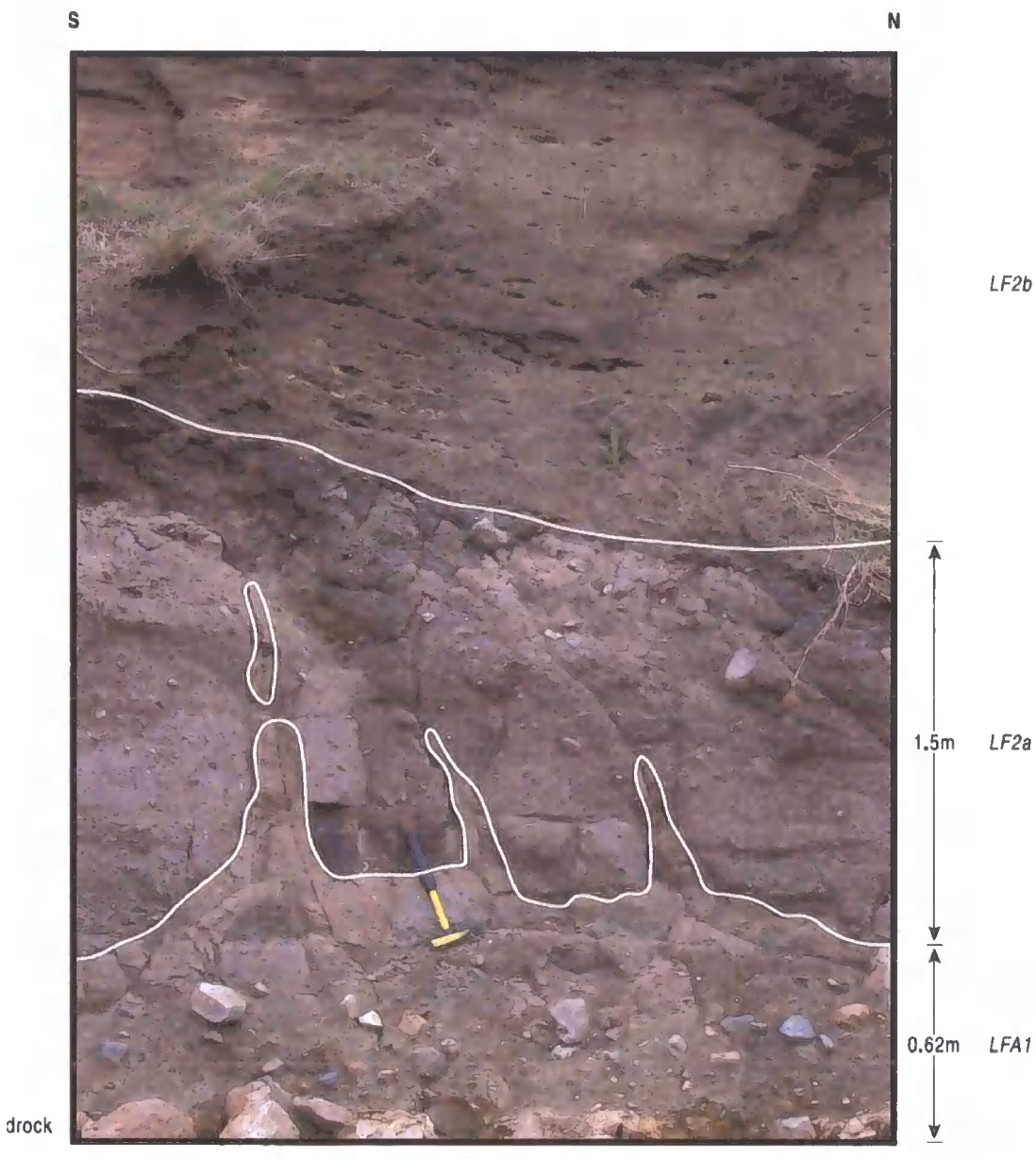

Figure 3.5: Photograph of pipe structures in Section 2a.
LF 1a is a massive diamicton, coloured 10YR 5/2. It is gravel-rich and has a sharp, erosive upper contact. It rests directly on Magnesian Limestone bedrock.
LF 2a is a massive, gravel-poor, silty diamicton coloured 10YR 3/3. Granite, Carboniferous Limestone and coal are common. Clasts are striated and faceted. Within LF 2a, pipe structures have been intruded upwards from LFA 1. These have a sandy texture, and are overturned to the south (180°). They are coloured 10YR 5/3.
LF 2b comprises thinly cross-bedded, well-sorted, fine sands.

LF 2a: Micromorphology

LF 2a is a dense, dark brown diamicton, with a small number of sub-rounded to rounded, matrix-supported skeleton grains, predominantly in the fine sand to silt size fraction (Table 3). Sample 10 (Figure 3.6) shows a highly variable structure. The limestone

bedrock has been drawn up into the diamicton forming a stringer structure, and matrix material has been squeezed downwards into the limestone. Numerous smaller angular flakes and coal grains are evenly distributed across the slide. Aligned clay particles along the boundary of the diamicton and bedrock indicate shearing (Table 4.2; Figure 3.6). There is a strong presence of rotational structures, Type II pebbles, and a strong skelsepic and masepic plasmic fabric.

LF 2b: Rippled and laminated sand and clay facies

The nested lenses of sands within LFA 2 include sequences of laterally variable, laminated, draped-rippled and deformed sands and clays (Figure 3.2). Although each channel fill has a unique sedimentary signature, they consistently have closed edges and flat tops, and generally consist of discrete inter-laminated sand and clay beds that have undergone varying degrees of soft sediment loading and dewatering deformation (cf. Mills, 1983). In a number of locations, channel walls have partly disintegrated, dropping diamicton fragments into the channels.

Typical characteristics include Type A climbing ripples, overlain by alternating sand and clay planar laminations, often deformed by soft-sediment deformation. In Section 9d, there is a diamicton (LFA 1) with a boulder pavement at its top, resting on Magnesian Limestone bedrock (Figure 3.7). A rippled sand bed (Type A Ripples, Allen, 1963) with a scoured lower contact and a gravel lag near the base overlies this (LF 2b). The sand is heavily deformed with convoluted bedding and recumbent folds overturned towards the south. Type A climbing ripples above this deformed bed grade conformably into a massive sand. The interbedded sand and clay above this is strongly deformed: the clay beds have been folded and the sands show extensive evidence of dewatering with flames and ball and pillow structures. This is overlain by a planar laminated sand and clay bed, which is capped by a sandy, massive diamicton (LF 2a) with an erosive, sharp lower contact. Adjacent sections exhibit repeated changes between planar laminated bedded sands, interlaminated sand and clay couplets, and Type B climbing ripples (Allen, 1963) with ripple drapes.

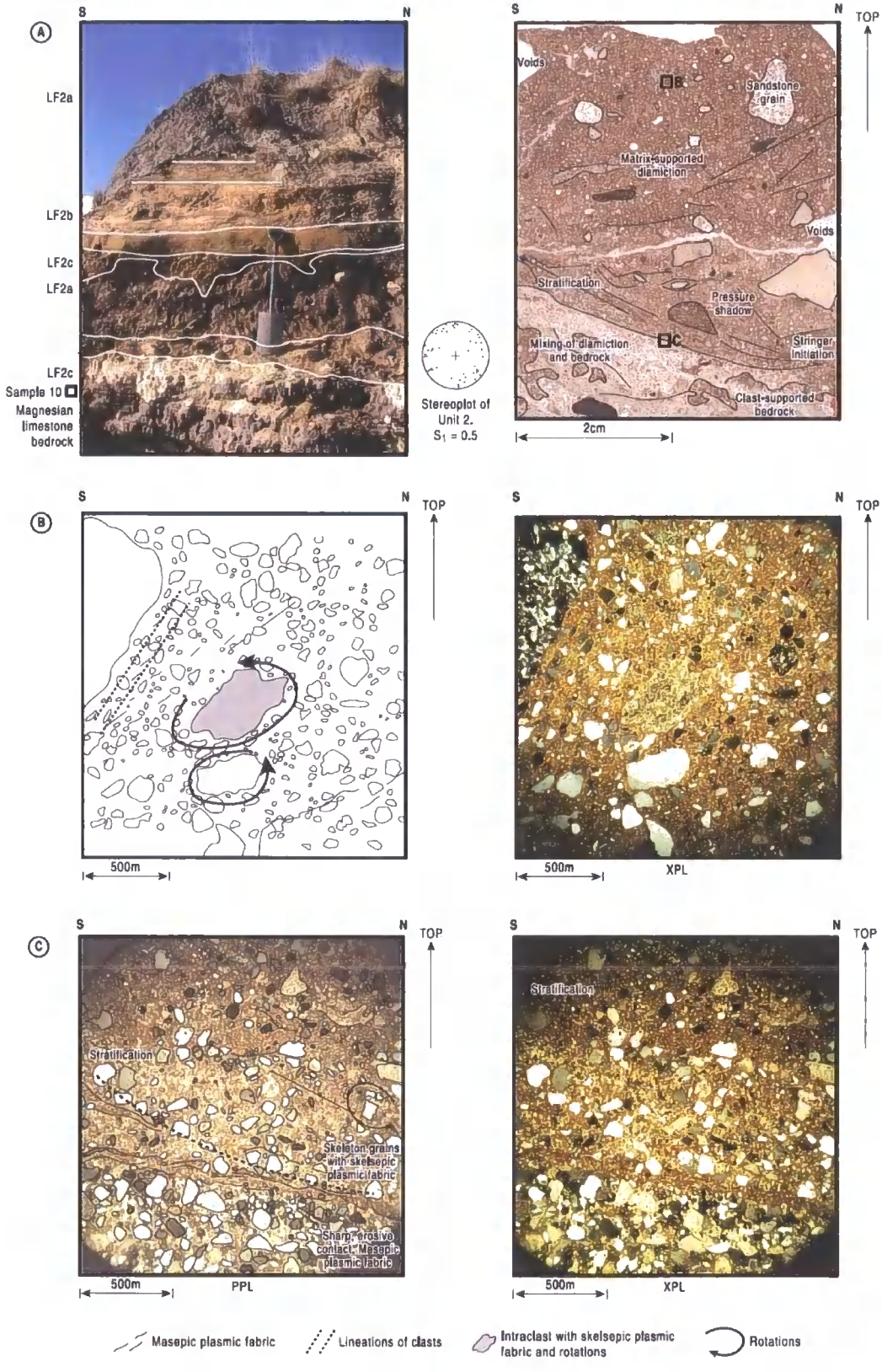

Figure 3.6: Photograph of Section 10 with thin section and photomicrographs of Sample 10, taken from the basal diamicton of Section 10. The slide shows characteristic, strongly birefringent plasmic fabric, Type II Pebbles, lineations of clasts, rotational structures and grain stacking, indicative of ductile deformation in a high strain environment.

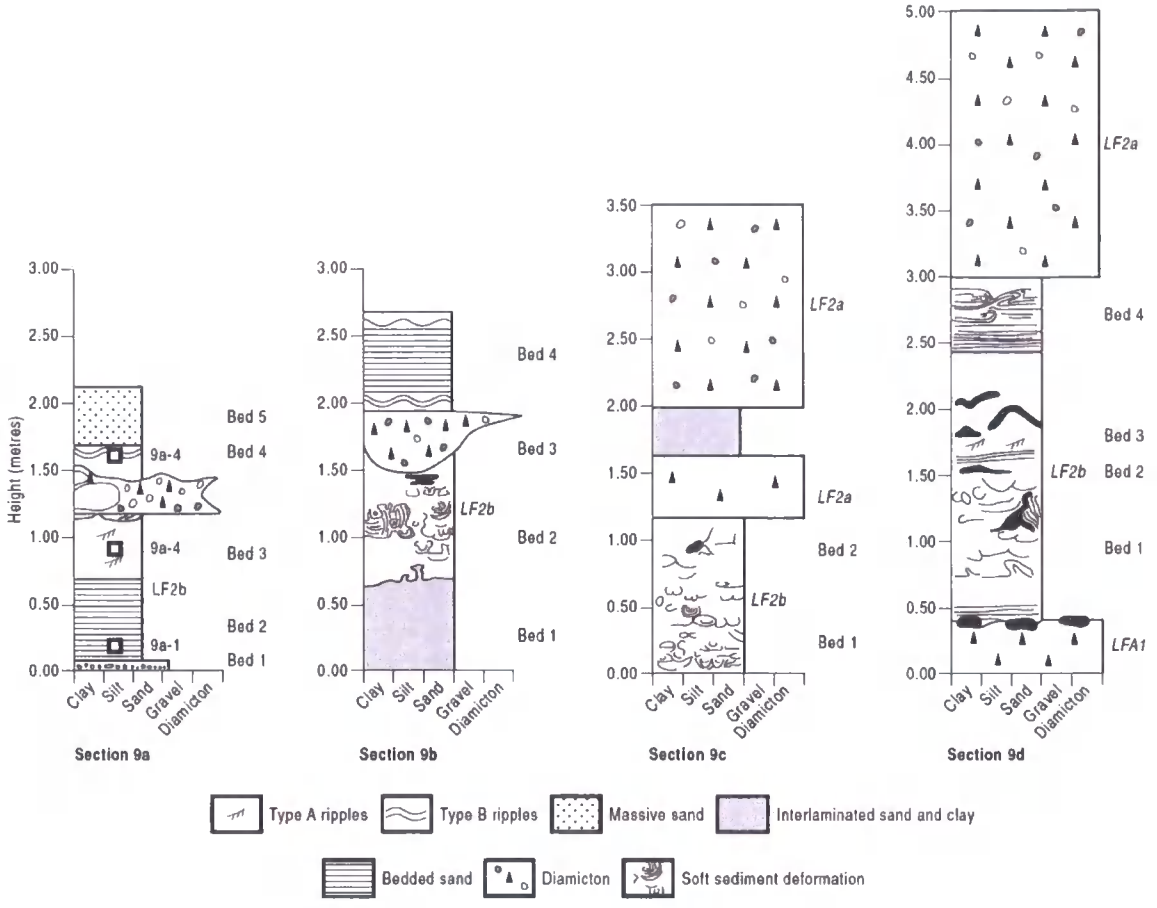

Figure 3.7: Vertical profiles of Section 9.

Section 9a begins with 20 cm of coarse, poorly sorted sand (10YR 4/3) resting on bedrock, which is overlain by 75 cm of planar laminated sand and clay (10YR 3/4) with a sharp lower contact. These conformably grade into Type A climbing ripples. The ripples are unconformably overlain by a matrix supported, massive diamicton (10YR 4/4; LF 2a). This is overlain by Type B clay draped-ripples and then by planar bedded sand and clay (LF 2b).

Section 9b has a well-sorted, fine, laminated sand (LF 2b) at the base, which is overlain by a well-sorted sand with ball and pillow and flame structures. Embedded within this is a diamicton with sharp, scoured contacts. It is overlain by ripple and planar laminated fine sand and clay.

Section 9c starts with a strongly deformed, fine, well sorted sand, overlain by a massive fine sand and then by a clast rich diamicton with sharp, erosive contacts. This is overlain by 0.5 m of laminated sand and clay.

Section 9d starts with a massive, over-consolidated gravel-rich diamicton (LF 2a). This contains stringers emanating from the Magnesian limestone bedrock. It is overlain directly and unconformably by heavily deformed sand with a sharp, scoured lower contact, and features recumbent folds, overfolds, and convolute lamination (LF 2b). This is overlain by Type A climbing ripples, and then by more strongly deformed sand. This grades into a planar laminated sand.

In Section 9d, Bed 3, clay and sand laminations are strongly folded and anastomosed into overfolds and recumbent folds. Bed 4 consists of planar laminated sand and clay, with a sharp, erosive lower contact. LF 2a, a dark brown, massive, gravel-poor diamicton caps the sequence.

LF 2b: Micromorphology

Thin-section analysis of the interlaminated channel fills (LF 2b) shows both primary sedimentary structures and secondary deformation. Samples 9a-1 and 9a-2 (from Beds 1

and 2 of Section 9a, Figure 3.7) show a predominance of thinly bedded sands. The well-sorted fine sand skeleton grains, with rare larger coal grains, are mostly clast supported, and are predominantly sub-angular to angular. Matrix material is largely absent apart from in small, localised patches distributed across the slides (Table 3.1). Elongate grains are aligned sub-parallel with each other.

Sample 9a-4, from Bed 4, has macroscopic, upward-fining, sand and silt-clay laminations, is normally faulted, and has recumbent folds (Figure 3.8). The moderately sorted sand laminations are clast supported. Skeleton grains are sub-rounded to sub-angular, with rare larger grains including sandstone, limestone, and fossiliferous coal. The inversely graded coarse laminations have sharp contacts, and contain thin lenses of masepic plasmic fabric. In contrast, the normally-graded fine sand and silt laminations are matrix-supported, with graded basal contacts. Within the fine clay laminations, there are rip-up clasts and numerous water-escape structures (Figure 3.8).

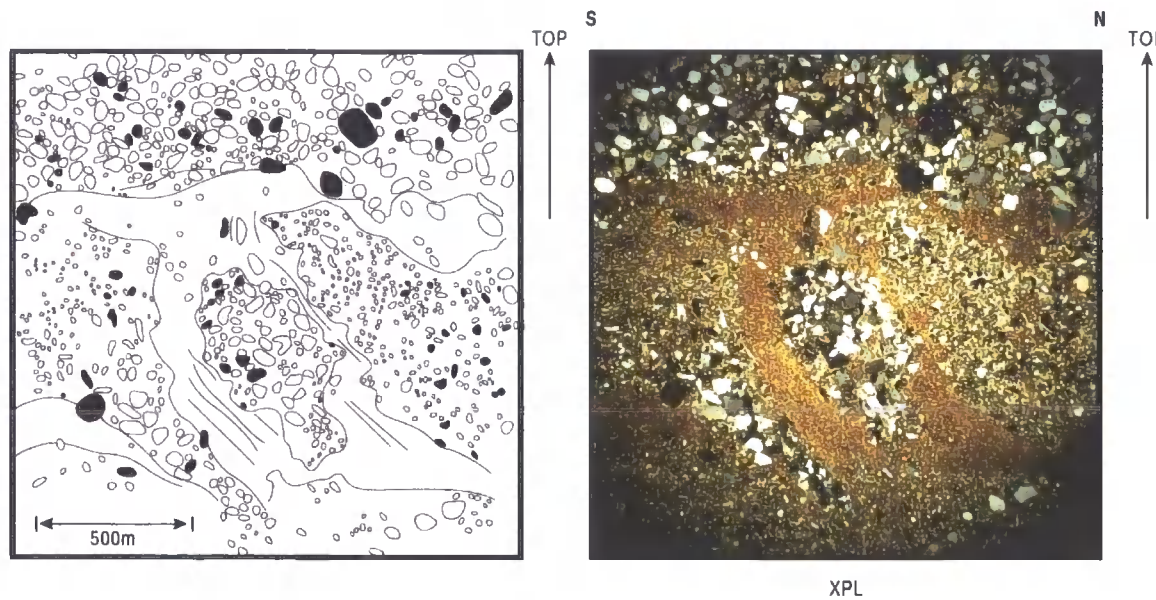

Figure 3.8: Photomicrograph of deformed bedding in thin section sample 9a-5, demonstrating strong masepic plasmic fabric development, which is highlighted on the sketch.

In Section 2 (Figure 3.2), a channel incises into the underlying diamicton (LFA 1). The interlaminated sands and silts (LF 2b) within the channel are heavily deformed, and a series of recumbent folds are overturned to the south. A thin-section sample taken from one recumbent fold (axis c. 070°) demonstrates polyphase brittle and ductile deformation (Figure 3.9). The primary planar- and ripple-cross laminations are normally graded. Some masepic plasmic fabric development is apparent sub-parallel to the bedding. The sequence

is compressively folded from a northerly direction and then crosscut by two phases of normal faults, which have triggered water escape structures that have pierced the clay laminae and caused fluidisation of the coarser sand laminae (Figure 3.9).

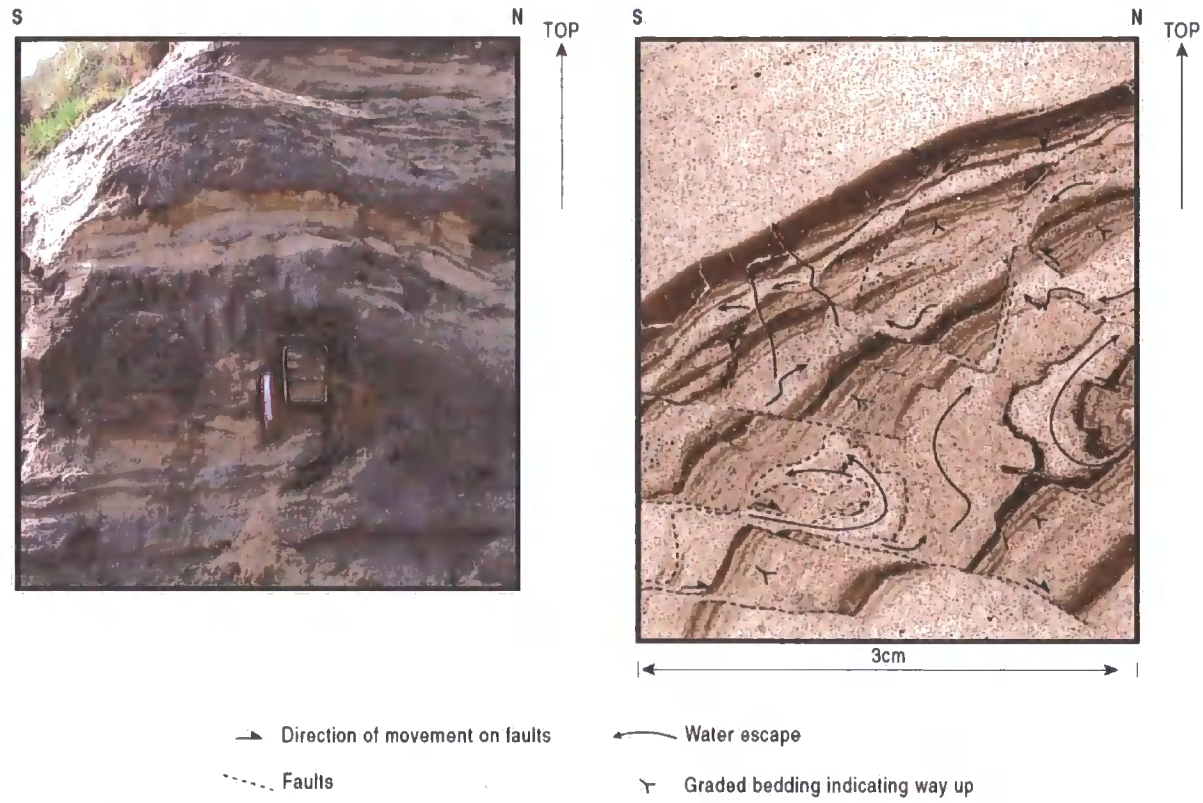

Figure 3.9: Microfaults and water escape structures relating to overfolding in Section 2b. Primary sedimentary lamination (graded bedding with planar and ripple cross lamination). Compaction causes masepic plasmic fabric development sub-parallel to bedding. Compression from the north caused overfolding, with the offset nature of the faults being conjugate, indicating vertical compression. Faulting has been accompanied by liquidisation of sands and water escape.

LF 2c: Coarse sand and gravels

There are channels exposed in Sections 6, 7 and 10, where a channelised, coarse, poorly sorted, bedded sand and gravel is well exposed (Figure 3.2). For example, the incised gravel bed in Section 7 exposes a well-sorted, planar-bedded, cobble gravel, with a sharp, erosive, undulating bottom contact, and a flat top contact.

LF 2d: Clastic dyke facies

Numerous medium to coarse, clast-supported gravel dykes with sharp, erosive contacts vertically dissect the diamicton (LF 2a) in Section 5 (Figure 3.10). Smaller dykes occur as branched offshoots from the larger dykes (LF 2d). The clastic dykes have clear-cut, sharply

erosive boundaries. Juxtaposed to the coarse gravels is an infill of fine, calcreted, thinly bedded sands (LF 2b), which are strongly deformed and contorted. These dykes transform laterally into sub-vertically orientated crudely bedded gravel strata (LF 2d), which fan out into the overlying diamicton (LF 2a). The lithologies of LF 2d are similar to those of the underlying LF 2a, with Magnesian Limestone the most abundant lithology. Intraclasts of diamicton occur within LF 2d.

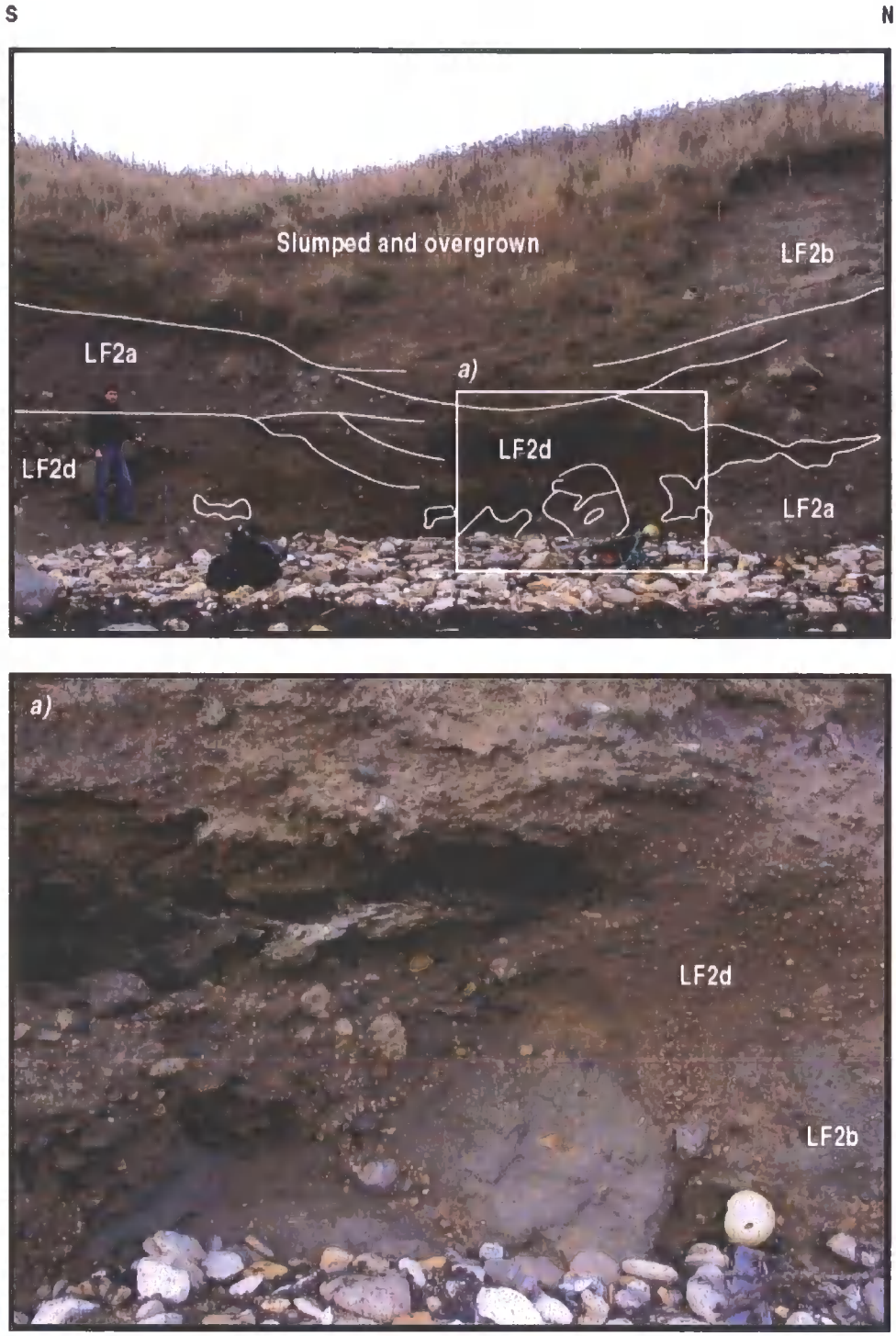

Figure 3.10: Photographs of Section 5.

LF 2a: **Massive, matrix-supported diamicton, 10YR 3/3, dark brown. Gravel-poor. Unconformable, sharp contacts with LF 2d.**
LF 2d: **Coarse, massive, poorly-sorted, clast-supported gravel dyke. Coarsest gravel in the centre. Gravel is sub-angular to angular. Sharp, erosive, unconformable contacts. Interbedded with horizontally bedded, calcreted, strongly deformed and contorted fine sand. Yellowish-brown colour (10YR 5/4).**
Fans out into Planar-bedded, coarse sand and gravel, matrix-supported.
LF 2b: **Planar-bedded, well-sorted, coarse sand. Fines upwards into well-sorted fine sand and clay. Pebble lag at base.**

3.3 Lithological, Geochemical and Biological Analysis

3.3.1 Lithological Analysis

Three bulk samples (from Sections 1, 2, and the pipes in 2) and two gravel samples (from Sections 1 and 2) were analysed from LFA 1. LFA 1 is a diamicton with high percentages of sand (Table 3.2). The samples reacted vigorously to 10 % hydrochloric acid. Four bulk samples from sections 1, 2, 4, and 10, and three handpicked clast samples from sections 1, 2 and 10 were taken from LF 2a. Both LFA 1 and LF 2a have similar particle-size distributions (Table 3.2). LF 2a has a weak to moderate reaction to hydrochloric acid. The fine laminated sand facies of LF 2b was sampled in Section 9a. It is a yellowish-brown, well-sorted sand (Table 3.2) that reacts vigorously to HCl.

Table 3.2: Average particle size distribution. For detailed PSA, see Appendix IV.

	LFA 1	LF 2a	LF 2b
% Gravel	11.82	11.76	0.00
% Sand	18.36	17.37	17.60
% Silt	39.10	38.88	72.50
% Clay	30.70	33.99	9.90

Clast Lithological Analysis

Magnesian Limestone dominates LFA 1 (Table 3.3) with 48.5 % of the clasts, and Carboniferous Limestone is present in smaller amounts (12.6 %). There are also relatively low amounts of Whin Sill dolerite erratics (0.8 %), and very low amounts of quartzite (1.6 %), andesite (0.5 %) and porphyries (0.2 %). Other erratics within LFA 1 include Old Red Sandstone (0.7 %), greywackes (7.6 %), and coal (1.6 %; Table 4.3). Notably, there is a lack of distinctive Lake District erratics and granites (cf. Francis 1972). For raw data, refer to Appendix IV.

LF 2a is poorer in Magnesian Limestone (33.1 %) and richer in Carboniferous Limestone (18.1 %) than LFA 1 (Table 3.3). There are slightly higher percentages of igneous clasts present, including pink porphyries (0.8 %), rhyolites (0.8 %) and granites (0.2 %), typical of the Cheviots region (see Chapter 2), schist typical of the Scottish Highlands, and Whin Sill dolerite (2.0 %), a local Permian igneous lithology.

Table 3.3: Average Clast lithology results from Whitburn Bay, 8-32 mm. Sandstones are distinguished on their quartz, feldspar and arenite content. For detailed raw counts, refer to Appendix IV.

	Clast Lithology	LFA 1 Average %	LF 2a Average %
Igneous	*Diorite*	0.00	0.20
	Granite	0.00	0.21
	Gabbro	0.00	0.20
	Rhyolite	0.00	0.82
	Andesite	0.51	0.72
	Porphyry	0.17	0.83
	Felsite	0.00	0.17
Metamorphic	*Slate*	0.00	0.49
	Schist	0.00	0.75
Sandstone and Sedimentary	*Sandstone*	10.59	12.09
	Arenite Sandstone	0.68	1.55
	Quartzitic Sandstone	8.05	6.11
	Siltstone	0.16	0.70
	Breccia	0.16	0.00
Jurassic	*Ironstone*	1.57	1.76
	Mudstone	0.80	2.11
Triassic	*Brown Orthoquartzite*	1.05	0.61
	Red Orthoquartzite	0.17	0.74
	White Orthoquartzite	0.35	0.37
	White Vein Quartz	0.00	0.43
Permian	*Magnesian Limestone*	48.46	33.10
	Yellow Sands	1.54	2.79
	Whin Sill Dolerite	0.83	1.97
Carboniferous	*Carboniferous Limestone*	12.55	18.12
	Coal	1.63	1.72
Devonian	*Chert*	0.19	0.57
	Old Red Sandstone	0.67	0.66
	Shale	0.00	0.17
Ordovician and Silurian	*Arkose Sandstone*	2.25	2.36
	Greywacke	7.61	5.63
Total (n)		***512***	***1073***

Heavy Mineral Analysis

The most prominent heavy mineral in LFA 1 is dolomite (excluded from Table 3.4 due to strong skew). The far-travelled suite constitutes an abundance of medium-grade metamorphic minerals such as clinozoisite (14.6 %), andalusite (9.7 %), kyanite (9.6 %), garnet (16.6 %) and olivine (5.6 %). Biotite (1.8 %) and tourmaline (3.5 %), common in many igneous rocks, are also present (Table 3.4).

The heavy-mineral suite of LF 2a has significant amounts of clinopyroxenes (4.68 %) and kyanite (8.8 %), and small amounts of rutile (2.3 %) and baryte (0.2 %), differentiating LF 2a from LFA 1 (Table 3.4). Detrital rutile is sourced from high grade, regionally metamorphosed terranes or sediments, while amphiboles are likely to be sourced from

various crystalline bedrock types. LF 2b is comparatively rich in igneous or high-grade metamorphic minerals, such as clinopyroxenes (5.9 %), rutile (2.9 %) and amphiboles (2.9 %; Table 3.4).

Table 3.4: Average Heavy Minerals (percent non-opaques) in glacial deposits at Whitburn Bay (excluding carbonates due to strong skew). Combined results of multiple samples. For raw mineral counts, refer to Appendix IV.

	SAMPLE	LFA 1	LF 2a	LF 2b
	n	***3902***	***669***	***1528***
	% Opaques	76.22	69.91	84.26
	% Non Opaques	23.78	30.09	15.74
	% Heavy Minerals	2.37	8.28	13.82
Silicate group	*Olivine Group*	5.54	3.77	5.02
	Zircon	3.72	5.69	9.62
	Sphene	1.56	1.62	1.67
	Garnet Group	16.57	18.59	25.52
	Sillimanite	0.45	3.24	0.00
	Andalusite	9.70	9.71	3.35
	Kyanite	9.61	8.78	4.18
	Staurolite	1.83	2.77	0.42
	Chloritoid	0.22	0.62	0.00
	Tourmaline Group	3.50	2.90	8.37
Epidote group	*Zoisite / clinozoisite*	14.61	7.80	5.86
	Epidote	2.35	2.58	0.84
Pyroxene group	*Enstatite*	2.47	1.01	2.51
	Hypersthene	0.21	0.09	1.26
	Diopsidic Clinopyroxene	1.85	3.14	4.18
	Augitic Clinopyroxene	0.87	1.54	1.67
Amphibole group	*Tremolite*	0.54	0.00	0.00
	Actinolite	0.31	0.00	0.00
	Hornblende	0.57	0.77	2.93
Mica group	*Muscovite*	9.16	11.63	5.44
	Biotite	1.77	2.37	0.84
	Chlorite Group	5.68	2.87	5.02
Oxides	*Rutile*	0.63	2.30	2.93
	Brookite	0.56	1.02	1.67
	Spinel Group	0.23	0.61	0.00
	Anatase	0.17	0.35	0.00
Sulphates	*Baryte*	0.31	0.19	0.00
Sulphides	*Sphalerite*	0.00	0.00	0.42
Phosphates	*Apatite*	5.01	4.04	6.28

Geochemical Analysis

Metals analysis of the matrix by ICP-MS indicates that LFA 1 is high in silicon, sodium, magnesium, aluminium, potassium, calcium, iron, manganese and titanium (Table 3.5). ICP-MS reveals that LFA 1 and LF 2a have similar elemental compositions. The

metals suite of LF 2b has noticeably higher proportions of magnesium and calcium than the diamicton samples (Table 3.5).

Table 3.5: Average Heavy Metals results at Whitburn Bay

Element	Lithofacies (average concentration mg/kg)		
	LFA 1	LF 2a	LF 2b
Li_7	59	68	41
Be_9	2	2	1
B_{11}	51	67	41
Si_{14}	278688	301196	31
Na_{23}	3823	4375	3650
Mg_{24}	1708	1525	3400
Al_{27}	29600	32475	18900
K_{39}	11550	11725	13100
Ca_{44}	17475	15800	30600
Ti_{48}	3763	4365	3070
V_{51}	76	88	53
Cr_{52}	75	87	50
Fe_{57}	31775	35200	24800
Mn_{55}	389	529	595
Co_{59}	14	15	10
Ni_{60}	39	45	28
Cu_{63}	22	26	17
Zn_{66}	62	51	44
As_{75}	8	8	8
Mo_{98}	5	7	2
Ag_{107}	1	2	1
Sb_{123}	0	0	0
Ba_{137}	337	351	404
Pb_{206}	19.25	22.75	23

Principal Components Analysis

A comparison of LFA 1 and LF 2a (Table 3.3) shows that locally sourced, non-durable lithologies dominate LFA 1, whereas LF 2a has a larger component of far-travelled and igneous erratics (Figure 3.11). Most of the variation could be accounted for by variation between the crystalline, Permian and Carboniferous groups, which have strong correlation indices. On a ternary plot of these three variables (Figure 3.11), the two diamicton lithofacies are well differentiated, with sample WH14, from Section 10, in between. A PCA on both the correlation and the covariance matrices replicates this result. The low

percentages of crystalline rocks and high percentages of Permian rocks are the main factors differentiating LFA 1 from LF 2a. A correlation PCA (Figure 3.11) on the total metals suite fails to distinguish the three lithofacies and indicates strong within-till heterogeneity. Sample WH13 from the sands and sample WH07 from LFA 1 show consistent differences to the other samples.

3.3.2 Biostratigraphy

Palynological analysis indicates that abundant wood fragments and well-preserved palynomorphs are present, with lower proportions of non-woody plant tissue (Riding, 2007). The palynomorphs are dominated by the long-ranging Carboniferous spores *Densosporites* and *Lycospora pusilla*. Lower numbers of *Endosporites globiformis*, *Florinites* spp., and *Radiizonates* spp., were also present, and are indicative of the Westphalian (Smith & Butterworth, 1967). *Tripartites trilinguis* and *Tripartites vestustus* suggest some Namurian input, possibly from the Newcastle coalfield.

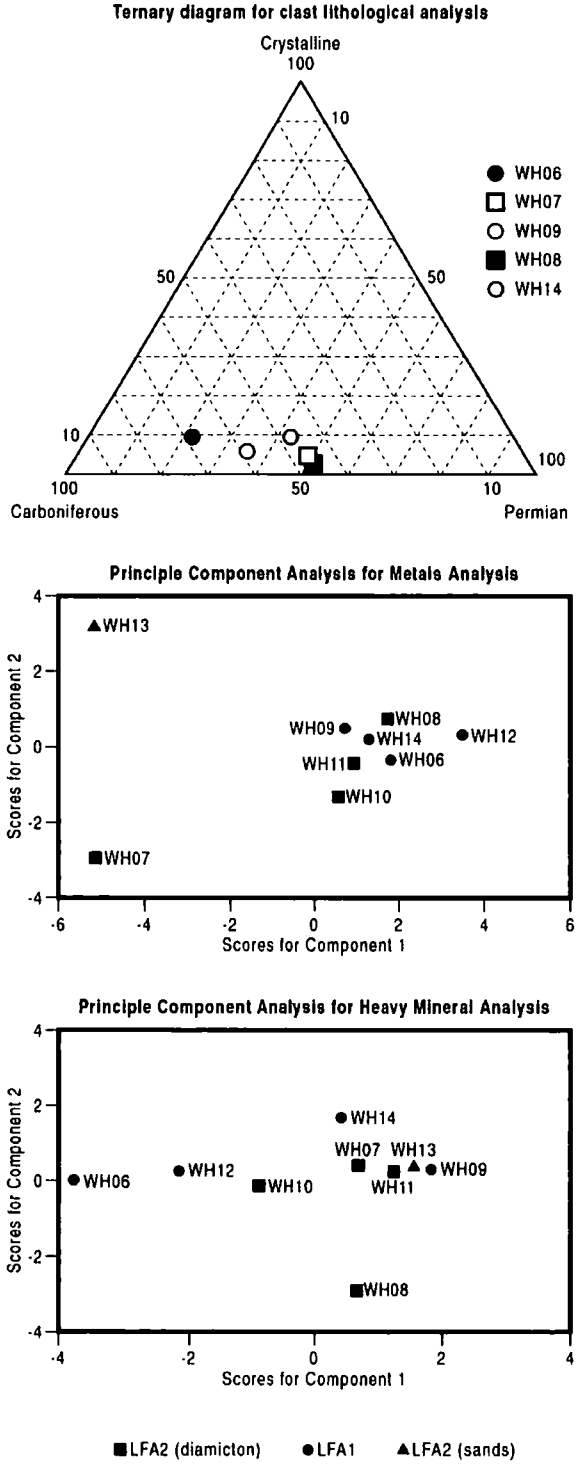

Figure 3.11: Principle Component Analysis and ternary diagram of heavy-mineral analysis, clast lithological analysis, and metals analysis.
The ternary diagram shows LFA 1 (circles) and LF 2a (circles) clast counts. Rippled sand facies (LF 2b; WH13) is denoted by triangles.
The first component of the metals PCA analysis explains 47 % of the data, and is explained mostly by the proportions of lithium, boron, aluminium, calcium, titanium, vanadium, beryllium, cobalt, nickel, iron, chromium and copper. Component 2 explains 19 % of the data, and is explained by potassium, manganese, arsenic, molybdenum, silver, antimony and barium.
For the heavy mineral PCA correlation, sulphides were excluded from the analysis due to low numbers; carbonates were excluded due to strong skew. The strong first component, with 52 % of the variation, is explained by the proportion of the silicate group, pyroxene, and micas in the sample. The second component, with 19 % of the variance, is explained by oxides and then by pyroxene. In this analysis, samples WH07 (LFA 1) and WH13 (LF 2b) do not stand alone, but correlate with the other samples.

3.4 Interpretation

3.4.1 Lithofacies Association 1

Subglacial traction till

LFA 1 has the macro-scale characteristics of a subglacial traction till (Evans *et al.*, 2006). These include striated, exotic, faceted clasts, far-travelled heavy minerals, an over-consolidated, matrix-supported structure, and clustered clast macro-fabrics (Benn & Evans, 1998; Evans *et al.*, 2006). The micromorphological analysis also supports an interpretation of LFA 1 as a subglacial traction till. Associations of rotational structures, rounded Type II and III pebbles, grain lineations, masepic plasmic fabrics and skelsepic plasmic fabrics denote ductile deformation (van der Meer, 1997; Hiemstra & Rijsdijk, 2003) and grain rotation in a till matrix (van der Meer, 1997; Nelson *et al.*, 2005). The rotation of skeleton grains has caused preferential alignment of clay particles (Roberts & Hart, 2005), through the transmission of stress perpendicular to the particle edges. Crushed grains imply high stress, low strain conditions in a brittle environment (Menzies *et al.*, 2006). The combination of both brittle and ductile deformation structures suggests polyphase deformation. The common rotational structures, and the lack of flow, marbling and tile structures, preclude a genesis by mass movement or debris flow (Lachniet *et al.*, 2001; Menzies & Zaniewski, 2003). Sample 1-3 (Section 1, Figure 3.5) shows where LFA 2 was emplaced over LFA 1. The two varieties of masepic (bimasepic) plasmic fabric indicate strong shear in two directions. The numerous soft sediment clasts indicate cannibalisation of pre-existing sediments.

LFA 1 is thus interpreted as a terrestrial subglacial traction till with evidence for both lodgement and deformation, which varied spatially throughout Whitburn Bay. The striated clasts with aligned long axes and the boulder pavement in Section 1 are indicative of lodgement (Menzies *et al.*, 2006). In contrast, LFA 1 in other sections (e.g. 2a, 3, and 10) at Whitburn Bay demonstrates structures indicative of extensional deformation, such as stringer initiation, weak clast macro-fabrics, massive, homogenous diamictons, and micromorphological evidence of extensive ductile deformation.

The Boulder Pavement

The boulder pavement occurs at the top of LFA 1. Striae and clast macro-fabrics are north-easterly orientated, consistent with fabric evidence from LF 2a, indicating that the second phase of ice flow directly overrode the boulders. There are several competing theories for boulder pavement formation, ranging from lodgement (Boulton & Paul, 1976), deformation with formation by the sinking of clasts through the deforming layer (Clark, 1991; van der Wateren, 1999; Glasser *et al.*, 2001), and a continuum between deformation, meltout and lodgement with subsequent extensive abrasion, truncating and striating the upper surfaces (Hicock, 1991). Boulton (1996) maintained that during erosion of the till down to the A/B interface, dense clasts, on being exposed, resist being drawn into glacier flow and remain immediately above the A/B interface, concentrating larger clasts from the mobilised till. Jørgensen and Piotrowski (2003) argued that a boulder pavement is an erosional surface, indicating truncation and removal of underlying sediments. Lodgement and extensive abrasion at the sole of the ice sheet truncates, orientates and striates the upper surfaces of boulder pavements.

A simple erosional mechanism best explains the boulder pavement at Whitburn Bay (Figure 3.12). As the boulders are orientated, planated, and striated strongly in one direction, it is unlikely that they have sunk through the deforming layer, as this would have led to multiple striae directions and to rotation of clasts (Jørgensen & Piotrowski, 2003). The clustering of the boulders at one level suggests that they are some sort of lag deposit. This may be the result of the down-ice removal of till matrix by ice, leaving a boulder lag, or the result of meltwater activity at the ice/bed interface, which removed the matrix to leave a lag of coarser material. Crudely stratified and sorted sand and gravel lenses and channels within the pavement point to a surplus of meltwater at the ice/bed interface, which would support this latter hypothesis. The boulders were lodged into the deforming substrate as ice began to flow north-north-east to south-south-west, causing planation and striation before eventual burial by further till accretion (LF 2a). The strong unimodal orientation of the clast long axes supports this. This model suggests abundant meltwater at the ice/bed interface, perhaps during the quiescence of the first flow phase, and before the second phase of ice flowing northeast to southwest, which planated and striated the boulder pavement, and deposited LF 2a.

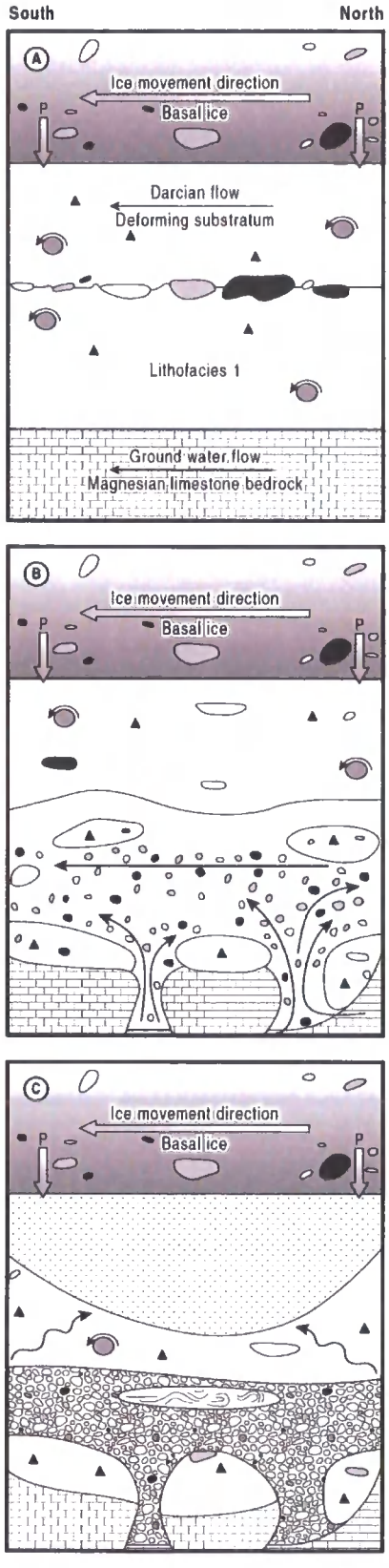

Figure 3.12: Cartoon depicting formation of the boulder pavement and hydrofracture at Whitburn Bay. Ice overburden pressure is denoted by *P*.
A. First ice lobe advances and deposits LFA 1. Ice lobe quiesces. Boulders melt out of ice. Second ice lobe advances, lodges boulders and imposes striations on them. Boulder pavement represents an erosional surface.
LFA 2 is deposited over the top of the boulders. High amounts of meltwater are inefficiently evacuated as porewater flow under high pressure.
B. Hydrofracture is initiated. Bedrock fractures, and groundwater is piped under pressure towards ice-bed interface. Channels form and the water flows away under the ice-sheet.
C. Once the main force of water is dissipated, course gravels and bedded sands are deposited. They are subsequently glaciotectonised. A later-phase nye channel forms above.

3.4.2 Lithofacies Association 2

LF 2a: Subglacial Traction Till

Faceted, striated, exotic clasts and the over-consolidated nature of the diamicton, indicate that LF 2a is also a subglacial traction till (Evans *et al.*, 2006). The variable localised incorporation of LFA 1 indicates that extensive deformation has homogenised and mixed the two tills. A PCA of the heavy mineral content shows strong inter-sample heterogeneity, but no dichotomy between the diamictons (Figure 3.11). The failure of this method to discriminate between the lithofacies could be a result of the small sample numbers, as this can create an artificially high skew.

Clast macro-fabrics and striae are poorly clustered, but indicate general ice movement from the north-north-east. The low and variable S_1 values from the clast macro-fabrics could suggest extensive deformation (cf. Evans *et al.*, 2006), possibly driven by fluctuating subglacial conditions and water pressure. Hart (2007) argued that weak clast macro-fabric strengths reflect clast interaction and a dominance of deformation and rotation, and furthermore that large grain size and low sorting emphasises rotation, leading to low clast macro-fabric strength in subglacial diamictons. Others argue that soft, water saturated sediments such as LF 2a behave as Coulomb plastic materials (Larsen & Piotrowski, 2003). Clasts become aligned parallel to the shear direction when exposed to high strain rates, giving a high fabric strength. Weak fabrics are therefore associated with low shear strains (Hooyer & Iverson, 2000; Larsen & Piotrowski, 2003). Larsen & Piotrowski (2003) argued that strong clast macro-fabrics only develop under conditions of strain homogeneity and uniform local conditions. The weak and variable clast macro-fabrics at Whitburn Bay therefore reflect heterogeneity in strain, water content, and till rheology.

In Section 2a, the overturned pipe structures are evidence of the squeezing of the soft, saturated LFA 1 into LF 2a under a high ice overburden pressure (Figure 3.13). They are overturned towards the southeast, supporting this direction of ice flow. These features have a low preservation potential, and are unlikely to have survived the process of lodgement (Nelson *et al.*, 2005), suggesting that they postdate the deposition of LFA 2. In all, the highly variable and often weak clast macro-fabric strengths, as well as the preservation of the pipe structures and canal fills, suggest a low strain deformation signature within LFA 2 (cf. Evans *et al.*, 2006). They may have formed contemporaneously with till accretion of LF 2a. As LFA 1 became buried by an increasingly thick layer of sediment, sealing the

lower hydraulic pathways and increasing overburden pressure, and the deforming layer moved upwards (the 'A Horizon), the lower non-dilated 'B Horizon' would have undergone little deformation, despite ongoing ice movement and till deformation in the 'A Horizon' above (cf. Boulton & Hindmarsh, 1987). The pipes would have formed in saturated, confined conditions and could have experienced little deformation.

Micromorphological analysis of LFA 2 reveals numerous micro-scale deformational structures, such as circular structures with associated skelsepic fabrics, associated with aligned grains and grain lineations (Table 3.3). Elongate grains near the shear plane have rotated until they are aligned plane-parallel. Crushed grains and strong masepic plasmic fabrics indicate pervasive strain and high pressure. These features are indicative of subglacial deposition and deformation (van der Meer, 1997; Carr, 2001). Thin section 10 shows in detail the junction of LF 2a with the underlying bedrock, and further supports a subglacial till interpretation, based on the strong presence of circular structures, crushed grains, Type II pebbles, and a strong plasmic fabric (Figure 3.6). The bedrock has been entrained into the till with evidence of stringer formation and cannibalisation of the lower soft, dolomitic limestone.

LF 2b and 2c: Nested Nye channels

The isolated channelised forms, with concave-up bases and flat tops, and the strong variation in height of these channels, preclude a proglacial origin. Distal proglacial sandur systems are characterised by trough cross-bedded, cyclic fining-upward sequences of gravels, sands and silts with slip face migration of longitudinal and linguoid braid bars. This gives rise to planar cross-beds, with abundant ripple-drift and cross-lamination (Maizels, 1995). Distal proglacial outwash sediments typically exhibit megaripple migration on point-bar surfaces, producing large-scale trough cross-beds. The lack of bars, dunes and tabular bedding in the Whitburn channel systems suggests that they are subglacial glaciofluvial sediments (Collinson, 1986). They are a low energy subglacial braided canal network, as defined by Walder and Fowler (1994), which was active beneath the ice sheet that formed the traction tills. The channels formed at the ice-bed interface, and were later buried by till accretion. This interpretation is in agreement with previous process-based research further north in Northumberland (Eyles *et al.*, 1982).

This type of distributed subglacial drainage system is inefficient, and can result in low energy flows and ponding beneath the ice sheet. These systems operate when pore-water

flow cannot evacuate all the excess water in the system (Benn & Evans, 1996). Such systems have long been recognised in the geological record as broad lenses of sorted sediment within the tills with concave-up lower contacts and nearly planar upper contacts (e.g. Dreimanis *et al.*, 1986; Shaw, 1987; Lunkka, 1994). Englacial conduits rarely extend further than 200 m into the ice sheet (Fountain & Walder, 1998; Piotrowski *et al.*, 2006), indicating that the sequence at Whitburn Bay formed in a submarginal environment. Ductile deformation, despite the high drainage capacity of the bed, would therefore have occurred close to the ice margin under low cryostatic pressures.

Swift *et al.* (2002) argued that seasonal reorganisation of subglacial drainage can occur beneath many temperate and polythermal glaciers, resulting in distributed and channelised configurations, with the development of a hydraulically efficient, channelised subglacial drainage system during the ablation season. This would involve higher-pressure, channelised, faster flowing canals (such as LF 2c; Section 7) and slower moving, lower energy, distributed drainage systems (such as LF 2b; Section 9) evolving (perhaps seasonally) throughout the year. These lower energy channels also demonstrate flow variability at smaller scales, with evidence of periodic quiescence and ponding, as well as periods of faster flow, demonstrated by the juxtaposition of Type A and B ripples, planar lamination and clay drapes, which represent alternations of fast flow and suspension settling under low- or no-flow conditions. This indicates periodic quiescence of the channel with little sediment input (cf. Ashley *et al.*, 1982; Ashley *et al.*, 1985). Repeated changes between planar laminated sands and Type B climbing ripples in Section 9d (Allen 1963) represent fluctuating flow, indicating slowly migrating ripples with high vertical aggradation rates (cf. Ashley, 1995), with ripple drapes indicating water ponding. Interlaminated sand and clay beds indicate repeated quiescence and fast flow in the channels. A pebble lag near the basal contact in Section 9d points to traction current activity with bedload saltation. LF 2b and LF 2c therefore demonstrates fluctuations of meltwater discharge at multiple scales, and perhaps seasonally.

An alternative explanation for the laminated clay and sand facies at Whitburn Bay could be backfilling of subglacial canals during times of low or no water flow, related to ice-contact lake level fluctuations. There is extensive evidence of such proglacial lakes in County Durham and Yorkshire (Smith, 1994). During periods of low lake levels, high submarginal discharge in these channels would have resulted in the deposition of rippled and bedded sands, but during periods of high ice marginal lake levels, backfilling of the

channels could have caused ponding and clay drape lamination. The canal fills could thus be related to the activity of local lakes such as Glacial Lake Wear. Indeed, episodically changing lake levels, related to both seasonal variations in meltwater and to the movement of ice lobes, have been suggested in Glacial Lake Wear (Smith, 1994). The geometry of these sand infills is therefore significantly different to the tabular, widespread, subaerial glaciofluvial sands and gravels presented by Francis (1972).

The laminations of LF 2b are locally strongly deformed; their load and water-escape structures indicate deformation and remobilisation of the water-saturated beds, suggesting rapid deposition (Glasser *et al.*, 2001) or a high overburden pressure. The laminated sand and clay channels have closed edges, flat tops, and undulating, convex bottom contacts, indicating that they were incised into the diamicton, perhaps in a period of higher energy flow (van der Meer *et al.*, 2003). The consistent overturning of folds to the south also suggests glaciotectonic disturbance as ice flowed southwards. This is supported by the micromorphological analysis, which shows compression of the primary bedding structures and masepic plasmic fabric development sub-parallel to bedding, followed by conjugate fault development as folds have been compressed, overturned, and extended (Figure 3.9). Compression has elevated porewater pressure within the sand beds, which has been released during faulting, causing fluidisation of sands and water escape and injection structures.

LF 2d: Hydrofracture

The sub-vertical clastic dykes in Section 5 (Figure 3.10) are the result of the escape of high-pressure groundwater beneath the ice sheet; i.e., as hydrofracture fills (Evans *et al.*, 2006). Tensional cracks are infilled by sediment fluidised by the escaping water. Hydrofractures occur where fluid pressure exceeds the tensile strength of the sediment and the smallest component of the ice overburden pressure (Rijsdijk *et al.*, 1999). Juxtaposed thinly bedded, calcreted sands, and coarse, well-sorted gravels indicate variable flow regimes.

At Whitburn Bay, subglacial meltwater would have discharged into the Magnesian Limestone aquifer. The overlying tills acted as aquicludes, hydraulically confining the bedrock (as also observed by Rijsdijk *et al.* (1999) at Killiney Bay, Ireland). When the supply of meltwater exceeded the capacity of the bedrock aquifer, water pressures rose beneath the overlying till. When the water pressure exceeded the tensile strength of the till,

it caused tensile fracturing, which enabled hydrofracturing (Figure 3.12). The discharge of water was sufficient to fluidise the sands and gravels, transport them through the hydrofracture and inject them into the overlying sediments. A high percentage of calcium carbonate in the ground water, derived from the bedrock, resulted in calcretion of the gravels. Hydrofractures and high porewater pressures may be related to the coarse-grained channels operating at the ice/bed interface. These discrete, hydraulically efficient channels are highly erosive and incise into the deforming layer at the ice/bed interface, suggesting effective evacuation of subglacial meltwater. They were later buried by continued till accretion. Hydrofracturing and channel formation was therefore associated with increasing basal water pressures during the accretion of LFA 2 from ice overriding from the north.

Ultimately, LFA 1 and LFA 2 represent a mosaic of processes operating subglacially at the time of sediment deposition, at both the macro- and the micro-scale (cf. Piotrowski *et al.*, 2004). The hydrofracture and infilled canals clearly show that basal water pressures fluctuated at Whitburn Bay during the deposition of LFAs 1 and 2, as will have pore water pressures, which have been influential in the degree of till deformation (cf. Boulton *et al.*, 2001). Multiple switches in different modes of deposition and deformation resulted in the variable appearance of the two tills and the boulder pavement at Whitburn Bay (cf. Piotrowski *et al.*, 2004; Piotrowski *et al.*, 2006).

3.4.3 Provenance of the Whitburn Bay tills

Heavy mineral sources

Both LFA 1 and LF 2a are rich in clinozoisite, which is common in schists and is a product of low- to medium-grade metamorphism (Mange & Maurer, 1992). Both tills are rich in olivine and pyroxenes (Table 3.4), which could be sourced from an ultramafic to mafic igneous sources. The Permian Whin Sill Dolerite, which outcrops extensively to the north and northeast of Whitburn (Smith & Francis, 1967), may have been a primary source of detrital pyroxene. However, this microgabbroic intrusion does not contain olivine, indicating that a separate basic igneous source was also supplying detritus. One such potential source of both olivine and clinopyroxene is the Carboniferous volcanic rocks (olivine and clinopyroxene phyric basalts) and high-level intrusions of Northumbria, the Midland Valley of Scotland, and locally within the Southern Uplands. As olivine is not very robust, it is likely to have been sourced from nearer areas, such as Northumbria.

The metamorphic assemblage of heavy minerals within both LFA 1 and LF 2a is consistent with a source terrane that includes a significant proportion of upper greenschist to upper amphibolite facies of regionally metamorphosed pelitic mudstones. The two key mineral assemblages are, firstly, garnet, staurolite and chloritoid, and secondly, garnet, andalusite and kyanite. Each assemblage is found only in specific areas of polydeformed and metamorphosed orogenic belts. In particular, the Highlands and Islands of Scotland are the sole source for chloritoid (Mange *et al.*, 2005). The garnet-staurolite-chloritoid assemblage is characteristic of Stonehavian-type metamorphism, developed in a small area to the east of Stonehaven close to the Highland Boundary Fault, implying a possible source in northeast Scotland (Stephenson & Gould, 1995; Trewin, 2002). The garnet-andalusite-kyanite assemblage (possibly with sillimanite) is a higher grade assemblage developed in the Buchan-type metamorphism of northeast Scotland (Stephenson & Gould, 1995).

Younger sedimentary rocks may be a source of reworked minerals. Tourmaline in particular is very resistant and is common in many sedimentary rock types. Further research should include the identification of the heavy mineral suites in sedimentary rocks in the Southern Uplands and Midland Valley, as well as in northern England. This does not explain the presence of non-durable mafic minerals, which would not have survived reworking.

Overall till provenance

The dominant lithologies in LFA 1 are principally locally sourced Magnesian Limestone, sandstones, Carboniferous Limestone, Whin Sill Dolerite and Old Red Sandstone. The Carboniferous Coal Measures immediately to the west and north of eastern Durham are sources for the coal and sandstones of LFA 1. Whin Sill dolerite is a local Permian intrusive igneous rock, with abundant outcrops to the north and west of the area. LFA 1 is largely a locally derived till. Old Red Sandstone outcrops to the north-west.

The heavy-mineral assemblage suggests that ice entrained material sourced from northwestern England, the Southern Uplands, the Midland Valley, and possibly further north from northeastern Scotland. Clast macro-fabrics and striae orientations support a first phase of ice flow from west to east, which crossed the Pennines through the Tyne Gap and deposited the lower traction till. If the northwest to southeast ice-flow interpretation is correct, East Grampian minerals within LFA 1 are most easily explained by the reworking of older northerly-derived glacigenic sediments situated on the Durham coastal lowlands.

The palynomorph assemblages within LF 2a indicate a likely derivation from the Newcastle coalfield, to the north. A lack of Magnesian Limestone in LFA 2 compared with LFA 1 (Figure 3.11) indicates that LF 2a has been isolated from the local Permian bedrock by a mantle of earlier till (LFA 1), which is widespread in the Durham region (Beaumont, 1967). The distinctive pink granites, rhyolites and porphyries within LFA 2 are from the Cheviots; its greywackes may come from the Southern Uplands, while the Grampian Highlands are sources of schist and slate.

The combination of dioritic / granitic lithics with the metamorphic mineral assemblage of LF 2a suggests that material was sourced from the Dalradian Supergroup, exposed in northeastern Scotland. Sources of Old Red Sandstone and Carboniferous sandstone and limestones extend eastwards into the North Sea, where they terminate against the North Sea Central Graben. Any ice feeding down the coast from the Scottish Highlands would have had to cross this area, and may also have coalesced with ice from the Midland Valley. The lower percentages of olivine and pyroxenes within LF 2a suggest that the Midland Valley had less influence on this till. These minerals could also have been derived from reworking of the lower LFA 1.

Collectively, this evidence indicates a northerly source as far north as the East Grampian Highlands, before ice coalesced with the Tweed ice stream, and entrained Cheviot erratics. A clast macro-fabric and striae on the boulder pavement indicating a north-north-westerly flow direction supports this interpretation.

3.5 Discussion

3.5.1 Evolution of the glacigenic sequence at Whitburn Bay

Recent research has highlighted the fact that there is large spatial variability in basal friction below ice sheets, and that glacier beds are mosaics of sliding, deformation, lodgement and ploughing (e.g., Piotrowski *et al.*, 2004; Nelson *et al.*, 2005; Evans *et al.*, 2006). Whitburn Bay demonstrates this well, with evidence for lodgement in the form of a boulder pavement, adjacent to extensive evidence for deformation and hydrofracturing.

Glacigenic sediments at Whitburn Bay can be understood through a multiphase model of development (Figure 3.13). The first phase involved the arrival of an ice lobe from the west, which deposited LFA 1 (Figure 3.14). This ice originated from Scotland and entered eastern England via the Tyne Gap, some time after 21-22 cal. yr BP based on correlation with the Dimlington type site (Cameron *et al.*, 1992; Bateman *et al.*, 2008). It was later superseded by ice flowing northeast to southwest, which lodged and planated the boulder pavement and deposited LFA 2 (the Horden Member in County Durham and the Bolders Bank Till in the offshore area (Catt, 2007)). The simplest interpretation of a secondary northeast to southwest ice-flow is deflection by Fennoscandian ice in the North Sea. This however conflicts with recent research, which indicates decoupling by the Fennoscandian and British ice sheets by the Late Devensian (Carr *et al.*, 2006).

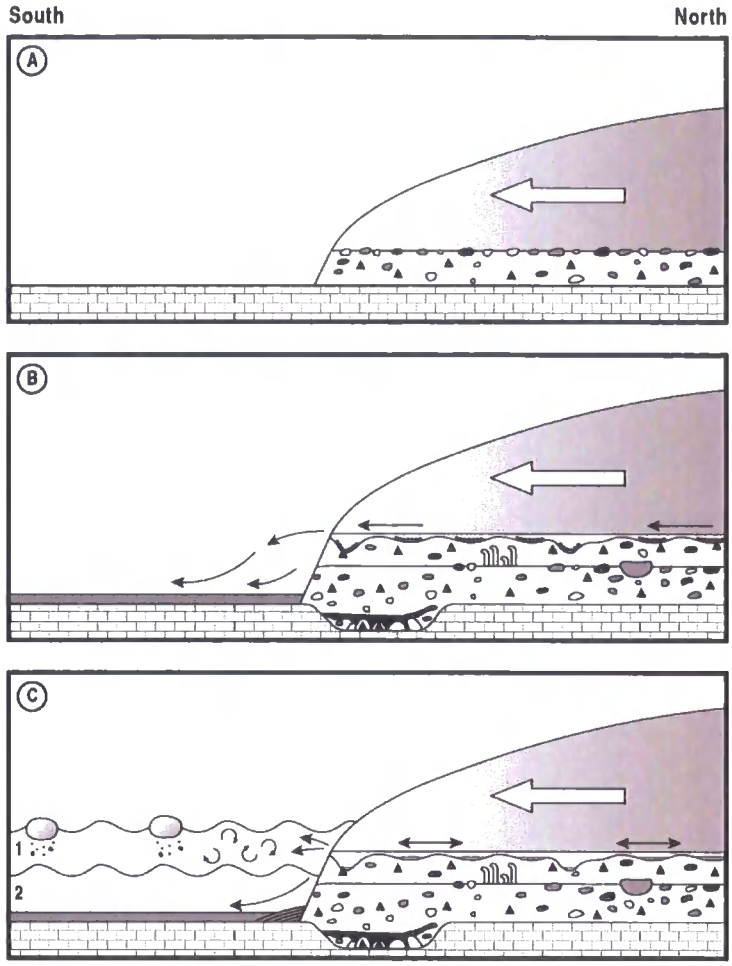

Figure 3.13: Land-system development at Whitburn Bay.
A. First ice lobe advances and deposits LFA 1. Ice lobe stagnates prior to retreat, and boulders melt out. As the second ice lobe advances, it striates and lodges the boulder pavement, as an erosional surface.
B. The deposition of LFA 2 buries the boulder pavement. A well-developed discreet ice-marginal, subglacial drainage system drains the glacier subaerially. Pipe structures and hydrofracture are formed. The sediments are extensively tectonised.
C. Discrete drainage system may evolve seasonally into a distributed, braided, subglacial canal system. Low flow periods, possibly seasonal or diurnal, results in quiescence in the channels. As the ice lobes retreat, Glacial Lake Wear was formed in between them. The depth of the lake varied between several high stands (C1 and C2). The lake may have periodically back-filled the canals, resulting in quiescence and ponding.

3.5.2 East Coast Surging

The initiation of the boulder pavement may have been triggered by a period of basal ice melting as flow from the west waned, resulting in aqueous washing of matrix material. The boulders were later lodged and abraded by the ice flowing from the north that deposited LFA 2 (Figure 3.14). A channelised subglacial drainage system of multiple braided canals developed beneath the ice, which may have changed, possibly seasonally, to a discrete, higher pressure drainage system of more efficient Nye channels. The sedimentary signal within the canals was controlled by a fluctuating internal drainage system; alternating periods of current flow and ponding suggest an inefficient hydraulic regime, which is often typical of surging glaciers (Björnsson, 1998). It is possible that fluctuating local lake levels also influenced the hydraulic efficiency in these submarginal canal environments, although this is difficult to substantiate.

Björnsson (1998) argued that glacial surges and fast ice flow are associated with subglacial distributed drainage systems, because an increase in pore-water pressure can lead to the decoupling of the ice from its bed (Björnsson, 1998). Decoupling can allow sliding to occur (Boulton *et al.*, 2001). Additionally, when ice overrides a wet subglacial till, enhanced flow velocities may also result from till deformation and sliding at the ice/bed interface (Ng, 2000; Boulton *et al.*, 2001).

Modelling by Boulton & Hagdorn (2006) showed that a powerful ice stream flowed down the eastern coast of Britain; its advance to the Wash embayment triggered the initiation of Glacial Lake Humber. Recent Optically Stimulated Luminescence dates on the highstand of this lake (Bateman *et al.*, 2008) of 16.6 ± 1.2 ka BP suggest that the BIIS was flowing at the western edge of the North Sea Basin, possibly during Heinrich Event 1, depositing the Skipsea Member and the Bolders Bank Formation. The Skipsea Member overlies silts dated to 21.7 cal. ka BP (Penny *et al.*, 1969). Eyles *et al.* (1994) argued that this east coast ice stream experienced recurrent onshore surging against the rising bedrock surface of Holderness and Lincolnshire. The deforming bed mosaic and subglacial canal evidence from Whitburn could therefore support the existence of such a surge lobe during Heinrich Event 1, which is supported by external evidence from modelling and the dates of 16.6 ka BP from Lake Humber.

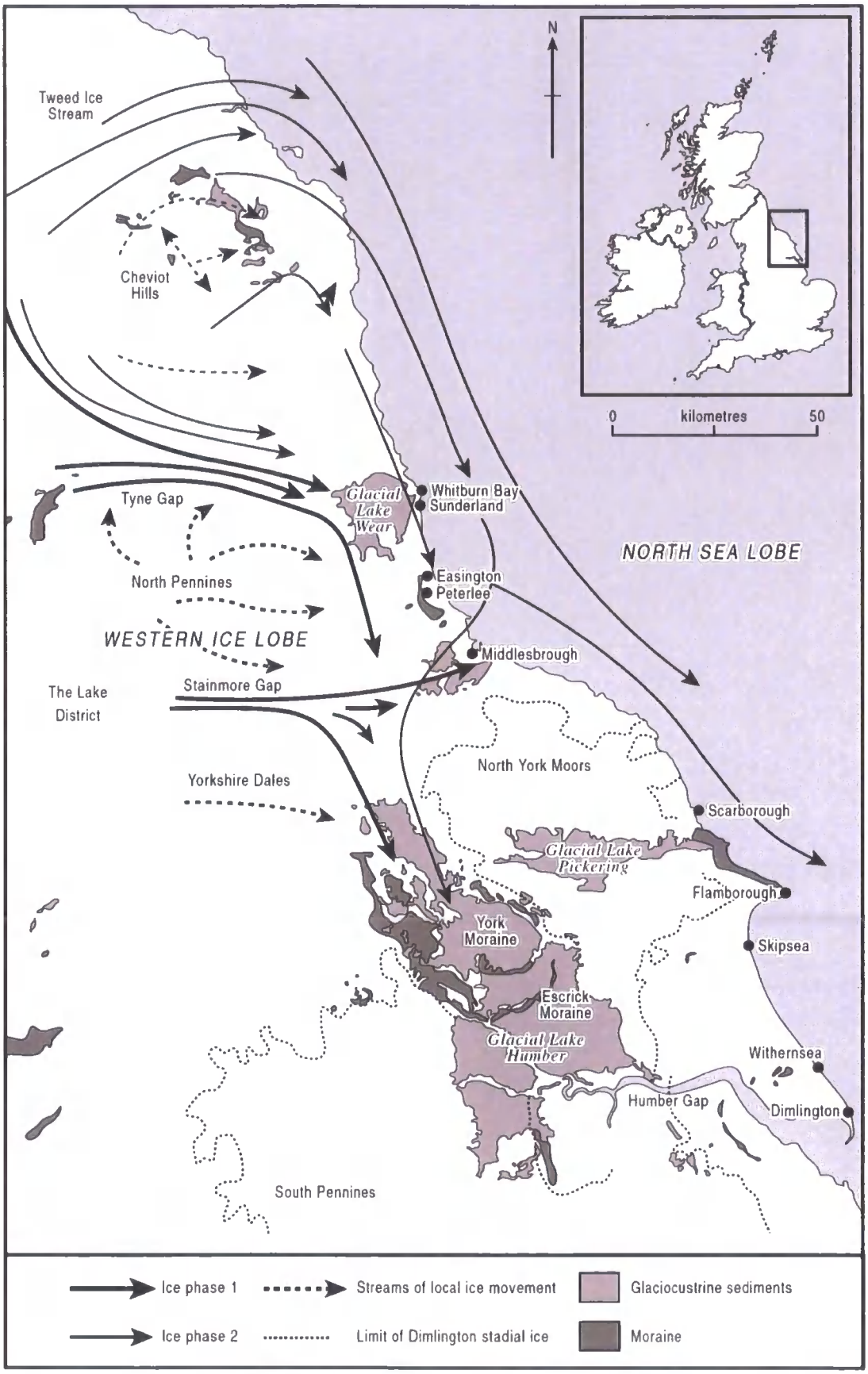

Figure 3.14: Map showing inferred ice flow directions, overlain onto the BRITICE data set for the northeast region (Clark *et al.* 2004). Ice flow around the Tweed area from Raistrick (1931).

3.5.3 Implications for Quaternary Stratigraphy of eastern England

The locally derived Blackhall Member (LFA 1) at Whitburn Bay was previously correlated with the Skipsea Member of Holderness (Francis, 1972) due to its stratigraphical position, but this is disputed here because of the provenance data. We favour an origin for ice flowing across the Pennines through the Tyne Gap. The Blackhall Member shows a distinct west-to-east movement, and comprises mainly local clasts. Previous work has suggested that it is limited in extent, and there seems to be no equivalent further south than County Durham (Beaumont, 1967). Therefore, the Blackhall Member does not appear to correlate with the Skipsea Member. Instead, the mineralogy, particle size, erratic content and characteristics of the Skipsea Member indicate a correlation with the Horden Member (Table 3.6).

The macrofabrics of the Horden and the Skipsea Members indicate deposition by ice moving inland from the North Sea basin. Ice is suggested to have originated from the Southern Uplands, streamed down the eastern coast of Britain (Eyles *et al.*, 1994), invaded the North Sea Basin and deposited the Skipsea Member and the Bolders Bank Fm (Cameron *et al.*, 1992; Carr *et al.*, 2006). The movement inland could have resulted from coalescence of British ice with Scandinavian ice offshore in the North Sea. Sejrup *et al.* (2000; 2005) and Carr *et al.* (2006) argued that the British and Fennoscandian ice sheets had decoupled by this stage, but the southerly extension of the North Sea Lobe during the latter phases of the LGM cannot have occurred without the continued presence of Scandinavian ice offshore. The presence of heavy minerals derived from the eastern Grampian Highlands indicates a distant northerly source. The presence of these minerals indicates that the ice has been deflected strongly southwards, suggesting that contact with Scandinavian ice offshore is needed to direct the ice flow. Shap erratics within the Skipsea Member are derived from coalescence of the Durham and Tees ice lobes in the Tees Gap. Hence, this work suggests that the southward-flowing North Sea Lobe was the second ice lobe to transgress the Durham area, but the first ice body to reach the Holderness coast during the LGM.

Table 3.6: Comparison of characteristics of Skipsea Member at Dimlington, and Horden Member at Whitburn Bay (Penny & Catt, 1967; Madgett & Catt, 1978; Evans *et al.*, 1995; Catt, 2007).

	Skipsea Member	Blackhall Member (LFA 1)	Horden Member (LFA 2)
Type Site	Dimlington, Yorkshire	Blackhall's Rocks, Durham	Horden, Durham
Colour	Very dark greyish brown. 10YR 3/2	Dark yellowish-brown. 10YR 4/4	Dark brown. 10YR 3/3
Sedimentology	5-9 m thick. Interbedded diamictons, discontinuous bodies of stratified sediments	Massive, matrix supported diamicton. Common cobbles of local origin. Boulder pavement at top.	Matrix-supported diamicton. Nested channels within diamicton.
Particle Size	22-38 % clay, 32-42 % silt, 22-42 % sand	31 % clay, 39 % silt, 18 % sand, 12 % gravel.	33 % clay, 38 % silt, 17 % sand, 11 % gravel.
Erratic content	Chalk, shale, greywacke, Cheviot porphyries, granites, Whin Sill Dolerite, Carboniferous and Magnesian Limestone, coal, rhomb porphyry	Magnesian Limestone, Carboniferous Limestone, Carboniferous sandstones, Greywacke, Old Red Sandstone.	Cheviot rhyolite and andesite, granite, Carboniferous Limestone, Magnesian Limestone, Old Red Sandstone, schist, greywacke.
Heavy Minerals	Enriched in amphibole and epidote, poor in chlorite and biotite.	Enriched in clinozoisite, micas, kyanite, and amphiboles.	Significant amounts of pyroxene, kyanite, epidote, limited chlorite and biotite.
Palynology	None available	None available	Carboniferous spores: Westphalian and Namurian.
Macrofabric	NNE-SSW direction; WNW-ESE fold axes	Moderately strong; NW to SE.	Weak macrofabric, NE to SW.
Age	Overlies Dimlington Silts: >21.7 cal. ka BP	None available	None available

3.6 Conclusions

Research at Whitburn Bay supports the existence of a complex, multi-lobate, Late Devensian BIIS along the east coast of Britain. The traction tills LFA 1 and 2 represent ice flow from two different directions within the same glaciation. The Blackhall Member (LFA 1) originated in northwestern England, possibly sourced from the Midland Valley and western Southern Uplands. It may also have a component of ice from northeastern Scotland. It flowed south, before passing through the Tyne Gap. There is little evidence of a Lake District ice source. The Horden Member (LFA 2) was deposited by an ice lobe flowing down the eastern coast of Britain, which may have originated as far north as the eastern Grampian Highlands and which is dominated by Cheviot and Northumbrian erratics. The boulder pavement was deposited as a lag through a combination of subglacial erosion and aqueous winnowing as ice flow from the west waned and was later lodged and abraded by ice moving southwards.

The braided canal system preserved in the Horden Member suggests a fluctuating low-flow subglacial drainage system, which, juxtaposed with high-energy gravel channels, reflects periodic changes in the subglacial drainage hydraulic regime. Hydrofracturing supports the notion of extreme variations in subglacial drainage, which may have triggered the development of high-energy channels at the ice-bed interface. The episodic changes from rapid water flow to quiescence in these submarginal channels indicate periodic ponding events. Seasonal re-organisations of the subglacial drainage system could have resulted in the juxtaposition of sand and very high-energy gravel channels. Fluctuating lake levels in the proglacial Glacial Lake Wear may have contributed to this variation, as high lake levels would have resulted in backfilling of the channels, quiescence, and the formation of draped lamination. Evidence for basal decoupling, extreme fluctuations in subglacial porewater pressure, and the presence of a deforming bed supports the notion of a fast flowing ice lobe in the vicinity of Whitburn Bay and further south such as at Holderness (Boulton & Hagdorn 2006; Eyles *et al.* 1994; Evans *et al.* 1995). The mineralogy, lithologies and process interpretation of the Horden Member demonstrates that it is correlative with the Dimlington Stadial Skipsea Member and possibly the Bolders Bank Fm in Yorkshire and offshore respectively. This may suggest that the North Sea ice

lobe flowing south was the second ice lobe to transgress the Durham region, but the first ice mass to cross the Holderness coast during the LGM.

CHAPTER 4

Hawthorn Hive to Blackhall Rocks

4.1 Introduction

The history of the interaction between the BIIS and the FIS throughout the Quaternary remains poorly understood. Recent research in Norfolk has presented three alternative models, with Scandinavian ice proposed during MIS 12 and 6 (Hart & Pelgar, 1990; Lunkka, 1994), just during MIS 6 (Hamblin *et al.*, 2005), and just during MIS 12 (Pawley *et al.*, 2008). These rapidly evolving models require rigorous, quantitative testing in other regions of the United Kingdom to ensure their robustness and applicability. The Quaternary stratigraphy in County Durham is therefore key to our understanding of glacial / interglacial history in Britain, as this area has previously provided evidence of multiple glaciations. This chapter uses the stratigraphic nomenclature proposed by Bowen (1999c).

The next three chapters present results from mapping, section logging, thin-section analysis and petrological and geochemical analysis of sediments exposed in coastal cliff sections in the Easington District of County Durham (Figure 4.1). Facies architecture and sedimentology at Hawthorn Hive is presented in this chapter. The Easington District of County Durham was the type site chosen by Smith and Francis (1967) for the Blackhall and Horden tills (see Chapter 1), and here, stacked sequences of Quaternary sediments are well exposed over the course of several kilometres (Bridgland & Austin, 1999).

The Magnesian Limestone bedrock in this region is covered with a mantle of complex Quaternary sediments, including a raised beach at a height of 33 m (see Chapter 5). Buried palaeo-valleys are infilled with a series of tills and bedded sands and gravels, and numerous steeply incised 'denes' are occupied by small streams. During the Twentieth Century, coal mining and the dumping of colliery waste on the beaches obscured much of the cliffs, making research difficult. The 'Turning the Tide' programme of the 1990s and subsequent coastal erosion has re-exposed much of the natural cliff line, which, combined with shallow excavations, has made research of the glacigenic sediments possible once again.

Figure 4.1: Map of eastern County Durham, showing the location of Shippersea Bay. Sites investigated in greater detail in this thesis are highlighted (in bold). National Grid (NZ) lines are shown.

4.2 Research Aims and Objectives

4.2.1 Rationale

Reconstructing the ice-ocean-climate interactions for the last BIIS at the LGM is important for predicting future cryosphere responses to climatic change, as contemporary changes in the mass balance of large polar ice sheets is likely to have a large impact upon the human environment. Additionally, providing sound geological data for glaciological modellers is vital to allow the testing and development of ice sheet models.

This region is critically located to capture interlobate ice sheet dynamics during the LGM glaciation. Firstly, the Easington district is characterised by a different set of glacigenic sediments to Whitburn Bay, with abundant glaciofluvial gravels and no evidence of proglacial lakes. Glacigenic sediments are exposed in this location for several kilometres, allowing their nature to be characterised. Secondly, Warren House Gill has previously provided evidence of multiple glaciations (see Chapter 1), and so is a key site to investigate the long-term Quaternary history of northern England. Three sites are investigated in detail: Hawthorn Hive (this chapter), Shippersea Bay (Chapter 5), and Warren House Gill (Chapter 6). These sites were the only places where the sediments are accessible; high cliffs mean that in the majority of places, sampling is not possible. The lithological and geochemical data from all sites are compared in Chapter 6, and regional correlations are drawn in Chapter 8.

4.2.2 Research aims and objectives

This research aims to establish the interactions between British and Scandinavian ice sheets in northern England. This is a key area for reconstructing their past dynamics, as it is a region affected closely by competing ice lobes. County Durham contains some of the most northerly reported Scandinavian glacial sediments (Clark *et al.*, 2004b), so it is crucial in determining the interaction between British and Fennoscandian ice during the Quaternary. It is also important to establish why, given the far greater distances involved, the FIS reached eastern England during the Pleistocene before the BIIS, and why specifically and only during MIS 6 and possibly MIS 12 (Clark *et al.*, 2004b). To achieve this aim, there are four key objectives, determined by previously published research:

1. To map and log coastal exposures of glacigenic sediments between Hawthorn Hive and Blackhall Rocks, County Durham.
2. To determine the genesis of the glacigenic sediments in the study area, with particular reference to former ice flow direction indicators, provenance of the glacigenic sediments and their depositional history.
3. To determine the age of the Pleistocene glaciations of the Co. Durham coast using stratigraphical techniques, luminescence dating techniques, and amino acid racemisation dating.
4. To determine the stratigraphy of the glacigenic sediments in Co. Durham, and to test and identify regional correlatives.
5. To determine the timing and dynamics of Scandinavian ice in the North Sea, and its influence on ice on the eastern coast of Britain, and to constrain the western limit of the FIS.

Previous work on the Quaternary sediments of northeast England, in particular the work by Trechmann and Beaumont, has highlighted a number of controversies and unknowns that remain to be answered. Firstly, can the Warren House Formation be identified and its genesis, provenance and age determined? A quantitative reassessment of the Warren House Formation will allow the proposed correlation to the Bridlington Member of northeast Yorkshire (Catt & Penny, 1966) to be tested. Secondly, there remain a number of questions regarding Trechmann's interglacial loess. Firstly, loess is normally deposited in cold, steppe environments, and not interglacials. Therefore, can Trechmann's loess be identified, and the mode of deposition determined? What is the age of the loess, and can this provide a stratigraphical tool in the age of the Warren House Formation?

Finally, the 'Main Cheviot Drift' of the Durham coastline (Trechmann, 1952) remains controversial. What were the modes of deposition and the genesis of the tills? Have the tills been glaciotectonically deformed? What was the provenance of the tills? Did the ice that deposited them originate from the west (Lake District) or the northeast? What was the role of the North Sea Lobe in their deposition? Can the tills be correlated between Whitburn Bay, Shippersea Bay, Hawthorn Hive, and Blackhall Rocks? What is the relationship of the tills with the Skipsea and Withernsea members of the north Yorkshire coast? Building on these, some key hypotheses regarding LGM glaciations in Durham can be identified:

1. The uppermost glacigenic sediments on the Durham coast are Devensian tills. The North Sea Lobe from the north deposited the upper Horden Member.

2. Ice flowing from the west, through the Tyne Gap, deposited the lower Blackhall Member.
3. These tills correlate with tills at Whitburn Bay.

In order to answer these research questions, and to test the identified hypotheses, the eight kilometres from Hawthorn Hive to Blackhall Rocks were mapped and logged in order to understand the stratigraphic context. Three sites were chosen for study in detail: Hawthorn Hive, Shippersea Bay (presented in Chapter 4), and Warren House Gill. Trial pits at Warren House Gill through the colliery waste exposed the lowest glacial sediments of the buried valley for the first time in decades. In the next three chapters, the sedimentary logs and sketches, thin sections, and petrological and geochemical results from these sites are presented and interpreted. The genesis, provenance, and local and regional correlatives of these lithofacies associations are analysed.

4.3 Facies Architecture: Hawthorn Hive to Blackhall Rocks

The facies architecture between Hawthorn Hive and Blackhall Rocks is presented in Figure 4.2. For full-size, high-resolution photographs, see Appendix III. Hawthorn Hive is located at the mouth of Hawthorn Dene, which is a steeply incised contemporary river valley cut through the glacigenic sediments and Magnesian Limestone bedrock (Figure 4.2). Within the bay, just north of this dene, is a buried valley infilled with diamicton and sorted sediments. The colliery waste in the cove protects the cliff, so exposures in the buried valley are currently limited and are covered with trees. At 24 m above the colliery waste in the buried valley, a tabular cobble gravel is well exposed, which is underlain and overlain by diamictons. This gravel is very poorly sorted to well sorted, ranging from coarse sand to large boulders, and clasts within it are angular to rounded. Within the gravel, balls of diamicton are preserved. The Magnesian Limestone rises again steeply to the north, and exposures further north than here are very high and inaccessible.

This sequence of two diamictons separated by a widespread cobble to clast gravel facies continues southwards from Hawthorn Hive. It is obscured periodically by slumping, but the sequence is continuous. At 500 m south of Hawthorn Hive, the Easington Raised Beach rests directly on the Magnesian Limestone bedrock. The tabular gravels are absent at this point, but poorly sorted sands, cross-bedded sands with foresets picked out with coal, and gravels do overly the beach. The upper diamicton onlaps onto these gravels and the lower diamicton pinches out against the beach. The beach lies in the cove of Shippersea Bay in the lee of Beacon Hill, which possibly gave it some protection during the glaciation that brought about the deposition of the overlying sands and diamicton. These beach gravels are well calcreted and contain bedded, well-sorted sands, and rounded cobble and clast gravel bearing shells. To the south of Shippersea Bay, the sequence of gravels separating two diamictons continues. Slumping obscures the direct relationship of these gravels to the beach, and the cliff is too high and steep to allow closer observation. In places, the lower diamicton is absent and bedded sands rest directly on the bedrock, overlain by the upper diamicton. Here and there, these sands are a bright red colour (Figure 4.3). South of Foxholes Dene, the sedimentology is markedly different (Figure 4.2). The bright red sands become more prominent southwards, and are discontinuously exposed

here. The cobble gravel descends down to bedrock in Exposure K (Figure 4.3), and the bedrock dips down below the level of the colliery waste.

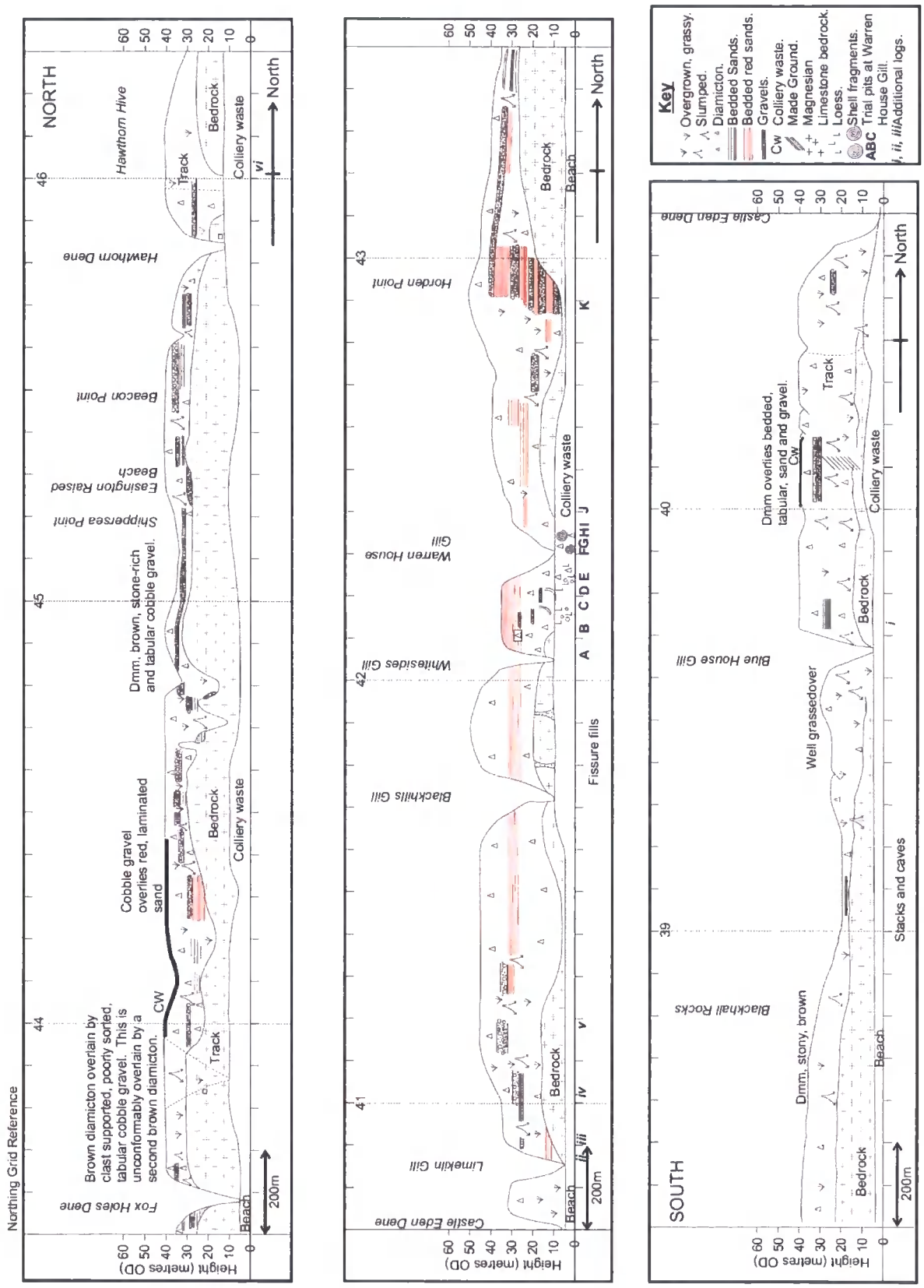

Figure 4.2: Facies Architecture: Hawthorn Hive to Blackhall Rocks

The height of the cliff is maintained by an infill of around 50 m of Quaternary diamicton. From 300 m south of Exposure K, the cobble gravel is absent. Steeply incised denes (Warren House Gill, Whitesides Gill, and Blackhills Gill) cut through the infill to the level of the colliery waste on the contemporary beach. The Magnesian Limestone is fissured and infilled with Early Pleistocene breccia, some of which is reported to contain Cromerian mammal fossils (Trechmann, 1952). The stratigraphy of this infilled valley is more complex, with the existence of a limited exposure of a third diamicton at the base of the buried valley. It is overlain by a beige silt, previously interpreted as a loess.

South of Blackhills Gill, the height of the bedrock rises sharply. The red sands are exposed for a short distance, but disappear some 400 m south of Blackhills Gill (Figure 4.4). The cobble gravel returns and is inconsistently exposed or obscured by mass movement processes until Limekiln Gill. Logs *ii* to *v* (Figure 4.4 and Figure 4.6) record detail of the stratigraphy at this site. Castle Eden Dene (Figure 4.5) is a large, wide palaeovalley, containing a modern (misfit) stream. The tabular cobble gravel fades out after this site. The exposures are poor and are badly slumped until Bluehouse Gill (Figure 4.5). South of here, the bedrock again rises. Two diamictons are well exposed above the bedrock, but the cobble gravel is absent.

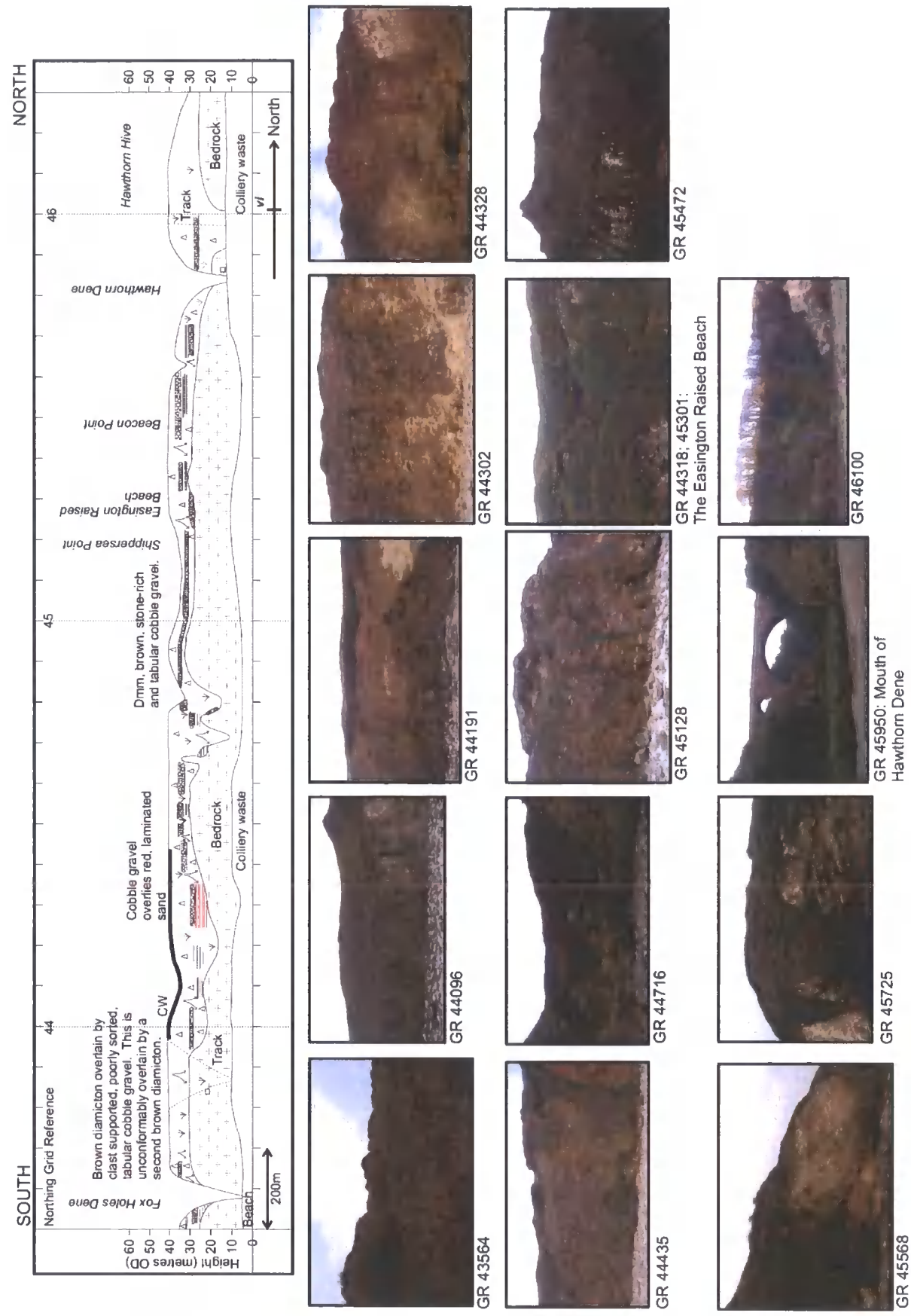

Figure 4.3: Facies Architecture: Hawthorn Hive to Foxholes Dene. Refer to Appendix III for larger photographs.

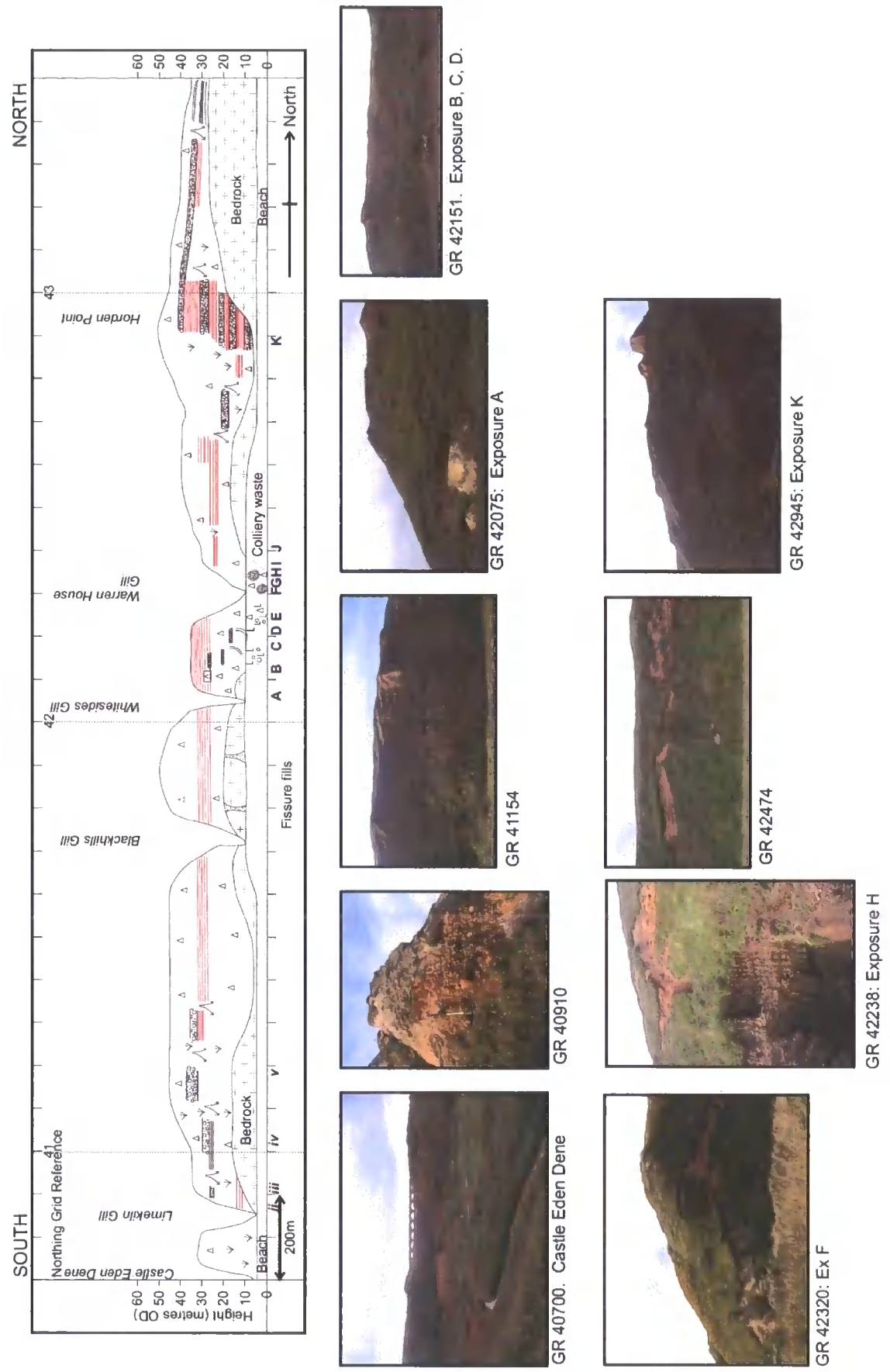

Figure 4.4: Facies Architecture: Foxholes Dene to Castle Eden Dene. Refer to Appendix III for larger photographs.

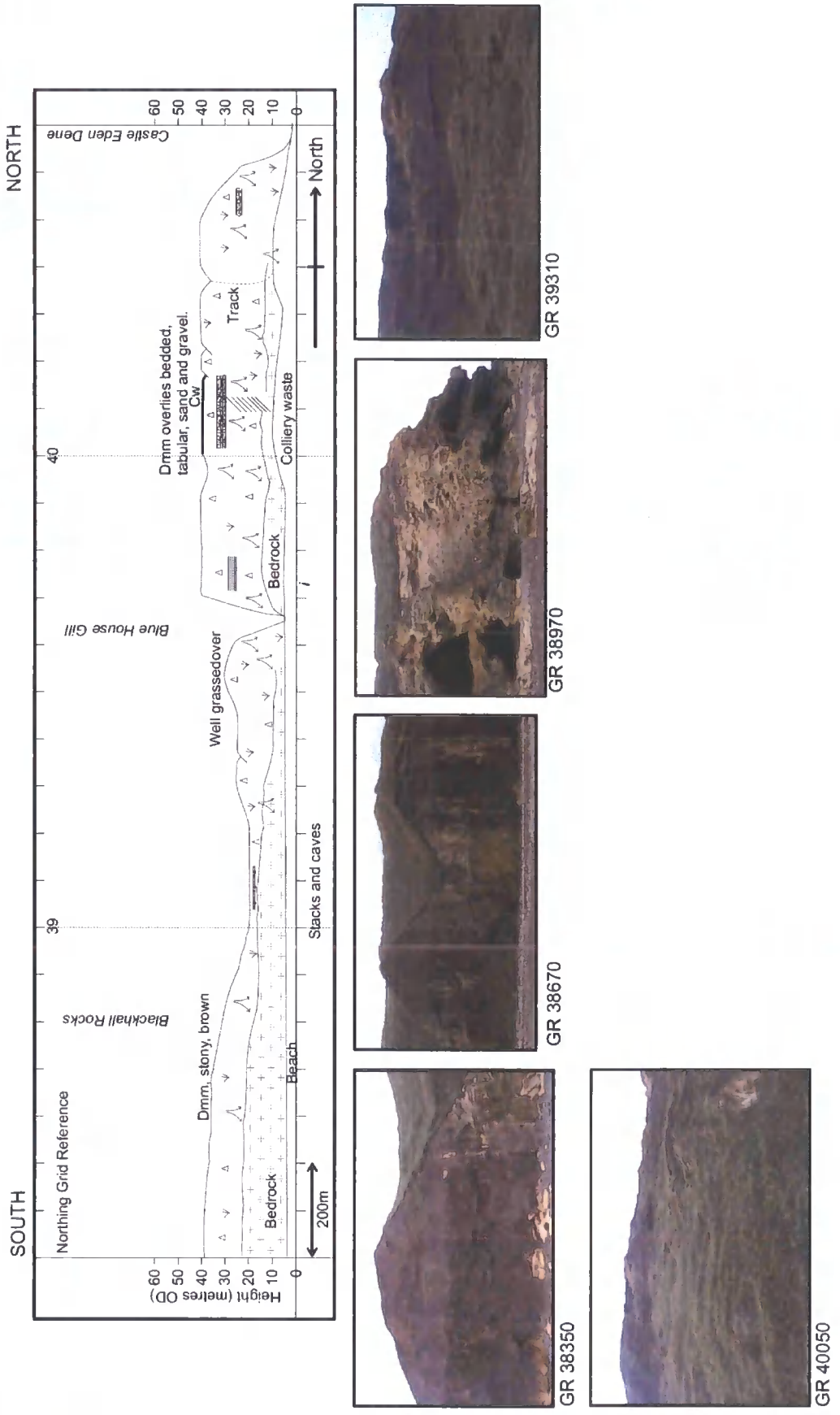

Figure 4.5: Castle Eden Dene to Blackhall Rocks. Refer to Appendix III for larger photographs

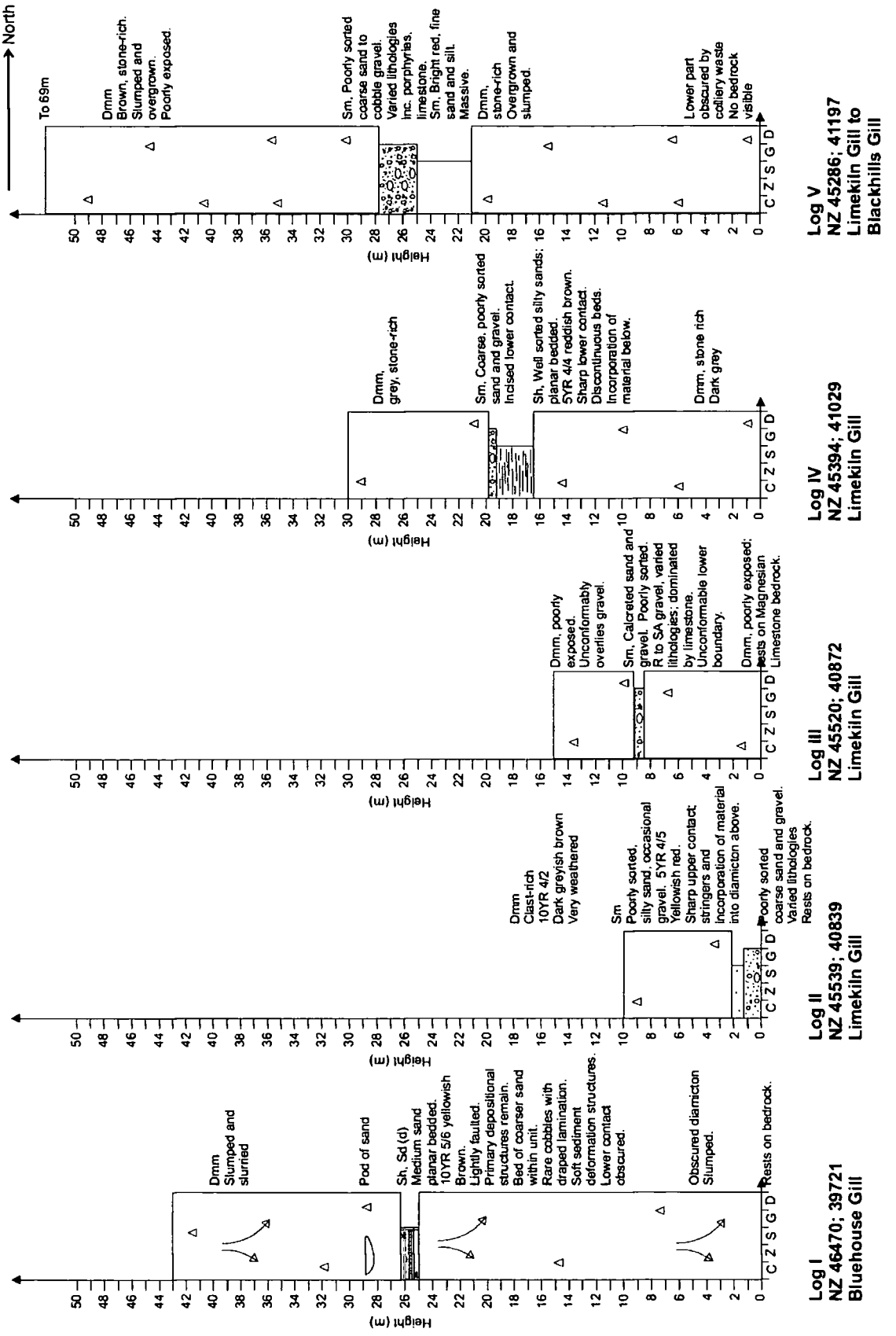

Figure 4.6: Vertical profiles, Hawthorn Hive to Blackhall Rocks.

From the analysis of the facies architecture, two diamictons can be seen to outcrop almost continuously along the section. They are separated by a sand or gravel deposit. At Warren House Gill, the facies architecture is more complex, with the existence of two sediments that do not occur elsewhere. Along the high limestone cliff tops, a basal diamicton is consistently overlain by a variable sand or gravel deposit with several facies. Firstly, it comprises well-sorted red-coloured sands, which exist only in the vicinity of Warren House Gill. North of Warren House Gill, there are bedded clast and cobble gravels, also red coloured, and the sorted sands and gravels which outcrop from Hawthorn Hive southwards. The uppermost deposit in the whole sequence outcrops continuously from Hawthorn Hive to Blackhall Rocks. It is a dark brown, clast-rich diamicton.

Previous researchers have identified two tills with intervening sands and gravels outcropping along the cliff tops in this area (Smith & Francis, 1967; Lunn, 1995; Bridgland & Austin, 1999). They have identified these as the Blackhall and Horden members (Thomas, 1999), with type sites at Blackhall Rocks and at Horden respectively, with the intervening Peterlee Sands and Gravels.

4.4 Hawthorn Hive

4.4.1 Sedimentology

The upland plateau of County Durham is characterised by large Permian stromatolite domes on reef dolomite. The bedrock is a multiphase de-dolomised collapse-breccia of Cycle 2 (Roker Dolomite) oolite (Smith, 1995b). On the south side of Hawthorn Dene, there is an abandoned meander loop with sinkholes. The modern stream has incised a new valley down to sea level (Hawthorn Dene) to the south of the palaeo-valley. Within the buried palaeo-valley at Hawthorn Hive (Grid Reference NZ 44081; 46130), the lower part of the buried valley is covered with colliery waste, slumping and vegetation. However, a small section is visible part way up, where two diamictons with intervening sands and gravels are visible. This was logged in detail (Figure 4.7) and sampled for lithological and geochemical analysis (indicated on Figure 4.7).

The lower diamicton (LFA 1) has a low-strength clast macro-fabric, showing little clustering of clasts along the a-axis. Gravel clasts are mostly angular to sub-angular, and are chiefly composed of limestone. Within the diamicton are tectonised, highly deformed sand lenses. Unconformably overlying the diamicton is a deposit of poorly-sorted, chaotic, angular boulders and gravels, containing numerous balls of diamicton (LF 2a; Figure 4.7). The gravel is clast-supported, incohesive, structureless, and includes various lithologies such as limestone, sandstone, greywacke, and coal. The gravel grades upwards into a well-sorted gravel (LF 2b; Figure 4.8), unconformably overlain by a second, upper diamicton (LFA 3). Twenty metres to the south of this exposure, these cobble gravels (LF 2b) are exposed as a well-sorted, bedded deposit containing rounded clasts. The sediment is strongly calcreted, and eroded to form a cave. The upper diamicton (LFA 3) is again well exposed and both it and LF 2b were sampled at this site.

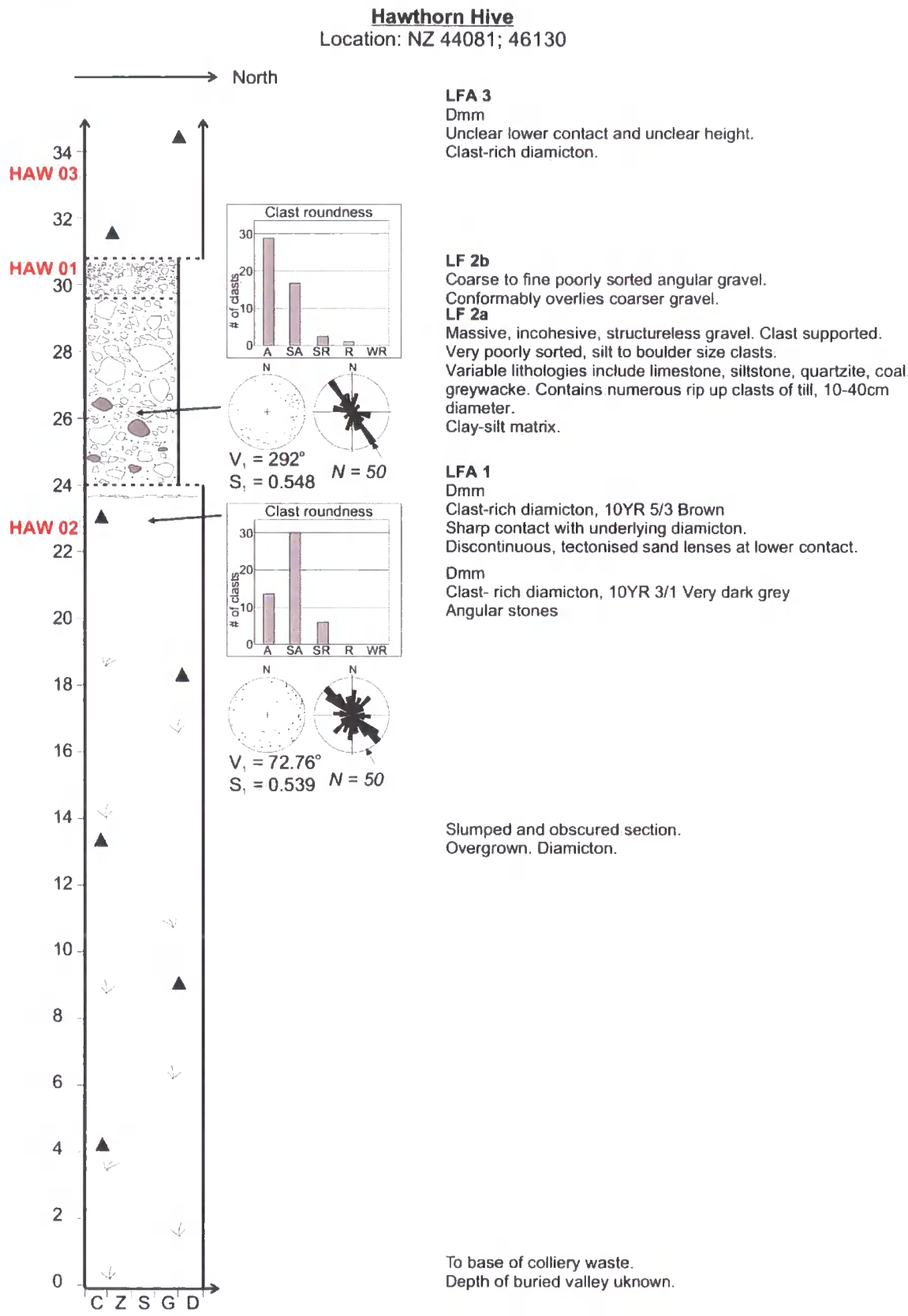

Figure 4.7: Section log, Hawthorn Hive. Lower clast fabric (LFA 1): $S_1 = 0.539$; $S_2 = 0.369$; $S_3 = 0.093$. Upper clast fabric (of LF 2a, gravels): $S_1 = 0.548$; $S_2 = 0.106$; $S_3 = 0.034$.

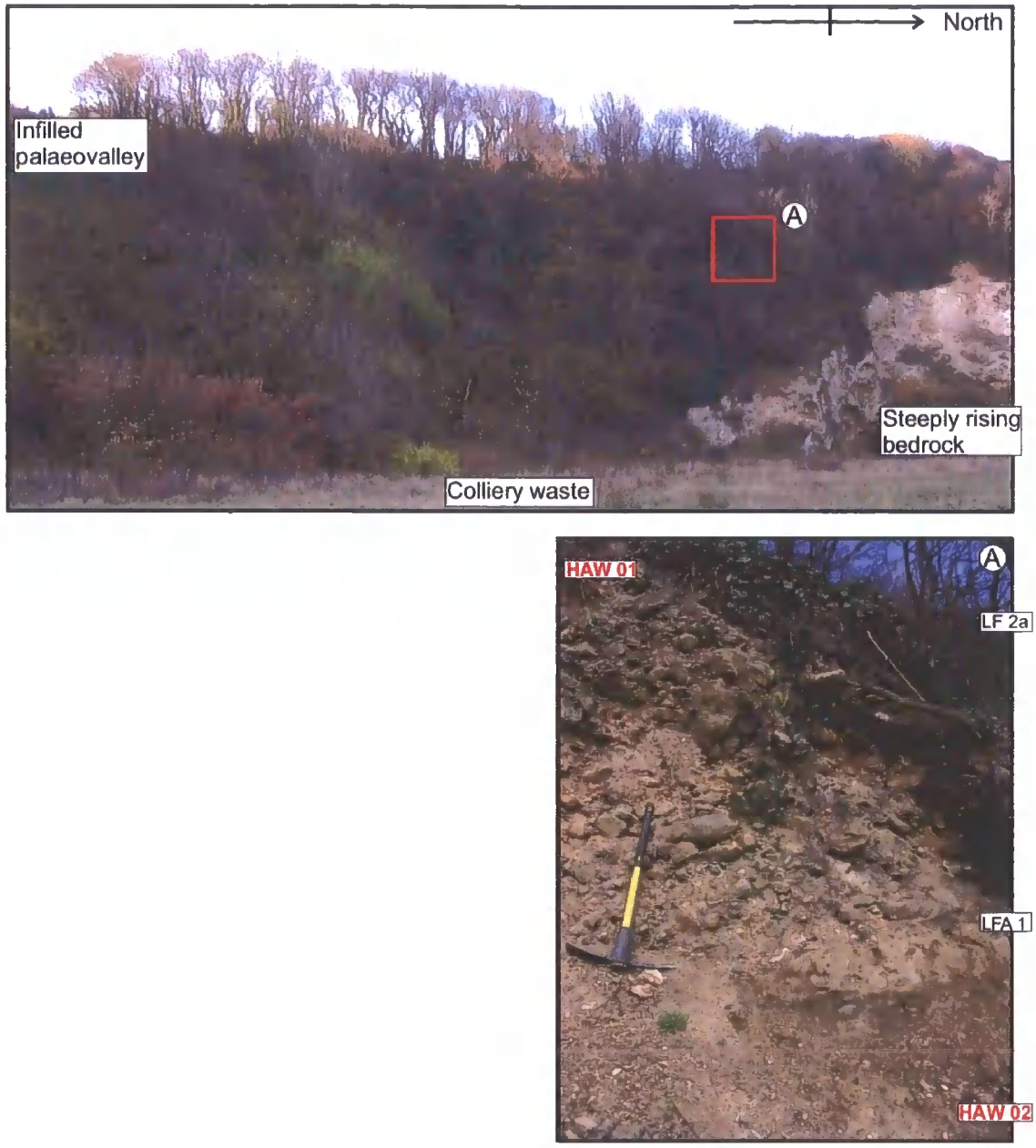

Figure 4.8: Photograph and detail of Hawthorn Hive.

4.4.2 Geochemical and Lithological Analysis

For detailed raw data, refer to Appendix IV. LF 2a (HAW 01) is the poorly-sorted coarse sand and gravel overlying LFA 1 at Hawthorn Hive (Figure 4.7). It is highly variable and changes from clast- to matrix-supported. The sands are yellowish-brown (10YR 5/4) in colour and very coarse. The clasts are sub-angular to sub-rounded in shape. Sample HAW 02 is the lower matrix-supported, laminated diamicton (LFA 1), directly and unconformably underlying the poorly-sorted gravels. It exhibits a vigorous reaction to HCl,

and has a silty clay matrix. Sample HAW 03 is the gravel-rich, weathered, upper diamicton, overlying the coarse sand and gravel (LFA 3). It is a dark brown colour (10YR 3/3). The diamicton has a very mild reaction to HCl. The gravel is strongly faceted, and mostly sub-angular in shape. The diamicton appears to be weathered.

Table 4.1 shows that both LFA 1 and LFA 3 have a large proportion of silt, though LFA 3 is a finer-grained diamicton with a larger proportion of clay. LFA 1 is coarser-grained, with significantly higher percentages of gravel than the upper diamicton. LF 2b in this location is dominated by the gravel and coarse sand fraction, with very little fines.

Table 4.1: Particle size distribution, Hawthorn Hive. For detailed raw counts, refer to Appendix IV.

Particle Size	HAW 02 Lower diamicton LFA 1	HAW 01 Gravels LF 2b	HAW 03 Upper diamicton LFA 3
% Clay	9.30	0.69	18.97
% Silt	37.91	3.23	40.04
% Fine sand	14.77	4.09	19.84
% Coarse sand	16.14	36.79	13.82
% Fine gravel	7.89	24.91	6.40
% Coarse gravel	13.99	30.29	1.94

Clast-lithological analysis of LFA 3 reveals a strikingly different suite of lithologies compared to the two lithofacies below (Table 4.2). Magnesian Limestone is present in only small amounts, with only 27.6 % of the counts. LFA 3 is enriched in greywacke (11.3 %), Carboniferous Limestone (13.1 %), sandstone (13.9 %), quartzitic sandstone (8 %), and small numbers of igneous and metamorphic erratics such as rhyolite (1.2 %), andesite (1.5 %), schist (0.9 %), granite (0.9 %), and gabbro (0.3 %). This contrasts with LFA 1 (the lower diamicton) and LF 2b (the sands and gravels), which are dominated by Magnesian Limestone (76.9 % to 70.1 %), with small amounts of Carboniferous material, and few far-travelled erratics.

LF 2b (HAW 01) is dominated by a significant percentage of locally derived dolomite and calcite (51.42 %). All three samples are enriched in garnet, andalusite and kyanite, while LFA 1 (HAW 02) and LFA 3 (HAW 03) have small amounts of staurolite and chloritoid (Table 4.3). LFAs 1 and 3 are also enriched in pyroxenes, tourmaline, epidote, and lawsonite in comparison to LF 2b.

Table 4.2: Average percentages of clast lithologies at Hawthorn Hive, 8-16, and 16-32 mm. For detailed raw counts, refer to Appendix IV.

	Lithology	HAW 02 LFA 1 Lower Diamicton	HAW 01 LF 2b Gravels	HAW 03 LFA 3 Upper Diamicton
	N	***425***	***551***	***337***
Igneous	*Diorite*	0.00	0.18	0.00
	Granite	0.71	0.00	0.89
	Gabbro	0.24	1.81	0.30
	Rhyolite	0.47	1.27	1.19
	Andesite	0.00	0.00	1.48
	Basalt	0.00	0.73	0.00
	Porphyry	0.00	0.18	0.00
	Felsite	0.24	0.00	0.00
Metamorphic	*Slate*	0.00	0.00	0.00
	Schist	0.00	0.00	0.89
Sandstone and sedimentary	*Sandstone*	9.42	2.36	13.94
	Quartzitic sandstone	2.12	0.00	8.01
	Siltstone	0.94	0.00	2.97
	Breccia	0.00	0.00	0.00
Cretaceous	*Chalk*	0.00	0.18	0.00
	Flint	0.00	0.00	0.00
Jurassic	*Ironstone*	0.24	0.54	0.59
	Mudstone	0.00	4.90	3.26
Triassic	*Red marl*	1.41	0.00	1.19
	Brown orthoquartzite	1.65	0.18	0.30
	Red orthoquartzite	0.00	0.00	0.59
	White orthoquartzite	0.00	0.54	0.00
	Brown vein quartz	0.00	0.00	0.00
	Red vein quartz	0.00	0.00	0.00
	White vein quartz	0.24	0.00	0.00
Permian	*Whin Sill Dolerite*	0.24	1.27	1.48
	Magnesian Limestone	70.12	76.86	27.60
	Yellow Sands	1.41	0.36	0.59
	New Red Sandstone	0.00	0.00	0.00
Carboniferous	*Carboniferous Limestone*	3.06	4.54	13.06
	Chert	0.00	0.00	0.00
	Coal	0.47	0.18	2.08
Devonian	*Old Red Sandstone*	0.00	0.18	2.67
	Shale	0.94	0.00	0.00
Ordovician and Silurian	*Arkose sandstone*	0.00	0.36	6.64
	Greywacke	6.12	4.36	11.28

Table 4.3: Average percentages of heavy mineralogies (percentage non-opaques) at Hawthorn Hive, size fractions 63-125 and 125-250 µm. For detailed raw counts, refer to Appendix IV.

	Heavy Mineral Phase	HAW 02 LFA 1 Lower Diamicton	HAW 01 LF 2b Gravels	HAW 03 LFA 3 Upper Diamicton
	n	***2633***	***1926***	***2640***
	% Opaques	76.58	67.98	81.43
	% Non-Opaques	23.42	32.02	18.57
	% Heavy Minerals	1.49	6.41	1.43
Silicate Group	*Olivine GP*	2.12	0.48	0.97
	Zircon	9.65	0.88	4.44
	Sphene	2.73	1.67	1.23
	Garnet GP	20.64	6.95	13.62
	Sillimanite	1.47	0.24	0.75
	Andalusite	3.49	7.12	4.46
	Kyanite	6.04	3.21	6.78
	Staurolite	0.23	0.00	0.90
	Chloritoid	0.31	0.00	0.19
Epidote Group	*Zoisite / Clinozoisite*	6.34	6.74	6.60
	Piemontite	0.00	0.71	0.00
	Epidote	3.33	0.48	6.78
	Lawsonite	0.31	0.00	0.51
	Axinite	0.07	0.00	0.04
	Pumpellyite	0.23	0.00	0.00
	Tourmaline GP	3.07	0.00	3.20
Pyroxene Group	*Enstatite*	0.66	0.00	1.06
	Hypersthene	0.84	0.00	0.08
	Diopsidic Clinopyroxene	1.67	0.24	1.99
	Augitic Clinopyroxene	1.41	1.67	1.69
Amphibole Group	*Tremolite*	0.00	0.00	0.03
	Ferriactinolite	0.69	0.00	0.00
	Hornblende	0.35	0.00	0.27
	Diallage	0.04	0.00	0.00
	Glaucophane	0.02	0.00	0.00
Mica Group	*Muscovite*	6.01	7.87	7.19
	Glauconite	0.08	0.00	0.07
	Biotite	6.60	8.55	9.83
	Chlorite GP	2.25	0.88	3.27
Oxides	*Rutile*	3.27	0.24	1.77
	Brookite	4.21	1.19	2.81
	Spinel GP	0.21	0.00	0.08
	Anatase	0.09	0.00	0.27
Carbonates	*Dolomite / Calcite*	9.71	51.42	17.23
Sulphates	*Baryte*	0.00	0.00	0.17
Sulphides	*Sphalerite*	0.02	0.00	0.00
Phosphates	*Apatite*	3.22	0.48	2.41
	Monazite	0.65	0.00	0.32

The metals analysis at Hawthorn Hive (Table 4.4) indicates that while all samples are enriched in the common elements, there is considerable variation in the low abundance metals. For example, LFA 3 is impoverished in zinc, but enriched in nickel, chromium and lithium. LFA 1 is impoverished in sodium and aluminium, but enriched in magnesium, lead and rubidium. LF 2b is enriched in sodium, aluminium, calcium, manganese, zinc, cadmium, and strontium (Table 4.4).

Table 4.4: Metals analysis of Hawthorn Hive.

	High Abundance Elements (mg / kg)						
SAMPLE	**Na_{23}**	**Mg_{24}**	**Al_{27}**	**K_{39}**	**Ca_{44}**	**Ti_{48}**	**Fe_{57}**
LFA 1 (HAW 02) Lower Diamicton	2456	4938	7568	13244	29500	2827	22940
LF 2b (HAW 01) Gravels	16300	2020	138000	12400	117000	1540	24100
LFA 3 (HAW 03) Upper Diamicton	2807	1687	24945	13325	13924	3962	32803

4.4.3 Summary of Hawthorn Hive

In summary, Hawthorn Hive is a bay in which a buried palaeovalley is exposed in cross-section. A modern stream (Hawthorn Dene) has made a re-incision down to sea level to the south of the buried palaeovalley. The buried palaeovalley is infilled with tens of metres of Quaternary sediments. Two diamictons are exposed in superposition, with intervening coarse, unsorted, chaotic gravels grading to sorted, rounded, bedded gravels (LF 2b). The lower diamicton (LFA 1) exhibits deformed sandy inclusions. It is difficult to access the upper diamicton (LFA 3), which is extensively weathered, but it appears to be massive. Both diamictons and gravel contain large amounts of locally derived Permian and Carboniferous clasts, with some further-travelled igneous and metamorphic erratics.

4.4.4 Process Interpretation

LFA 1: The Lower Diamicton

LFA 1 at Hawthorn Hive infills a palaeovalley of unknown depth. This diamicton is interpreted as a subglacial till, based on the following criteria: its over-consolidated, diamict texture, the presence of exotic erratics and deformed sandy inclusions, the bullet-shaped and striated clasts. These characteristics indicate a combination of deformation and lodgement (cf. Sharp, 1984; Nelson *et al.*, 2005; Hart, 2007). The clast macro-fabric

indicates ice flow from northwest to southeast. The deformed sandy lenses are interpreted as the product of local erosion and entrainment followed by progressive attenuation during shearing (cf. Hart & Roberts, 1994; Roberts & Hart, 2005; Hart, 2007). LFA 1 is laterally extensive along the coast of Durham, although it pinches out against the flanks of the Easington Raised Beach.

LF 2b: The Middle Gravel

The sedimentary characteristics of the overlying boulder-cobble-gravel satisfy the criteria for a debris flow (Eyles, 1987; Maizels, 1995); these include the lack of sorting, the presence of a wide range of clast sizes and forms, the dispersed clast macro-fabric, and the poorly-sorted, structureless, clast-supported sedimentation. The lack of fines indicates winnowing by water. The presence of till balls and non-durable lithologies such as coal indicates that this must be an ice-proximal setting; downstream transportation would rapidly eradicate these soft lithologies. Therefore, the bouldery debris overlying the subglacial till below is probably an ice-contact debris flow (as defined by Eyles & Miall, 1984).

The sorting increases higher up the section and the grain size decreases; non-durable lithologies disappear and the rounding of clasts increases. This is consistent with further sorting and rounding by flowing water, and indicates increased downstream transportation and distance from the glacier terminus. This gravel is very extensive south of Hawthorn Hive and forms a laterally extensive tabular deposit. In places, it grades into bedded sands and either coarser or finer gravels. The high carbonate content of the Magnesian Limestone has contributed to the calcretion of the gravels in several places. The laterally extensive nature of these gravels suggests that this is glaciofluvial deposit (Maizels, 1995). This type of system is more common distally, as immediate proglacial outwash tends to be characterised by deep, single-thread, high energy, erosive courses high in transport capacity. Proglacial outwash fans are characterised by the lack of fines and unstable channel networks. Bank erodibility is enhanced by the non-cohesive sediments with little silt and clay. Fines are removed in suspension, leaving only medium to coarse-grained materials to form bank materials (Maizels, 1995). The heterogeneity reflects variations in the erosive power of the water that deposited the cobble gravel.

A proglacial outwash sandur interpretation effectively explains the tabular sands and gravels outcropping south of Hawthorn Hive. The variability in the sands and gravels,

resulting from channel migration and bar formation, is explained by this subaerial glaciofluvial mechanism. The coarse particle-size distribution suggests a proximal environment, as meltwater streams rapidly lose competence and discharge quickly lessens (Maizels, 1995), leading to a progressively finer bedload. Clast-supported, heterogeneous, sub-rounded gravels with a wide variety of textures are typical of glacial outwash deposits. Sheet floods are common in the areas in front of ice sheets, which are usually of low relief. The low relative relief of the Durham plateau and the tabular nature of the gravels suggests that this lithofacies was deposited by sheet flow as part of a proglacial outwash fan (cf. Rust & Koster, 1984; Maizels, 1995).

Lithologically, LF 2b shows an affinity with LFA 1 and is distinct from the overlying LFA 3; the high percentage of Magnesian Limestone and low percentage of Carboniferous Limestone and sandstone suggests that it is derived from LFA 1. It is therefore likely to be genetically associated with the lower traction till and the earlier ice sheet to cover the region.

LFA 3: The Upper Diamicton

The diamicton overlying the gravel is difficult to access and has been strongly affected by slope processes. It was difficult to obtain an accurate clast macro-fabric. However, the diamicton also bears the hallmarks of a subglacial till (Evans *et al.*, 2006); these include the lateral extent, the over-consolidated matrix, and the presence of bullet-shaped, far-travelled, striated erratics. LFA 3 is laterally extensive and extends as an unbroken till sheet from Hawthorn Hive to Blackhall Rocks. It shows strong similarity to the diamicton overlying the raised beach in Shippersea Bay (see Chapters 5 and 6).

4.4.5 Provenance Interpretation

LFA 1: The Lower Till

LFA 1 at Hawthorn Hive (sample HAW 02) has a limited suite of clast lithologies. Firstly, there is a significant locally-derived and Pennine component, comprising significant quantities of Magnesian Limestone (70 %), Carboniferous Limestone (3.1 %), sandstone (9.4 %) and other Carboniferous and Permian lithologies (such as yellow sandstone, coal, shale, and Whin Sill Dolerite). The igneous erratics were too indistinct to determine their provenance but could be derived from the Grampian Highlands or elsewhere. There is a minor amount of Triassic red marl (1.4 %), sourced from fissures in

the limestone or immediately offshore. The heavy-mineral suite contains more far-travelled species, indicative of a high-rank metamorphic source terrane. These include the garnet-andalusite-kyanite assemblage, diagnostic of Buchan-type metamorphism (Trewin, 2002). Garnet, staurolite and chloritoid are indicative of Stonehavian-type metamorphism, from near the Highland Boundary fault (Stephenson & Gould, 1995). The ferromagnesian minerals (olivine and pyroxenes) are typical of the Carboniferous volcanic rocks such as the basalts of the Midland Valley of Scotland, southwards. The Whin Sill Dolerite is also a probable source for the pyroxenes, but it cannot explain the olivine component.

LFA 3: The Upper Till

LFA 3 at Hawthorn Hive (HAW 03) has a diverse range of clast lithologies. These include a significant amount of Carboniferous Limestone (13.1 %) but a relatively low percentage of Magnesian Limestone (27.6 %). There are a greater proportion of other Carboniferous lithologies, such as coal (2.1 %). Granites and other igneous erratics occur in greater numbers than in HAW 02. The presence of schist (0.9 %) indicates an input from the Dalradian of northern Scotland (cf. Johnson, 1991). The acid porphyries and basalts could be derived from the Midland Valley of Scotland southwards (cf. Trewin, 2002). Old Red Sandstone is a typical lithology of the Midland Valley of Scotland, and greywacke is associated with the Southern Uplands. This sediment therefore is more northerly derived, and was less influenced by local lithologies. The low percentage of Magnesian Limestone indicates that the till was isolated from the bedrock by a mantle of pre-existing sediments, and many of the lithologies within it are derived from erosion of this lower sediment. This explanation has previously been invoked by Beaumont (1967).

This is also supported by the high-rank metamorphic heavy mineral assemblage. The high numbers of kyanite, andalusite and garnet are indicative of Buchan-type metamorphism, located near Aberdeen (Trewin, 2002). There are low numbers of ferromagnesian minerals, which are probably sourced from the Carboniferous volcanic rocks and high-level intrusions of northern Britain. These porphyritic basaltic rocks are widely exposed in the Midland Valley of Scotland, and locally within the Southern Uplands (Cameron & Stephenson, 1985).

The lithologies and heavy minerals of the upper and lower tills at Hawthorn Hive are very similar, suggesting a similar provenance for each. The majority of the differences can be explained by the upper till being isolated from the bedrock, and deriving many of its

lithological components from erosion of LFA 1. The clast macro-fabrics and striae noted by Beaumont (1967) (Figure 1.5), the distribution of the upper till (LFA 3) as mapped by the BGS (Figure 1.6) and drumlins (Livingstone *et al.*, in prep) and outwash deposits in the Tyne Gap (Yorke *et al.*, 2007) indicates the presence of two separate ice lobes, which may have been sourced in the same region of the Scottish Highlands.

4.5 Conclusions

Facies architecture from Hawthorn Hive to Blackhall Rocks and section logging at Hawthorn Hive clearly identifies five lithofacies associations. Two are present only at Warren House Gill, but LFAs 1, 2b and 3 clearly extend southwards from Hawthorn Hive to Blackhall Rocks. A thick sequence of sediments infills a buried palaeovalley at Hawthorn Hive. LFA 1 is interpreted at Hawthorn Hive as a subglacial till, exhibiting predominantly local and Pennine erratics. LFA 2 exhibits many facies. The facies present at Hawthorn Hive is interpreted as a debris flow, overlain by proximal glaciofluvial outwash. The upper till, LFA 3, exists as a uniform, unbroken till sheet. It exhibits local and Pennine lithologies, but in substantially fewer quantities than LFA 1. LFA 3 contains higher numbers of northerly and Scottish erratics.

Previous researchers have interpreted these sediments as subglacial tills and glaciofluvial outwash sands and gravels, with LFA 1 being the Blackhall Member, LFA 2 the Peterlee Sands and Gravels, and LFA 3 the Horden Member (Francis, 1972; Lunn, 1995; Thomas, 1999). This work therefore supports previous interpretations, but adds valuable detail and provenance information, indicating a Pennine transport pathway for LFA 1 (the Blackhall Member).

CHAPTER 5

The Easington Raised Beach

5.1 Introduction

A version of this chapter is in press in the *Proceedings of the Geologists' Association* (see Appendix II). The Easington Raised Beach (NZ 44318, 45301) is exposed in the cliffs above Shippersea Bay, on the coast of County Durham (Figure 4.1), 20 km north of the Tees estuary. It is the most northerly known Middle Pleistocene interglacial deposit in England, and, as such, is a geological SSSI (Site of Special Scientific Interest). The beach lies on the eastern flank of Beacon Hill, a resistant reef dolomite knoll rising to 85.7 m O.D., which might account for its survival of at least one glaciation (Bridgland & Austin, 1999). It was first described and interpreted by Woolacott (1900) and then by Trechmann (1931a), who both recognised it as an interglacial beach. Set into the Magnesian Limestone bedrock (Figures 5.1 and 5.2), it is approximately 2.5 m thick, and extends laterally for about 15 m (Trechmann, 1952). Bowen *et al.* (1991) confirmed the deposit as an interglacial beach, describing it as a calcreted shelly gravel with an abundant temperate molluscan fauna of littoral character, resting on a rock platform *c.* 33 m above O.D. (Figure 5.1). Descriptions of the beach have reported eight stratified beds with common 'bored' clasts, marine molluscs, the brachiopod *Rhynconella psitticea* and an assemblage of shallow water foraminifera (Bowen *et al.*, 1991; Bridgland, 1999). It has been noted that local Magnesian Limestone clasts are progressively diluted upwards through the deposits (Bridgland & Austin, 1999). Reported exotic components include Scandinavian rocks, possibly derived from the Warren House Formation that crops out 3 km to the south, and Cheviot granite, Borrowdale Volcanics, and Whin Sill Dolerite (Trechmann, 1931a). More angular gravels containing coal that immediately overlie the beach are of glacial origin, and relate to gravel that crops out in Hawthorn Hive, 800 m to the north of Shippersea Bay (Figure 4.1). Conventional amino acid chronology suggested a correlation of the beach deposits with MIS 7, although it was also recognised that there were apparently reworked specimens showing greater shell mineral diagenesis, perhaps from MIS 9 (Bowen *et al.*, 1991). The Easington Raised Beach is overlain by the Horden Member, and the Blackhall Member pinches out against its flanks (Bridgland & Austin, 1999; Figure 5.1).

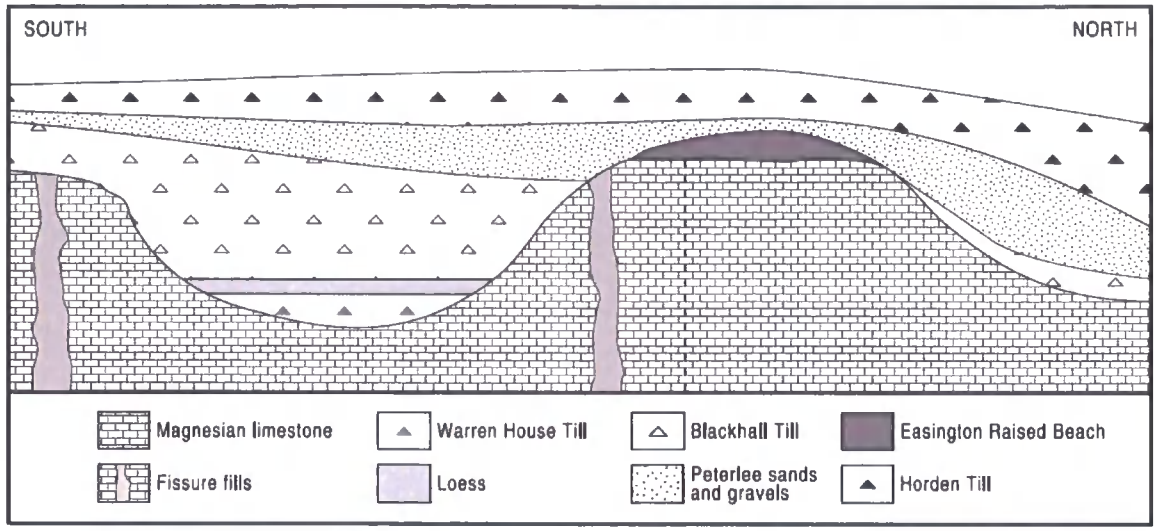

Figure 5.1: Simplified stratigraphy of coastal glacigenic sediments in County Durham. Modified from Bridgland and Austin (1999).

The age and stratigraphical relations of the Easington Raised Beach are of considerable interest in understanding the history of glaciation in coastal north east England, where particular significance is placed upon the recognition of a till of Scandinavian origin, the Warren House Formation (Thomas, 1999), at Warren House Gill, Horden (Figure 4.1, Trechmann, 1952; Lunn, 1995). The occurrence of Scandinavian lithologies in the raised beach (cited above) has led to the suggestion that it post-dates the Warren House Formation (Trechmann, 1952; Lunn, 1995; Teasdale & Hughes, 1999), although this view originated at a time when the Pleistocene record was viewed in the context of relatively few glaciations. The Easington Raised Beach was one of the first British deposits to be attributed to an interglacial (Trechmann, 1931a). The raised beach is also important for understanding regional long-term uplift and sea level change during the Quaternary.

Recent reinterpretation of the stratigraphy and provenance of the North Sea Drift in Norfolk raises questions regarding the timing and dynamic interaction between the British-Irish Ice Sheet (BIIS) and the Fennoscandian Ice Sheet (FIS) at different times during the Quaternary (Lee *et al.*, 2002; Lee *et al.*, 2004; Hamblin *et al.*, 2005). Under the recently proposed model (Hamblin *et al.*, 2005), the FIS reached the British coastline only during MIS 6. This model details a multiple BIIS event stratigraphy stretching back to MIS 16, but is yet to be validated elsewhere in the UK. One of the major obstacles to validation is the occurrence of the 'Warren House Formation' in County Durham (Trechmann, 1931b;

Thomas, 1999), as this would appear to predate the MIS 7 raised beach (Bowen *et al.*, 1991; Lunn, 1995), implying that it is older than the MIS 6 Scandinavian glaciation of Norfolk and eastern Yorkshire, and suggesting multiple incursions of Scandinavian ice to the British coastline.

The aim of this research has been to develop a chronostratigraphic and lithostratigraphic framework within which to test the stratigraphical relationship of the Easington Raised Beach and the Warren House Formation. Furthermore, developing a reliable chronostratigraphy for these sediments will also allow long-term uplift in northern England during the Quaternary to be better quantified.

5.2 Sedimentology and Stratigraphy

Three lithofacies associations are recognised overlying the bedrock in Shippersea Bay (Figure 5.2). Directly overlying the bedrock is LFA 1, comprising well-sorted, bedded to massive sands and gravels with a fossil shell gastropod fauna. It is unconformably overlain by massive, incohesive and structureless, coarse and poorly sorted sands and gravels (LF 2a) and well-sorted, cross-bedded sands (LF 2b). This lithofacies is overlain by a dark brown diamicton (LFA 3).

Two exposures (Sections A and B) are accessible from the cliff-top coastal path (Figure 5.2). In Section B, LFA 1 lies directly on bedrock, and consists of well-bedded, well-sorted sands and gravels (LF 1a and LF 1b; Figure 5.4). They are overlain by a poorly-sorted, massive, sandy gravel (LF 2a) and then by a well-sorted sand, with foresets picked out by fine grains of coal (LF 2b). The sand is overlain by a dark brown, clast-rich diamicton (Figure 5.3; LFA 3; the Horden Till), but the contact is obscured. A lower, brown diamicton (the Blackhall Till) pinches out against the flanks of the raised beach (Bridgland & Austin, 1999).

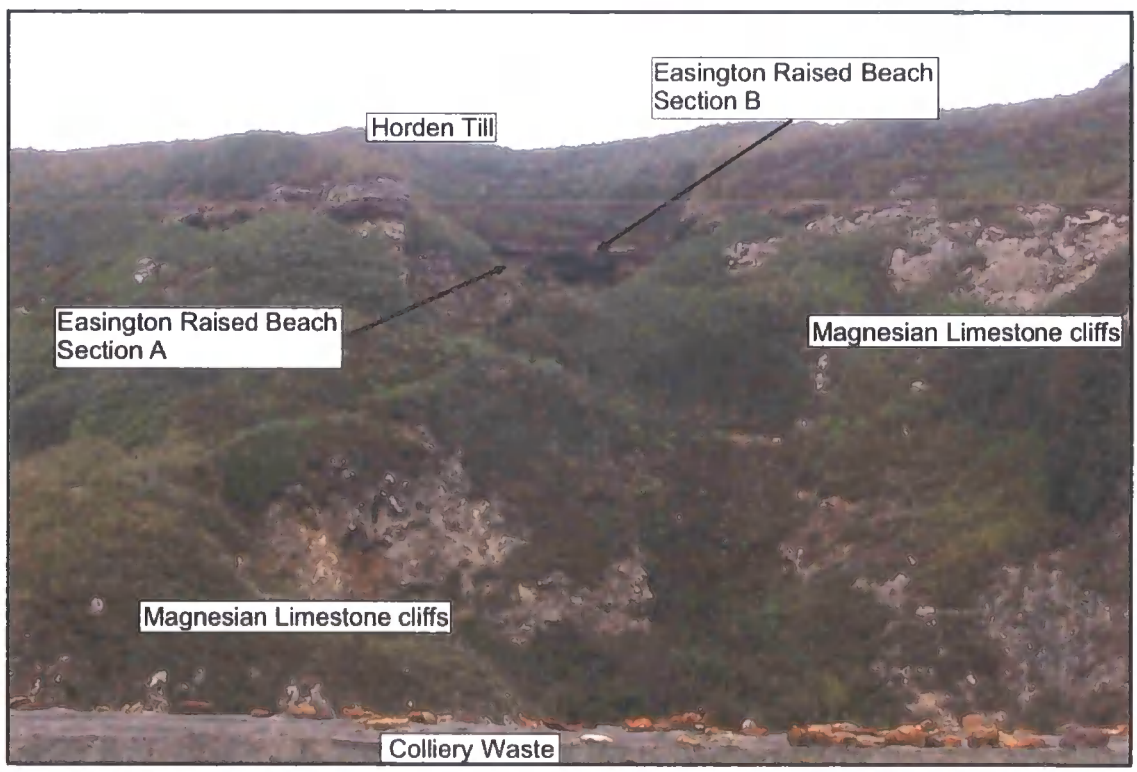

Figure 5.2: Photograph of the Easington Raised Beach, Shippersea Bay, Grid Reference: NZ 44318; 45301.

LF 1a at Section B (Figure 5.3 and Figure 5.4) consists of five planar beds with graded, conformable contacts of massive sand and rounded gravel. These beds are neither cemented nor consolidated but are very well-sorted, with strong imbrication of clasts (Figure 5.3), and are very pale brown in colour (10YR 7/4). These well-sorted, well-rounded, clast-supported gravels (LF 1a, Bed 3) are predominantly composed of Magnesian Limestone. There are uncommon clasts of Carboniferous Limestone, greywacke, orthoquartzite, vein quartz, flint, and sparse igneous rocks such as granite, porphyries, and rhyolite. Softer lithologies (typically limestones) frequently display borings by annelid worms and molluscs. There are frequent gastropod shells within LF 1a, Section A. LF 1a, Bed 4, is a very coarse cobble-gravel with stones imbricated seawards, presumed to result from swash. LF 1b (Section B; Figure 5.4B) consists of cemented, well-rounded, alternating well-sorted sand and gravel beds. The cemented sands that show ripple lamination (Bed 2) were sampled for OSL and U-series dating (see Table 1). The beds contain a similar suite of gravel clast lithologies.

LF 2a (Section B, Figure 5.4) is significantly different in character from the underlying LFA 1. It is a chaotic, coarse, gravelly, poorly-sorted sand with abundant angular to sub-angular clasts including coal, which is completely absent from LFA 1 at this section. Stratigraphically above this structureless facies is a current-bedded, well-sorted fine sand (LF 2b), with foresets picked out with coal grains, but the contact was not exposed. A small trial pit from the path above the raised beach proved that this body of sand is overlain by LFA 3 (Figure 5.3), a weathered, dark yellowish-brown diamicton (10YR 3/6), massive in appearance and with numerous angular to sub-angular clasts of predominantly local lithologies such as Permian and Carboniferous sandstones and limestones.

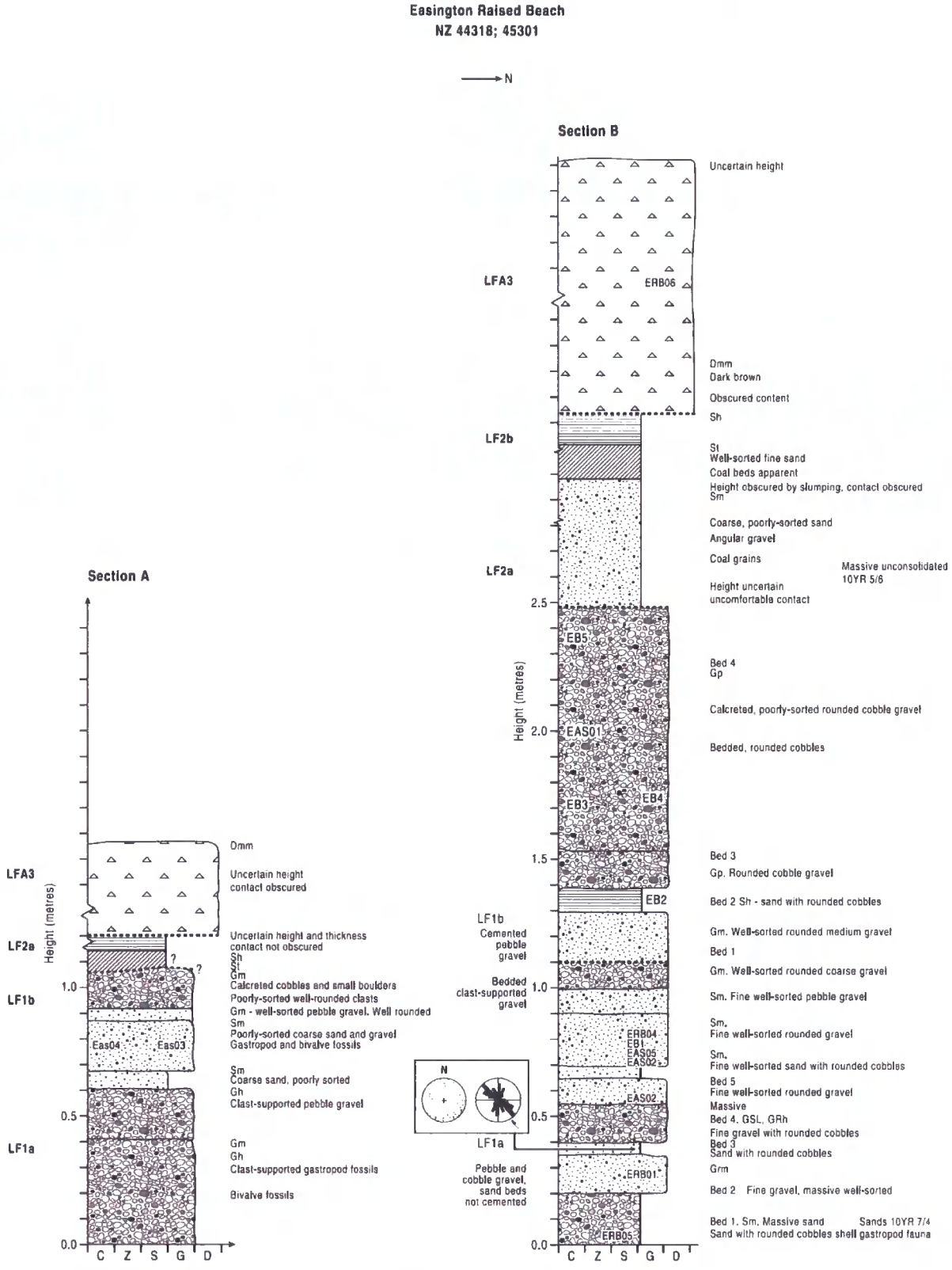

Figure 5.3: Sedimentary logs of Sections A and B, showing LFAs 1 to 3, Shippersea Bay

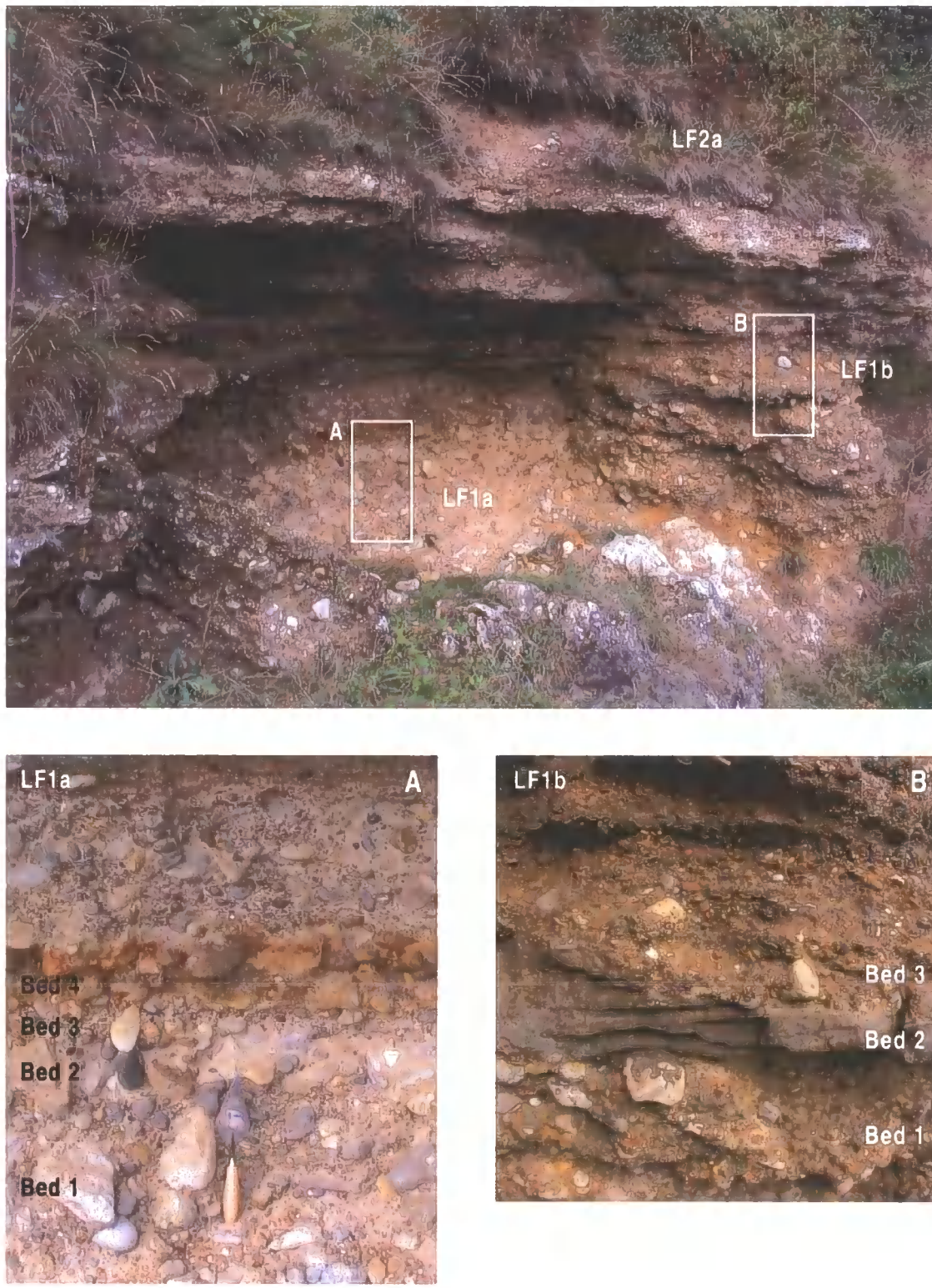

Figure 5.4: Photographs of the Easington Raised Beach, Section B.

Inset Photograph A: Detailed photograph of LF 1a, loose sand and gravel, not calcreted. Bed 1: rounded shingle gravel. Bed 2: Well-sorted sand with rounded cobble gravel. Bed 3: well-sorted fine, rounded gravel. Bed 4: iron-stained cobble gravel.

Inset Photograph B: Detailed photograph of LF 1b. Bed 1: Stratified, calcreted, clast-supported gravel with rare porphyries. Bed 2: Laterally short and disjointed, calcreted, thinly ripple-cross bedded fine sand with rare fine gravel. Bed 3: Poorly-sorted gravelly sand with rare porphyries.

5.3 Geochemical, Lithological, Biological and Chronostratigraphical Analysis

5.3.1 Lithological and Geochemical Data

Multiple bulk samples were taken from the raised beach (Table 5.1). In LFA 1, there is a strongly bi-modal particle-size distribution, with a combination of very well-sorted sand beds and gravels comprising a less well-sorted range of particle sizes from coarse sand to gravel. In general, LFA 3 above the beach has moderate percentages of all particle sizes (Table 5.2). For detailed particle size results, refer to Appendix IV.

The clast lithology of LFA 1 is profoundly different from that of the overlying diamicton (LFA 3, Table 5.3). First, LFA 1 is vastly richer in Magnesian Limestone (79 to 84 %), but greatly impoverished in sandstone (≤ 0.3 %) compared with LFA 3. Secondly, LFA 1 contains flint erratics (0.8 to 2.3 %), and more porphyries, quartz and orthoquartzite. LFA 3, in contrast, is enriched in Whin Sill Dolerite (4.3 %) and contains sparse igneous and metamorphic erratics, such as basalt (1.7 %), gabbro (1.3 %) and slate (0.2 %) (Table 5.3). Geochemical analysis also reveals LFA 1 to be consistently different in character to the overlying LFA 3 (Table 5.4). Compared to the former, LFA 3 is impoverished in sodium, magnesium, calcium, but significantly enriched in iron, titanium, lithium, boron, vanadium, cobalt, nickel, copper, and zirconium (Figure 5.5).

The contrast between LFA 1 and LFA 3 is highlighted further by the results of heavy mineral analysis (Table 5.5), which show that LFA 1, unlike LFA 3, have abundant epidote (10.3 %) and related minerals such as zoisite (4.6 %), as well as andalusite (4.1 %) and kyanite (6.2 %). The locally-derived mineral dolomite contributes a significant amount (15.1 %) to the heavy mineral suite of LFA 1.

Table 5.1: Sample locations, Easington Raised Beach

Location	Description	Sample	Analysis
Section B. LFA 3.	Diamicton	ERB 06	PSA, Heavy Minerals, Clast Lithology
Section B. LF 1a (Bed 3)	Well-sorted gravel (far right of section)	ERB 03	PSA, Heavy Minerals, Clast Lithology
Section B. LF 1a (Bed 1).	Well-sorted gravel (far left of section)	ERB 04	PSA, Heavy Minerals, Clast Lithology
Section B. LF 1a (Bed 2).	Well-sorted gravel	ERB 01	PSA, Heavy Minerals, Clast Lithology, Shell Identification
Section B. LF 1a (Bed 1).	Well-sorted sand	ERB 05	PSA, Heavy Minerals, Clast Lithology

Location	Description	Sample	Analysis
Section B. LF 1b (Bed 4)	Bedded, rounded cobbles, poorly-sorted	EAS 01	OSL
Section B. LF 1a (Bed 5)	Well-sorted fine sand	EAS 02	OSL
Section B. LF 1a (Bed 2)	Calcreted well-sorted bedded sand	EAS 05	OSL
Section A. LF 1a (Bed 6a)	Sand and gravel, poorly sorted	EAS 03	OSL
Section A. LF 1a (Bed 6a)	Sand and gravel, poorly sorted	EAS 04	OSL

Location	Description	Sample	Analysis
Section B. LF 1a (Bed 2).	Well-sorted gravel	EaERB01NI1bF	AAR
Section B. LF 1a (Bed 2).	Well-sorted gravel	EaERB01NI1bH*	AAR
Section B. LF 1a (Bed 2).	Well-sorted gravel	EaERB01NI2bF	AAR
Section B. LF 1a (Bed 2).	Well-sorted gravel	EaERB01NI2bH*	AAR
Section B. LF 1a (Bed 1).	Well-sorted gravel (far left of section)	EaERB04NI1bF	AAR
Section B. LF 1a (Bed 1).	Well-sorted gravel (far left of section)	EaERB04NI1bH*	AAR

Location	Description	Sample	Analysis
Section B. LF 1b (Bed 2)	Calcreted well-sorted bedded sand	EB 1	U-Series
Section B. LF 1b (Bed 3)	Cemented pebble-gravel	EB 2	U-Series
Section B. LF 1b (Bed 3)	Cemented pebble-gravel	EB 3	U-Series
Section B. LF 1b (Bed 4)	Bedded, rounded cobbles, poorly-sorted	EB 4	U-Series
Section B. LF 1b (Bed 4)	Bedded, rounded cobbles, poorly-sorted	EB 5	U-Series

Table 5.2: Average particle size distribution of the beach sands and gravels and the diamicton above.

Particle Size	LF 1a Beach sand	LF 1a Beach gravel	LFA 3
	ERB 05	*ERB 04*	*ERB 06*
% Clay	0.28	0.69	15.28
% Silt	1.10	3.23	32.79
% Fine sand	87.48	4.09	21.15
% Coarse sand	11.14	36.79	13.51
% Fine gravel	0.00	24.91	3.14
% Coarse gravel	0.00	30.29	14.13

Table 5.3: Average percentages of clast lithologies at Shippersea Bay, 8-16, and 16-32 mm. For detailed raw counts, refer to Appendix IV.

	Clast Type	*LFA 1*			*LFA 3*
		ERB 01	*ERB 04*	*ERB 03*	*ERB 06*
	n	*1077*	*987*	*679*	*464*
Igneous	*Diorite*	0.00	0.00	0.00	0.00
	Granite	0.84	1.62	0.44	0.65
	Gabbro	0.00	0.00	0.00	1.29
	Rhyolite	1.39	0.81	0.59	0.00
	Andesite	0.00	0.20	0.15	1.94
	Basalt	0.00	0.00	0.00	1.72
	Porphyry	4.09	5.27	5.60	0.00
Metamorphic	*Slate*	0.00	0.00	0.00	0.22
	Schist	0.00	0.00	0.00	0.00
Sandstone and Sedimentary	*Sandstone*	0.28	0.00	0.00	45.69
	Siltstone	0.00	0.00	0.00	4.31
	Breccia	0.00	0.00	0.00	2.16
Cretaceous	*Chalk*	0.00	0.00	0.00	0.00
	Brown Flint	0.00	2.33	1.47	0.00
	Black Flint	0.84	0.41	1.47	0.00
Jurassic	*Ironstone*	0.00	0.00	0.00	0.65
	Mudstone	0.00	0.00	0.00	3.02
Triassic	*Brown orthoquartzite*	0.28	0.51	0.00	0.00
	Red orthoquartzite	1.86	1.11	0.88	0.86
	White orthoquartzite	3.44	2.74	3.98	1.29
	Brown vein quartz	0.09	0.61	0.00	0.00
	Red vein quartz	0.09	0.00	0.29	0.00
	White vein quartz	5.66	4.15	2.50	0.00
	Red marl	0.46	0.00	0.00	0.00
Permian	*Magnesian Limestone*	79.39	79.43	83.95	20.69
	Yellow Sands	0.56	0.00	0.15	0.86
	Whin Sill Dolerite	0.19	0.00	0.15	4.31
	New Red Sandstone	0.00	0.00	0.00	0.22
Carboniferous	*Carboniferous Limestone*	0.28	0.41	1.33	1.29
	Chert	0.00	0.00	0.00	0.22
	Coal	0.00	0.00	0.00	0.00
Devonian	*Shale*	0.00	0.00	0.00	0.43
	Old Red Sandstone	0.00	0.00	0.00	1.29
Silurian	*Greywacke*	0.28	0.00	0.00	4.74
Other	*Shell*	0.00	0.41	0.00	2.16

Table 5.4: Geochemical analysis of sediments in Shippersea Bay

	High Abundance Elements (mg / kg)						
SAMPLE	Na_{23}	Mg_{24}	Al_{27}	K_{39}	Ca_{44}	Ti_{48}	Fe_{57}
ERB 05 LF 1a; Beach sand	27100	6440	204000	12000	203000	1110	19500
ERB 01 LF 1a; Beach gravels	6570	7550	328000	10500	53800	493	6290
ERB 06 LFA 3; Diamicton	2811	433	22456	12388	10558	4113	33355

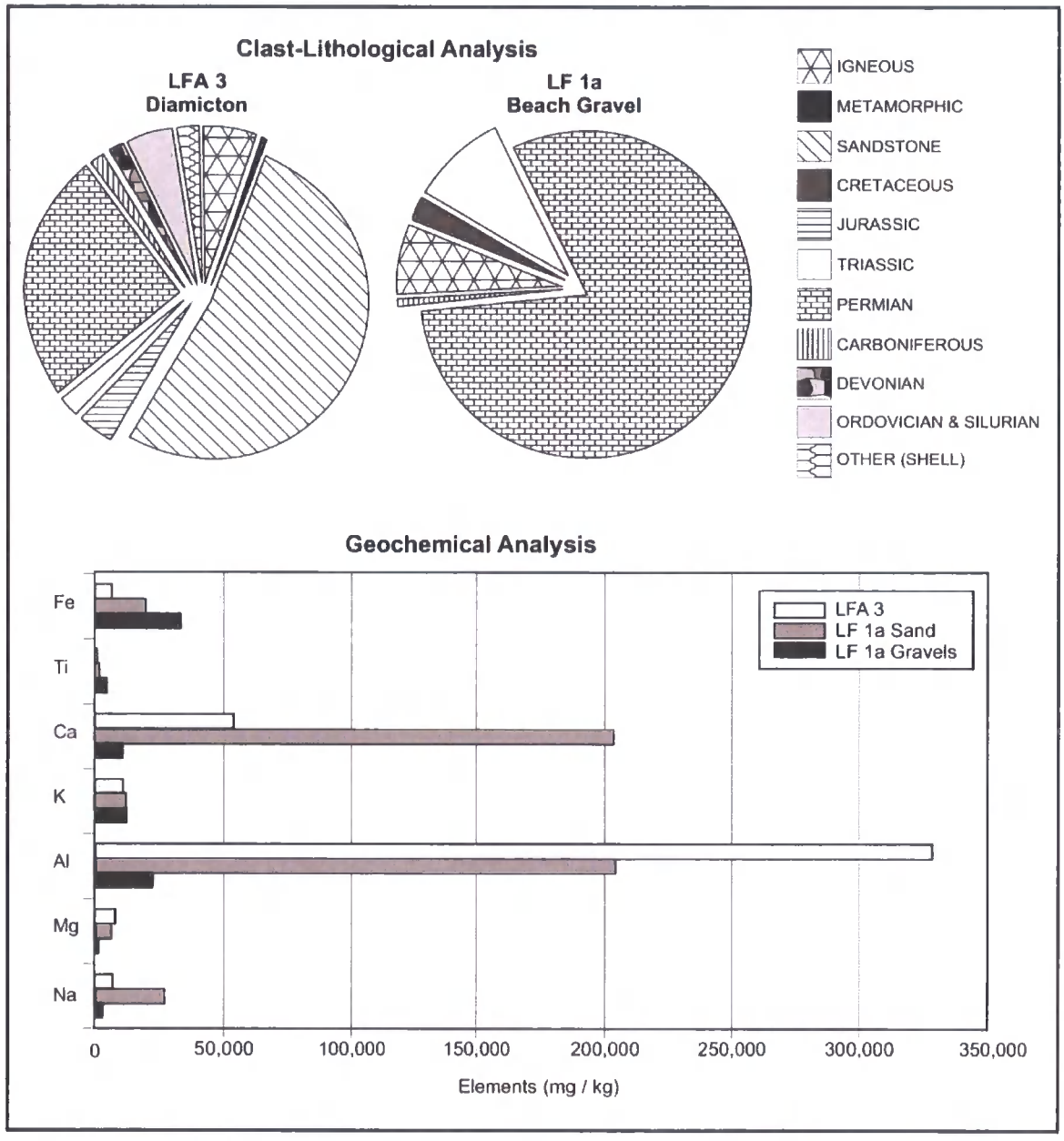

Figure 5.5: Pie charts of average clast-lithological analysis and bar charts of geochemical analysis, Shippersea Bay.

Table 5.5: Average percentage heavy minerals in sediments in Shippersea Bay. For detailed raw counts, refer to Appendix IV.

	Heavy Mineral Phase	LFA 1	LFA 3
	n	***8796***	***2048***
	% Opaques	89.04	73.29
	% Non Opaques	10.96	26.71
	% Heavy Minerals	2.17	0.40
Silicate Group	*Olivine GP*	0.34	0.19
	Zircon	4.90	11.58
	Sphene	1.98	3.45
	Garnet GP	13.03	30.25
	Sillimanite	1.44	0.18
	Andalusite	4.07	2.63
	Kyanite	6.24	2.24
	Staurolite	1.23	0.37
	Chloritoid	0.19	1.74
Epidote Group	*Zoisite / Clinozoisite*	4.55	1.61
	Piemontite	0.00	0.00
	Epidote	10.33	0.19
	Lawsonite	0.88	0.00
	Axinite	0.00	0.55
	Pumpellyite	0.00	0.00
	Tourmaline GP	2.80	2.63
Pyroxene Group	*Enstatite*	1.66	1.32
	Hypersthene	0.00	2.29
	Diopsidic Clinopyroxene	2.87	3.36
	Augitic Clinopyroxene	3.03	4.34
Amphibole Group	*Tremolite*	0.00	0.00
	Ferriactinolite	0.00	0.37
	Hornblende	0.00	0.39
	Diallage	0.00	0.37
	Glaucophane	0.00	0.19
Mica Group	*Muscovite*	8.63	6.63
	Glauconite	0.00	0.00
	Biotite	8.43	7.85
	Chlorite GP	2.33	2.21
Oxides	*Rutile*	1.74	6.23
	Brookite	1.65	1.09
	Spinel GP	0.00	0.18
	Anatase	0.00	0.18
Carbonates	*Dolomite / Calcite*	15.19	0.73
Sulphates	*Baryte*	0.00	0.00
Sulphides	*Sphalerite*	0.00	0.00
Phosphates	*Apatite*	2.13	4.26
	Monazite	0.39	0.37

5.3.2 Biological Data

LFA 1 contains numerous whole gastropod shells. The following species were identified: *Littorina litoralis, Littorina littorea, Littorina saxatilis, Nucella lapillus, Gibbula umbilicalis*, and *Patella vulgata.* This fauna, which confirms and adds to previous findings (Bowen *et al.*, 1991), is indicative of a warm littoral environment, such as that presiding on the modern beach at Shippersea Bay. Foraminifera (counted and identified by William Austin) are also present in these sands (Table 5.6). LFA 1 contains a relatively low diversity assemblage of benthic foraminifera, characteristic of temperate intertidal and sub-tidal environments (Murray, 1979). These assemblages are consistent with a high energy depositional setting, such as a beach deposit, where many of the specimens have undergone abrasion and breakage during the transportation / depositional processes.

Table 5.6: Foraminifera of LFA 1, the Easington Raised Beach. Courtesy of Dr. William Austin.

Foraminifera species	Abundance
Ammonia beccarii	Abundant
Elphidium williamsoni	Common
Cibicides lobatulus	Common
Elphidium excavatum	Common
Elphidium macellum	Common
Elphidium incertum	Rare
Haynesina germanica	Rare
Elphidium albiumbilicatum	Rare
Rosalina sp.	Rare

5.3.3 Chronostratigraphy

Introduction

Three independent dating methods were applied to LFA 1. The first was Optically Stimulated Luminescence (OSL) dating, which is a direct method of dating mineral sediments. It can only be used for sediments rich in quartz and/or feldspar grains that were exposed to light at the time of deposition; this makes it highly suitable for wind-blown, fluvial and beach sediments, and therefore applicable to this study (Lian, 2007). The context and depositional environment of the sample sites, however, must be well understood if the dates are to be correctly interpreted. OSL dating works with sediments from the Middle to Late Pleistocene (Lian & Roberts, 2006), making it a valuable radiometric technique for studying interglacial deposits. This was conducted by Dr.

Pawley, of Royal Holloway, University of London. The report is presented in Appendix IV.

The second dating technique, amino acid racemisation analysis (e.g., Miller & Clarke, 2007), has been previously applied to the Easington Raised Beach deposits, using an earlier methodology measuring the racemisation of a single amino acid in the whole shell fraction (cf. Bowen *et al.*, 1991). The analyses reported here used a new technique; improvements in the methodology mean that multiple amino acids were analysed from the intra-crystalline fraction of protein, which forms a closed system (Penkman *et al.*, 2007; Penkman *et al.*, 2008). A closed system is essential for the application of amino acid geochronology, because the majority of organic matter within fossil biominerals is potentially subject to contamination and / or leaching. As diagenetic reactions are used to assess the original properties and burial history of the sample, the degradation products of the organic matter must be retained within the biomineral: this is the case in closed systems (Penkman *et al.*, 2008). The method is based on the extent of protein decomposition, which increases with time, although there is an increased rate of breakdown during warm stages and a decrease in cold stages. Amino acids can exist in two forms, L and D, and only L-amino acids are formed in shells; modern shells have a DL ratio of close to zero. However, when an organism dies a spontaneous reaction occurs called racemisation, until there is an equal number of D- and L- amino acids, i.e., a D/L value of 1. This work was carried out by Dr. Penkman and Miss Demarchi, of the University of York. Refer to Chapter 2.9.1.

A third application of geochronology was the attempted use of the uranium-series method to measure the age of the calcareous cement in the upper part of the raised beach sequence, this being an appropriate technique for dating calcium carbonate precipitates of this sort (Candy *et al.*, 2004). This was carried out together with analysis of the stable isotopes of oxygen and carbon (refer to Chapter 2.9.3). This work was conducted by Dr. Candy, also of RHUL, whose report is presented in Appendix IV.

Optically Stimulated Luminescence

The Easington Raised Beach was dated by OSL by Dr. Pawley at Royal Holloway, University of London (see Appendix IV). OSL samples were collected from LFA 1 by hammering opaque plastic tubes into the face of the cleaned section (Figure 5.3 and Figure 5.6). A carbonate cemented sand bed was sampled (EAS 05) as an intact block, with the

light-exposed edges removed by dissolution using 10 % HCl. In estimating burial history, it was assumed that the site had been buried by 13 m of Late Devensian glacigenic sediments for the past 23 ka, and prior to this, a burial depth of 2 ± 1 m was assumed based on the thickness of the raised beach sediments that overlie the sampling locations. An underestimate of the burial depth would result in a commensurate underestimate in estimated age; thus, if the beach was buried by 10 m consistently prior to the Late Devensian, perhaps by an earlier glacial deposit, subsequently removed, then this would imply a 9 % increase in the estimated age.

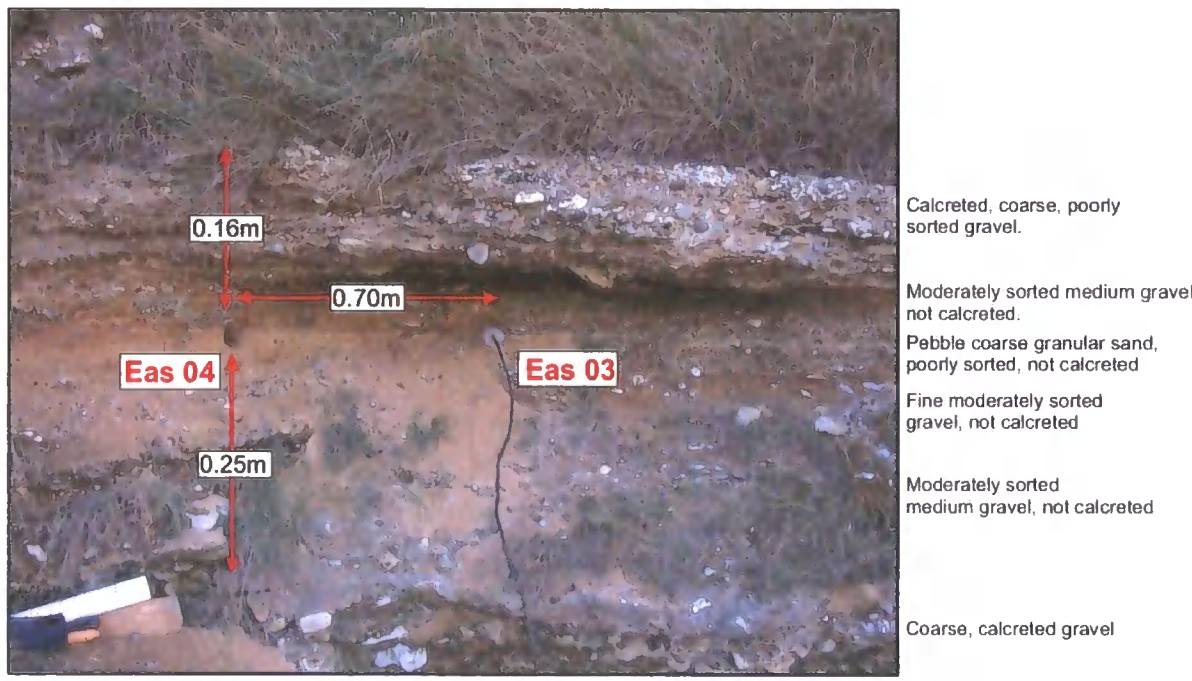

Figure 5.6: Location of samples EAS 04 and EAS 05. LF 2a, Section A, Easington Raised Beach

Dose recovery tests of 200 Gy were performed by Dr. Pawley on groups of four aliquots in each sample with the average measured / given dose ratio being 1.06 ± 0.04 m, very close to unity and confirming the ability of these samples to measure a known laboratory dose. The results of the quartz OSL dating are shown in Table 5.7 alongside the dose rate data and D_e estimates from between 12 and 22 aliquots per sample. When the OSL ages are compared to the marine isotope curve (Figure 5.7) derived from the ODP677 site (Shackleton *et al.*, 1990), four out of five dates are within errors of MIS 7 and range from 153 ± 17 to 250 ± 30 ka BP.

If the systematic uncertainties scaled on each date are combined in quadrature, a mean and error of 201 ± 28 ka is obtained which will cover systematic uncertainties in beta

source calibration, gamma-ray spectrometry calibration, dose rate conversion factors, beta dose attenuation factors, water content, cosmic dose/burial depth, and internal quartz dose. These ages support previous interpretations by Bowen *et al.* (1991) using conventional amino acid geochronology.

Table 5.7: Results of OSL dates, Easington Raised Beach, courtesy of Dr. Pawley.

Sample	*n*	Burial depth (m)	K (%)	U (ppm)	Th (ppm)	Water (%)	Dose rate (Gy/ka)	De (Gy)	Age (ka)
EAS01	16	2.0 ± 1.0	0.43	2.01	2.05	5	1.20 ± 0.11	184 ± 9	**153 ± 17**
EAS02	13	2.0 ± 1.0	0.45	2.31	1.66	5	1.14 ± 0.11	223 ± 17	**196 ± 26**
EAS03	12	2.0 ± 1.0	0.37	1.61	1.98	5	1.10 ± 0.11	260 ± 27	**237 ± 35**
EAS04	22	2.0 ± 1.0	0.46	1.84	2.02	5	1.20 ± 0.11	300 ± 21	**250 ± 30**
EAS05	14	2.0 ± 1.0	0.30	0.90	0.70	7	0.70 ± 0.10	130 ± 14	**188 ± 33**

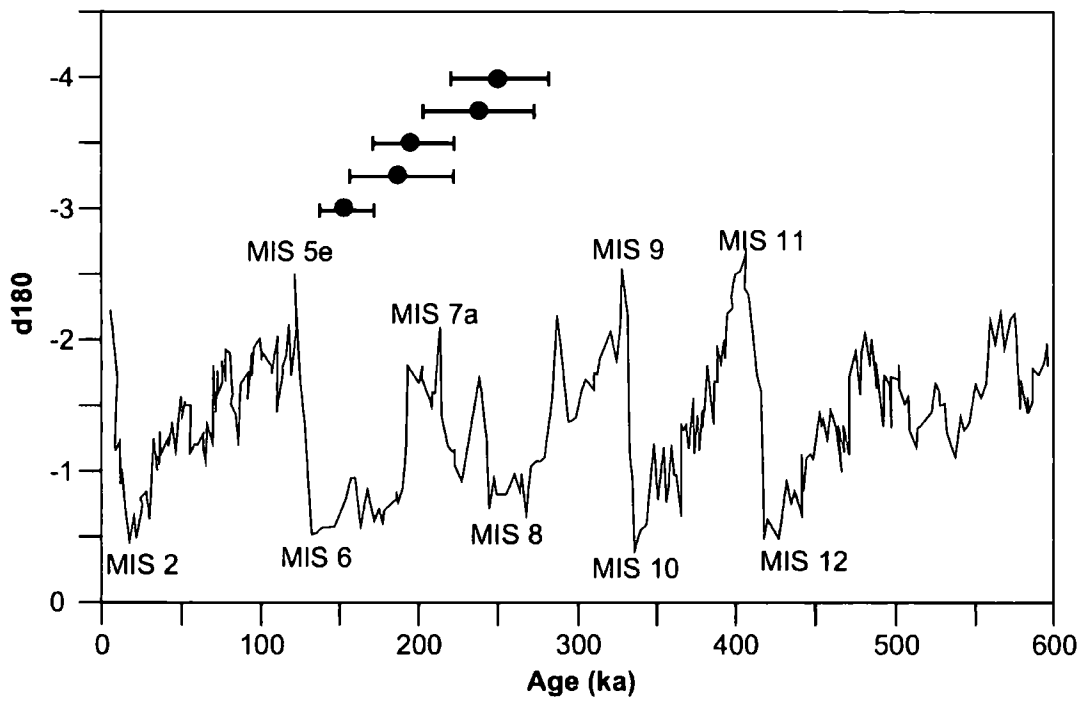

Figure 5.7: Comparison of OSL ages with the marine isotope record derived from the ODP677 site (Shackleton et al., 1990). Image courtesy of Dr. Pawley.

Amino Acid Racemisation

Amino acid racemisation analysis (e.g., Miller & Clarke, 2007), has been previously applied to the Easington Raised Beach deposits, using an earlier methodology measuring the racemisation of a single amino acid in the whole shell fraction (cf. Bowen *et al.*, 1991). Dr. Penkman and Miss Demarchi of York University analysed three *Nucella lapillus* gastropod shells for the degradation of intra-crystalline proteins. Two shells were taken from sample ERB01, and one shell from the ERB04. Two subsamples were taken from

each shell: one for analysis of the free amino acids (FAA) and one for the total amino acids, which include the peptide bound amino acids (Total Hydrolysable amino acids; THAA). The data from five amino acids (aspartic acid / asparagine (Asx), glutamic acid / glutamine (Glx), serine (Ser), alanine (Ala) and valine (Val)) are reported (Table 5.8), as these amino acids yield baseline resolution.

Table 5.8: Amino acid data on Nucella shells from the Easington Raised Beach. Error terms represent 1 S.D. about the mean for the duplicate analyses for an individual sample. Each sample were bleached (b) with the free amino acid fraction signified by 'F' and the total hydrolysable fraction by 'H*'. Each sample thus has a unique identifier. Results courtesy of Beatrice Demarchi and Kirsty Penkman of the University of York.

Sample	Asx D/L	Glx D/L	Ala D/L	Val D/L	[Ser]/[Ala]
ERB01 NI1bF	0.778 ± 0.016	0.297 ± 0.009	0.435 ± 0.004	0.260 ± 0.001	0.172 ± 0.005
ERB01 NI1bH*	0.614 ± 0.000	0.199 ± 0.000	0.295 ± 0.006	0.175 ± 0.003	0.170 ± 0.003
ERB01 NI2bF	0.779 ± 0.001	0.391 ± 0.093	0.436 ± 0.002	0.270 ± 0.000	0.167 ± 0.010
ERB01 NI2bH*	0.618 ± 0.000	0.208 ± 0.001	0.322 ± 0.002	0.188 ± 0.000	0.165 ± 0.000
ERB04 NI1bF	0.791 ± 0.000	0.304 ± 0.005	0.428 ± 0.003	0.274 ± 0.006	0.174 ± 0.001
ERB04 NI1bH*	0.619 ± 0.001	0.206 ± 0.000	0.306 ± 0.001	0.175 ± 0.001	0.153 ± 0.001

The results were compared to data from *Nucella* from other Quaternary Early Pleistocene interglacial beach and coastal deposits from around eastern England: Bramerton Crag, Sidestrand Crag and the Mya Bed (overlying the Freshwater Bed) at West Runton (Norton, 1967; Rose *et al.*, 2001; Rose *et al.*, 2002; Lee *et al.*, 2006; Riches *et al.*, 2008). All the diagenetic indicators (D/L and [Ser]/[Ala]) indicated a coherent increase in protein degradation with time for this species (Figure 5.8). The diagenetic indicators therefore strongly suggested a much younger age for the Easington deposits than for the other sites, therefore the Easington Raised Beach must be younger than the type Cromerian. The values obtained suggest that the deposits are not as young as the Devensian. Thus, with the paucity of previous data using this methodology acting as a major constraint on resolution, the new analyses placed the Easington deposit as younger than the Cromerian and older than Devensian. Assignment to a particular MIS will not be possible until a larger database of results from interglacial marine sites is available; as they stand, these results do not contradict the MIS 7 age implied by the OSL (above) and the earlier conventional amino acid analyses (cf. Bowen *et al.*, 1991).

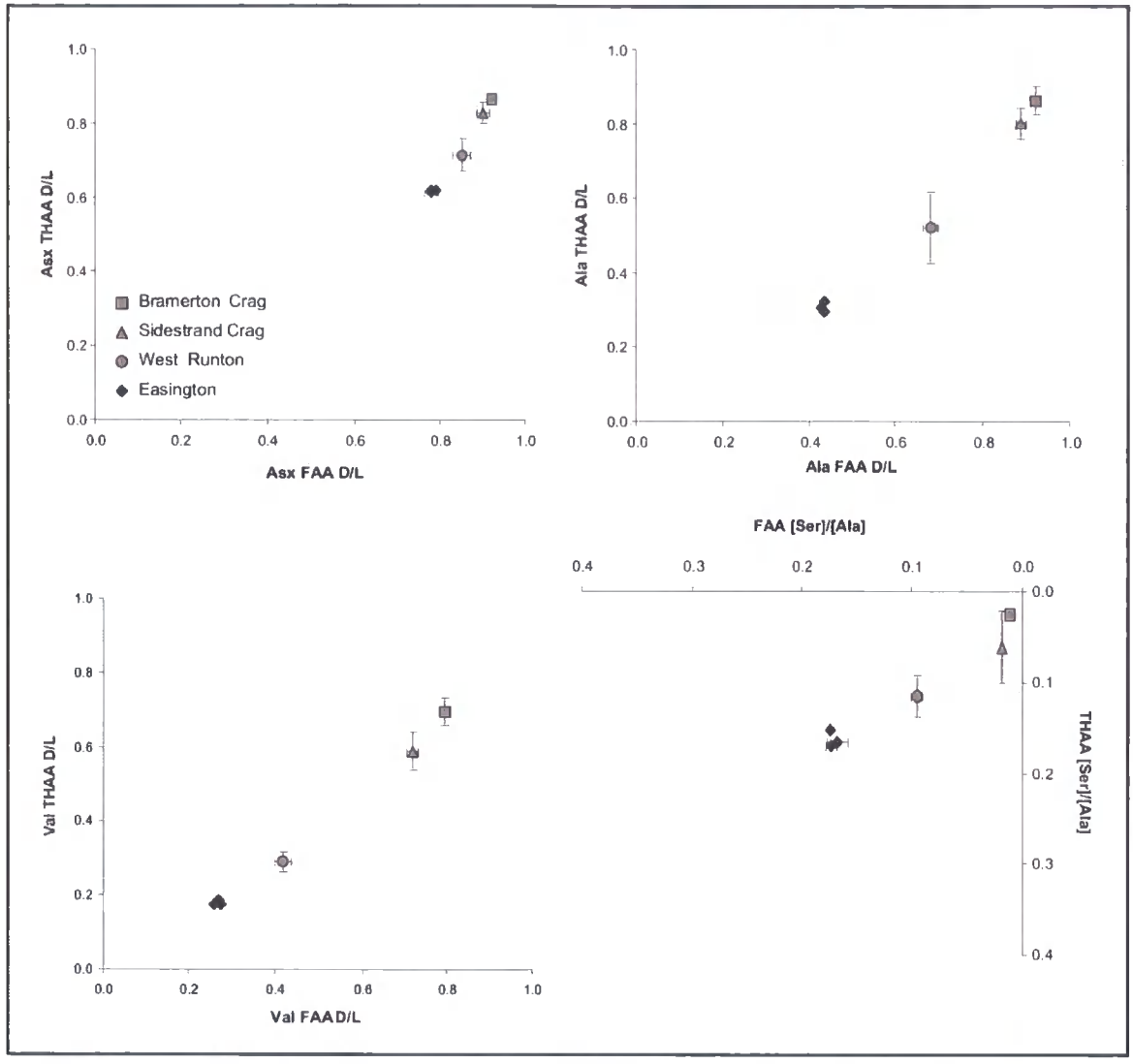

Figure 5.8: D/L values of Asx, Ala, Vak and [Ser]/[Ala] for the free (FAA) and Total Hydrolysable Amino Acid (THAA) fractions of the bleached Nucella lapillus shells from the Easington Raised Beach, compared with shells from the Cromerian type site (West Runton), and Crag deposits of Early Pleistocene age (from Sidestrand and Bramerton).

Data for Easington are represented with one standard deviation around the mean of the replicates for each individual sample. Comparison sites are represented with two standard deviations around the mean for the site. The axes for the [Ser]/[Ala] data are plotted in reverse, so that the direction of increased protein degradation for each of the indicators remains the same. Note: different scales on the *y*-axes. Courtesy of Beatrice Demarchi.

Stable Isotope Geochemistry and U-series dating

Stable isotope geochemistry and U-series dating was conducted by Dr. Candy (Candy, 2008, see Appendix IV). To assess the U-series chronology and date of cementation of the beach, densely cemented samples were taken from representative sediment fabrics within the raised beach sequence. These included well-sorted medium sands, gravels with a medium sand matrix, and open-framework gravels. Thin sections were prepared according to procedures outlined in Lee and Kemp (1994). Candy (2008) observed that the thin

sections of the three samples showed that the carbonate cement matrix to be dominated by secondary calcite spar, which is typical of calcification in the phreatic zone (Tucker & Wright, 1990; Preece *et al.*, 2007). In the sand samples, where small pore size means that there is minimal room for cement crystal growth, the cement was characterised by small (10 μm) spar crystals. In the open-fabric gravels, the calcite crystals are larger (300 μm). Candy (2008) observed that in both the sand-dominated and open-framework sediments, the calcite crystals are fibrous in form and exhibit an isopachous arrangement, with cements of consistent thickness growing around the pore rim (Figure 5.9).

Candy (2008) proposed that the petrography and the stable isotopic composition of the Easington cements are characteristic of carbonate precipitation by phreatic (groundwater) processes. The coarse-spar cements are indicative of calcite precipitation in association with regularly recharging waters. Their isopachous arrangement implies that the pores were permanently filled with water. Both the oxygen and carbon isotopic values of the Easington cements are consistent with those of interglacial 'groundwater' carbonates (Figure 5.10), with no indication of precipitation under marine conditions (Candy, 2008).

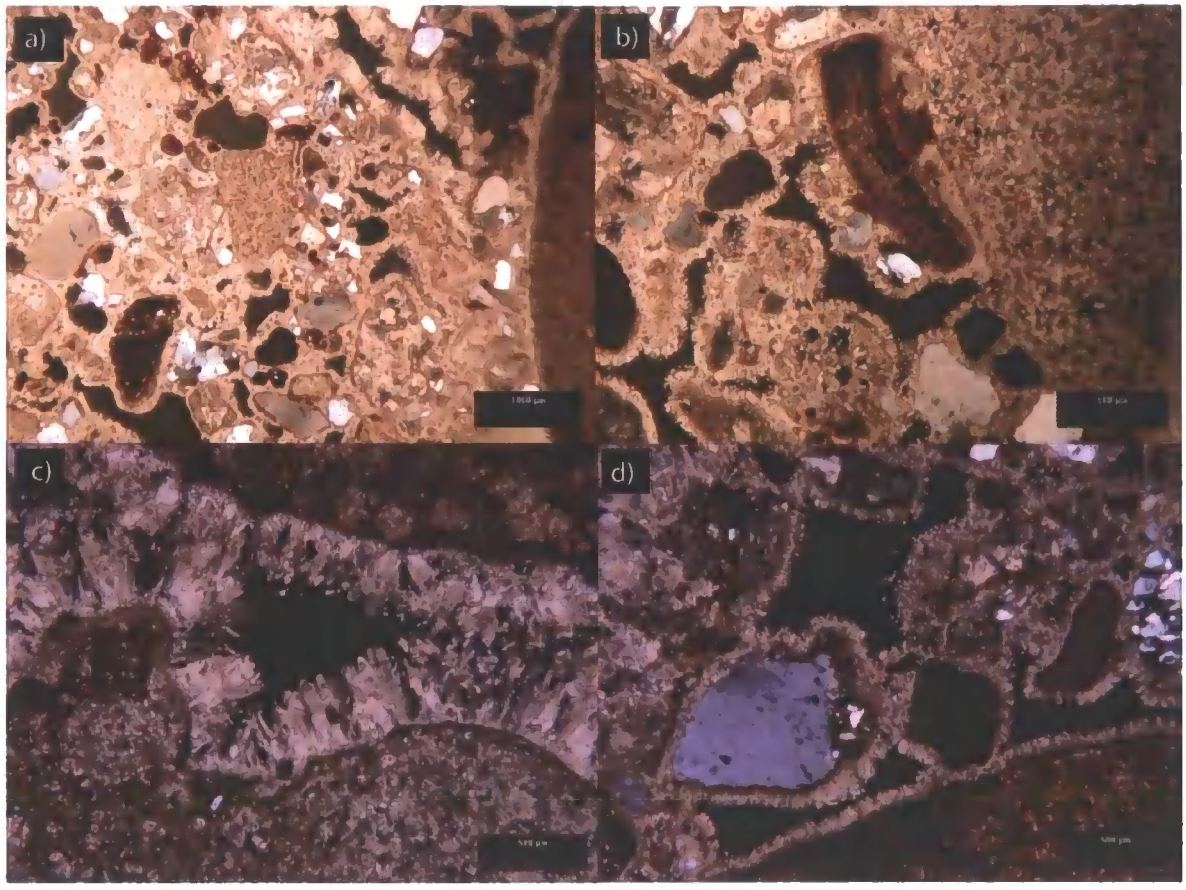

Figure 5.9: Photomicrographs of the microstructure of the Easington beach cement.

a) Low power view of the sediment and cement matrix.

b) Carbonate cements within the sandy fabric, fibrous calcite crystals in an isopachous arrangement.

c) Carbonate cements within the open-framework gravels.

d) Carbonate cements within the pebble-gravel with sandy matrix. All photo-micrographs are shown in cross-polarised light. From Candy (2008); refer to Appendix IV.

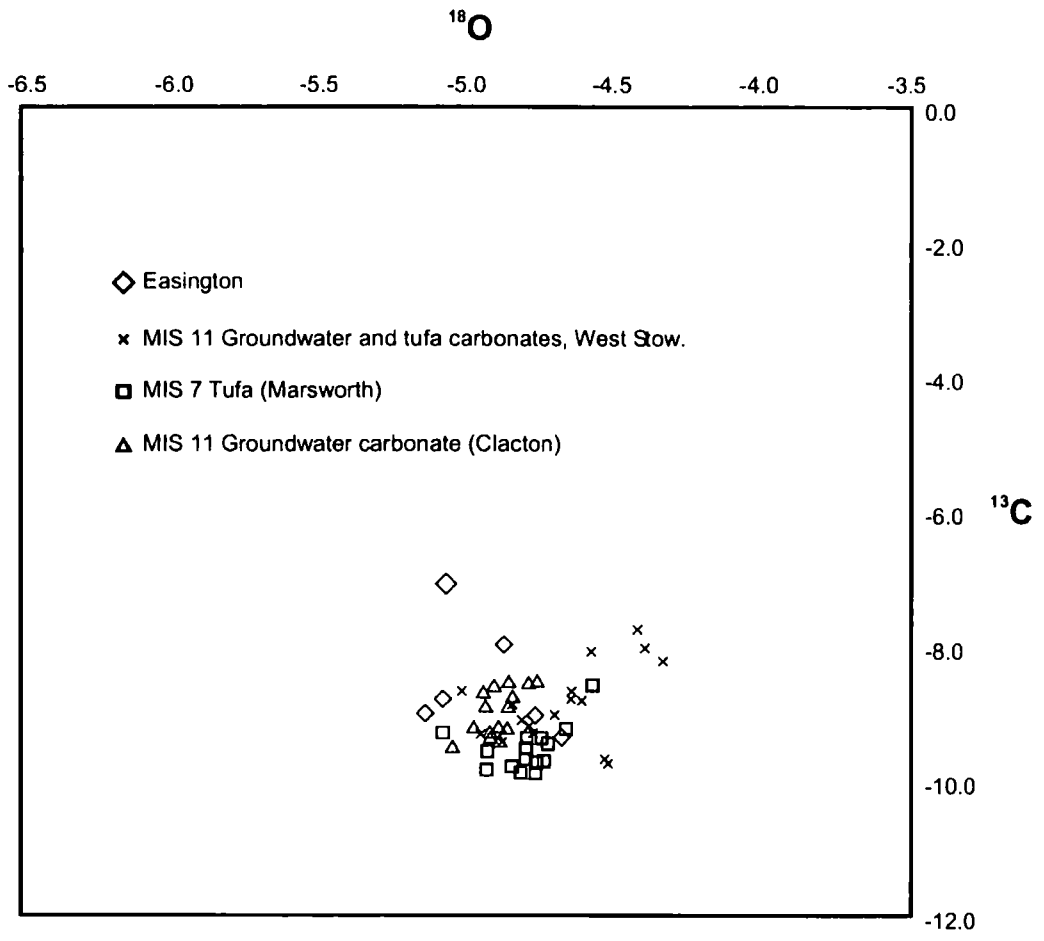

Figure 5.10: Comparison of the stable oxygen and carbon isotopic composition of the Easington Raised Beach with groundwater and tufa sediments from British interglacials (MIS 7 and MIS 11). From Candy (2008).

In an attempt to constrain the age of the raised beach deposits, Dr. Candy took five samples of the carbonate cements for $^{230}Th/U$ dating. The most suitable material was the large spar cement accumulations from the open-framework gravels, as cements in these contexts can grow into open pores, resulting in low amounts of detrital contamination with the cement lattice. Also, the relatively thick accumulations of cements means that any surfaces that have undergone weathering can be removed before analysis. The derived ages scatter between 7,470 ± 120 years and 39,360 ± 450 years (Table 5.9).

Candy (2008) suggested that the concentration of ^{232}Th (80 to 250 ppb) and the $^{230}Th/^{232}Th$ activity ratio (1 to 6.8) could indicate detrital contamination (cf. Candy *et al.*, 2005), which would overestimate the true age of the carbonate cement. However, although concentrations of thorium are high, they are low compared to concentrations of uranium (850-1000 ppb). In many carbonate systems, such a high level of uranium relative to thorium would mean that the effect of detrital contamination should be minimal, and the

$^{230}Th/^{232}Th$ activity ratio should be >>20. That this is not the case in the Easington samples is likely to be a function of the very young age of the cement (Candy, 2008), as when a sample is very young, very little ^{230}Th will have accumulated through radioactive decay. As a consequence, the $^{230}Th/^{232}Th$ activity ratio will be relatively low, making the samples appear heavily contaminated. Candy (2008) applied a detrital correction to this dataset (following Ludwig and Paces (2002) and Sharp *et al.* (2003)), which altered the ages slightly, but the three Holocene ages remained Holocene, and the two Devensian ages remained Devensian.

Table 5.9: Age of cementation from U-series dating. From Candy (2008); refer to Appendix IV.

Sample	EAS1	EAS2	EAS3	EAS4	EAS5
U (ppb)	853	834	900	1029	925
Th (ppb)	243	125	250	82	169
$(^{230}Th/^{238}U)$	0.305	0.066	0.096	0.155	0.08
2σ	(-0.003)	(-0.001)	(-0.003)	(-0.002)	(-0.001)
$(^{234}U/^{238}U)$	0.104	1.15	1.149	1.157	1.158
2σ	(-0.007)	(-0.005)	(-0.006)	(-0.006)	(-0.006)
$(^{230}Th/^{232}Th)$	3.582	1.543	1.202	6.831	1.538
2σ	(-0.015)	(-0.022)	(-0.021)	(-0.068)	(-0.022)
Age (years)	39,360 ± 450	7,470 ± 120	10,940 ± 310	18,300 ± 260	9,070 ± 160

This data therefore indicates that cementation occurred primarily during the Holocene (Candy, 2008). An interglacial interpretation is supported by the stable isotope geochemistry, which would require a constant and persistent water table (which would be more likely to occur during an interglacial). The two samples placing cementation in the Devensian are therefore curious, and suggest that cementation could span 40,000 years, and that the relevant groundwater processes are only weakly related to climate (Candy, 2008). Alternatively, the cementation could be multi-phase, and these older ages could be averages. At localised points within the cement, there is evidence that carbonate was precipitated during multiple phases and does not represent a single phase of carbonate precipitation (Candy, 2008).

5.4 Discussion

5.4.1 Depositional Processes

LFA 1: Sorted sands and gravels

LFA 1 in the sheltered cove of Shippersea Bay is interpreted as a raised beach, supporting interpretations by Trechmann (1952) and Bowen *et al.* (1991). The presence of bored clasts indicating littoral bivalves and annelid worms, the seaward dipping imbrication, the well-sorted sands and gravels, the well-rounded clasts, and fossil littoral gastropods and foraminifera all suggest a temperate-climate beach interpretation. The dating evidence from this and earlier studies indicates that the beach formed during MIS 7, which was the penultimate interglacial (Bowen, 1999c). The height of the beach, at 33 m O.D., can be related to progressive regional uplift in northern England. This is the case with south coast raised beaches such as in west Sussex (Westaway *et al.*, 2006), although the uplift history in east Durham has undoubtedly been complicated by repeated depression and recovery from glacial ice loading and perhaps also by its proximity to the subsiding North Sea basin. An age of MIS 7 and a height of 33 m would indicate a long-term uplift rate of ~0.19 mm a^{-1}, which is in keeping with a regional pattern of increasing uplift rates across England, and is comparable with that in the Pennines (Westaway, in press). There is an increase in uplift northwards, which is related to the thinner (30-32 km thick, Chadwick & Pharaoh, 1998) and hotter Palaeozoic crust, with surface heat flow in many localities ~90 Mw m^{-2} (Lee *et al.*, 1987), due to the significant radiogenic heat production in Palaeozoic granite intrusions (Westaway, in press). The lower crust is therefore much less viscous than in the south of England, and is capable of flowing to a greater extent in response to surface processes, essentially driving isostatic uplift in response to rapid erosion (England & Molnar, 1990). Westaway (in press) attributed the uplift to redistribution of mobile lower crustal material, driven by repeated loading and unloading as a result of the growth and decay of ice sheets and the rise and fall of sea level (these being, in any case, interrelated), as well as erosional unloading of the land area (Westaway *et al.*, 2002). The process is progressive and affects areas of younger crust worldwide (Bridgland & Westaway, 2007), although in glaciated areas like northern England its influence is generally masked by the considerably more rapid (but reversible) effects of glacio-isostasy.

Trechmann (1952) argued that Scandinavian lithologies present within the beach were derived from the 'Scandinavian Drift' (Warren House Formation), implying that the beach was younger than the till. No Scandinavian lithologies were found in the beach during the course of the present study, however. There are rare incidences of flint, but it is difficult to prove that they originated from the Warren House Formation. They could have been derived from another deposit, now removed by subsequent processes (as, indeed, could the Scandinavian clasts reported from the beach by Trechmann).

Unsorted sands and gravels (LF 2a) and diamicton (LFA 3)

The coarse, gravelly sands (LF 2a) immediately overlying the raised beach are interpreted as glaciofluvial in origin. They are massive, incohesive, poorly sorted, and contain numerous erratics. In LF 2b, there are foresets emphasised by grains of coal, which is not present in the high-energy environment of the beach. The overlying diamicton, LFA 3 (the Horden Till), has been weathered. This is supported by the presence of roots, pedogenesis, oxidisation, and the removal of less durable minerals (cf. Eyles & Sladen, 1981). The presence of striated, sub-angular to sub-rounded, far-travelled stones, and the unsorted character all support an interpretation as a subglacially-derived till, originating from a combination of processes at the ice-bed interface, including lodgement, glaciotectonic deformation, and grinding (Hart & Boulton, 1991; Hindmarsh, 1997; Larsen *et al.*, 2004). This is firmly supported by more rigorous investigations of other diamictons correlated with the Horden Till at Whitburn Bay (Chapter 3) and Warren House Gill (Chapter 6).

4.4.2 Cementation of the Easington Raised Beach

Candy (2008) argued that the U-series data indicate that the cementation of the raised beach (LFA 1) was a Late Quaternary phenomenon. The stable isotope geochemistry suggests that the cement precipitation in LF 1b occurred in an interglacial climate (Figure 5.13). This is supported by the necessity for a constant and persistent water table (which would be more likely to occur during an interglacial). However, two of the derived ages place cementation during the Devensian (Table 5.9). There is, therefore, the possibility that cementation spans the last 40,000 years, and that the groundwater processes responsible for cementation are only weakly related to the prevailing climate. The cementation could also be multi-phase, and although the main phase occurred during the Holocene, earlier phases

may have occurred during previous interglacials. Whether the ages obtained were averages, or whether there are genuine glacial stage cements within the beach is difficult to prove, however, at localised points within the cement there is evidence that carbonate was precipitated during multiple phases and does not represent a single phase of carbonate precipitation.

Candy (2008) proposed that the cementation of the beach required dissolution of significant amounts of carbonate from within the hydrological system, and for the re-precipitation of carbonate within the beach gravels as a result of a change in carbonate solubility. The overlying Devensian till is crucial to this story. During an interglacial, the expansion of vegetation and soil forming processes across the surface of the till would lead to the dissolution of detrital carbonate, due to the presence of organic acids and the high partial pressure of CO_2 in the soil atmosphere. This causes it to be taken up into solution as carbonic acid. Downward percolation of waters through this till is slow, due to the low permeability of this deposit. As these vadose waters enter the highly permeable raised beach deposits, the increased rate of water flow, increased pore size, and increased pH are more conducive to carbonate precipitation. Carbonate consequently precipitates as dense spar crystals. The till overlying the beach is therefore critical to the precipitation of the raised beach cement matrix (*ibid.*). It is likely that widespread cementation of the raised beach was not possible until after the LGM and the deposition of this till. However, the emplacement of an older MIS 6 till, now removed, over the top of the beach, might have led to an earlier phase of cementation.

5.4.3 Provenance

The Raised Beach

LFA 1 contains a varied suite of heavy minerals (Table 5.5). The presence of far-travelled high-rank metamorphic minerals (such as kyanite, andalusite, zoisite, amphiboles and detrital micas) indicates littoral reworking of pre-existing, glacigenic sediments. It is possible that this includes the 'Scandinavian Drift' (Trechmann, 1915, 1952), now the Warren House Formation (Thomas, 1999), but it is also possible that these minerals were derived from other, now locally non-extant (eroded), glacigenic deposit(s). Locally-derived minerals such as dolomite (15.2 %) are abundant, along with stable minerals such as garnet (13.0 %) and zircon (4.9 %). Clast lithological analysis confirms the input of some reworked, far-travelled material (Table 5.3). While the majority of the clasts are locally-

derived limestones, the flints, quartzite, vein quartz, acid porphyries (probably Scottish) and granites are outside regional fluvial drainage networks (Cameron & Stephenson, 1985; Johnson, 1995; Stephenson & Gould, 1995; Strachan *et al.*, 2002; Trewin, 2002), and indicate that older glacigenic deposits must have been reworked. The only currently extant source for quartz, quartzite and flint erratics in the local vicinity is the Warren House Formation, but this does not exclude pre-existing glacigenic deposits now no longer remaining. The absence of non-durable lithologies such as coal, sandstone, mudstone etc., probably reflects the high-energy nature of the beach environment.

The glaciofluvial sands and gravels (LFA 2) and the subglacial till (LFA 3)

The glaciofluvial sands and till overlying the raised beach at Shippersea Bay share many provenance characteristics with other upper-most glacial sediments in County Durham. Although the till here shows signs of weathering, provenance-specific indicators remain. For example, the presence of slate indicates a source from the Grampian Highlands of Scotland. Granite, gabbro, acid porphyries, and basalt are all probably derived from the Scottish Highlands and the Midland Valley (Cameron & Stephenson, 1985; Stephenson & Gould, 1995; Davies *et al.*, in press). Old Red Sandstone is a typical lithology of the Midland Valley of Scotland and northwest of the Cheviots (Cameron & Stephenson, 1985). The low percentage of Magnesian Limestone in the till implies separation of ice from the bedrock at the time of subglacial erosion by a mantle of older till (the Blackhall Till; cf. Davies *et al.*, in press), and that most of the limestone clasts were derived secondarily through erosion of this older till, as suggested by Beaumont (1967). Clasts of dolerite were probably derived from the Whin Sill, which crops out to the north (Smith, 1994; Randall, 1995).

Heavy-mineral analysis of LFA 3 in Shippersea Bay reveals a characteristic garnet-staurolite-chloritoid assemblage, indicative of Stonehavian-type metamorphism, which indicates input of material derived from near the Highland Boundary Fault. The presence of the garnet-andalusite-kyanite assemblage suggests input from Buchan, near Aberdeen (Stephenson & Gould, 1995; Trewin, 2002), which is comparable to other Devensian tills in the area (refer to Chapter 3).

5.4.4 Implications

The Easington Raised Beach contains a varied heavy mineral suite and varied gravel clast lithologies, clearly demonstrating the input of far-travelled material. This suggests that marine erosion, acting upon pre-existing glacigenic deposits, introducing this material into the raised beach. For the lithologies to have reached such high percentages, the glacigenic deposit must have been widespread. Previous authors (Trechmann, 1931a; Francis, 1972; Lunn, 1995; Thomas, 1999) have suggested the Warren House Formation as the source. Currently however, this is preserved only in the bottom of a deeply incised pre-Devensian valley, although it could previously have been more widespread.

LFA 3, overlying the raised beach (Bridgland & Austin, 1999), is clearly distinguished by the low proportion of Magnesian Limestone and the high proportion of sandstone. It contains far-travelled erratics, namely gabbro, andesite and basalt, sourced from the Southern Uplands and the Grampian Highlands. The heavy-mineral assemblage shows a clear input from near the Highland Boundary Fault.

Although this study agrees with the interpretation of LFA 1 as a raised beach, and direct dating has indicated an MIS 7 age, this study found no evidence of Scandinavian erratics within the raised beach. However, Scottish acid porphyries and granites and Cretaceous flints suggest erosion of a sediment that flowed from offshore eastern England in a westerly direction. This could include an ice sheet sourced in Scandinavia, and rhomb porphyries could therefore potentially exist within the beach in very low numbers.

The vast majority of the clasts within the beach are locally derived bedrock lithologies. The large number of quartzose lithologies and rare flint lithologies bears resemblance to the lithologies within the Warren House Formation. However, these lithologies are very durable and could survive several cycles of reworking. Therefore there is no clear lithostratigraphical evidence that the beach includes derived clasts from the Warren House Formation.

5.5 Conclusions

This study is the first fully quantified sedimentological, petrological and lithological analysis of the Easington Raised Beach, also providing in-depth analysis of the sedimentary structures. The presence of well-sorted sands, and well-rounded, imbricated, cobble-gravel with annelid worm and molluscan borings, and of warm-climate, littoral shells from species such as *Nucella lapillus* and *Patella vulgata*, and shallow, sub-tidal and temperate foraminifera, combine to indicate that this is a temperate beach. New dating applications have confirmed earlier attributions to MIS 7. The cement matrix was formed by groundwater percolation during the Holocene in relation to the overlying subglacial till.

This study found no evidence of Scandinavian erratics within the raised beach. However, Scottish acid porphyries and granites and Cretaceous flints suggest reworking from a sediment that was sourced offshore from eastern England. This study agreed with previous workers that the sediments were deposited in a warm, littoral environment during a period of high sea level during MIS 7.

The diamicton overlying the beach is the Horden Till, as defined by Francis (1972). It is very weathered and contains numerous sandstone lithologies. It shows a clear provenance from north-eastern England, with derived material from further away, including the Grampian Highlands. The lower Blackhall Till pinches out against the flanks of the beach.

CHAPTER 6

Warren House Gill

6.1 Introduction

The regional Quaternary geology of this area was described in Chapter 1, and the local facies architecture was reported in Chapter 4. This chapter presents results from detailed section logging, sedimentology, thin-section analysis, and quantitative provenance analysis from Warren House Gill, County Durham.

6.1.1 Rationale

Lee *et al.* (2006) recently highlighted the complex interactions between ice and climate at Pakefield on the Norfolk coast, with repeated evidence for ice incursions, sea level fluctuations, and changing coastal environments (Lee *et al.*, 2006). Recent chronostratigraphical work has highlighted the complexity of Middle Pleistocene glaciations (Lee *et al.*, 2002; Rose *et al.*, 2002; Lee *et al.*, 2004). Understanding these long-term climatic changes and the climatic, oceanic and cryospheric response to them is important in understanding contemporary climatic fluctuations.

Whilst numerous global glacial episodes are recognised from deep ocean cores (Shackleton, 1967; Shackleton & Opdyke, 1973), forcing terrestrial evidence into this stratigraphical framework is fraught with difficulty (Bowen, 1999b). Nevertheless, the recent research in Norfolk has aroused questions regarding the dynamics of Quaternary glaciations. A key part of this is reconstructing the presence of Scandinavian ice in Britain and in the North Sea, and the extent of its coalescence with and influence on the BIIS during the Quaternary. Only by reconstructing these past events can we understand the context for Quaternary climatic change, its timescales, its 'normality', and its likely future patterns. In addition, it is important to provide sound geological data and robust stratigraphical models of previous cryospheric responses to climate change. These data can be used by mathematical modellers to test and train ice-sheet models. These models can then be used to predict future ice-ocean-climate interactions, particularly in the field of the response of the Greenland ice sheet to oceanic warming and likely resulting sea level rise.

Warren House Gill has previously provided evidence of multiple glaciations, with reported Scandinavian erratics. It is ideally located to independently, critically test recent models proposed in Norfolk. It is therefore a key site in understanding British Quaternary stratigraphy.

6.1.2 Previous Research

Previous research in northern England has indicated the existence of a sequence of glacigenic sediments, consisting of three tills with intervening aeolian and fluvial deposits. Trechmann (1952) proposed that the sequence in Warren House Gill (see Figure 1.1, page 6) consisted of a 'Scandinavian Drift' deposited by an 'Older Glaciation', which was overlain by interglacial loess. He also argued that Shippersea Bay (Figure 4.1) contained a raised beach which he named the "Easington Raised Beach" (see Chapter 5), and contended that it was deposited during an interglacial postdating the formation of the Scandinavian Drift (Trechmann, 1952). Thomas (1999) renamed the Scandinavian Drift the 'Warren House Formation'.

Other workers correlated the Warren House Formation with the Bridlington Member (formerly the Basement Till; Table 1.4, Lewis, 1999) of Yorkshire, and assigned it to MIS 6 (Catt, 1991b). However, the Warren House Formation has been interpreted as stratigraphically older than the Easington Raised Beach, dated to MIS 7 (this study, Chapter 4); therefore, its age and the stratigraphy remain controversial. These sediments are overlain by the Devensian Blackhall and Horden Members, which were correlated to the Skipsea Member of Yorkshire (Francis, 1972), and which are the southern extension of the tills exposed in Whitburn Bay. The Quaternary sediments in County Durham can therefore provide substantial new information and evidence to test evolving theories of British and Fennoscandian ice sheet interactions during the Quaternary. The more northerly position of the Warren House Formation enables the dynamics and interactions of these Middle Pleistocene ice sheets to be better reconstructed and the models proposed for Norfolk to be independently tested, so it is a crucial area for research.

6.1.3 Research Aims and Objectives

As outlined in Chapter 4 above, this research aims to understand the interaction between the British and Fennoscandian ice sheets during the Quaternary. The principle

objectives, outlined in Chapter 4.2.2, are to determine the genesis, provenance and stratigraphy of these glacigenic sediments, and their regional stratigraphical significance. Based on the previous research, outlined in Chapter 1, three key hypotheses have been identified:

1. There have been multiple glaciations in northeast England throughout the Pleistocene.
2. The oldest glacial sediments at Warren House Gill represent a till of Scandinavian provenance, of MIS 6 age.
3. The Easington Raised Beach is stratigraphically younger than the Warren House Formation and represents the succeeding interglacial.

In order to achieve these aims and objectives, and to test these hypotheses, systematic sampling was conducted at Warren House Gill. First, using original logs compiled by Trechmann (Trechmann, 1952), targeted shallow excavations were conducted to expose all the lithofacies expected. This was followed by detailed stratigraphical analysis (through sketches, vertical profiles and levelling) and identification of lithofacies. Systematic bulk and thin-section sampling of all lithofacies was then conducted, with multiple and replicate samples from each lithofacies. Where possible, samples were taken throughout a vertical profile (e.g., as in Exposure C).

6.2 Sedimentology and Stratigraphy

6.2.1 Facies Architecture

Warren House Gill (Grid Reference NZ 4772, 4234) is a contemporary stream valley, incised into Quaternary deposits infilling a deep, buried palaeo-valley. The bedrock is a collapse-breccia of Roker Dolomite, a facies of the Magnesian Limestone. It is a SSSI for its geological and ecological interest, and the limestone grassland is part of a European Special Area for Conservation. The National Trust owns the land. Colliery waste and slumping obscures most of the cliffs, and a JCB was therefore used to excavate eleven trial pits (Figure 6.1). This and some better exposed sections enabled detailed study of hitherto unseen sediments and their stratigraphic relationships, close inspection of their sedimentary and deformation structures, and extensive sampling. Several detailed vertical profiles (labelled A to K) along a 500 m cliff were logged and sketched in detail. The sediments are laterally variable and exhibit considerable changes in character across the buried palaeo-valley. Nevertheless, similarities between stratigraphic facies in different trial pits allowed correlation into lithofacies associations (LFAs; Figure 6.2 and Figure 6.3). Five lithofacies associations are identified here.

First is LFA 1, the Basal Shelly Diamicton; previously named the 'Scandinavian Drift' by Trechman (1952) and later renamed the 'Warren House Formation' by Thomas (1999). LFA 1 contains three facies: LF 1a (massive, grey diamicton); LF 1b (diamicton with bedded sands); and LF 1c (deformed association of interbedded grey shelly diamicton and pink silts (LFA 2)). LFA 1 is overlain by beige silts (LFA 2), interpreted by Trechmann (1952) as loess. LFA 3, the Middle Diamicton, directly and unconformably overlies this silt. It is continuous with LFA 1 identified Hawthorn Hive. LFA 3 is macroscopically heterogeneous and comprises several different lithofacies. LF 3a is a dark brown diamicton. LF 3b is a tectonised diamicton interbedded with red sands, seen in Exposure D2. Gravelly, bedded sands occur frequently at around 10 m O.D., these form LF 3c. In Exposure E1, well-sorted, planar bedded sands (LF 3d) are interbedded with LF 3a. In Exposure C, two more facies are exposed; LF 3e, which is a thickly bedded well-sorted clay, and LF 3f, a laminated diamicton (Figure 6.3).

LFA 3 is overlain by LFA 4, which exhibits two facies at Warren House Gill. These are red, bedded sands and silts (LF 4a), and the intimately associated cobble gravel in

Exposure K (LF 4b). The final lithofacies association is LFA 5, the Upper Diamicton, which is macroscopically massive, clast rich, and directly and unconformably overlies LFA 4. LFA 5 exists as an unbroken diamicton sheet from Hawthorn Hive southwards.

Combined with the macroscale sedimentology, this gives a powerful tool for the interpretation of glacigenic sediments. This technique was used in conjunction with lithological, geochemical, petrological and chronostratigraphical techniques to aid process interpretation, stratigraphical correlation and provenance interpretation. The locations of bulk, thin section and OSL samples are shown on Figure 6.3.

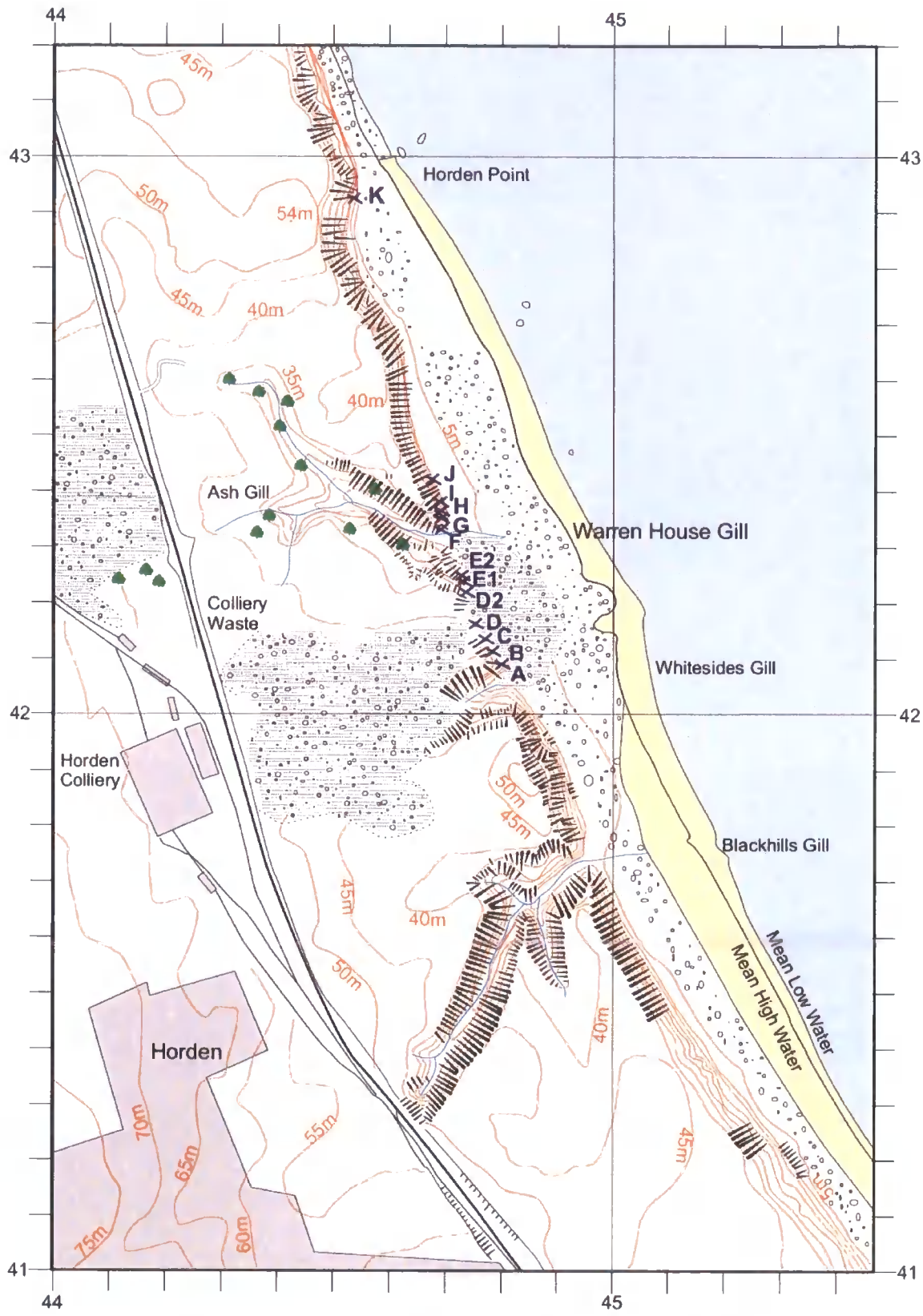

Figure 6.1: Map showing location of trial pits (letters A to I) and exposures (letters J and K) at Warren House Gill.

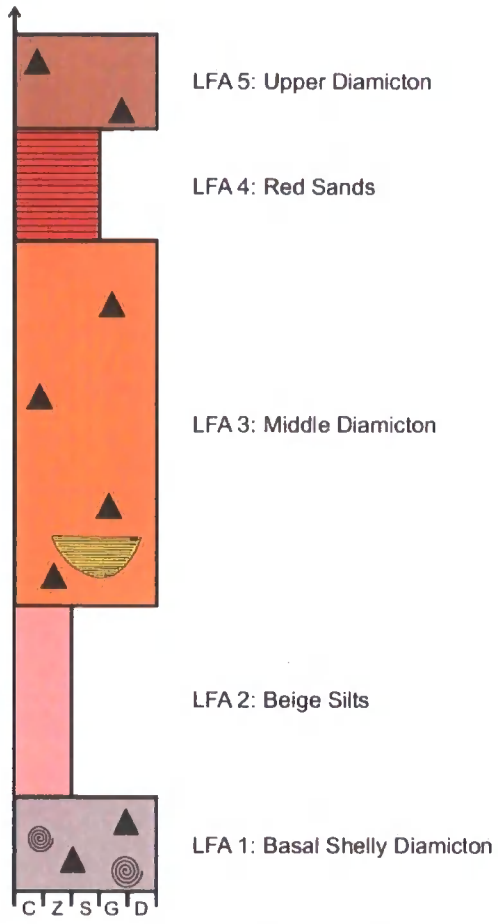

Figure 6.2: Simplified composite stratigraphy, Warren House Gill

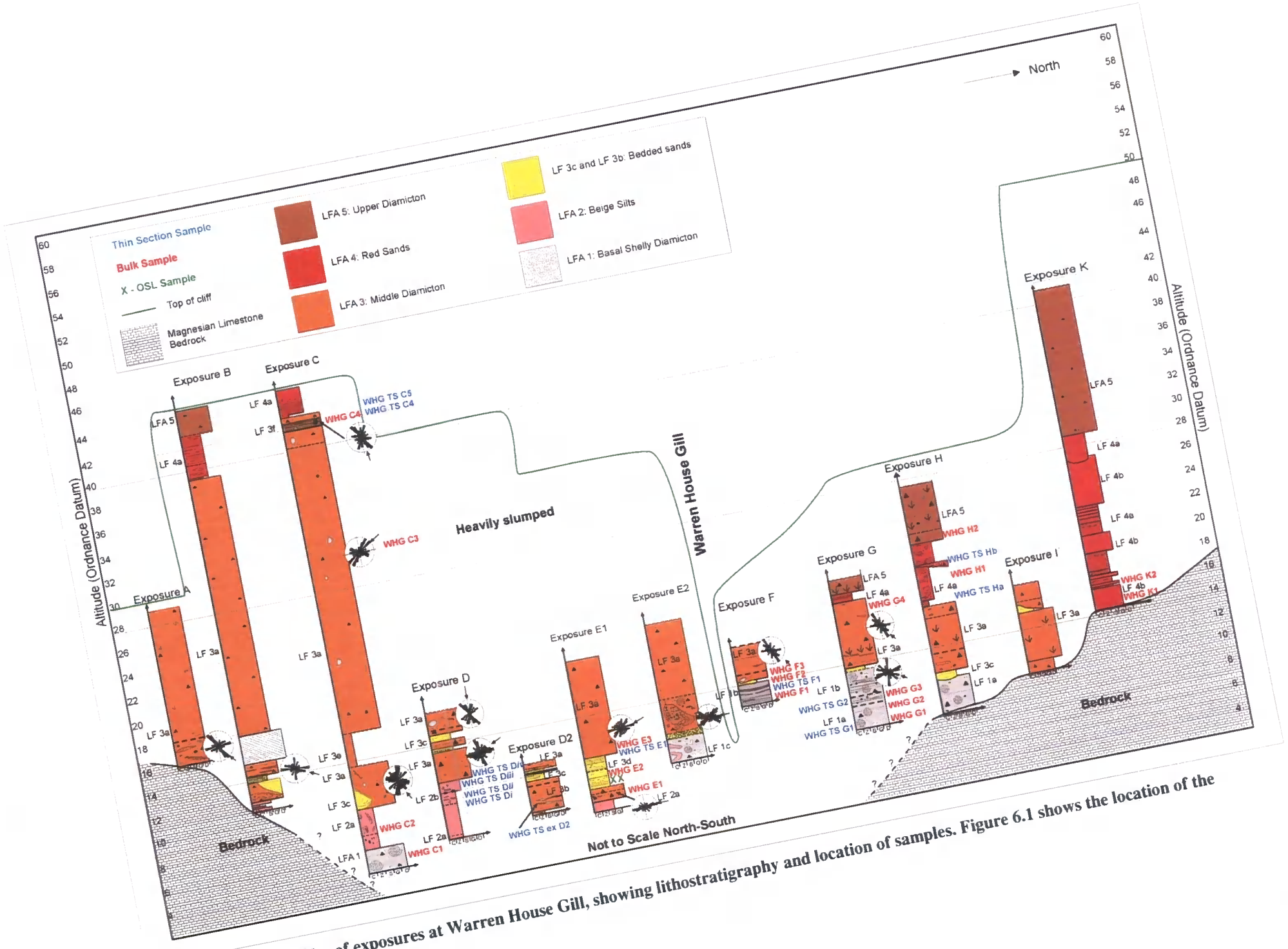

Figure 6.3: Vertical profiles of exposures at Warren House Gill, showing lithostratigraphy and location of samples. Figure 6.1 shows the location of the exposures.

6.2.2 LFA 1: The Basal Shelly Diamicton

Sedimentology and Stratigraphy

Three facies of LFA 1 are exposed at Warren House Gill, exposed in trial pits F, G, and H. LF 1a is a massive, clay-rich diamicton with very rare gravel clasts. LF 1b is slightly coarser, with more gravel, and deformed sandy lamination. LF 1c is a tectonite with apparent mixing between LFA 1 and LFA 2.

LFs 1a and 1b: Massive to laminated diamicton

Exposure G lies 20 m to the north of Exposure H (NZ 47724; 42343). The trial pit and the cliff above show four facies (see Figures 6.5, 6.6 and 6.7). At the base it is a very dark grey, massive, fissile, clast-poor diamicton (LF 1a), bearing broken fragments of marine bivalve shells. The gravel content increases with height in the trial pit. At 2 m height, there is a conformable contact with an overlying second diamicton (LF 1b), with a colour change to a yellowish brown and then to a dark olive brown. Gravel clasts increase in number, and deformed sand laminations appear (Figure 6.6). A clast macro-fabric taken from this location (Figure 6.4 and Figure 6.5) shows little clustering along the a-axis, with a wide variety of dip angles. The clasts are mostly sub-angular in shape, with significant numbers of angular to sub-rounded varieties. Common clast lithologies include chalk, flint, red marl, igneous erratics, quartz, and orthoquartzite. This facies is overlain by coarse, gravelly sand with an incised, unconformable, convex lower contact (LF 3c). The contact is difficult to observe as it coincides with a step in the trial pit, and is too high to clean. LF 3a, which has a significantly higher clast content, overlies this and then by the red, planar bedded sands (LF 4a).

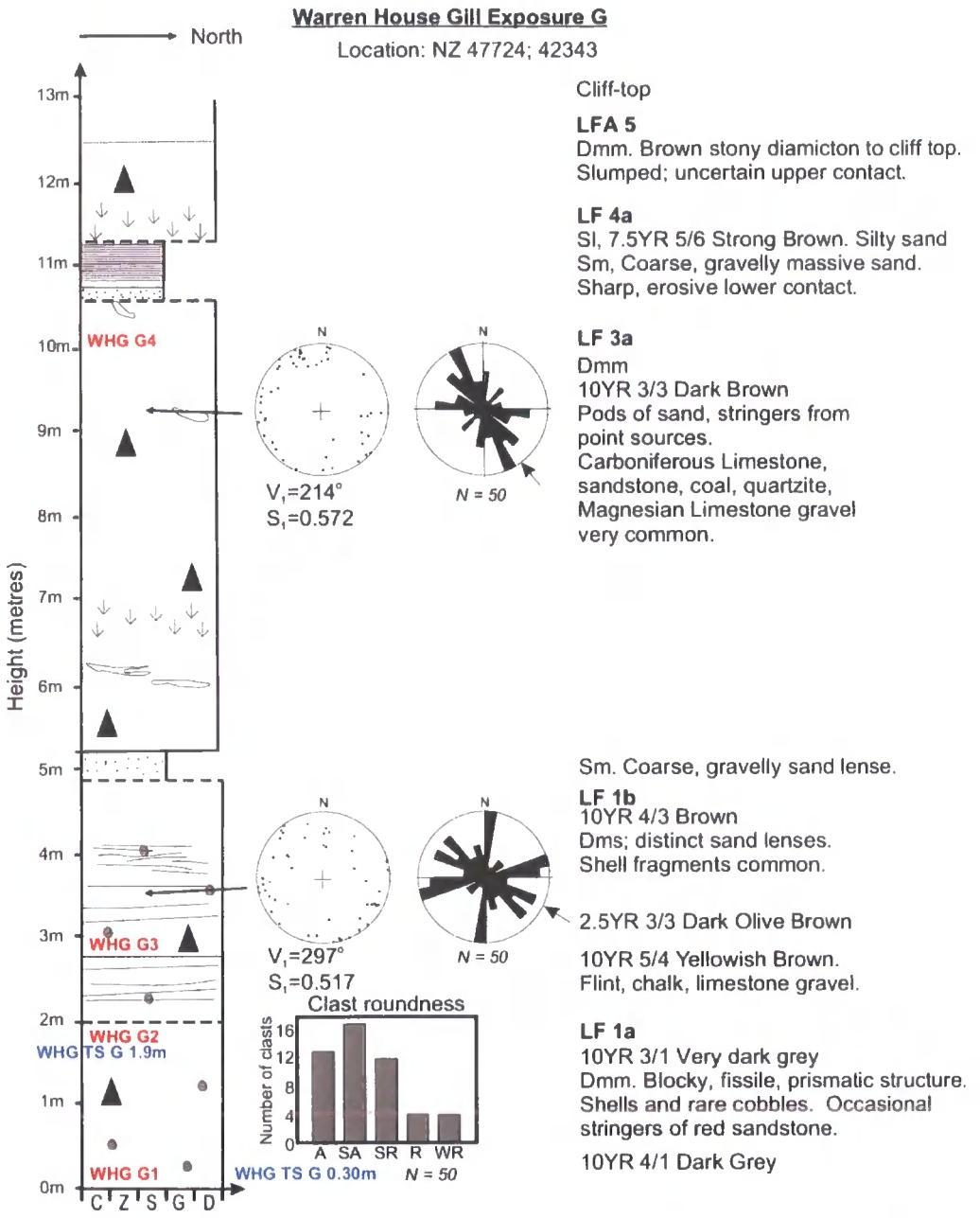

Figure 6.4: Vertical Profile of Exposure G, Warren House Gill, showing location of bulk (red writing) and thin section (blue writing) sampling points. Lower clast fabric (LF 1b; $S_1 = 0.517$; $S_2 = 0.337$; $S_3 = 0.147$). Upper clast fabric (LF 3a; $S_1 = 0.572$; $S_2 = 0.269$; $S_3 = 0.091$).

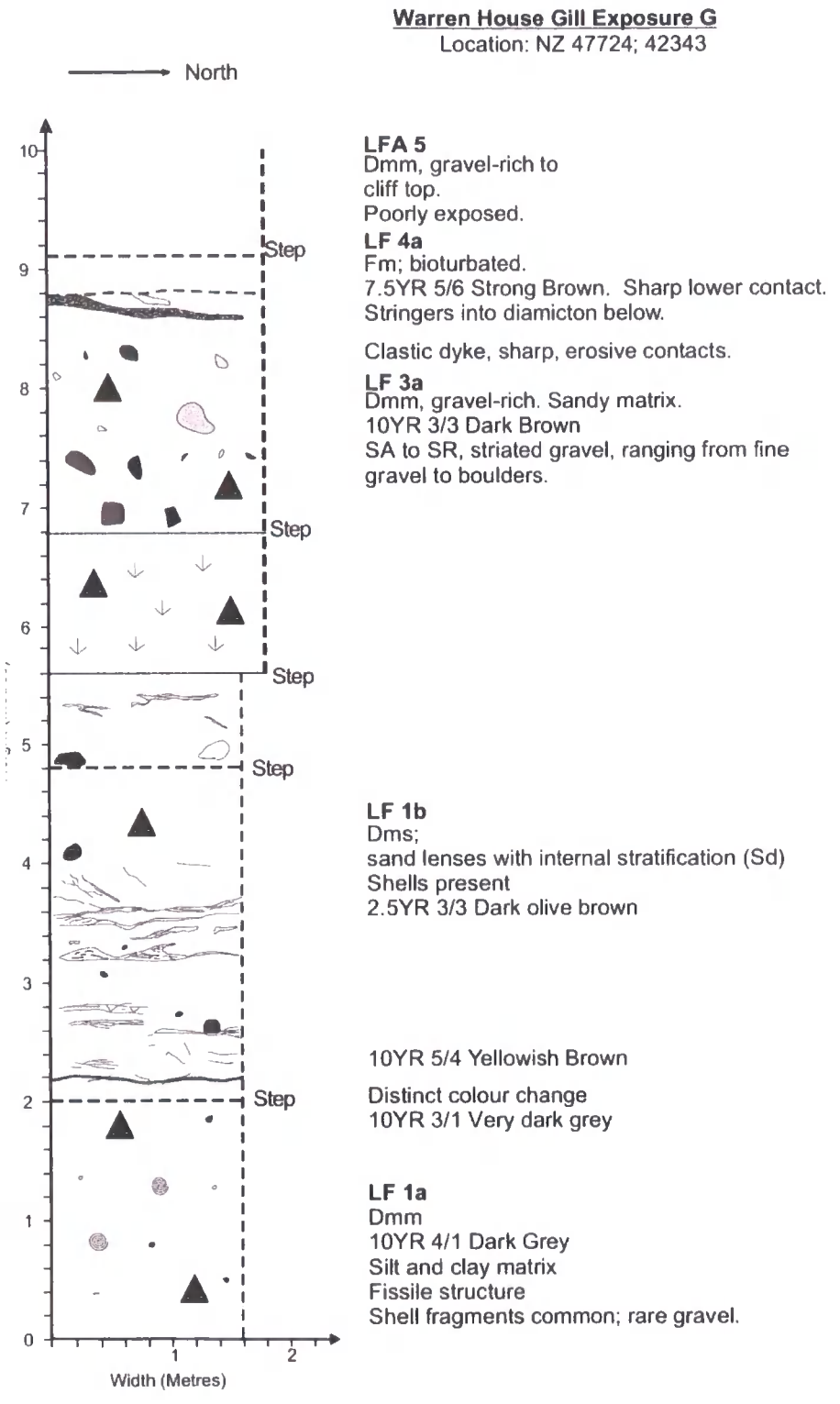

Figure 6.5: Sketch of LF 1a to LF 4a at Exposure G, Warren House Gill.

Figure 6.6: Photograph A. Exposure G, Warren House Gill. Photograph B: LF 1b, showing tectonised laminations. Pickaxe is 90 cm long. Photograph C: Detail of LF 1b.

In Exposure F (located at NZ 44713; 42320), two diamictons are exposed in superposition (Figure 6.7). The basal diamicton, LF 1b, is a macroscopically laminated, shell bearing (broken marine bivalves), clast poor, dark grey, fissile diamicton. The laminations are sheared, and deformed. A bed of coarse, poorly sorted, bedded sand, with a scoured, convex basal contact (LF 3c), overlies the diamicton. This is overlain by a gravelly diamicton (LF 3a).

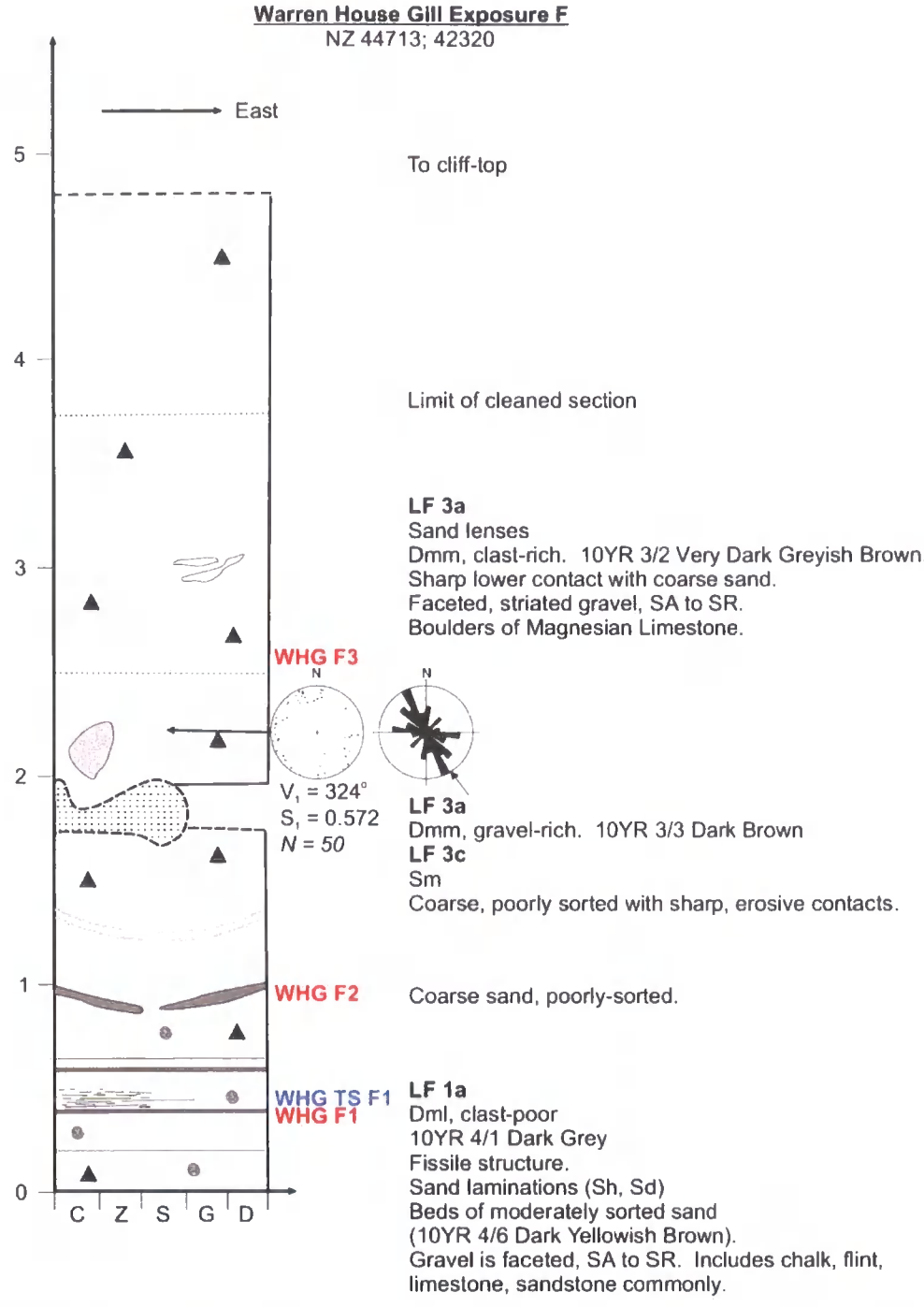

Figure 6.7: Vertical Profile of Exposure F at Warren House Gill, showing location of bulk (red writing) and thin section (blue writing) sampling points. The clast fabric S vales are: $S_1 = 0.572$; $S_2 = 0.334$; $S_3 = 0.093$. 50 measurements were made.

LF 1c: Tectonite

Exposure E2 (Figure 6.8), on the southern side of the current stream, is markedly different in character to Exposure G. It is the only trial pit to expose the contact between LFAs 1 and 2. LF 1c is a clast-poor grey diamicton bearing fragments of bivalve shells, chalk and flint gravel, and red marl clasts. Folded into this diamicton are narrow laminae

of yellowish-brown silt (LFA 2), which are extended, faulted, folded and deformed, with stringers extending from the silt into the diamicton. This is the northern limit of the silts; the outcrop narrows and is poorly preserved in this exposure. A matrix-supported, diamict gravel overlies the whole facies (LF 3c), and is in turn overlain by a gravel-rich diamicton (LF 3a), within which is a large pod of crudely bedded, overturned, gravelly sand (LF 3c).

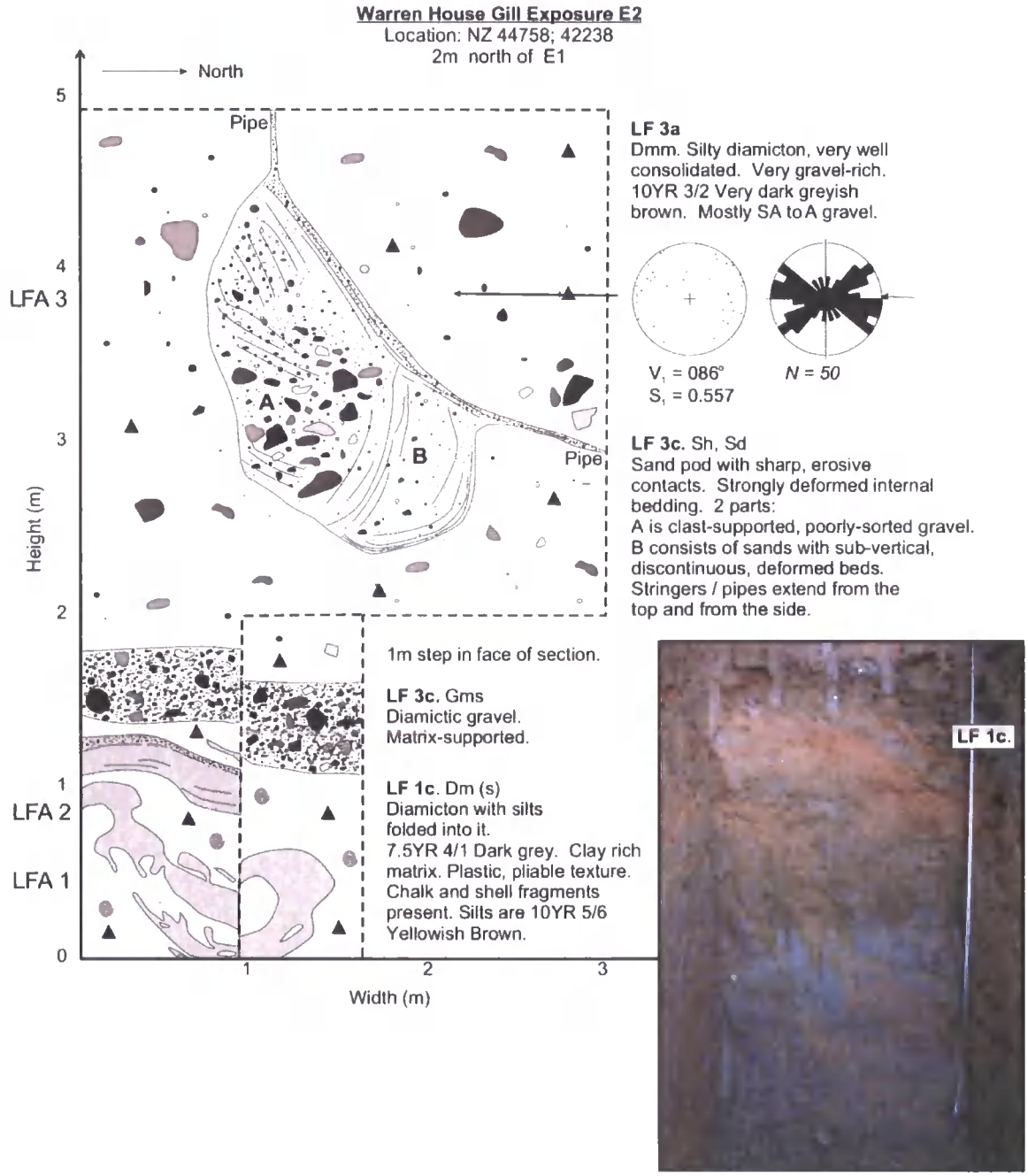

Figure 6.8: Detailed sketch of Exposure E2, with photograph of LF 1c, the tectonised contact between LFAs 1 and 2. LFA 1 and LFA 2 are folded together. Clast fabric from LF 3a ($S_1 = 0.557$; $S_2 = 0.31$; $S_3 = 0.134$).

Thin-section analysis

A summary of all the thin sections is presented in Table 6.1. WHG TS F1 was taken from LF 1b, Exposure F (Figure 6.7 and Figure 6.9). On macroscopic inspection, the sample is a massive, dense, brown, matrix-supported diamicton. There are occasional red marl grains and fine gravel clasts.

On microscopic inspection, the skeleton grains are poorly sorted and range in size widely from silt to fine gravel. They are sub-angular to sub-rounded and are mostly less than 100 μm. The plasma is of variable density as can be seen on the macroscopic slide and is distinctly banded (Figure 6.9). The rare planar voids are inferred to be laboratory induced. There are shell fragments and marine microfossils present in the thin section. There is some highly deformed graded bedding within the diamicton. Structural analysis reveals stratification as well as many deformation structures, such as occasional rotational structures with associated necking structures, Type II Pebbles, and Type III Pebbles with their own internal plasmic fabric, multiple clay domains, and rare grain lineations. There are rare crushed grains with fragments separated by plasma (Figure 6.10 C). The plasmic fabric reveals a moderately developed skelsepic and masepic plasmic fabric with a strong birefringence (Figure 6.10). The plasmic fabric has multiple crosscutting directions, with varieties of masepic plasmic fabric. There are also regions of omnisepic plasmic fabric.

Table 6.1: Micromorphological summary of thin sections of LFA 1 at Warren House Gill.

Sample	Location	Lithofacies	Skeleton			Matrix		Void type	Sedimentary Structures				Deformation Structures												Plasmic Fabric				
			Sorting	Grain shape <500µm	Grain shape >500µm	Texture	Microfabric		Laminations	Dropstones	Microfossils	Dump Structures	Section Elements	Faulting	Folding	Rotations	Grain lineations	Pressure Shadow	Crushed Grains	Grain stacks	Pebble Type I	Pebble Type II	Pebble Type III	Water escape	Fluidised Bedding	Skelsepic	Lattisepic	Masepic	Bi-Masepic	Unistrial
WHG G1	Ex G 0.3m	Massive shelly mud	D	SA - SR	A - SA	F		L	●●●	●	●		Be, Bo, F, Sh	●●	●●	●	●	●					●●●		●●●	●●		●		
WHG G2	Ex G 1.9m	Massive shelly mud	D	SA - SR	A - SA	F		L/P	●●		●		Ba, F, Be			●●	●●					●●	●●●		●●	●●		●●●		
WHG F1	Ex F 0.5m	Massive shelly Mud	D	SA	SA	F		L/P					Be		●	●			●				●●●		●	●●		●●●		

Key

Sorting

WS	Well sorted
MS	Moderately sorted
PS	Poorly sorted
D	Diamicton

Grain shape

WR	Well rounded
R	Rounded
SA	Subangular
A	Angular

Microfabric

H	Horizontal Microfabric
V	Vertical microfabric

Voids

P	Packing induced
L	Laboratory induced

Texture

F	Fine grained
C	Coarse (no fine silt/clay)
M	Medium (some fine silt/clay)

Section Elements

Ba	Banding
Bo	Boudinage
Be	Bedding
Sh	Shear
F	Flow
St	Stringer

●●● Indicates feature is strongly present / numerous

●● Indicates feature is present

● Indicates feature is rarely / occasionally present

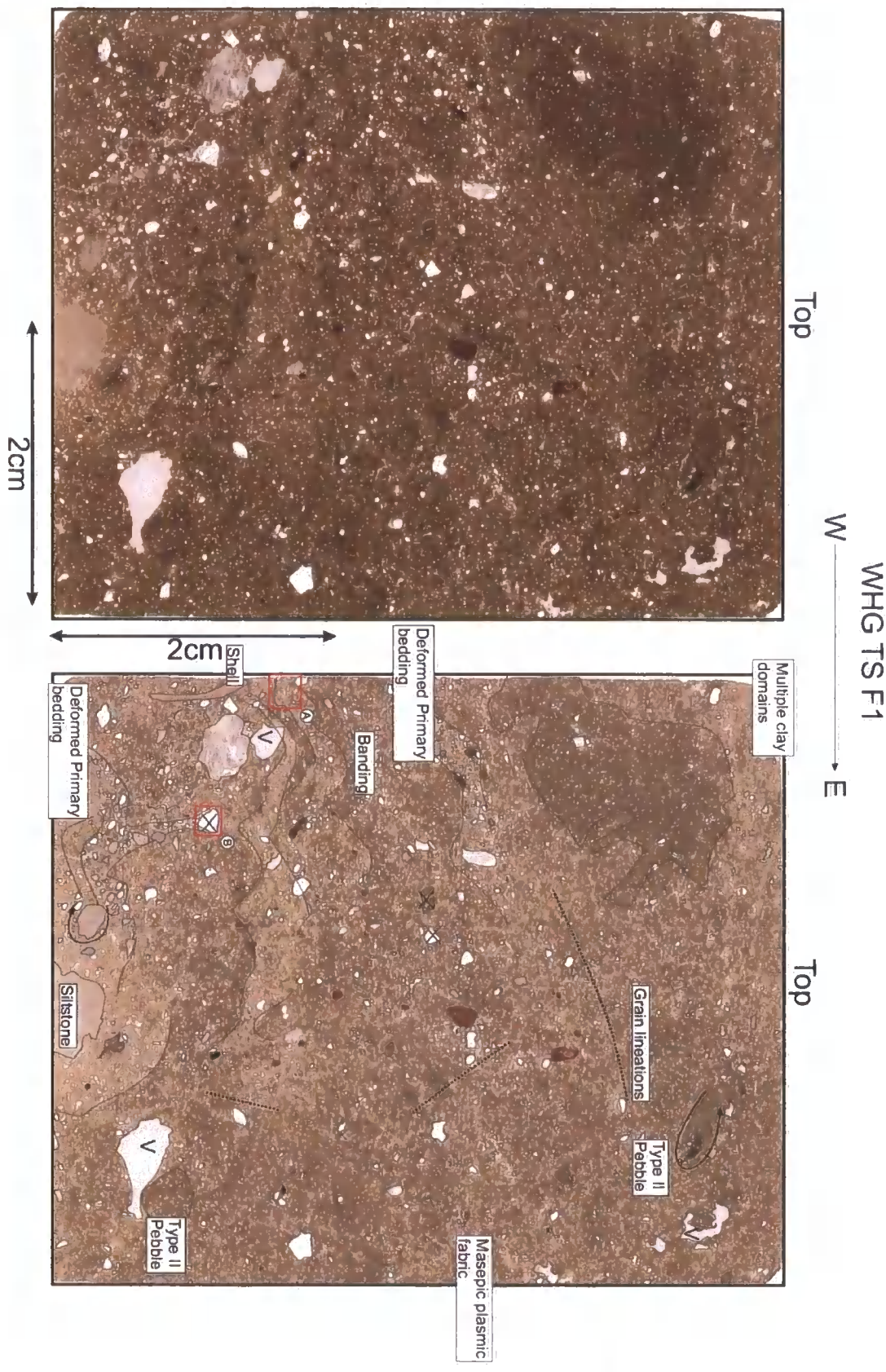

Figure 6.9: Photograph of thin section sample WHG TS F1. Box A (Figure 6.10) shows shears. Box B shows a crushed grain in detail. Grain lineations that are sub-resolution of the image and masepic plasmic fabric have been highlighted to show their orientation and position.

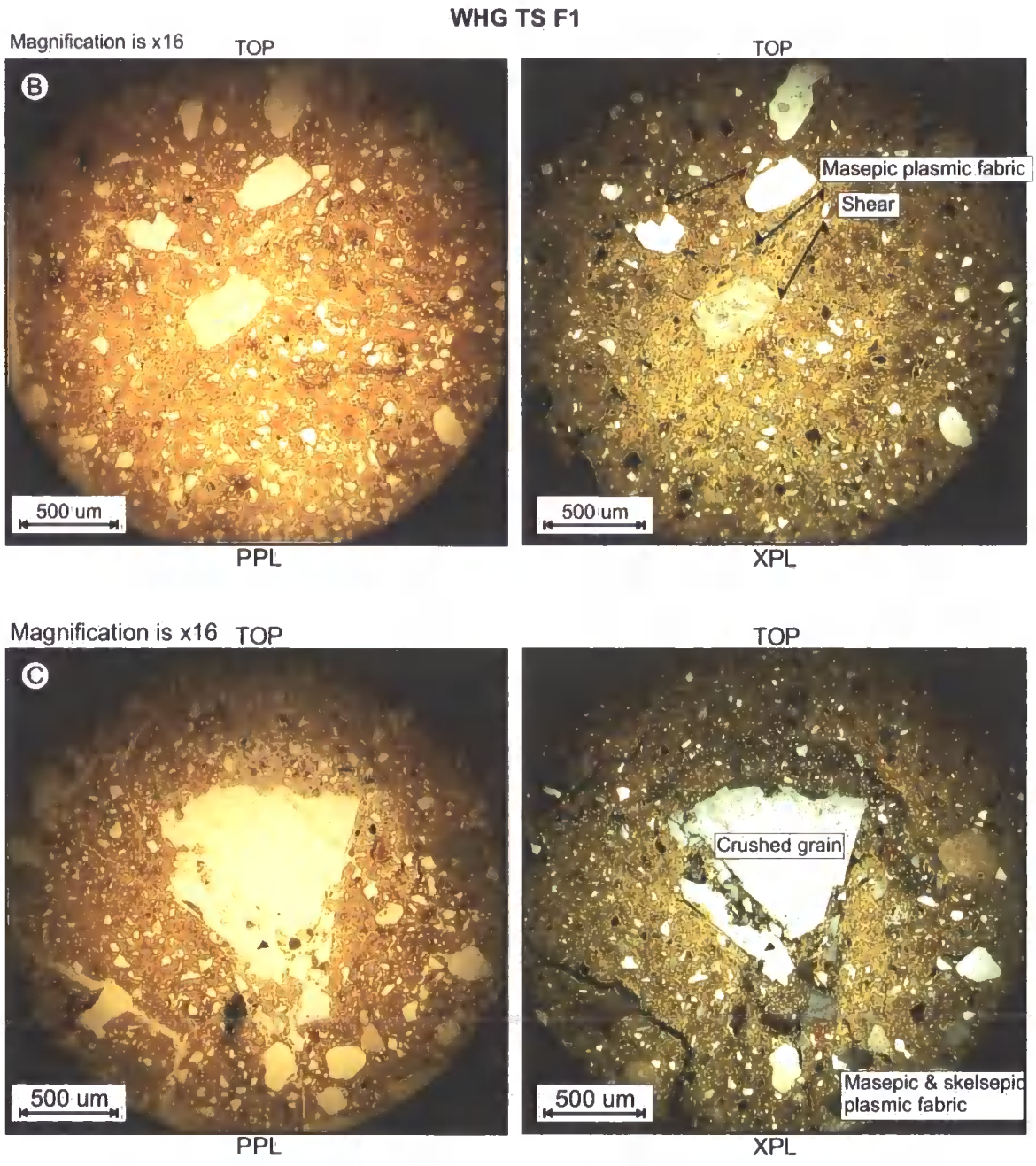

Figure 6.10: Photomicrographs, WHG TS F1, from LFA 1 Exposure F at Warren House Gill.

WHG TS G 0.30 m was taken from LF 1a, at the base of Trial Pit G, (summarised in Table 6.1). Massive at exposure, the thin section is a diamicton with many deformed and folded beds of sand with graded contacts (Figure 6.11). There is common fine gravel, including soft sediment pebbles, red marl, igneous lithic fragments, and quartz grains. There are shell fragments and marine microfossils. Textural analysis of the sand beds shows that they consist of a silt to fine sand matrix, and are moderately to poorly sorted. The grains are mostly sub-angular in shape. The diamicton beds have a very wide range of

grain sizes and shapes. The microfabric is horizontal in the clay matrix, sub-parallel to the beds.

There are abundant sedimentary structures within the slide. The voids within the slide are planar, bedding-parallel, packing-induced voids, with occasional laboratory-induced vugh voids. The graded sedimentary laminations are strongly deformed by soft sediment deformation and have been subjected to ductile 'flow' (Menzies *et al.*, 2006). There is a well-developed masepic plasmic fabric (Figure 6.12 A, B, and C). There is a limited amount of manganese staining. Boudinaged bedding is in evidence, crosscut by clay-lined normal faults (Figure 6.12 C) and associated in places with are pressure shadows with associated plasmic fabric development (Figure 6.12 A). Within the diamicton, there are lineations of grains with associated plasmic fabric development, rare rotations (Figure 6.12 A), a rotated intraclast with a tail, and pressure shadows. The central large intraclast has been loaded by a sand grain, splitting and rotating it (Figure 6.12 D and E). Figure 6.12 F shows a lamination which has been faulted downwards. The association with a grain lineation demonstrates the presence of shear.

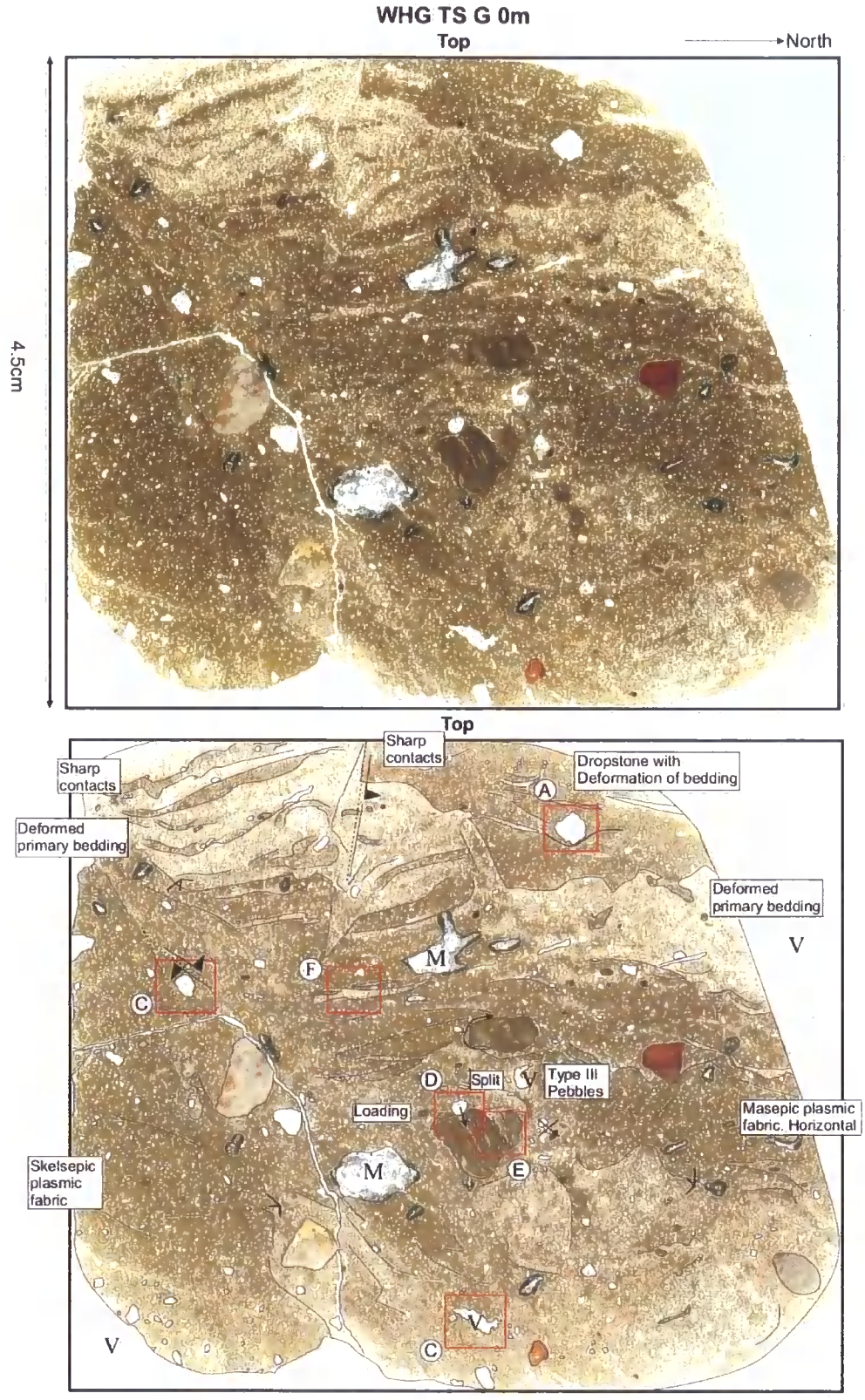

Figure 6.11: Scans of thin section sample WHG TS G 0 m, LF 1a. Boxes show location and context of photomicrographs in Figure 6.12. Location of sub-resolution features is annotated on the scan.

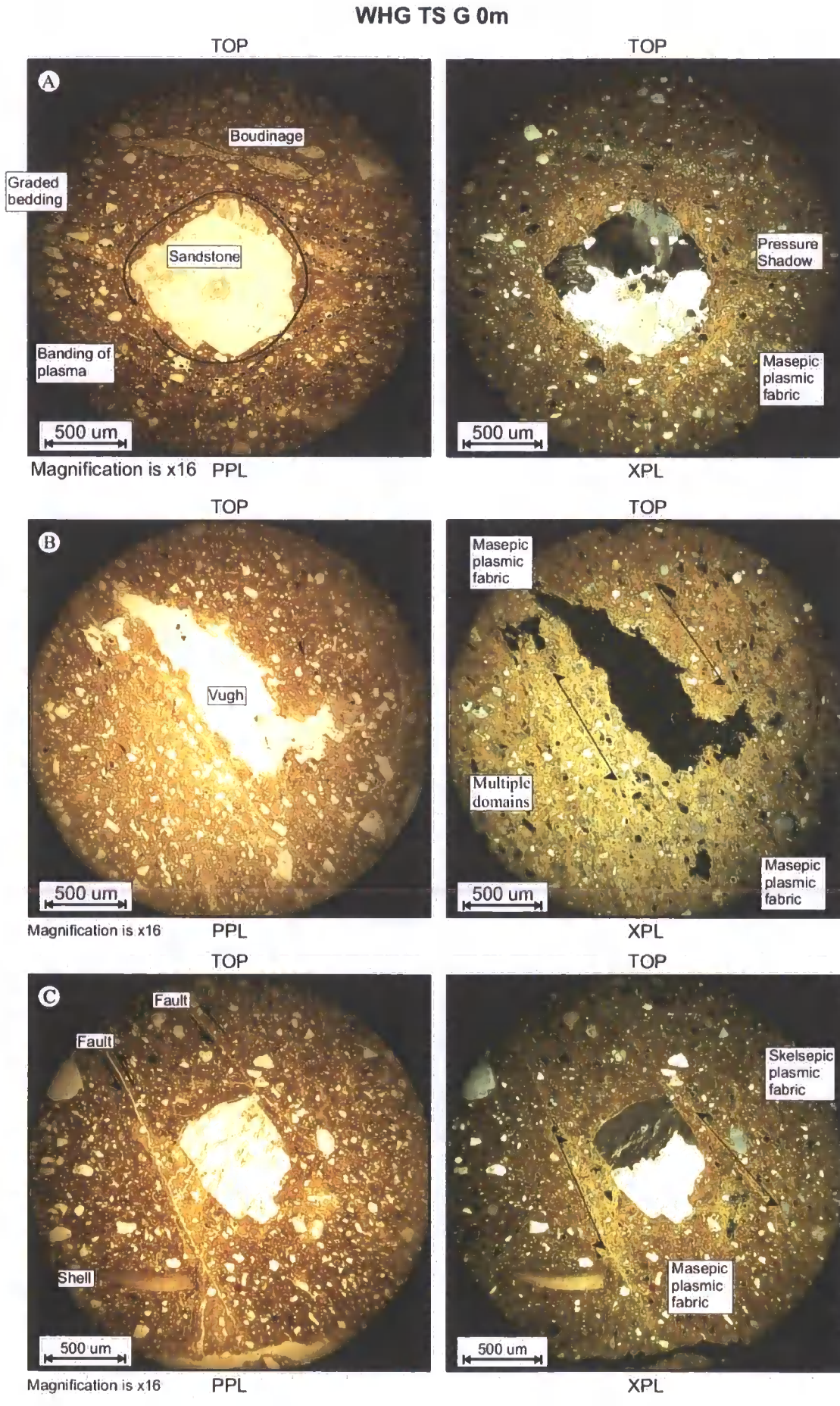
WHG TS G 0m
TOP
TOP
A
Boudinage
Graded bedding
Sandstone
Banding of plasma
500 um
Pressure Shadow
Masepic plasmic fabric
500 um
Magnification is x16
PPL
XPL
TOP
TOP
B
Vugh
500 um
Masepic plasmic fabric
Multiple domains
Masepic plasmic fabric
500 um
Magnification is x16
PPL
XPL
TOP
TOP
C
Fault
Fault
Shell
500 um
Skelsepic plasmic fabric
Masepic plasmic fabric
500 um
Magnification is x16
PPL
XPL

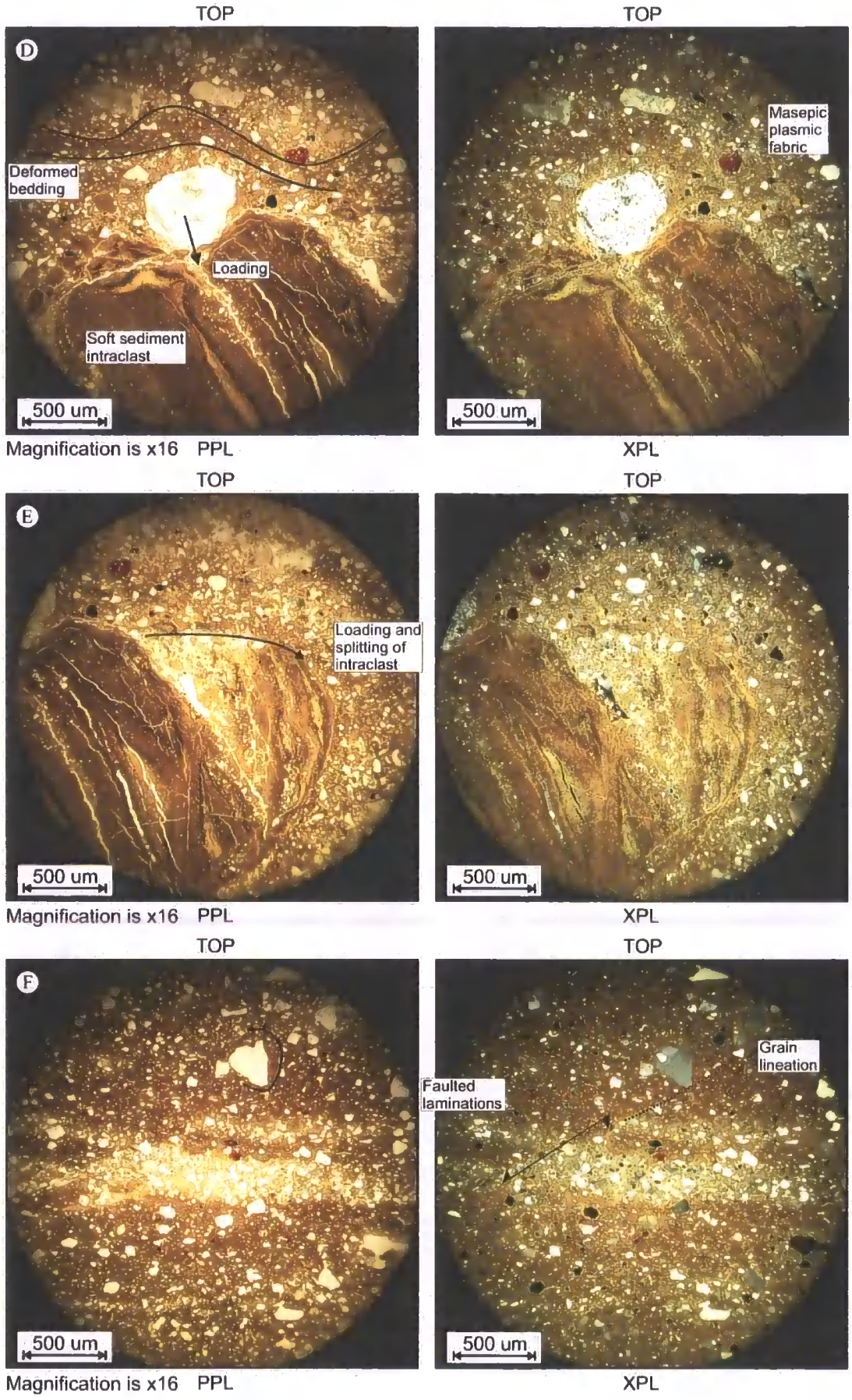

Figure 6.12: Photomicrographs, Thin section WHG TS G 0m. Locations are shown in Figure 6.11.

Thin section WHG TS G 1.9 m was sampled from LF 1b. In thin section, it is a dark brown, iron-stained diamicton with large vugh voids (Figure 6.13). It is mostly fine-grained with one large irregular schistose skeleton grain. There is poor impregnation in one part of the slide. Texturally, the diamicton is a fine sand or silt with some fine material. The skeleton grains are sub-rounded to sub-angular, with numerous angular fine skeleton grains. Skeleton grains are predominantly composed of quartz and plagioclase feldspar; red marl, sandstone, basalt, and other igneous lithic fragments are present. Soft sediment intraclasts, such as Type II and III pebbles, are present. There are rare microfossils and shell fragments.

Structural analysis reveals 'flow' of matrix material and ductile deformation, associated with masepic plasmic fabrics. The matrix is of variable density, and banding is present. There are abundant grain lineations associated with rotational structures, both with and without a core stone, again associated with masepic plasmic fabrics (Figure 6.14A and B). There are lineations of grains, with aligned long axes (Figure 6.14 C). A variation in the abundance of clay platelets has led to the variable intensity of the plasmic fabric.

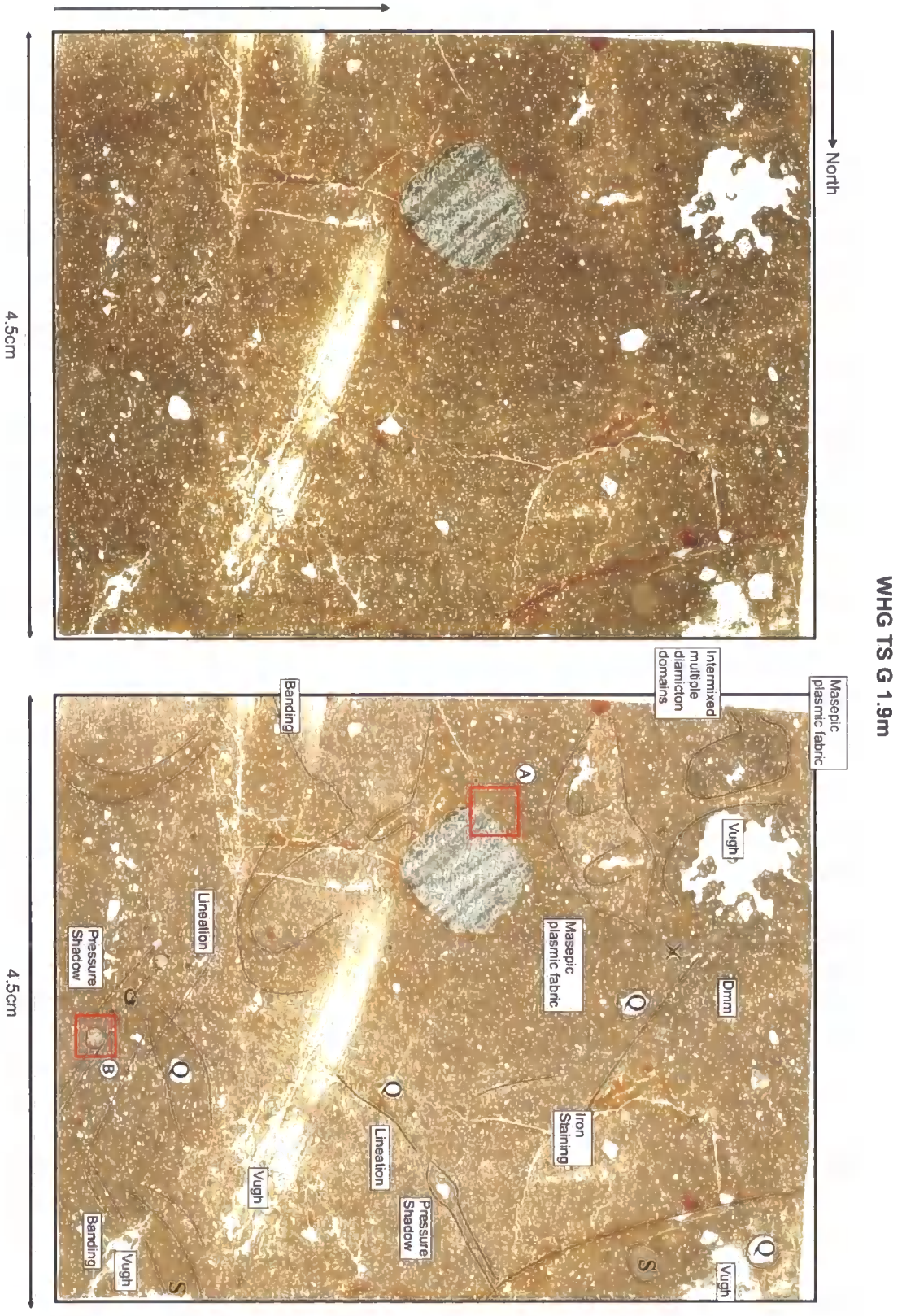

Figure 6.13: Warren House Gill thin section sample WHG TS G 1.9m. LF 1a, the Basal Shelly Diamicton. There is a large man-made vugh void in the centre of the slide (laboratory induced, due to poor impregnation). Location of masepic plasmic fabric and orientation and location of grain lineations are annotated onto the scan.

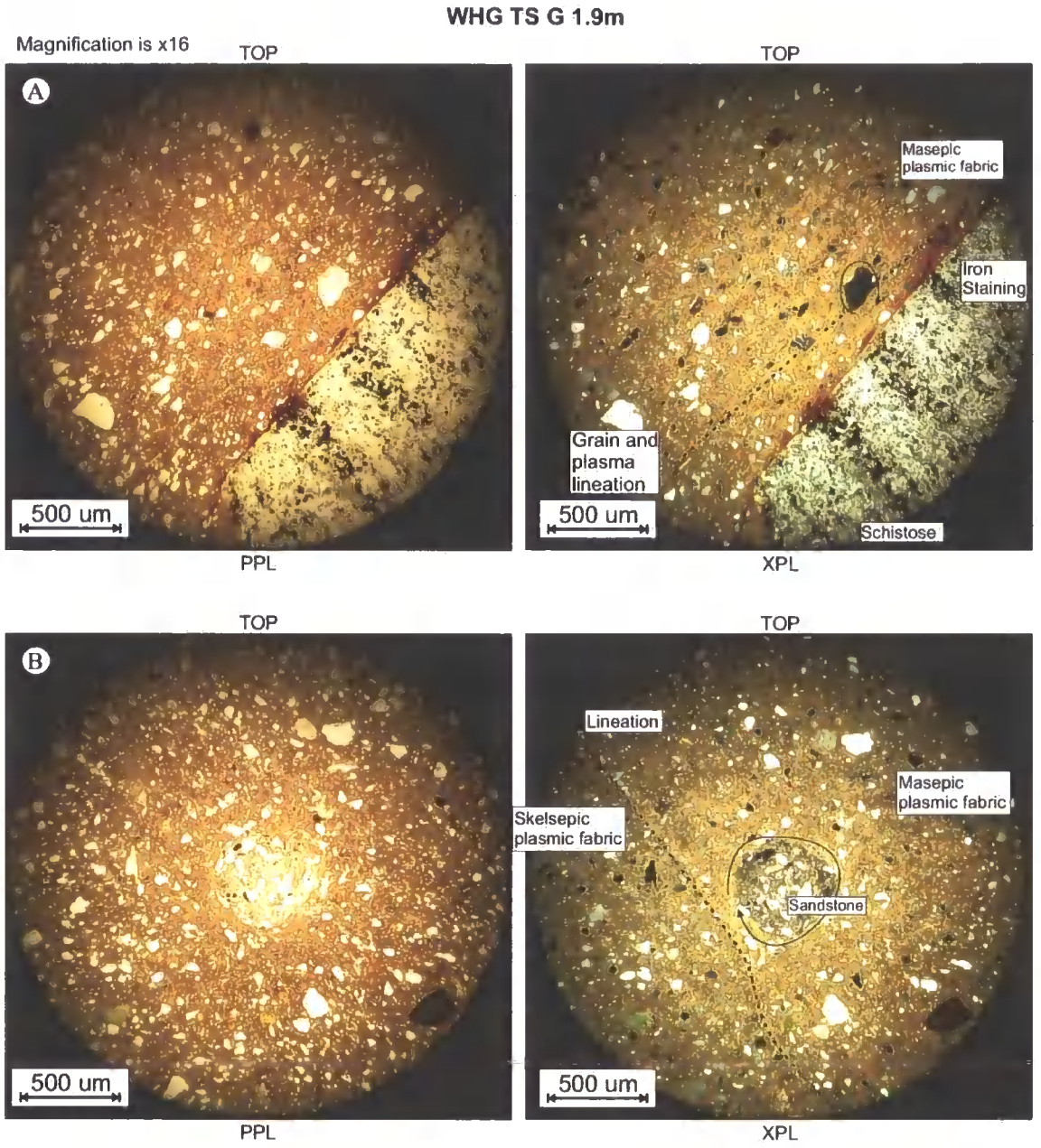

Figure 6.14: Photomicrographs of WHG S G 1.9 m, LFA 1, Warren House Gill.

6.2.3 LFA 2: The Beige Silts

Sedimentology and Stratigraphy

LFA 2 is a moderately well-sorted silt, stratified to laminated in places, and strongly deformed. In the southern end of the palaeovalley, LFA 2 rests on bedrock, but in the centre of the palaeovalley, it overlies LFA 1. LFA 2 pinches out and is absent in the north of the valley (trial pits F, G and H). It is overlain by LFA 3. LFA 2 is strongly variable, with each exposure showing different characteristics. Two principle lithofacies are

identified. LF 2a is a pink silt with race nodules, sandy laminations and deformed clay beds. LF 2a is best exposed in exposures B and C. In exposures C and D, the silts are over 5 m thick. LF 2b is a complex facies with upturned, interbedded silt and sand, with associated clay augen structures. LF 2b is exposed in Exposure D.

LF 2a: Massive to laminated silts

Figure 6.15 is a detailed sketch of LF 2a in Exposure B, showing 1.3 m of stratified, deformed silts on bedrock, overlain by a stratified diamicton (LF 3a; Figure 6.16). LF 2a is a yellowish-brown sandy silt with deformed, folded stratification. Soft sediment, loading and dewatering-style deformation is prevalent (Figure 6.17 A). Black beds are interbedded within the silts (Figure 6.17 B), but they contain no pollen or other discernible organics. The bottom contact is complex, undulating and uneven. The soft Magnesian Limestone bedrock is brecciated, and silt has been injected downwards (Figure 6.17 C). Stringers of limestone extend upwards into the silts above. At the bedrock interface, there are several well-rounded cobbles of exotic origin, including Carboniferous Limestone. Towards the top of LF 2a in Exposure B, the sediment is increasingly stratified. There are discontinuous planar beds of gritty sand interbedded within the silts, which pinch and swell. These grade into a 10 cm shear zone below LF 3a above. This pinches out to the northern end of the section. It is overlain by a gravel rich, dark grey diamicton (LF 3a; see Figure 6.3).

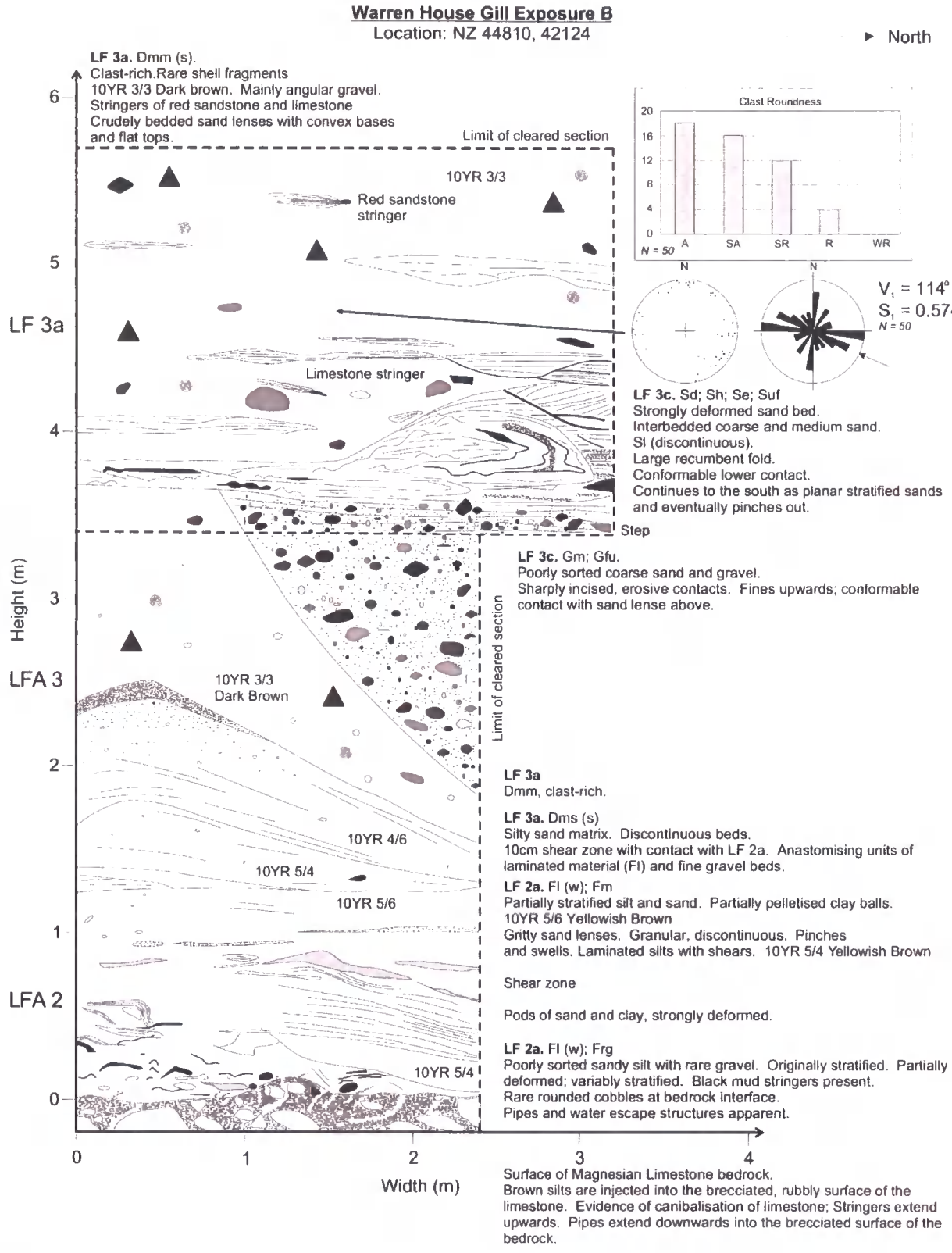

Figure 6.15: Detailed Sketch of Exposure B, LF 2a and LF 3a. Clast fabric (LF 3a): $S_1 = 0.574$; $S_2 = 0.363$; $S_3 = 0.063$.

Figure 6.16: Photograph of LF 2a and LF 3a, Exposure B. LF 2a lies on bedrock, and is overlain by a diamict facies with some bedding, which pinches out on the northern side of the section (LF 3a). This is overlain by a clast-rich diamicton (LF 3a), which contains well-bedded sands which are recumbently folded (LF 3c).

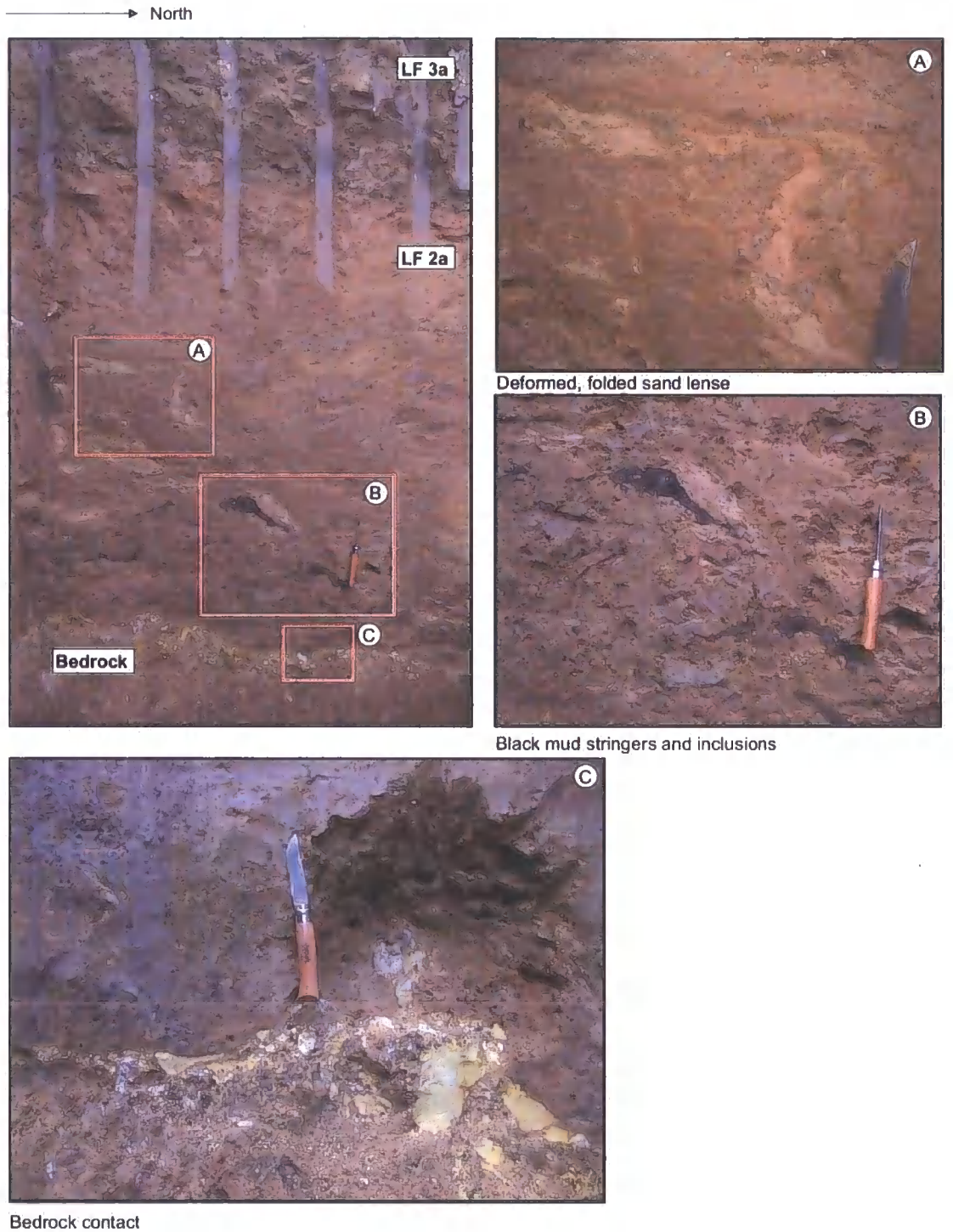

Figure 6.17: Detailed photographs of LF 2a, Exposure B. Photograph A shows deformed sand laminae. Photograph B shows deformed black inclusions. Photograph C details the nature of the contact with the soft, dolomised bedrock. Knife is 19 cm long when extended, and the blade only is 8 cm long.

LF 2a in Exposure C constitutes over 5 m of a fine grained, well-sorted silt, mostly massive with some fluidised sand and clay laminations, overlain by a diamicton (LF 3a). Flecks of coal within the silt are apparent, and carbonate 'race nodules' are present (numbered in Figure 6.18). LF 2a rests on a grey diamicton bearing shell fragments

(LFA 1) on bedrock. The contact of LFA 1 with LFA 2 was observed only in a borehole. This is overlain by strongly fluidised sand and clay beds with numerous rounded clay intraclasts. Water escape, pipe, ball and pillow, and flame structures are abundant in this facies, indicating loading under saturated conditions. The upper contact with the diamicton above is sharp, undulatory and sheared.

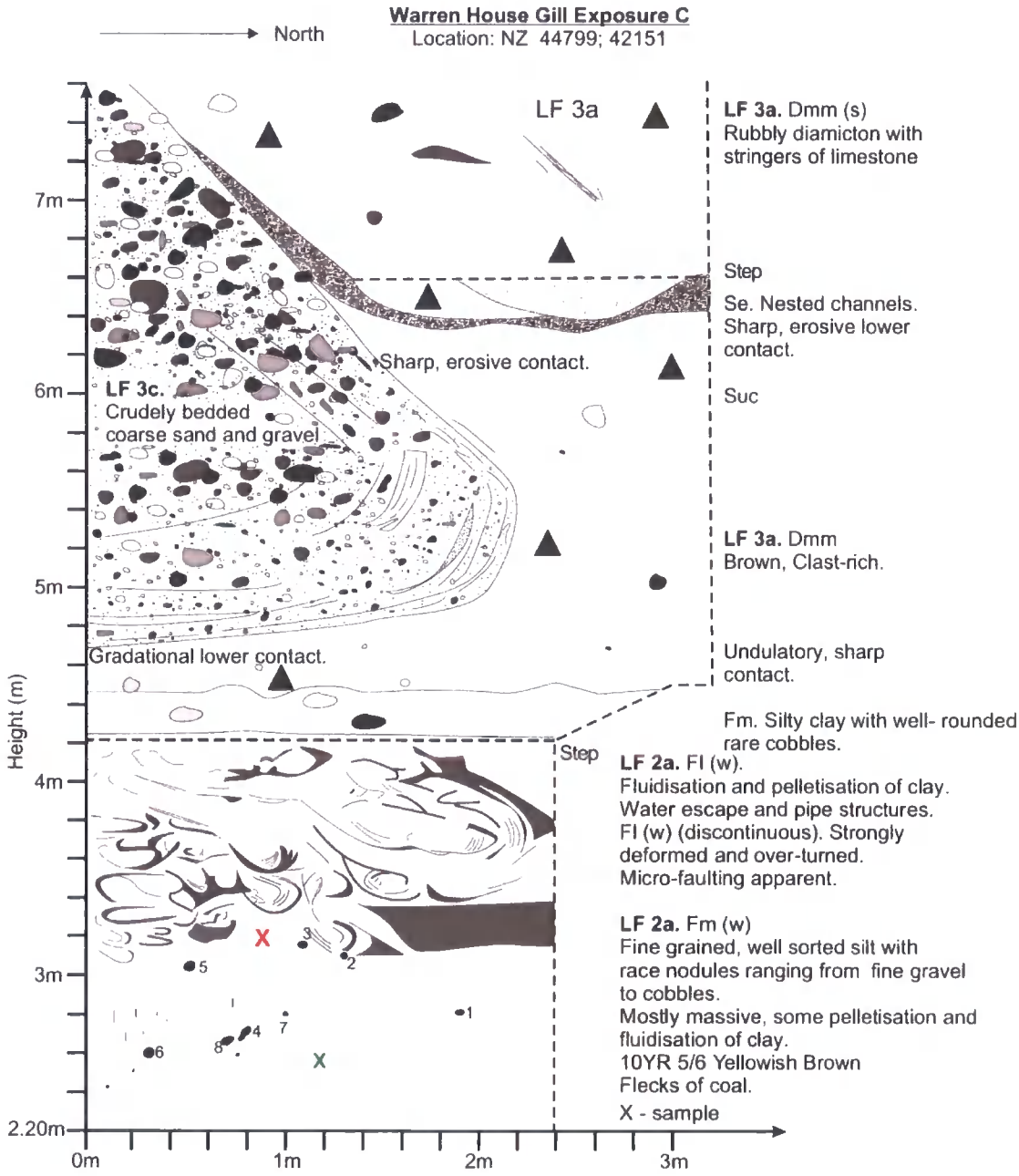

Figure 6.18: Detailed sketch of LF 2 at Exposure C, Warren House Gill, showing bulk (WHG C2; red cross) and OSL sampling locations (green cross). Numbers denote carbonate nodules in LF 2a. For vertical profile, refer to Figure 5.12. *Y*-axis shows height above bedrock (proved by coring but not observed in section to sketch).

LF 2b: Upturned, interbedded sands and silts

Exposure D is in the deepest part of the palaeovalley. Digging by the JCB revealed over 5 m of LFA 2, and did not reach the contact with either bedrock or LFA 1. At the base, LF 2a is exposed, which is similar to that in Exposure C, with well-sorted silty sands showing disturbed laminations, including tightly overturned folds (Figure 6.19). There is evidence of fluidisation of sand and clay. There are no apparent carbonate race nodules or rounded cobbles at this location. LF 2a is capped by a bed of well-sorted clay that dips downwards to the north. It swells sharply into two distinct clay pods with internal sub-vertical, deformed laminations (Figure 6.20 A, B and C). The sediment above the clay (LF 2b) is significantly different, with incoherent, interbedded sand and clay with a distinct sub-vertical nature. These complex interstratified sediments are heavily fluidised, and they contain rare shell fragments. Towards the contact with the overlying diamicton, the sediments become increasingly sub-horizontal to horizontal, resulting in more coherent laminations (Figure 6.20 D). This is overlain by a narrow, discontinuous bed of poorly-sorted gritty sand with some internal stratification, which grades into a 10 cm thick bed of well-sorted clay. There is evidence of cannibalisation of the sediments below, and the clay extends in places as stringers into the diamicton above. The clay bed contains rare clasts derived from the diamicton above. The upper contact is sharp and undulatory.

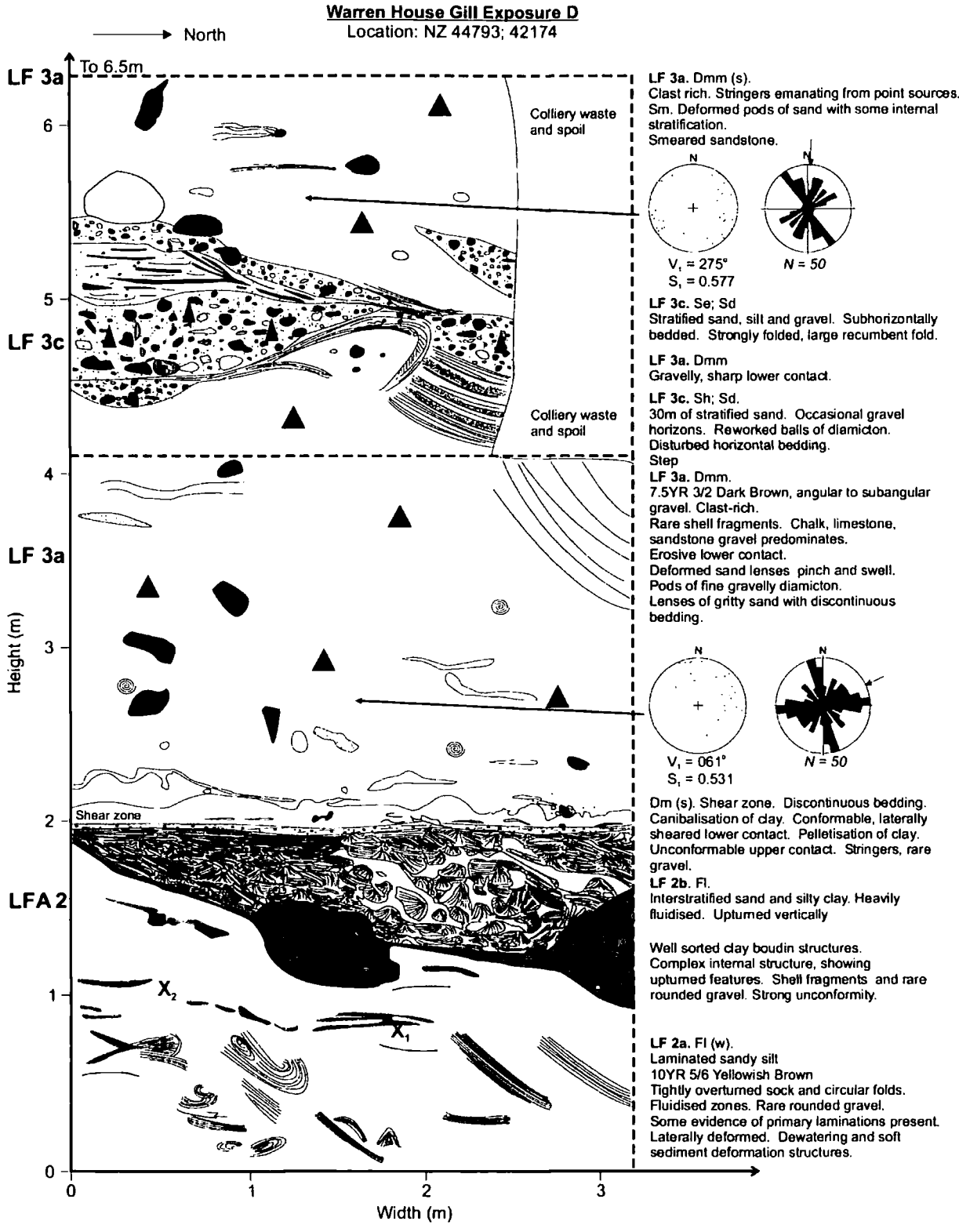

Figure 6.19: Detailed Sketch of LF 2a and LF 2b (silts) and LF 3a (Diamicton) and LF 3c (sands and gravels) in Exposure D, Warren House Gill. Green crosses show OSL sampling locations. Lower clast macro-fabric (LF 3a): $S_1 = 0.531$; $S_2 = 0.356$; $S_3 = 0.112$. Upper clast macro-fabric (LF 3a): $S_1 = 0.577$; $S_2 = 0.32$; $S_3 = 0.103$.

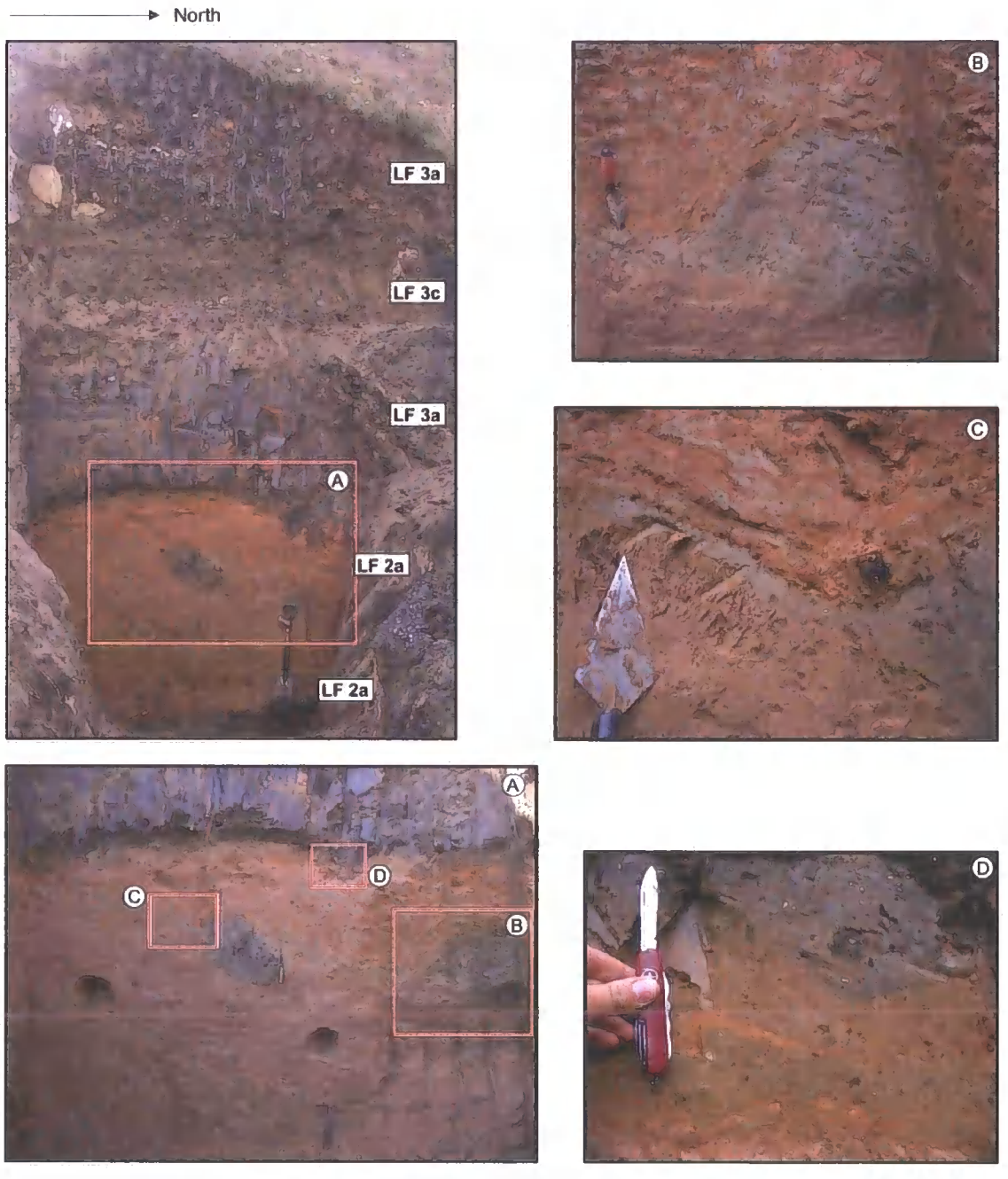

Figure 6.20: Photographs and detail of LFA 2, Exposure D, Warren House Gill.

Photograph A: LF 2a and LF 2b. Photograph B: Clay boudin structure, LF 2b. Photograph C: Contact LF 2a and LF 2b, showing well-sorted clay bed and boudin structure. Photograph D: Shear zone between LF 2b and LF 3a. Trowel for scale is 26 cm long. Spade is 1 m long.

Thin-section analysis

Three thin sections were sampled from LF 2a and LF 2b, Exposure D (Figure 6.21). WHG TS D*iv* (LF 3a) is presented in Chapter 6.4.2. The thin sections demonstrate the changing nature of these silts. The first thin section (WHG TS D*i*) was sampled from LF 2a in Exposure D at 1.3 m height (Figure 6.19). The silt is well-sorted with occasional deformed clay laminations. On macroscopic inspection, it has a variable texture showing extensive deformation of primary fluvial bedding structures. The slides are summarised in Table 6.2.

The skeleton grains mostly consist of well-sorted silt, predominantly quartz, and are angular to well-rounded in shape. Rare larger sand grains are sub-angular to sub-rounded in shape. The thin section has two large vugh (laboratory-induced) voids, which may be related to manganese staining of the sediments. There is a well developed, north-south aligned microfabric. Structural analysis reveals graded bedding structures including the foresets of a climbing ripple. This conformable, graded bedding has been extensively fluidised under saturated, loaded conditions (cf. Phillips *et al.*, 2007). Cutting through the deformed bedding are a series of crosscutting faults. A clay intraclast has been sheared and attenuated; this is associated with lineations of microfabric and small skeleton grains. This deformation is emphasised with the clear lattisepic and masepic plasmic fabric.

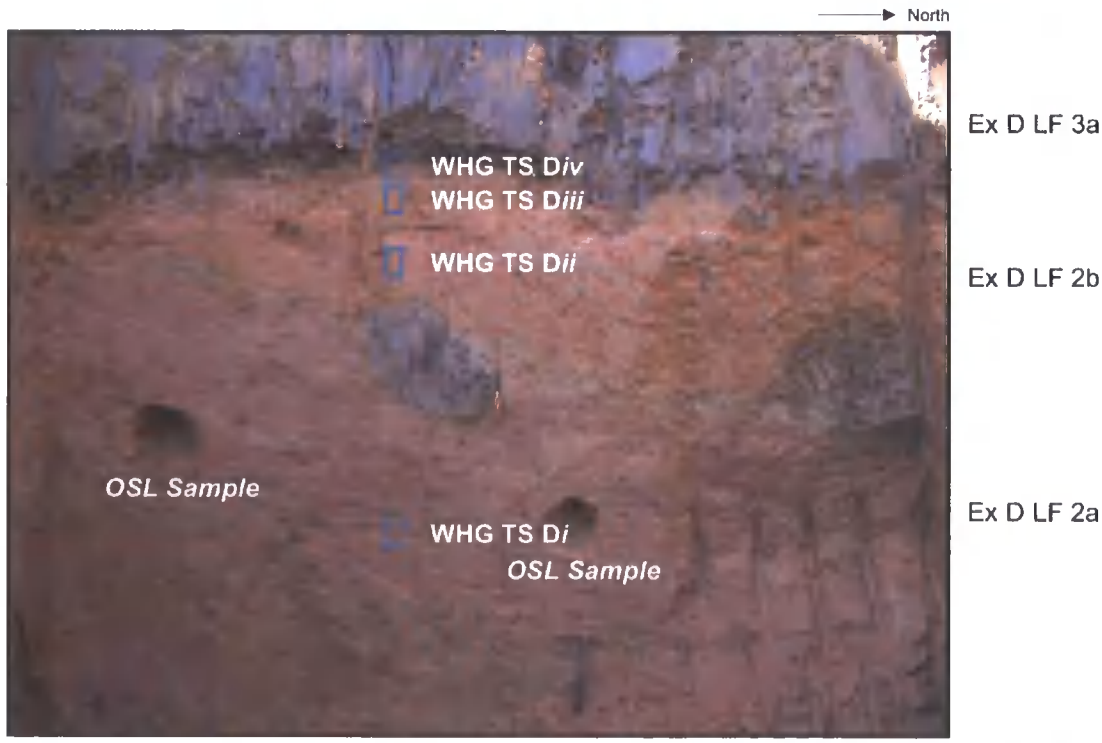

Figure 6.21: Location of thin section samples and OSL samples at Exposure D, Warren House Gill. Geological hammer is 32 cm long. Penknife is 19 cm long when extended.

Table 6.2: Summary of micromorphology of LFA 2, the Beige Silts.

Sample	Location	Lithofacies	Skeleton			Matrix		Void type	Sedimentary Structures				Deformation Structures														Plasmic Fabric				
			Sorting	Grain shape <500µm	Grain shape >500µm	Texture	Microfabric		Laminations	Dropstones	Microfossils	Dump Structures	Section Elements	Faulting	Folding	Rotations	Grain lineations	Pressure Shadow	Crushed Grains	Grain stacks	Pebble Type I	Pebble Type II	Pebble Type III	Water escape	Fluidised Bedding		Skelsepic	Lattisepic	Masepic	Bi-Masepic	Unistrial
WHG Di	Ex D 1.3m	LF 2a. Beige Silts	WS		A - WR	M	H	P/L	••				Sh Be	•		•								••	•••		••			•
WHG Dii	Ex D 1.65m	LF 2b. Deformed sand and clay	WS	SA	SA - SR	M	H	L	••				F		••	••	•						•••	•	•••		•	••			
WHG Diii	Ex D 2.2m	LF 2b. Shear zone in beige silts	WS		SR	F / M		L/P					Be St										•••				•	•			

Key

Sorting

WS	Well sorted
MS	Moderately sorted
PS	Poorly sorted
D	Diamicton

Grain shape

WR	Well rounded
R	Rounded
SA	Subangular
A	Angular

Microfabric

H	Horizontal Microfabric
V	Vertical microfabric

Voids

P	Packing induced
L	Laboratory induced

Texture

F	Fine grained
C	Coarse (no fine silt/clay)
M	Medium (some fine silt/clay)

Section Elements

Ba	Banding
Bo	Boudinage
Be	Bedding
Sh	Shear
F	Flow
St	Stringer

••• Indicates feature is strongly present / numerous

•• Indicates feature is present

• Indicates feature is rarely / occasionally present

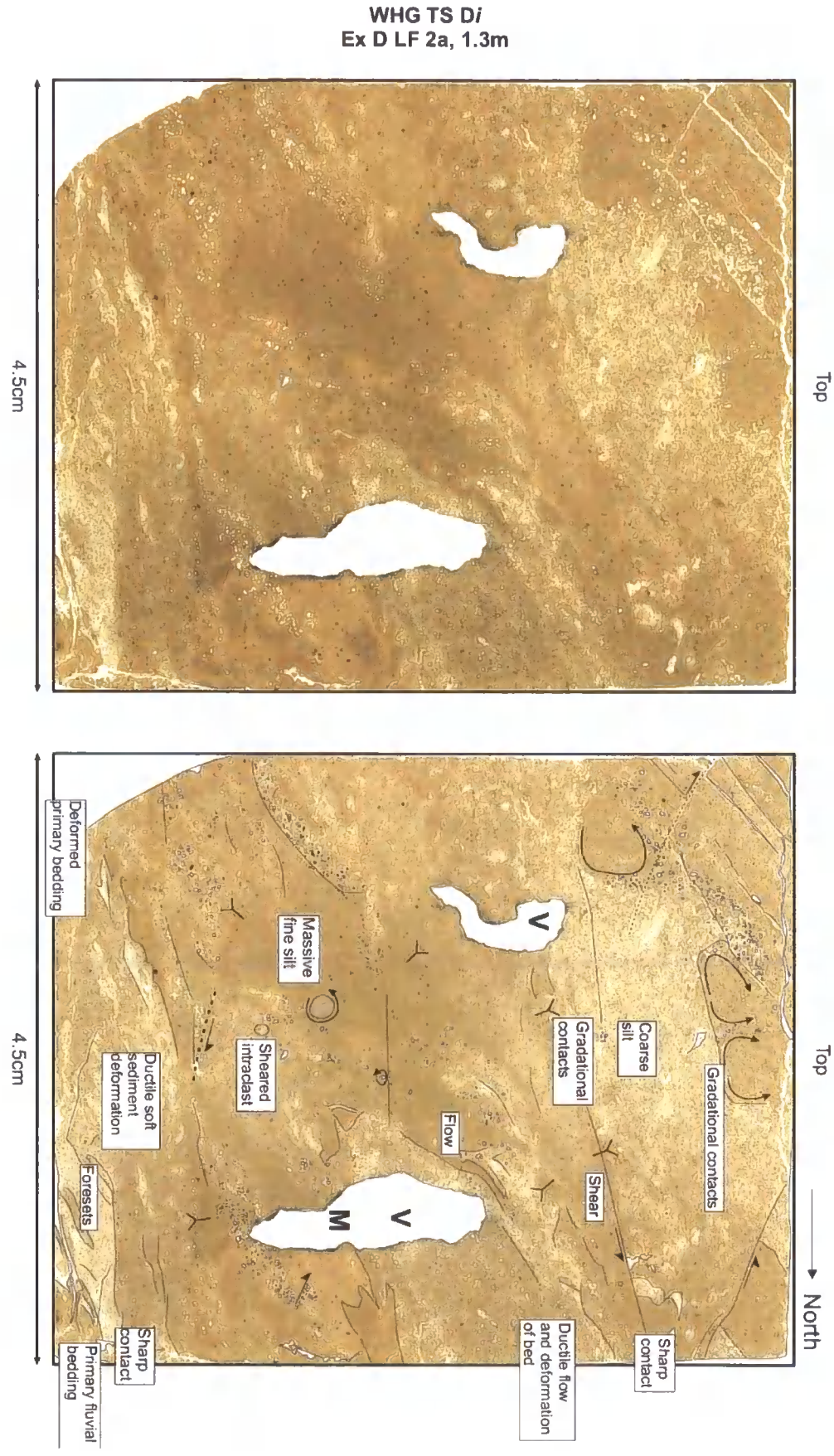

Figure 6.22: Photograph of Thin Section sample WHG TS D*i*. The matrix material is deformed and intermixed, exhibiting ductile deformation.

The second thin section (WHG TS D*ii*) was sampled from LF 2a of Exposure D, at a height of 1.65 m (Figure 6.21). On a macroscopic inspection, it is a strongly deformed silt with deformed, disjointed clay-lined beds. The slide constitutes mostly well-sorted silt with some sand grains. There are also Type III Pebbles visible (van der Meer, 1997). Iron staining along particle-size boundaries is apparent.

Textural analysis indicates that the silt grains are predominantly angular to sub-angular in shape, while the larger sand grains are more edge-rounded. The matrix is composed of silt skeleton grains with some clay matrix material. The voids are vugh-type, with some bedding-parallel voids, probably caused during packing. The slide has some evidence of primary deposition in water, which has been strongly deformed. There has been 'flow' of the bedding (Menzies *et al.*, 2006). This deformation is related to the development of a common latti/skelsepic plasmic fabric within the clay matrix.

Thin section WHG TS *Diii* was taken from the top of LF 2b in Exposure D, at a height of 2.2 m (Figure 6.23). This is a macroscopically homogenous, moderately well-sorted, massive silt. It has numerous larger, rounded, clay intraclasts. Textural analysis of the skeleton grains reveals that the silt consists mostly of angular to sub-angular grains of even distribution. The slide is mostly homogenised, but there are some indications of crude primary bedding. The only deformation structures are the numerous rounded Type III Pebbles, sometimes with their own plasmic fabric development. The matrix displays a weakly developed latti/skelsepic plasmic fabric.

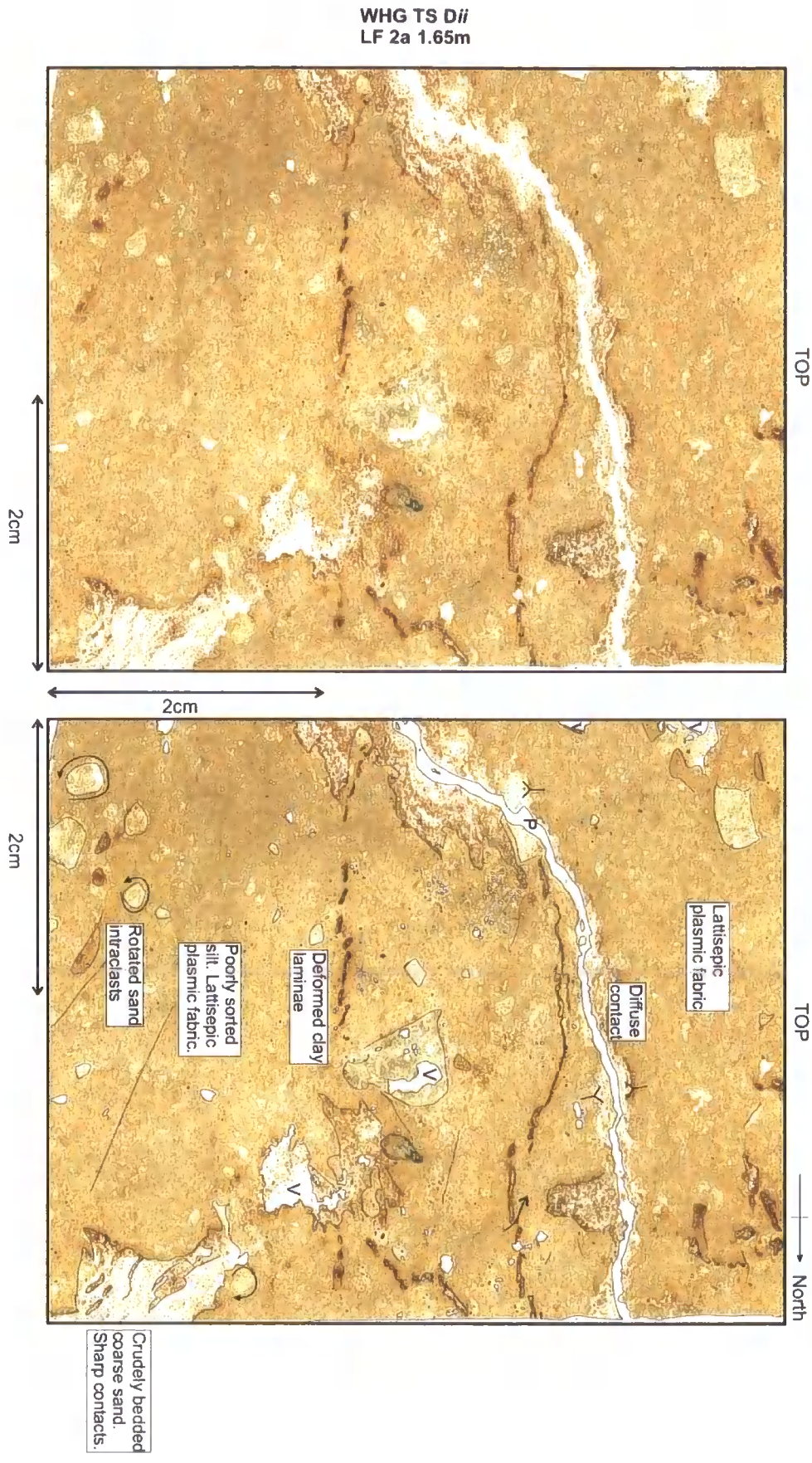

Figure 6.23: Scan of WHG TS D*ii*, taken from LF 2a in Exposure D. LF 2a, height 1.65 m. Location of plasmic fabric development is noted.